

CRANFIELD UNIVERSITY

ALEXANDER JAMES MABBOTT

THE OVERMATCHING OF UK POLICE BODY ARMOUR

CRANFIELD DEFENCE AND SECURITY

PhD thesis
Academic Year: 2015

Supervisors: Dr Debra Carr and Mr Stephen Champion
December 2015

CRANFIELD UNIVERSITY

CRANFIELD DEFENCE AND SECURITY

PhD Thesis

Academic Year 2015

Alexander James Mabbott

THE OVERMATCHING OF UK POLICE BODY ARMOUR

Supervised by Dr Debra Carr and Mr Stephen Champion
December 2015

© Cranfield University 2015. All rights reserved. No part of this publication may be reproduced without the written permission of the copyright owner.

ABSTRACT

Police officers and other personnel in the UK routinely wear body armour that provides protection from specific threats. Typically, 'soft' armours, usually formed from multiple layers of fabric, can protect wearers from fragmentation and low velocity (handgun) ballistic threats, while 'hard' armours, formed from ceramic and composite plates, offer protection from high velocity (rifle) threats. Protection from stab and/or slash attack is predominantly provided by utilising chain mail and laminated solutions. The question has been raised however, of what would happen when armour is overmatched with a greater threat than it is designed to protect against.

A limited number of studies have been published in the open source literature regarding the overmatching of soft body armour.

This research aims to increase the understanding of overmatching, by investigating the effect of both i) soft fabric body armour designed to protect from handgun ammunition being challenged by high velocity rifle projectiles and ii) knife and spike resistant armour protecting against low velocity handgun projectiles.

A subsection of the research considered three tissue simulants in order to find the most suitable for investigating the effects of overmatching armour. A method for recording the damage produced in the simulants was also developed; from which comparison of damage to different targets was possible.

Following the tissue simulant investigation, gelatine blocks 10% in concentration were selected and used to investigate the overmatching of two types of UK police body armour. Three different arrangements were setup, namely 10% gelatine blocks 500mm, 10% gelatine blocks 250mm in length, and porcine thoracic walls arranged to simulate a thorax.

Testing blocks 500mm in length was a set-up typical to ballistic investigations; the blocks were capable of capturing the majority of the projectiles' damage, with the damage produced in both unprotected and protected (on the front face only) targets compared. Based on anthropometric measurements, testing 10% gelatine blocks 250mm in size was more representative of a torso sized target. With the blocks smaller, armour was placed on both the front and back face of targets. This is more representative of how armour would be worn in a real life scenario; patrolling UK police officer wearing armour that protects both the front and back of their torso. Finally, the use of porcine samples arranged to simulate both protected and unprotected thoraxes enabled comparisons of the damage seen in homogenous tissue simulants to damage in non-homogenous material typical to those found in the human torso.

The outcomes from testing three different targets with two ammunition and armour

combinations revealed the effect of overmatching armour is not one that can be generalised and predicted for all overmatching scenarios. The presence of armour on the rear face of targets based on typical measurements of human chest depth, increased the chances of the projectiles tested remaining within the targets.

ACKNOWLEDGEMENTS

There are only so many ways I can say thank you, and yet so many people to thank, so please bear with me as I take this opportunity to pay tribute those who without whom this thesis would not have been possible.

Mum and Dad: it's done! Thank you for everything. For all the favours, from days and nights spent correcting my use of the English language, to collecting documents on my behalf, even when they weren't quite as close to your location as I believed... I truly wouldn't have had this opportunity without your support and push to further myself. And it's okay Dad, it got me a job in the end! Thank you to my big sisters too. Your words of encouragement through the toughest times were invaluable.

To Deb – I truly could not have asked for a better supervisor. You are a credit to your profession and I know I'm not that only one who thinks so. Being fortunate enough to have had your supervision, support, and advice has made me not only a better academic but a better person. You work so hard, and your expertise and knowledge knows no bounds. You are a true role model, particularly to those of us who are grammatically challenged! Thank you. I will always, always be indebted to you, and I will come back and make gelatine for you anytime!

To Steve, for getting me involved with the mucky job that is gelatine production, I've come a long way thanks to you. I may have cursed you once or twice for your ballistic and aerodynamic input, but ultimately I am better off for the expertise you shared with me. Thank you.

To Professor Ian Horsfall, for always being in support of the work I have carried out for the Impact and Armour group. One of my fondest memories will always be PASS 2012. Within the Impact and Armour group, a big thank you goes to Dave, Mike, Claire, Alan; the range staff. For getting stuck in with me for the numerous hours I spent down the range, from shaking gelatine out of their boxes, to holding bits of meat for photographs, nothing was too much to ask of you, and it made my task a lot easier. Tea breaks were always a welcome break from staring at the computer screen and always a good laugh too!

To my office buddies past and present: Rocky, Ryan, Cat and Leigh. It's been a long time coming and without the snacks, throw-and-catch sessions, practical jokes, tunes, late nights and the joint suffering; I wouldn't be writing my acknowledgments page right now. You're some of the smartest people I've come across and I can't wait to graduate with you!

I have a few final shout-outs to my fellow Cranfieldians, who through either assistance or friendship, made this a little easier. In particular, to Dan and Charlene, who have been through this ordeal and come out the other side of it with flying colours. Your advice has been invaluable, and I truly have the utmost respect for what you have achieved. Thanks also to Iain Mackay for accepting all the challenges I posed you during the last few years.

Thank you to the Engineering and Physical Sciences Research Council for sponsoring the project. I would also like to extend my gratitude to the Home Office's Centre for Applied Science and Technology (CAST) and in particular Chris Malbon, who provided the materials needed to complete this research. Support was also provided to me by The Worshipful Company of Armourers and Brasiers, who made it possible for me to attend PASS 2012 and 2014 to present my research. A final thank you for the support I received from the Ballistics Injury Archive, and in particular Leslie Payne, whose knowledge was truly invaluable during the early stages of my studies.

To the Lakers, the guys back home, and friends both sides of the Atlantic, thanks for not getting too bored hearing about the trials of being a student, still. The professional student career is nearly at an end and I look forward to catching up with everyone and making up for lost time.

Last but not least, Annie. For being there through the most stressful times; being patient, being the distraction, being the motivation, talking and listening through topics I bet you never thought you'd hear about. Not to mention making ISB2014 the best conference known to man. Thank you.

CONTENTS

ABSTRACT.....	i
ACKNOWLEDGEMENTS.....	i
CONTENTS.....	iii
LIST OF FIGURES.....	x
LIST OF TABLES.....	xv
NOMENCLATURE.....	xxii
Chapter 1 : INTRODUCTION.....	1
1.1 Relevance of the subject.....	2
1.2 Aim and outline of the study.....	3
1.3 Structure of the thesis.....	4
Chapter 2 : LITERATURE REVIEW.....	6
2.1 Ammunition.....	6
2.1.1 Cartridge case nomenclature.....	6
2.1.2 Projectile.....	8
2.1.2.1 Expanding projectiles.....	9
2.1.2.2 Fragmenting projectiles.....	10
2.1.2.3 Projectile velocity.....	10
2.1.3 Summary.....	11
2.2 Wound ballistics.....	12
2.2.1 External ballistics.....	12
2.2.1.1 Ballistic coefficient.....	13
2.2.1.2 Drag force and drag coefficient.....	14
2.2.1.3 Stability.....	16
2.2.1.3.1 Yaw.....	17
2.2.2 Theories of wounding capability.....	18
2.2.2.1 Expected Kinetic Energy (EKE).....	20
2.2.3 Wounding mechanisms.....	21
2.2.3.1 Crushing and lacerating of tissue.....	22
2.2.3.1.1 Deceleration in tissue.....	22
2.2.3.1.2 Yawing in tissue.....	24
2.2.3.2 Temporary Cavitation.....	26
2.2.3.3 Shock waves.....	29
2.2.3.4 Bullet expansion and fragmentation.....	29

2.2.3.5 Contamination.....	30
2.2.5 Summary.....	32
2.3 Tissue simulants.....	33
2.3.1 Ballistic soap.....	34
2.3.2 Gelatine.....	34
2.3.2.1 10% gelatine.....	35
2.3.2.2 20% gelatine.....	36
2.3.2.3 10% blocks vs 20% blocks – which blocks to use?.....	37
2.3.2.4 Temperature.....	38
2.3.2.5 Block size.....	40
2.3.2.5.1 Anthropometric measurements of the human torso.....	41
2.3.2.6 Calibration.....	41
2.3.3 Polymer based gels.....	42
2.3.4 Perma-Gel™.....	43
2.3.5 Summary.....	44
2.4 Body Armour.....	47
2.4.1 History.....	47
2.4.2 Forms of body armour.....	48
2.4.2.1 Soft body armour.....	48
2.4.2.1.1 Para-aramids.....	49
2.4.2.1.2 UHMWPE.....	50
2.4.2.1.3 Polyamides.....	51
2.4.3 How does body armour work?.....	51
2.4.4 Body armour failure mechanisms.....	53
2.4.5 UK Police soft body armour.....	54
2.4.7 Summary.....	56
2.5 Review of previous overmatching armour investigations.....	57
2.5.1 The shielding capacity of the standard military flak jacket against ballistic injury to the kidney (O’Connell <i>et al.</i> , 1988).....	57
2.5.2 The personal protective equipment provided for combatants: The part played by wearing a protection vest in the behaviour of projectiles. Wounding outcomes (Breteau <i>et al.</i> , 1989).....	58
2.5.3 Small Arms vs Soft Armour (Prather, 1994).....	59
2.5.4 Study on the wound ballistics of fragmentation protective vests following penetration by handgun and assault rifle bullets (Missliwetz <i>et al.</i> , 1995).....	62
2.5.5 The destabilising effect of body armour on military rifle bullets (Knudsen and Sørensen, 1997).....	65

2.5.6 Is the wounding potential of high velocity military bullets increased after perforation of textile body armour? (Lanthier, 2003; Lanthier <i>et al.</i> , 2004)	66
2.5.7 Miscellaneous	67
2.5.8 Case studies.....	68
2.5.9 Summary	70
2.6 Overall summary of literature review	71
Chapter 3 : EXPERIMENTAL SELECTION AND JUSTIFICATION OF A TISSUE SIMULANT	72
3.1 Introduction.....	72
3.2 Part A – Depth of penetration of 5.5mm ball bearings	72
3.2.1 Materials and methods	73
3.2.1.1 Simulants.....	73
3.2.1.1.1 Gelatine	73
3.2.1.1.2 Perma-Gel™	74
3.2.1.2 Ball bearings	76
3.2.1.3 Depth of penetration testing method.....	76
3.2.1.4 Depth of penetration analysis.....	79
3.2.2 Results.....	80
3.2.2.1 Depth of penetration results for 5.5mm BBs in 10% gelatine, 20% gelatine and Perma-Gel™	85
3.2.2.2 Depth of penetration results for 5.5mm BBs in 10% and 20% gelatine	87
3.2.2.3 Depth of penetration results for 5.5mm BBs in re-melted Perma-Gel™	88
3.2.3 Discussion of depth of penetration testing.....	88
3.3 Part B – Baseline simulant tests.....	92
3.3.1 Materials and methods	92
3.3.1.1 Simulants.....	92
3.3.1.2 Ammunition	92
3.3.1.3 Baseline simulant method	94
3.3.1.4 Baseline simulants analysis.....	95
3.3.1.4.1 High speed video analysis.....	99
3.3.2 Results.....	100
3.3.2.1 Projectile construction	100
3.3.2.2 .223 Remington Federal Premium® Tactical® Bonded® results	103
3.3.2.2.1 ANOVA results.....	106
3.3.2.3 9 x 9mm FMJ results.....	110
3.3.2.3.1 ANOVA results.....	114
3.3.3 Discussion of baseline simulant tests.....	118

3.3.3.1	Baseline tests with .223 Remington Federal Premium® Tactical® Bonded® projectiles.....	118
3.3.3.2	Baseline tests with 9mm Luger projectiles	119
3.3.3.3	Overview of baseline tests	120
3.4	Part C – Ballistic testing of porcine samples	122
3.4.1	Materials and methods	122
3.4.1.1	Target materials	122
3.4.1.1.1	Porcine samples	122
3.4.1.1.2	Gelatine	123
3.4.1.2	Ammunition	123
3.4.1.3	Ballistic testing method.....	124
3.5.1.4	Analysis.....	126
3.5.1.4.1	Comparison of results from porcine and baseline testing.....	129
3.4.2	Results.....	130
3.4.2.1	.223 Remington Federal Premium® Tactical® Bonded® results	130
3.4.2.1.1	Distance to projectiles ANOVA	133
3.4.2.1.2	Distance to .223 Remington Federal Premium® Tactical® Bonded® projectiles (non-rib striking shots removed) ANOVA.....	134
3.4.2.2	9 x 9mm FMJ results.....	135
3.4.3	Discussion.....	136
3.5	Discussion on the selection and justification of a tissue simulant.....	138
3.5.1	Perma-Gel™	138
3.5.2	Gelatine	138
3.6	Chapter summary	140
Chapter 4 : THE OVERMATCHING OF ARMOUR.....		141
4.1	Introduction.....	141
4.2	Part A: Armoured gelatine blocks 500mm in length	141
4.2.1	Materials and methods	141
4.2.1.1	10% gelatine.....	141
4.2.1.2	Body armour	142
4.2.1.3	Ammunition	143
4.2.1.4	Ballistic testing method.....	143
4.2.1.5	Analysis.....	144
4.3.1.6	EKE deposited and high speed video analysis.....	144
4.2.2	Results from .223 Remington Federal Premium® Tactical® Bonded® rounds ..	145
4.2.2.1	ANOVA results.....	152
4.2.2.1.1	Neck length	152

4.2.2.1.2	Body length.....	152
4.2.2.1.3	Representation of maximum ellipsoid volume	152
4.2.2.1.4	Fissure area	153
4.2.2.1.5	EKE.....	154
4.2.2.1.6	Distance to projectile	155
4.2.2.1.7	Projectile expansion.....	156
4.2.2.1.8	Maximum temporary cavity location.....	157
4.2.2.1.9	Maximum diameter of the temporary cavity	157
4.2.3	Discussion of .223 Remington Federal Premium® Tactical® Bonded® results .	158
4.2.4	Results from 9mm Luger rounds	163
4.2.4.1	ANOVA results.....	168
4.2.4.1.1	Fissure area	168
4.2.4.1.2	EKE.....	168
4.2.4.1.3	Maximum temporary cavity location.....	170
4.2.4.1.4	Maximum diameter of the temporary cavity	170
4.2.4.1.5	90 ° Yaw	171
4.2.5	Discussion of 9mm Luger results	172
4.3	Part B: Armoured gelatine blocks 250mm in length	177
4.3.1	Materials and methods	177
4.3.1.1	10% gelatine.....	177
4.3.1.2	Body armour	178
4.3.1.3	Ammunition	178
4.3.1.4	Ballistic testing method.....	178
4.3.1.5	Analysis.....	179
4.3.1.6	Kinetic energy deposited and high speed video analysis.....	179
4.3.2	Results from the interactions of .223 Remington Federal Premium® Tactical® Bonded® rounds with 10% gelatine targets 250mm in length	180
4.3.2.1	Order of magnitude	186
4.3.2.2	ANOVA results.....	187
4.3.2.2.1	Neck length	188
4.3.2.2.2	Body length.....	188
4.3.2.2.3	Representation of maximum ellipsoid volume	188
4.3.2.2.4	Fissure area	189
4.3.2.2.5	Kinetic energy deposited.....	190
4.3.2.2.6	Maximum temporary cavity analysis.....	191
4.3.2.2.7	Projectile expansion	192
4.3.3	Discussion of .223 Remington Federal Premium® Tactical® Bonded® results .	193

4.3.4 Results from 9mm Luger rounds	197
4.3.4.1 Order of magnitude	201
4.3.4.2 ANOVA results.....	202
4.3.4.2.1 Fissure area	203
4.3.4.2.2 Kinetic energy	203
4.3.4.2.3 Maximum temporary cavity analysis.....	204
4.3.5 Discussion of 9mm Luger results	205
4.4 Part C: Armoured simulated thoraxes.....	208
4.4.1 Materials and methods	208
4.4.1.1 Porcine samples	208
4.4.1.2 10% gelatine.....	209
4.4.1.3 Ballistic testing method of protected simulated thoraxes	209
4.4.1.4 Analysis.....	212
4.4.2 Results.....	216
4.4.3 Results from .223 Remington Federal Premium® Tactical® Bonded® projectiles	216
4.4.3.1 ANOVA results.....	218
4.4.3.1.1 Distance to projectile	218
4.4.3.1.2 Entry dimensions in anterior thoracic walls.....	219
4.4.3.1.3 Exit dimensions in posterior thoracic walls	220
4.4.4 Discussion of .223 Remington Federal Premium® Tactical® Bonded® results	221
4.4.5 Results from 9mm Luger projectiles.....	223
4.4.5.1 ANOVA results.....	225
4.4.5.1.1 Entry dimensions in anterior thoracic walls.....	225
4.4.5.1.2 Exit dimensions in posterior thoracic walls	226
4.4.6 Discussion of 9mm Luger results	227
4.5 Summary of parts A, B and C of Chapter 4.....	229
4.6 Overall discussion on overmatching UK police armour.....	230
4.6.1 Overmatching using targets of 10 % gelatine blocks 500mm in length	230
4.6.2 Overmatching using targets of 10 % gelatine blocks 250mm in length	231
4.6.3 Overmatching using simulated thoraxes as targets.....	234
Chapter 5 CONCLUSIONS AND SUMMARY.....	236
5.1 Conclusions.....	236
5.1.1 Tissue simulant comparison.....	236
5.1.2 Conclusions from the study of overmatching HG2 protected 10% gelatine blocks 500mm in length with .223 Remington projectiles.....	236

5.1.3 Conclusions from the study of overmatching KR1/SP1 protected 10% gelatine blocks 500mm in length with 9mm Luger projectiles	237
5.1.4 Conclusions from the study of overmatching HG2 protected 10% gelatine blocks 250mm in length with .223 Remington projectiles.....	238
5.1.5 Conclusions from the study of overmatching KR1/SP1 protected 10% gelatine blocks 250mm in length with 9mm Luger projectiles	238
5.1.6 Conclusions from the study of overmatching protected simulated thoraxes	239
5.2 Limitations of this study on the overmatching of UK police armour	239
5.3 Summary	241
5.4 Recommendations.....	242
REFERENCES	243
APPENDIX A – Ballistic calculations	256
APPENDIX B – Gelatine data sheet.....	261
APPENDIX C – Method for the preparation of 10% (by mass) gelatine (32kg block)	262
APPENDIX D – Method for the preparation of 20% (by mass) gelatine (32kg block)	263
APPENDIX E – Explanation of statistical methods used.....	264
APPENDIX F – Depth of penetration raw data.....	274
APPENDIX G – 10% gelatine quality control check	284
APPENDIX H – SEM spectra	287
APPENDIX I – Ethics committee approval letter	290
APPENDIX J – Method for estimation of EKE	291
APPENDIX K – Publications generated from this research.....	295
APPENDIX L – Other publications the author was involved in during this research.....	327
APPENDIX M – Spreadsheets of tracking data collected from high speed videos (CD attachment).....	329

LIST OF FIGURES

CHAPTER 2

Figure 2-1: The calibre of a rifled barrel.....	7
Figure 2-2: Side and base views of an unjacketed (left) and jacketed 9mm bullet (right).	9
Figure 2-3: Side and front view of a (.357) partially-jacketed soft point (left) and a (.44) partially-jacketed hollow point bullet (right).....	10
Figure 2-4: A schematic diagram of drag.	15
Figure 2-5: A 9mm Luger projectile of mass 7.45 g (left) and an SS109 5.56 x 45mm projectile of mass 4 g (right) for which drag will be calculated throughout this section when the various factors are altered	16
Figure 2-6: A schematic diagram showing the forces acting on a non-spin-stabilised projectile.	17
Figure 2-7: A spin stabilised projectile yawing from the stage of precession through to nutation.	18
Figure 2-8: Schematic diagram illustrating the passage of a yawing projectile forming the permanent and temporary cavity. In this example the projectile exits the target backwards. .	22
Figure 2-9: Schematic diagram highlighting the effect of target depth on where yaw occurs (adapted from Vellema and Scholtz (2005)).....	26
Figure 2-10: Molecular arrangement of a para-aramid.....	50
Figure 2-11: Molecular arrangement of polyethylene	50
Figure 2-12: Molecular arrangement of Nylon 6,6.....	51
Figure 2-13: Schematic diagram showing the situation of the internal organs of a human torso. Police body armour must protect the heart (9), lungs (3), liver (5), kidneys (7) and spleen (11).....	55

CHAPTER 3

Figure 3-1: Typical example of the gelatine blocks produced.....	74
Figure 3-2: Moulds used for casting blocks.....	74
Figure 3-3: Roaster oven used for the melting of Perma-Gel™ raw base media	75
Figure 3-4: Example of a Perma-Gel™ block ready for testing	75
Figure 3-5: Sieving system used for the casting of larger Perma-Gel™ blocks.....	75
Figure 3-6: Perma-Gel™ block after being re-melted and cast into larger block.....	76

Figure 3-7: 7.56 x 51mm cartridge case, sabot and 5.5mm BB used for DoP testing.....	77
Figure 3-8: Schematic of the experimental setup for the depth of penetration testing of 5.5mm BBs.	78
Figure 3-9: Enfield Number 3 Proof Housing set up.....	78
Figure 3-10: Target set up complete with a 20% gelatine block	79
Figure 3-11: Penetration depth being measured with the use of a metal rod.....	79
Figure 3-12: Graph of impact velocity vs. DoP for all simulants.....	82
Figure 3-13: Graph showing mean impact velocity vs. mean (and s.d.) DoP for each velocity bin in all four simulants	83
Figure 3-14: Graph showing kinetic energy density vs. mean velocity bins in all four tissue simulants, together with results from the open literature*	84
Figure 3-15: A .223 Remington (62 grain; Federal Premium® Tactical® Bonded®)(left) and a 9mm Luger (124 grain; full metal jacket; DM11 A1B2).....	93
Figure 3-16: A mounted and sectioned .223 Remington Federal Premium® Tactical® Bonded®)(left) and a 9mm Luger, complete with hardness testing locations.	94
Figure 3-17: Gelatine block cut along the length of the tract to assess the permanent cavity damage	98
Figure 3-18: Schematic diagram of the measurements taken of the permanent cavities.....	98
Figure 3-19: Measurement of fissures – length (left) and height measurements (right), with visible debris present highlighted.	99
Figure 3-20: A still image of a typical 9mm Luger temporary cavity where the maximum diameter of the temporary cavity is being measured using the PCC 2.5 software	100
Figure 3-21: A still image of a typical 9mm Luger temporary cavity where the distance to the point of maximum expansion of the temporary cavity is being measured using the PCC 2.5 software.....	100
Figure 3-22: SEM analysis of a .223 Remington Federal Premium® Tactical® Bonded with composition labelled	102
Figure 3-23: SEM analysis of a 9mm Luger with composition labelled	102
Figure 3-24: Stills from high speed footage showing the formation and collapse of a typical temporary cavity produced in 10% gelatine by a .223 Remington Federal Premium® Tactical® Bonded® projectile.	105

Figure 3-25: Stills from high speed footage stills showing the formation and collapse of a typical temporary cavity produced in 20% gelatine by a .223 Remington Federal Premium® Tactical® Bonded® projectile. 106

Figure 3-26: Example of the flash that propagates through a Perma-Gel™ block after impact with by a .223 Remington Federal Premium® Tactical® Bonded® projectile..... 106

Figure 3-27: Stills from high speed footage showing the formation and collapse of a typical temporary cavity produced in 10% gelatine by a 9mm Luger projectile..... 114

Figure 3-28: Stills from high speed footage showing the formation and collapse of a typical temporary cavity produced in 20% gelatine by a 9mm Luger projectile..... 114

Figure 3-29: A front and back view of a typical example of the porcine thoracic wall tested 123

Figure 3-30: A front and back view of a typical example of a set of lungs tested 123

Figure 3-31: Schematic diagram showing the simulated thorax arrangement..... 124

Figure 3-32: View of the typical set up from the front showing the front thoracic wall with the skin facing the muzzle..... 125

Figure 3-33: Typical set up showing the arrangement of the thoracic walls and lungs 125

Figure 3-34: View of the set-up from the rear, with a 10% gelatine block placed adjacent to the porcine samples..... 126

Figure 3-35: Typical example of an entrance (left) and exit (right) shot into the front thoracic wall. These examples are after perforation of .223 Remington Federal Premium® Tactical® Bonded® round..... 127

Figure 3-36: Typical example of an entrance (left) and exit (right) shot into the lung. This damage was caused by a .223 Remington Federal Premium® Tactical® Bonded® round .. 127

Figure 3-37: Typical example of an entrance (left) and exit (right) shot into the back (second) thoracic wall. These examples were caused by a .223 Remington Federal Premium® Tactical® Bonded® round..... 127

Figure 3-38: Typical example of the bone debris seen in lung. This example was after perforation of a .223 Remington Federal Premium® Tactical® Bonded® round 128

Figure 3-39: Example of the lead debris seen in the tract in the lung after the perforation of a .223 Remington Federal Premium® Tactical® Bonded® round 128

Figure 3-40: Typical examples of the of bone fragments recovered during dissection of the thoracic samples..... 129

Figure 3-41: Typical examples of the lead debris recovered during the dissection of the thoracic samples.....	129
--	-----

CHAPTER 4

Figure 4-1: Typical examples of HG2 (Left) and KR1/SP1 body armour panels (right).	142
Figure 4-2: Typical target set up of 10% gelatine block 500mm in length with a body armour panel (HG2) on the front face.	143
Figure 4-3: Typical example of temporary cavity expansion produced by .223 Remington Federal Premium® Tactical® Bonded® projectiles in (top) 10% gelatine blocks 500mm in length and (bottom) armoured 10% gelatine blocks.	149
Figure 4-4: Expansion of .223 Remington Federal Premium® Tactical® Bonded® projectiles after penetration of armoured 500mm long gelatine blocks (left three columns) and after penetration of baseline 10% gelatine blocks (right three columns) from the front (top) and rear.....	150
Figure 4-5: Fibre and fabric debris recovered from all ten .223 Remington Federal Premium® Tactical® Bonded® shots into armoured 10% gelatine blocks 500mm in length	151
Figure 4-6: Typical example of temporary cavity expansion produced by 9mm Luger projectiles in 10% gelatine blocks 500mm in length (top) and armoured 10% gelatine blocks (bottom).....	167
Figure 4-7: 10% gelatine block 250mm in length, cut to size after 5.5mm BB quality control check shot was carried out.	177
Figure 4-8: Typical target set up of HG2 armour panels on the front and back face of a 10% gelatine block 250mm in length.....	179
Figure 4-9: High speed footage stills showing the typical process of a .223 Remington Federal Premium® Tactical® Bonded® projectile (A) entering a 250mm 10% gelatine block protected by HG2 armour on both the front and back face before (B) reaching the rear face and then travelling back through the gelatine block and exiting via the front face.	186
Figure 4-10: A front and back view of a typical example of the porcine thoracic walls tested	209
Figure 4-11: Typical front view of a protected simulated thorax	210
Figure 4-12: Schematic diagram of a protected simulated thorax arrangement.	211
Figure 4-13: Arrangement of the protected simulated thorax.....	211

Figure 4-14: Measurement of a typical exit hole in the anterior thoracic wall caused by .223 Remington Federal Premium® Tactical® Bonded® rounds. Fabric debris visible.212

Figure 4-15: A .223 Remington Federal Premium® Tactical® Bonded® round *in situ* in a posterior thoracic wall.....213

Figure 4-16: A 9mm Luger round recovered from *in situ* within a posterior thoracic wall. 213

Figure 4-17: A .223 Remington Federal Premium® Tactical® Bonded® round recovered from within a posterior thoracic wall during dissection.213

Figure 4-18: A typical permanent cavity complete with debris produced within 10% gelatine block that was situated in between two protected porcine thoracic walls after penetration of a .223 Remington Federal Premium® Tactical® Bonded® round.214

Figure 4-19: Typical fabric debris recovered from protected simulated thoraxes after perforation of 9mm Luger projectiles.214

Figure 4-20: Typical tissue debris recovered from 10% gelatine blocks that was situated in between two protected porcine thoracic walls after penetration of a .223 Remington Federal Premium® Tactical® Bonded® round215

APPENDIX J

Figure J-1: Screenshot displaying the location of the axis for a video of a .223 Remington projectile.291

Figure J-2: (Left) the front location used to track a .223 Remington projectile and (right) the centre of mass location used to track a 9mm Luger projectile.292

Figure J-3: Four columns produced from frame by frame analysis in PCC and the data produced from those columns.293

Figure J0-4: Typical example of a polynomial regression for a .223 Remington projectile that was fired into a block of 10% gelatine.....294

LIST OF TABLES

CHAPTER 2

Table 2-1: A breakdown of the ammunition mentioned in this thesis*	8
Table 2-2: Theories of wounding capability of projectiles on impact	19
Table 2-3: Specific gravities of selected tissues of the human body	24
Table 2-4: Chest depths from different anthropometric studies	41
Table 2-5: The minimum and maximum acceptable penetrations for different impact velocities (Jussila, 2004).....	42
Table 2-6: The advantages and disadvantages of three tissue simulants	44
Table 2-7: Anterior skin-to-organ distances when standing (Bleetman and Dyer, 2000)	56

CHAPTER 3

Table 3-1: Ballistic test variables	77
Table 3-2: Velocity bins used for data analysis	80
Table 3-3: Depth of penetration in 10% gelatine, 20% gelatine and Perma-Gel™	86
Table 3-4: Depth of penetration in 10% and 20% gelatine	87
Table 3-5: Measurements of permanent cavity and why they were taken.	96
Table 3-6: Micro hardness results.....	101
Table 3-7: Measurements collected from interactions of .223 Remington Federal Premium® Tactical® Bonded® with 10% gelatine blocks.....	103
Table 3-8: Measurements collected from interaction of .223 Remington Federal Premium® Tactical® Bonded® projectiles with 20% gelatine blocks.....	104
Table 3-9: Body length after penetration with .223 Remington Federal Premium® Tactical® Bonded® projectiles	107
Table 3-10: Representation of maximum ellipsoid volume after penetration of .223 Remington Federal Premium® Tactical® Bonded® projectiles.....	107
Table 3-11: Fissure area after penetration by .223 Remington Federal Premium® Tactical® Bonded® projectiles	108
Table 3-12: Distances .223 Remington Federal Premium® Tactical® Bonded® projectiles travelled within gelatine blocks	109
Table 3-13: Distance to maximum expansion of temporary cavity caused by .223 Remington Federal Premium® Tactical® Bonded® projectiles in gelatine targets	109

Table 3-14: Maximum diameter of temporary cavity produced by .223 Remington Federal Premium® Tactical® Bonded® projectiles in gelatine targets	110
Table 3-15: Measurements collected from interactions of 9mm Luger projectiles with 10% gelatine blocks	111
Table 3-16: Measurements collected from interactions of 9mm Luger projectiles with 20% gelatine blocks	112
Table 3-17: Fissure area after perforation of 9mm Luger DM11 A1B2 FMJ projectiles.....	115
Table 3-18: Distance to maximum expansion of temporary cavity caused by 9mm Luger projectiles in gelatine targets	115
Table 3-19: Maximum diameter of temporary cavity produced by 9mm Luger projectiles in gelatine targets	116
Table 3-20: Distance to first 90 ° yaw of 9mm Luger projectiles in gelatine targets	117
Table 3-21: Distance to second 90 ° yaw of 9mm Luger projectiles in gelatine targets.....	117
Table 3-22: Distance to third 90 ° yaw of 9mm Luger projectiles in gelatine targets	117
Table 3-23: Thoracic sample details	130
Table 3-24: Shot details – .223 Remington Federal Premium® Tactical® Bonded®	130
Table 3-25: .223 Remington Federal Premium® Tactical® Bonded® strike locations through target	131
Table 3-26: .223 Remington Federal Premium® Tactical® Bonded® entry and exit dimensions	131
Table 3-27: Distance to .223 Remington Federal Premium® Tactical® Bonded® projectiles	132
Table 3-28: Details of location and mass of fragments collected from samples after .223 Remington Federal Premium® Tactical® Bonded® shots	132
Table 3-29: Mass of .223 Remington Federal Premium® Tactical® Bonded® projectiles and fragments collected from 10% gelatine blocks	132
Table 3-30: Distance to .223 Remington Federal Premium® Tactical® Bonded® projectiles	133
Table 3-31: Distance to .223 Remington Federal Premium® Tactical® Bonded® projectiles (non-rib striking shots removed).....	134
Table 3-32: Shot details –9mm Luger DM11 A1B2.....	135
Table 3-33: 9mm Luger strike locations through target	135
Table 3-34: 9mm Luger entry and exit dimensions	136

Table 3-35: Details of location and mass of fragments collected from samples after 9mm Luger shots.....	136
--	-----

CHAPTER 4

Table 4-1: Measurements collected from baseline tests involving .223 Remington Federal Premium® Tactical® Bonded® projectiles and unprotected 10% gelatine blocks 500 mm in length.....	146
Table 4-2: Measurements collected from interactions of .223 Remington Federal Premium® Tactical® Bonded® projectiles with HG2 protected 10% gelatine blocks	147
Table 4-3: Summary of the mean results collected from protected and unprotected 10% gelatine blocks 500mm in length after penetration of .223 Remington Federal Premium® Tactical® Bonded® projectiles	151
Table 4-4: Body length created by .223 Remington Federal Premium® Tactical® Bonded® projectiles.....	152
Table 4-5: Representation of maximum ellipsoid volume after penetration of .223 Remington Federal Premium® Tactical® Bonded® projectiles.....	153
Table 4-6: Fissure area after penetration by .223 Remington Federal Premium® Tactical® Bonded® projectiles	153
Table 4-7: EKE of .223 Remington Federal Premium® Tactical® Bonded® projectiles (EKE calculated using the impact velocity of the projectile striking the gelatine block, calculated using PCC 2.5 software)	155
Table 4-8: EKE of .223 Remington Federal Premium® Tactical® Bonded® projectiles (EKE calculated using the impact velocity of the projectile striking the front armour park, from the Weibel Doppler radar)	155
Table 4-9: Distance to .223 Remington Federal Premium® Tactical® Bonded® projectiles in 10% gelatine 500mm in length	156
Table 4-10: Surface area of .223 Remington Federal Premium® Tactical® Bonded® projectiles after recovery from targets	156
Table 4-11: Distance to the location of the maximum temporary cavity produced by .223 Remington Federal Premium® Tactical® Bonded® projectiles.....	157
Table 4-12: Size of the maximum temporary cavity diameter produced by .223 Remington Federal Premium® Tactical® Bonded® projectiles.....	158

Table 4-13: Measurements collected from interactions of 9mm Luger with 10% gelatine blocks 500mm in length.....	164
Table 4-14: Measurements collected from interactions of 9mm Luger with KR1/SP1 protected 10% gelatine blocks 500mm in length.....	165
Table 4-15: Summary of the mean results collected from protected and unprotected 10% gelatine blocks 500mm in length after perforation of 9mm Luger projectiles	167
Table 4-16: Fissure area after penetration by 9mm Luger projectiles	168
Table 4-17: EKE deposited by 9mm Lugers in 10% gelatine blocks 500mm in length (EKE calculated using the impact velocity of the projectile striking the gelatine block, calculated using PCC 2.5 software)	169
Table 4-18: EKE calculated using the impact velocity of the projectile striking the front armour park, from the Weibel Doppler radar	169
Table 4-19: Distance to the temporary cavity maximum produced by 9mm Luger projectiles	170
Table 4-20: Size of the maximum temporary cavity diameter produced by 9mm Luger projectiles.....	171
Table 4-21: Distance to first 90 ° yaw of 9mm Luger projectiles in gelatine targets	171
Table 4-22: Distance to second 90 ° yaw of 9mm Luger projectiles in gelatine targets	172
Table 4-23: Distance to third 90 ° yaw (when it occurs) of 9mm Luger projectiles in gelatine targets (n = 5).....	172
Table 4-24: Measurements collected from interactions of .223 Remington Federal Premium® Tactical® Bonded® projectiles with 10% gelatine blocks 250mm in length.....	181
Table 4-25: Measurements collected from interactions of .223 Remington Federal Premium® Tactical® Bonded® projectiles with HG2 on the front face of 10% gelatine blocks 250mm in length.....	182
Table 4-26: Measurements collected from interactions of .223 Remington Federal Premium® Tactical® Bonded® projectiles with HG2 on the front and back face of 10% gelatine blocks 250mm in length	183
Table 4-27: Comparison of the summary statistics produced in all three 10% gelatine target types 250mm in length after impact by .223 Remington Federal Premium® Tactical® Bonded® projectiles	187
Table 4-28: Body length created by .223 Remington Federal Premium® Tactical® Bonded® projectiles in 10% gelatine targets 250mm in length.....	188

Table 4-29: Representation of maximum ellipsoid volume produced by .223 Remington Federal Premium® Tactical® Bonded® projectiles in 10% gelatine targets 250mm in length	189
Table 4-30: Fissure area produced in 10% gelatine blocks 250mm in length after penetration by .223 Remington Federal Premium® Tactical® Bonded® projectiles	189
Table 4-31: Kinetic energy deposited in 10% gelatine blocks 250mm in length by .223 Remington Federal Premium® Tactical® Bonded® projectiles	190
Table 4-32: Distance to the location of the maximum temporary cavity in 10% gelatine blocks 250mm in length produced by .223 Remington Federal Premium® Tactical® Bonded® projectiles	191
Table 4-33: Size of the maximum temporary cavity diameter produced in 10% gelatine blocks 250mm in length by .223 Remington Federal Premium® Tactical® Bonded® projectiles	192
Table 4-34: Expansion of .223 Remington Federal Premium® Tactical® Bonded® projectiles after striking the target	193
Table 4-35: Measurements collected from interactions of 9mm Luger with 10% gelatine blocks 250mm in length.....	197
Table 4-36: Measurements collected from interactions of 9mm Luger with KR1/SP1 body armour panels on the front face of 10% gelatine blocks 250mm in length	198
Table 4-37: Measurements collected from interactions of 9mm Luger with KR1/SP1 body armour panels on the front and back face of 10% gelatine blocks 250mm in length	200
Table 4-38: Comparison of the summary statistics produced in all three 10% gelatine target types 250mm in length after impact by 9mm Lugers	202
Table 4-39: Fissure area in 10% gelatine blocks 250mm in length after penetration by 9mm Luger projectiles	203
Table 4-40: Kinetic energy deposited by 9mm Lugers in 10% gelatine blocks 250mm in length.....	204
Table 4-41: Distance to the temporary cavity maximum in 10% gelatine blocks 250mm in length produced by 9mm Luger projectiles	205
Table 4-42: Size of the maximum temporary cavity diameter produced in 10% gelatine blocks by 9mm Luger projectiles.....	205
Table 4-43: Thoracic sample details	216
Table 4-44: .223 Remington Federal Premium® Tactical® Bonded® shot details	216

Table 4-45: .223 Remington Federal Premium® Tactical® Bonded® strike location through target	217
Table 4-46: .223 Remington Federal Premium® Tactical® Bonded® entry and exit dimensions	217
Table 4-47: Distance to .223 Remington Federal Premium® Tactical® Bonded® projectiles	217
Table 4-48: Mass of .223 Remington Federal Premium® Tactical® Bonded® projectiles and fragments collected from 10% gelatine blocks	218
Table 4-49: Details of location and mass of fragments collected from porcine samples after perforation by .223 Remington Federal Premium® Tactical® Bonded® projectiles	218
Table 4-50: Distance to .223 Remington Federal Premium® Tactical® Bonded® projectiles after penetration of simulated thorax	219
Table 4-51: Anterior thoracic wall entry widths after penetration by .223 Remington Federal Premium® Tactical® Bonded® projectiles	220
Table 4-52: Anterior thoracic wall entry heights after penetration by .223 Remington Federal Premium® Tactical® Bonded® projectiles	220
Table 4-53: 9mm Luger DM11 A1B2 shot details	223
Table 4-54: 9mm Luger strike location through target	224
Table 4-55: 9mm Luger entry and exit dimensions	224
Table 4-56: Distance to 9mm Luger projectiles	224
Table 4-57: Mass of 9mm Luger projectiles and fragments collected from 10% gelatine blocks	225
Table 4-58: Details of location and mass of fragments collected from porcine samples after 9mm Luger shots.....	225
Table 4-59: Anterior thoracic wall entry widths after penetration by 9mm Luger projectiles	226
Table 4-60: Anterior thoracic wall entry heights after penetration by 9mm Luger projectiles	226
Table 4-61: Posterior thoracic wall exit widths after penetration by 9mm Luger projectiles	227
Table 4-62: Posterior thoracic wall exit heights after penetration by 9mm Luger projectiles	227

APPENDIX A

Table A-1: Ballistic table of a 9mm Luger parabellum (Ness and Williams, 2013)257

Table A-2: Ballistic table of a .223 Remington SS109 (Ness and Williams, 2013).....258

NOMENCLATURE

General glossary

<i>Areal density</i>	Mass per unit area, measured in kilograms per square metre (Denton and Daniels, 2002).
<i>Ammunition</i>	“(A round of ammunition) refers to a single, live, unfired, cartridge comprising the missile, cartridge case, propellant and some form of primer” (Heard, 2008, p. 48).
<i>Bloom strength/jelly strength</i>	(gel) The force, expressed in grams, necessary to depress the surface of a gelatine gel with a concentration of 6.67% w/w by 4mm with a standard plunger (12.5mm diameter) (Rousselot, 2014).
<i>Blue-on-blue</i>	“Relating to an attack in which soldiers, etc. are injured or killed by their own army or by soldiers on the same side as them” (Walter, 2008).
<i>Body armour</i>	Protective clothing “designed to protect the wearer against a range threats” (Tobin and Iremonger, 2006, p. 15).
<i>Calibre</i>	Diameter of the bore of a weapon, measured across the lands of the rifling (Greenwood <i>et al.</i> , 1987).
<i>Cannelure</i>	A groove or fluting around the cylindrical part of a bullet (Di Maio, 1999, p.22)
<i>Cavitation</i>	“The formation of cavities in something” (Allen, 2000, p. 220).
<i>Cavity</i>	“An empty or hollowed-out space within a mass” (Allen, 2000, p. 220).
<i>Centre of pressure</i>	“Point through which aerodynamic force can be regarded as acting” (Greenwood <i>et al.</i> , 1987, p. 451).

<i>Ergonomics</i>	“A science concerned with the relationship between human beings, the machines and equipment they use, and the working environment” (Allen, 2000, p. 471).
<i>Gel strength/jelly strength</i>	See Bloom.
<i>Gelatine</i>	“A virtually colourless and tasteless water-soluble protein prepared from collagen” (Pearsall, 1999, p. 588).
<i>Groove</i>	See Rifling.
<i>Handgun</i>	“Short-range weapons, such as revolvers and pistols, capable of being fired when held in one or both hands” (Allsop and Toomey, 1999, p. 284).
<i>Inertia</i>	“A property of matter by which it remains at rest or in uniform motion in the same straight line unless acted on by some external force” (Allen, 2000, p. 717).
<i>Land</i>	“Highpoints left in the barrel after cutting the rifling” (See Rifling) (Hornick <i>et al.</i> , 2008, p. 88)
<i>Overmatch</i>	“To be more than a match for, exceed or defeat” (Allen, 2000, p. 995).
<i>Penetrating</i>	“Having the power of entering, piercing or pervading” (Allen, 2000, p. 1028).
<i>Penetration</i>	“The act or an instance of penetrating” (Allen, 2000, p. 1028).
<i>Perforation</i>	“To make a hole through (something)” (Allen, 2000, p 1033).

<i>Perma-Gel™</i>	A clear synthetic material developed specifically as a soft tissue for the testing and comparison of different projectile types (Amick, 2006).
<i>Permanent cavity</i>	Void left after temporary cavity has collapsed following initial penetration (Janzon <i>et al.</i> , 1997).
<i>Rifle</i>	“Long barrelled weapon designed to be effective at long range, used for accurate shooting to 600 m or more” (Allsop and Toomey, 1999, p.288).
<i>Rifling</i>	“Spiral grooves that are cut the length of the interior or bore of barrel. Rifling consists of these grooves and the metal left between the grooves – the lands” (Di Maio, 1999, p.13).
<i>Sectional density</i>	“The ratio of mass to cross-sectional area A. The cross-sectional area equates to that of the projection of the bullet onto a plane perpendicular to the direction of movement” (Kneubuehl <i>et al.</i> , 2011, p. 65).
<i>Soft body armour</i>	Armour which is relatively soft, flexible and comprises multiple layers of fabrics (Chen and Chaudhry, 2005).
<i>Shock wave</i>	“A region across which there is a rapid pressure, temperature, and density rise, usually caused by a body moving supersonically in a gas or by a detonation” (Bresin, 2011, p 1292).
<i>Stability</i>	“The property of a body to recover equilibrium after being disturbed” (Allen, 2000, p 1363).
<i>Temporary cavity</i>	“When a projectile moves through a liquid or medium with similar properties, the material is accelerated away from the path of the projectile by high pressures created around its path” (Janzon, 1997, p. 27).
<i>Tukey’s HSD multiple comparison test</i>	A test or post hoc test performed after ANOVA has shown the null hypothesis has been rejected, which helps to determine the pattern of

significant differences among the means. Each mean in the rejected null hypothesis is compared to every other mean (Coolidge, 2006).

Yaw

“The deviation of a projectile in its longitudinal axis from the straight line of flight” (Belkin, 1979, p. 15).

Medical glossary

<i>Cellulitis</i>	“Inflammation of the connective tissue between adjacent tissues and organs. Commonly due to bacterial infection by streptococci” (Martin, 1996, p. 109).
<i>Contaminate</i>	“Make impure by exposure to or addition of a poisonous or polluting substance” (Pearsall, 1999, p. 306).
<i>Contusion</i>	“A region of injured tissue or skin in which blood capillaries have been ruptured; a bruise” (Pearsall, 1999, p. 310).
<i>Devitalise</i>	“To deprive of life, vigour, or effectiveness” (Allen, 2000, p. 581).
<i>Gas gangrene</i>	“Death and decay of wound tissue infected by the soil bacterium <i>clostridium perfringens</i> . Toxins produced by the bacterium cause putrefactive decay of connective tissue with the generation of gas” (Martin, 1996, p. 265).
<i>Haemorrhage</i>	“The escape of blood from a ruptured blood vessel, externally or internally” (Martin, 1996, p. 291).
<i>Infection</i>	“Invasion of the body by harmful organisms (pathogens), such as bacteria, fungi, protozoa, rickettsia, or viruses” (Martin, 1996, p. 335).
<i>Inoculation</i>	“The process by which infective material is brought into the system through a small wound in the skin or in a mucous membrane” (Thomson, 1981, p. 485).
<i>Inoculum</i>	“Any material that is used for inoculation” (Martin, 1996, p. 338).

<i>Myocyte</i>	“A muscle cell” (Martin, 1996, p. 430).
<i>Pericardium</i>	“The membrane surrounding the heart, consisting of two portions. The outer <i>fibrous pericardium</i> completely encloses the heart and is attached to the large blood vessels emerging from the heart. The internal <i>serous pericardium</i> is a closed sac of serous membrane” (Martin, 1996, p. 496).
<i>Pleura</i>	“The covering of the lungs (<i>visceral pleura</i>) and of the inner surface of the chest wall (<i>parietal pleura</i>)” (Martin, 1996, p. 517).
<i>Septicaemia</i>	“Widespread destruction of tissues due to absorption of disease-causing bacteria to absorption or their toxins from the bloodstream” (Martin, 1996, p. 597).

Abbreviations

AKE	ARRADCOM Kinetic Energy
ANOVA	analysis of variance
CAST	Centre for Applied Science and Technology
CNS	central nervous system
CV	coefficient of variation
d.f.	degrees of freedom
DoP	depth of penetration
EDX	energy dispersive x-ray
EKE	expected kinetic energy
F	F statistic
FMJ	full metal jacket
FMJTC	full metal jacket truncated cone
FPS	feet per second
fps	frames per second
FSP	fragment simulating projectile
GPMG	general purpose machine gun
HOSDB	Home Office Scientific Development Branch
HP	hollow point
Hv	Hardness Vickers
JHP	jacketed hollow point
L_p	penetration
MS	mean squared
N	number of replicates
NATO	North Atlantic Treaty Organisation
P	probability
PG	Perma-Gel TM
s.d.	standard deviation
SEM	scanning electron microscope
SJHP	semi-jacketed hollow point
SLR	self-loading rifle
ss	sum of squares
TM	Trademark

Variables and constants

ρ	density; kg/m ³
A	cross-sectional area; m ²
C _B	ballistic coefficient; kg/m ²
C _D	drag coefficient; dimensionless
d	diameter; m
F _D	drag force; N
h	height; mm
I	form factor; dimensionless
I	moment of inertia; kgm ²
KE	kinetic energy; J
l	length; mm
M	mass; kg
P	momentum; kgm/s
P _i	probability of a projectile being within body tissue at depth i
P _w	power theory (DeMuth, 1968); kg m ³ /s ³
R	retardation; m/s ²
S	distance; m
SD	sectional density; kg/m ²
SG	specific gravity; dimensionless
V	velocity; m/s
V ₁	starting velocity; m/s
V ₂	velocity at distance further along than V ₁ ; m/s
V _i	impact velocity; m/s
V _I	velocity of a projectile at depth I; m/s
W	angular velocity; rad/s
w	width; mm

Chapter 1 : INTRODUCTION

Numerous studies carried out on body armour have demonstrated that it is capable of protecting the wearer from a range of threats (e.g. Horsfall, 2000; Bleetman *et al.*, 2003; Carr *et al.*, 2012; Sakaguchi *et al.*, 2012). Threats such as blunt objects, knives, fragments, low velocity projectiles and high velocity projectiles can be nullified by body armour, as long as the level of protection matches the threat. But what happens when it doesn't? To overmatch is defined as "to match with a superior opponent" (Allen, 2000, p. 995). What happens when the threat is greater than the level of protection available and the armour is overmatched?

Research has shown that fabric armour systems can protect a wearer against fragmentation and low velocity bullets (e.g. Croft and Longhurst, 2007b; Hewins, 2010; Carr *et al.*, 2012; Pinto *et al.*, 2012). It is also accepted that the use of hard plates is required in order to stop perforation from high velocity bullets, as soft armours are ineffective against high velocity ammunition (Tobin and Iremonger, 2006). However, does this indicate that soft armours are simply ineffective against this threat, or do they make the situation worse by exacerbating the resulting wounds if the soft body armour is overmatched?

The interaction between perforating ammunition and soft body armour is an area that is not well understood. There is a paucity of studies in the peer-reviewed open source literature that investigate wounding behind soft armour caused by overmatching. In addition, the evidence presented by these studies is contradictory. It has been suggested that the specific body armour worn may not aid protection; rather it could exacerbate the wounding (Missliwetz *et al.*, 1995). Others have dismissed this, claiming that body armour does not affect the resultant wounds negatively, instead claiming it has a positive influence (Lanthier *et al.*, 2004). Further research in this area has been called for (Prather, 1994; Knudsen and Sørensen, 1997).

Direct comparisons of results from the previous research is problematic as each investigation has used different materials (different soft body armours, varying numbers of soft fabric layers, various types of ammunition as well as no or different simulants). However, this problem reflects issues likely to be faced in real life situations; great diversity exists in ammunition and body armour, and no two targets are going to be identical, nor struck in the same precise location under comparable conditions. This is one of the significant issues in addressing the issue of overmatching: every case is going to be unique and distinctive based on a number of factors.

Understanding the interaction that occurs between the ammunition and the soft armour during the perforation stage of an overmatched attack could be key. Possibilities include but are not limited to: causing an earlier transfer of energy to the target; initiating or increasing the level of yaw (including yawing-in-tissue) of the projectile; breaking up the projectile into smaller fragments; causing the projectile to deform; or a combination of the aforementioned possibilities. Developing a greater understanding of this interaction may help predict what may happen when certain ammunition types come up against specific armour types.

1.1 Relevance of the subject

This thesis is concerned with possible overmatching of police body armour. The risk to UK police officers has not necessarily changed over the history of law enforcement, but with technology improving, the threat constantly alters. Police officers in the UK routinely wear body armour designed to protect them against potential identified threats (Tobin and Iremonger, 2006). The body armour they wear is procured against a suite of standards issued by the Home Office's Centre for Applied Science and Technology (CAST) (Croft and Longhurst, 2007a; Croft and Longhurst, 2007b; Croft and Longhurst, 2007c).

For the year up to March 2014, 7,709 offences that involved firearms¹ (4,842 excluding air weapons) were recorded by police in England and Wales. Handguns were used in 2,130 cases (27.6%) - the most commonly used firearm after air weapons – while rifles were used 54 times (0.7%). Of the total firearms offences recorded, 1,426 caused injury (261 (18.3%) by handguns; 6 (0.4%) by rifles), 29 of which resulted in fatalities (18 (62.1%) by handgun, 1 (3.5% by rifle). Five of the recorded injuries were to on duty police officers, with no fatalities recorded, however since March 2003, five Police Officers have suffered fatal injuries from offences involving firearms (Office for National Statistics, 2015).

As well as the figures for firearm incidents in the UK, examples such as the 7th July 2005 co-ordinated attacks on London and the murder of Fusilier Lee Rigby on the 22nd May 2013 should be considered. These attacks, together with the UK's involvement in campaigns such as Iraq and Afghanistan, demonstrate that the UK is still vulnerable to extremist and terrorist attacks. This was highlighted further by the UK raising its terror threat level from substantial to severe (the second highest threat level possible) on 29th August 2014 (Home Office and May, 2014). Although there was a drop of 5% in firearms incidents from 2012/2013

¹ The term firearm in this statistic covers firearms that use controlled explosions to fire a projectile, imitation firearms and air weapons; as stated by the Firearms Act 1968.

to 2013/2014, and with firearm cases in 2013/2014 only accounting for 0.2% of the total recorded crime (Office for National Statistics, 2015), it is still necessary to anticipate that ballistic attacks could be carried out; attacks that could put patrolling police officers wearing body armour against an overmatched threat.

With that said, UK firearms officers are more probable targets of high velocity attacks than patrolling officers. Although the level of protection they wear is greater than that of a patrolling police officer, certain areas of a firearm officer's body will have only soft armour coverage. In addition, firearms officers themselves are equipped with high velocity weapons and ammunition. Therefore, they are at greater risk of encountering overmatching during potential attacks, or even in blue-on-blue incidents (so called 'friendly fire').

1.2 Aim and outline of the study

The aims of the research, each of which constitute a contribution to knowledge in this broad area, were to:

- ❖ Establish which tissue simulant would be best suited for research into overmatching; 10% gelatine, 20% gelatine and Perma-Gel™ were compared.
- ❖ Justify and establish a procedure for measuring post firing damage to the simulants so as to compare the effects of armour.
- ❖ Investigate the effects of overmatching HG2 armour (designed to protect against handguns) against the threat of rifle ammunition.
- ❖ Investigate the effects of overmatching KR1/SP1 (knife and spike resistant armour) against the threat of handgun ammunition.
- ❖ Analyse the effects of different target sizes with reference to anthropometric data.
- ❖ Compare the effects of having the same armour pack present on the rear face of the target as well as the front.
- ❖ Compare how damage to both protected and unprotected simulants fared against damage produced in a protected and unprotected simulated thoraxes (utilising porcine samples).

An initial study was conducted to establish which tissue simulant would be best suited for this research; 10% gelatine, 20% gelatine and Perma-Gel™ were compared. While

comparing these tissue simulants, a method was produced for measuring the damage that was caused, enabling the damage inflicted to different targets to be compared.

Once a tissue simulant had been chosen, trials were conducted to investigate the interactions of varying levels of UK police body armour (including baseline tests without armour) with specific ammunition types of interest to the UK Home Office. Body armour and ammunition choices were established through discussions with The Home Office Centre for Applied Science and Technology (CAST) who supported this work. Impact events were recorded using high-speed video, and post-failure analysis of body armour and simulants was completed before statistical analysis and comparisons were carried out. As the study continued, target types were altered so as to investigate the most torso like target, as this is the area that is protected by the body armour.

1.3 Structure of the thesis

After setting the scene for this research in Chapter One; Chapter Two is a literature review that covers the topics of importance for this project, namely: ammunition, wound ballistics, tissue simulants and body armour. An in-depth critical review of the previous studies carried out into the overmatching of soft armour is also included.

Chapter Three goes into further detail regarding tissue simulants discussed in the literature review section, and describes the process of testing three different materials and determining which simulant to use for the remainder of the study. Work involving the use of porcine thoracic samples to mimic a thorax for ballistic testing is also discussed in Chapter Three.

Chapter Four presents and discusses three trials that overmatched two types of UK police body armour (namely HG2 and KR1/SP1). The chapter is split into three parts, covering different target arrangements. Part A investigates the presence of these two armour types in front of 10% gelatine blocks 500mm in length, while Part B considers the role of armour that is overmatched both in front of and behind 10% gelatine blocks 250mm in length. Finally, based on the work that used porcine thoracic samples in Chapter Three, the effect of adding armour panels on the front and back face of these targets is investigated in Part C. The three overmatching trials of Chapter Four are brought together in a discussion at the end of the Chapter.

The thesis is brought to a close in Chapter Five, with the conclusions from the entire thesis presented, prior to the limitations of the study being discussed. The Chapter is completed with a final summary and recommendations for future work.

Chapter 2 : LITERATURE REVIEW

Four main topics will be discussed in this chapter: ammunition, wound ballistics, tissue simulants and body armour. This is followed by an in depth critical review of the previous studies into the overmatching of body armour.

2.1 Ammunition

A round of ammunition refers to a single, live, unfired cartridge, with a round of small arms ammunition comprising of four basic component parts: the cartridge case, the primer, the propellant and the projectile (Heard, 2008). Extensive discussion of all of these component parts is outside the scope of this thesis; however, ammunition nomenclature and projectiles will be covered.

2.1.1 Cartridge case nomenclature

Several systems of naming cartridges have been devised (NRA, 1970). The calibre of a weapon is the diameter of the internal surfaces of the barrel; the width of the bore. In a rifled barrel (a barrel with helical grooves), the calibre is the diameter of the bore, measured across the lands of the rifling (Greenwood *et al.*, 1987) (Figure 2-1). This forms the basis of cartridge nomenclature, though calibre designations may not be precise and exceptions exist (NRA, 1970; Heard, 2008).

Whether a cartridge is in imperial or metric measurements will generally indicate its origin (British/American or European), although a number of cartridges are identified by both metric and imperial systems. Cartridges in inches, with the zero removed from in front of the decimal point, are typically of British/American origin, e.g. .32" – a cartridge with a bullet 0.32" in diameter (Heard, 2008). The inclusion of a relative case length may also be given when more than one case length exists e.g. .32 short, .32 long (NRA, 1970). For European cartridges, measurements are in millimetres, e.g. 9mm. This can be followed with the length (in millimetres) of the cartridge case (e.g. 9mm Luger), or with a name (also known as the 9mm Parabellum), helping to distinguish among cartridges of the same calibre (Heard, 2008). In certain cases, more information is required to differentiate between ammunition, e.g. 5.56 x 45mm (M193) compared with the 5.56 x 45mm (NATO) (Allsop and Toomey, 1999), the latter being the NATO standard 62 grain round, the former the US developed 55 grain round.

The table below documents ammunition that will be mentioned in this thesis (Table 2-1). The sources from which they are mentioned cover The Home Office CAST's ballistic test standard (Croft and Longhurst, 2007b), ammunition that is of interest to CAST, and ammunition that has been used in previous studies of overmatching armour.

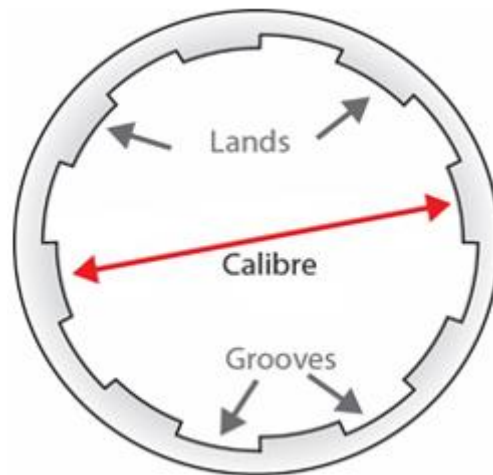


Figure 2-1: The calibre of a rifled barrel.

Table 2-1: A breakdown of the ammunition mentioned in this thesis*

Ammunition name and details	Synonyms	Armament examples	Typical bullet construction	Bullet mass (g)	Muzzle velocity (m/s)	Muzzle energy (J)
9mm Luger DM11 A1B2	9mm Parabellum; 9mm Luger; 9mm Patrone 08	Pistols marked '9 x 19' or other synonym. Predominant sub-machine gun cartridge throughout the world	Lead-core, steel jacketed with a gilding metal envelope.	8.00	396	627
.357 Magnum	.357 Smith & Wesson Magnum; 9.1 x 33 R.	Revolvers	Soft point flat nose lead core with a gilding metal partial jacket.	10.23	453	1011
5.45 x 39mm	5.45 M74; 5.45 Russian; 545 Kalashnikov	AK-74 series rifles and sub carbines, AK 107 and RPK-74.	Mild steel core with a 3mm lead plug in front and a hollow space at the tip, gilding metal jacket (7N6 type).	3.44	900	1417
5.56 x 45mm SS109	5.56 NATO; .223 Remington; 5.56 International	M16, M4 Carbine SCAR and SA80.	Lead-antimony core with a steel tip in a gilding metal jacket.	4.00	930 (from a 508mm barrel – M16)	1708
5.56 x 45 Federal Premium® Tactical® Bonded®	.223 Remington	As above	Open tip match lead core with a gilding metal jacket.	4.02	930	1736
7.62 x 39mm	7.62mm M43; 7.62 x 39 Soviet; 7.62 Kalashnikov	Includes but is not exclusive to: AK-47, AKM, M60, M62 and the PMK.	Mild steel core with a gilding-metal clad-steel jacket.	7.75-8.05	710-725	~ 2030
7.62 x 51mm	7.62 NATO; 7.62 International; .308 Winchester	FN FAL, H&K G3, M14 rifles and FN MAG, MG3 and M60 machine guns.	Lead-antimony core with a gilding metal jacket.	9.46-9.65	838-854	~ 3400

*Data and information in the table gathered with the aid of IHS Jane's weapons: Ammunition (Ness and Williams, 2013) and Ammunition – small arms, grenades and projected munitions (Hogg, 1998).

2.1.2 Projectile

The projectile, or bullet, is the part of the ammunition that leaves the muzzle of the firearm when fired (Di Maio, 1999). Originally a bullet was a lead sphere (e.g. musket balls); modern ammunition comes in a variety of bullet profiles, materials and construction to cater to a vast range of uses (Heard, 2008). Covering all varieties is beyond the scope of this research; however, some basic types of importance to this thesis will be discussed.

Small arms ammunition generally falls into two categories:unjacketed and jacketed (Figure 2-2). Unjacketed bullets can be made from a range of materials (predominantly metals), lead is by far the most common (Heard, 2008). A widespread metal that is cast easily, lead is an ideal material for projectile manufacture (Schwoeble and Exline, 2000). That said, lead projectiles are commonly alloyed with antimony and tin to increase hardness and thus penetration ability (Hornick *et al.*, 2008). Steel is also used.

Lead or steel cores, covered by a layer of harder material are known as jacketed bullets (Heard, 2008). The material can be constructed from gilding metal (copper and zinc), gilding metal-clad steel, cupro-nickel (copper and nickel), or aluminium (Di Maio, 1999). Jacketed bullets can come in the form of a full metal-jacket (FMJ) or a partially metal-jacket. The jackets used on FMJs typically encompass the bullet from the tip down to the base, leaving part of the core at the base exposed. As a result FMJs tend not to deform greatly during impact through soft tissues, often resulting in the complete perforation of targets. Partially jacketed bullets are typically jacketed from the base up, with part of the core left exposed (unjacketed) at the tip. This design encourages the expansion of bullets on impact, resulting in greater kinetic energy being deposited as well as penetration depths shorter than those typical for FMJ projectiles (Dodd, 2006; Hornick *et al.*, 2008).

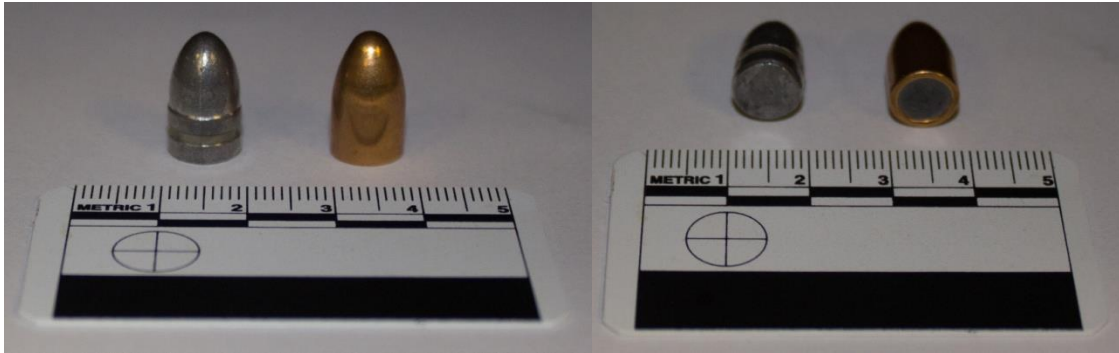


Figure 2-2: Side and base views of an unjacketed (left) and jacketed 9mm bullet (right).

2.1.2.1 Expanding projectiles

The aim of expanding projectiles is to create a large volume of tissue damage early in the target while depositing as much energy as possible. This is done by the projectile expanding to typically more than double its original diameter, causing it to slow due to greater resistance from the increased surface area (Hornick *et al.*, 2008). Two common types of expanding ammunition are hollow point and soft point (Figure 2-3). A hollow point bullet has an opening in the nose, while a soft point has an exposed tip (Haag and Haag, 2011). Due to aforementioned greater expansion, hollow points will penetrate tissue to lesser depths when compared to a FMJ bullet. This results in expanding bullets typically transferring more energy to a target too. Rapid expansion of a soft point round can produce wounds of up to twice the size of the projectile's original diameter (Byers *et al.*, 2005). Dum-dums are also an expanding type of ammunition. Constructed by trimming back the metal jacket to expose the lead core and placing a short metal tube into the nose of the bullet, dum-dums are designed to expand rapidly on impact. Although the 1899 Hague Convention outlawed this ammunition being used in warfare, the Convention is not applicable to civilian applications and police forces are not restricted from using this type of ammunition (Heard, 2008). Often, expanding ammunition is safer to use in an urban environment as it is less likely to perforate a target and hit someone else, thus controlling 'collateral damage' (Hornick *et al.*, 2008).

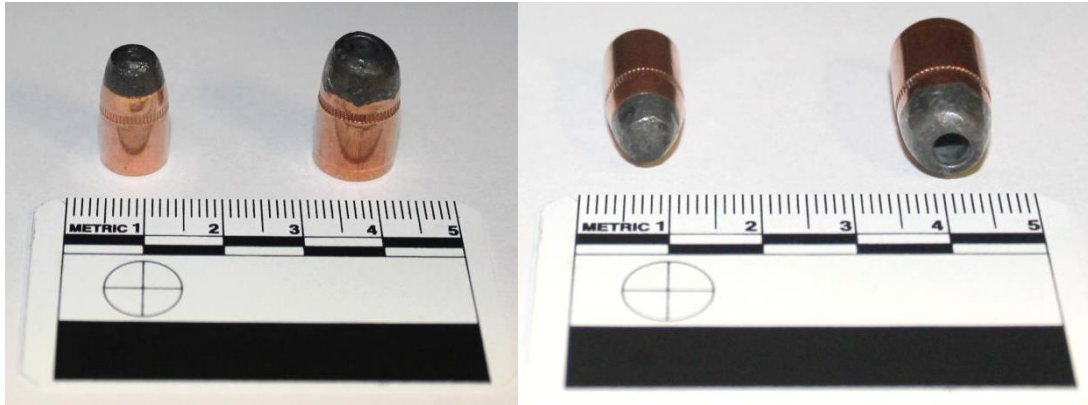


Figure 2-3: Side and front view of a (.357) partially-jacketed soft point (left) and a (.44) partially-jacketed hollow point bullet (right).

2.1.2.2 Fragmenting projectiles

Some types of ammunition have a tendency to fragment during an impact event/penetration of a target. Potential causes have been hypothesised to be due to the jacket of the bullet lacking the strength to cope with the high impact, causing the bullet to break at the cannelure. An alternative idea suggests the combination of high velocity (over 800m/s) and relatively large mass predisposes the bullet to fragment (Hiss and Kahana, 2000). Fragmenting and expanding ammunition will be discussed further in the wounding section of this literature review (*2.2.3.4 Bullet expansion and fragmentation*).

2.1.2.3 Projectile velocity

The definition of low and high velocity projectiles varies among sources. Fackler (1996b) states that in the UK, the boundary between low and high velocity is commonly referred to as 335m/s, the speed of sound in air. Contradictory to that, Tobin and Iremonger (2006) claim 500m/s has been quoted as the upper limit of ‘low velocity’, however, state the term has no formal definition. American researchers also fail to make the definition clear, with researchers quoting three varying limits; 610m/s, 762m/s, and 914m/s. To overcome this issue Fackler (1996b) proposed that velocity should be expressed in either numbers or a numerical velocity range.

Due to the lack of clarity in defining projectile velocity, work carried out in this thesis involving projectiles will either use the terms ‘handgun’ and ‘rifle’, or specific velocities expressed in numbers.

2.1.3 Summary

A small arms weapon uses a round of ammunition to fire a projectile, with the intention of striking, and in most cases causing damage to, a target. Many forms of small arms, and indeed ammunition, exist, producing a vast range of effects at the target. When a target is protected from ballistic threat, the projectile must overcome this protection in order to cause damage. This will depend on a number of variables; how the projectile reaches the target will depend on the forward motion and energy imparted into it overcoming resistant forces over the muzzle-to-target distance. Its effect on the target will vary with factors that include but are not limited to: size, shape, mass, velocity, aerodynamic forces, distance and material density of the target and any other materials (i.e. body armour) it must travel through to reach the intended target. The majority of these influences will be addressed in the next section of this literature review, wound ballistics.

2.2 Wound ballistics

A term allegedly first coined by Callender and French (Callender and French, 1935, cited by Bowyer *et al.*, 1997a), wound ballistics is the study of a projectile's effect on living tissue (Heard, 2008). Studies of wounds caused by projectiles had been carried out long before however, with John Hunter describing wounds caused by musket balls as early as 1792 (Payne, 1997).

Although wound ballistics is not a new area of research, it is a complex subject that is not completely understood (DeMuth, 1966; DeMuth, 1968; Adams, 1982). This is perhaps not surprising as a wide range of wounds and wound severities can be produced by a projectile. Variables include: shape, size, mass, velocity and available kinetic energy of the projectile, together with the variable physical and mechanical characteristics of the living target; all having an effect on the damage that is produced (Ryan *et al.*, 1997; Hiss and Kahana, 2000). Developments over time, not only in weapons and warfare methods, but also medical developments and treatment techniques, have played a role as well (Bowyer *et al.*, 1997a).

That said, knowing the basic concepts and certain properties of the moving projectile can aid in a better understanding of wound production (DeMuth, 1966; DeMuth, 1968). Barach (1986) states these critical properties include: impact velocity, energy release rate, yawing, retardation effects, bullet design and shape, target density and cavitation.

This section will discuss the scientific principles that explain how a projectile reaches a target; the theories proposed to explain what happens when a projectile strikes living tissue and the wounding mechanisms that are involved. This project is focused on projectiles defeating armour and penetrating or perforating the wearer; as a result, discussion of non-penetrating injuries will not be covered.

2.2.1 External ballistics

Before a projectile can inflict damage to an object, it must first reach the target. When a weapon is fired, the pressure created by the ignited propellant imparts energy into the projectile, driving it along the barrel of the weapon. External ballistics is the study of a projectile after it leaves the barrel. Below, a brief section on external ballistics will cover

the fundamentals which are important for terminal or wound ballistics; however, an in-depth review on external ballistics is outside the scope of this research.

2.2.1.1 Ballistic coefficient

Defined as “A numerical measurement that expresses a projectile’s efficacy to overcome air resistance” (Morris, 1992, p. 212), the ballistic coefficient is not as fundamental in external ballistics as it once was. Prior to WWII developments in: wind tunnels; free-flight spark photography; and high-speed electronic computers, calculating the drag coefficient of a single long range trajectory was only possible for a few projectile types, due to the labour and time of manual computation involved (McCoy, 2012). However, having this information for several standard reference projectiles meant trajectories for new projectiles could be calculated using a form factor, relating the unknown projectile’s form to one of the known reference standards, by means of differential corrections. The use of a ballistic coefficient, C_B , reduced a process that would have taken several weeks to a matter of days (DeMuth, 1969; McCoy, 2012):

$$C_B = \frac{SD}{I}, \quad (2.1)$$

where SD is the sectional density and I is a form factor dependant on the nose configuration of the projectile. The form factor is calculated using the known drag coefficient of standard projectiles. The ratio of a projectile’s mass to its cross-sectional area is described as sectional density:

$$SD = \frac{M}{A}, \quad (2.2)$$

where M is mass in kilograms (kg) and A is the cross-sectional area in square metres (m^2), giving the sectional density in kg/m^2 . Substituting equation 2.2 into 2.1 gives:

$$C_B = \frac{M}{IA}. \quad (2.3)$$

If a projectile's cross-sectional area is assumed to be circular:

$$A_{Circle} = \frac{\pi d^2}{4}, \quad (2.4)$$

then:

$$C_B = \frac{4M}{I\pi d^2}. \quad (2.5)$$

However, this is not the ballistic coefficient equation that is widely accepted, as Barach *et al.* (1986) presents:

$$C_B = \frac{M}{I d^2}. \quad (2.6)$$

The difference between eq. 2.5 and eq. 2.6 is a factor of $4/\pi$ and it is unclear what area is being used in eq. 2.6. As there is no explanation as to the shape of the object being assumed (and consequently why there is a lack of $4/\pi$ in eq. 2.5), it is reasonable not to use eq. 2.6. Further, technological developments have meant that calculating the drag coefficient of a specific projectile no longer takes several weeks, and with the correct equipment is more achievable. Since the drag coefficient can be calculated, and is a more direct description of how a projectile is affected by drag, ballistic coefficient will no longer be discussed.

2.2.1.2 Drag force and drag coefficient

Drag force opposes the forward motion of the projectile (Belkin, 1979) (Figure 2-4).

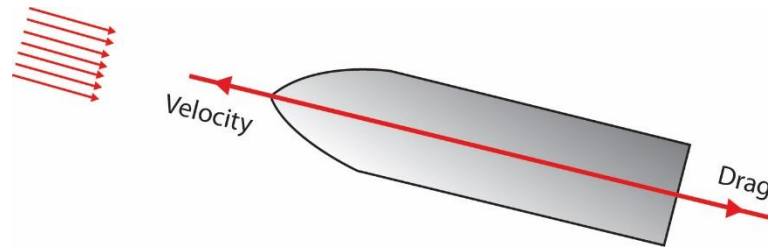


Figure 2-4: A schematic diagram of drag.

Drag force, F_D , is (McCoy, 2012):

$$F_D = \frac{1}{2} \rho V^2 A C_D, \quad (2.7)$$

where ρ is the density of air (1.2 kg/m^3), V is the projectile's mean velocity (m/s), A is the cross-sectional area of the projectile (m^2) and C_D is the drag coefficient². The drag force is measured in Newtons (N). Increasing these variables with respect to the regimes typical of the ballistic events considered in this thesis will result in a larger drag force. As it is squared, velocity will have the greatest influence, followed by density, before the lesser extents of area and drag coefficient. In ballistics, the measure of a projectile's deceleration due to drag is termed retardation (Belkin, 1978). Different formulas for retardation are presented without any derivation (Belkin, 1979; Adams, 1982; Barach *et al.*, 1986). In this thesis, the term retardation will not be used, and instead deceleration with respect to eq. 2.7 will be described.

Using the C_D derived from *Appendix A – Ballistic calculations*, the F_D for a 9mm Luger projectile of mass 7.45 g with a muzzle velocity of 396m/s travelling 10 m is 1.76 N. The F_D for an SS109 5.56 x 45mm projectile of mass 4 g with a muzzle velocity of 975m/s travelling 100 m is 4.49 N (Figure 2-5). Factors that alter the level of deceleration and how this affects injury caused by projectiles will be discussed later in this section. As different influences are discussed, the effect on the two aforementioned projectiles will be calculated to link the theory of the physics to what is witnessed in ballistic wounding.

² Drag coefficient is a dimensionless quantity used to describe an object's ability to overcome drag in fluid (Morris, 1992). Ballistic calculations beginning with deriving the C_D for projectiles of interest to this project can be found in *Appendix A – Ballistic calculations*.



Figure 2-5: A 9mm Luger projectile of mass 7.45 g (left) and an SS109 5.56 x 45mm projectile of mass 4 g (right) for which drag will be calculated throughout this section when the various factors are altered

2.2.1.3 Stability

The centre of mass (centre of gravity) of a projectile, where inertia can be considered to act, always lies on the line of flight. The point where aerodynamic forces act, is at a different location called the centre of pressure (Hopkinson and Marshall, 1967). The distance between the two locations is the overturning moment (Belkin, 1979) (Figure 2-6). During flight, a projectile is statically stable when the centre of pressure is behind the centre of gravity (Greenwood *et al.*, 1987). For example, an arrow; the centre of mass is at the front, while the centre of pressure is towards the rear. Not only does this ensure the stability of the arrow, but marginal deviation off the line of flight can be overcome and corrected (Hopkinson and Marshall, 1967). The opposite arrangement is seen in small-arms projectiles that do not have spin imparted to them; the centre of pressure is in front of the centre of mass, resulting in the majority of projectiles fired from small-arms being aerodynamically and directionally unstable (Barach *et al.*, 1986; Moss, 1997). This is because soon after firing, the centre of pressure would move off of the line of flight, with aerodynamic forces causing a positive overturning moment to act on the projectile, increasing the angle of deviation from the line of flight, making the projectile overturn (McCoy, 2012) (Figure 2-6). While overturning, the centre of pressure moves continuously, but always remains ahead of the centre of mass. Thus once started, overturning will continue (Hopkinson and Marshall, 1967). The process of overturning is known as tumbling, but as what the projectile is going through is still the result of yaw (see below) the term yawing is used too, and will be throughout this thesis.

In modern weapons, to stabilise a small-arms projectile in air, spin is imparted to it. Rifling in the barrel causes the projectile to spin as it exits the muzzle of the weapon (Heard, 2008). The spin of a projectile counteracts the aerodynamic forces acting on it, gradually returning the projectile to its line of flight. It is analogous to when a spinning top is knocked off balance; the stabilising forces gradually return it to a stable vertical position (Hopkinson and Marshall, 1967). Although a projectile with spin imparted to it remains stabilised, the aerodynamic forces still have an effect, causing a slight degree of deviation from the longitudinal axis of flight (Barach *et al.*, 1986; Sellier and Kneubuehl, 1994). The effects of this include yawing, tumbling, precession and nutation (Adams, 1982).

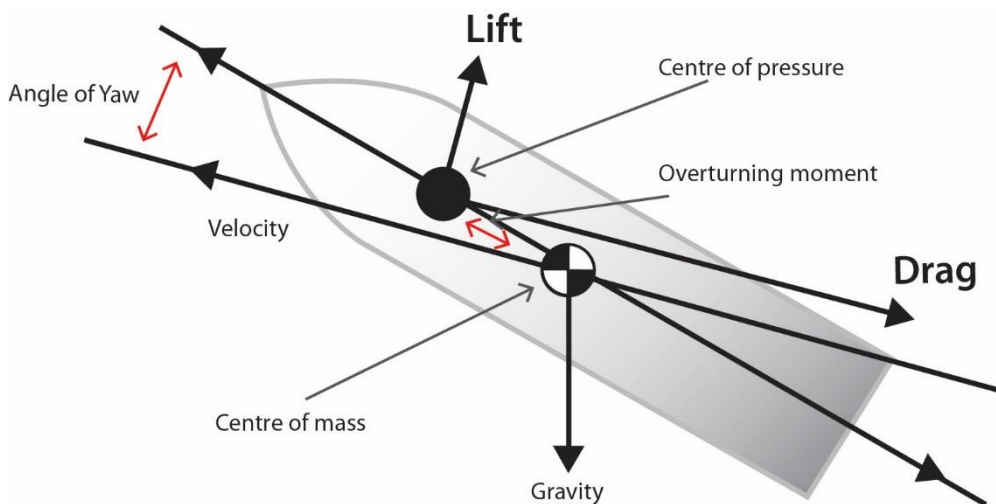


Figure 2-6: A schematic diagram showing the forces acting on a non-spin-stabilised projectile.

2.2.1.3.1 Yaw

Yawing is defined as the deviation of a projectile in its longitudinal axis from the straight line of flight (Belkin, 1979; Adams, 1982). The degree of yaw is the angle between the projectile's axis and the tangent to the trajectory (Hopkinson and Marshall, 1967). Yaw angles of a stabilised projectile during flight are small ($2 - 6^\circ$), with the maximal angle often seen early in a projectile's trajectory before it progressively reduces (Ryan *et al.*, 1997). Spin acting on a yawing projectile causes precession to occur. This is where the centre of mass acts as a fulcrum between the nose and the tail of the projectile, which are both tracing a circular course around the mean position of the longitudinal axis

(Hopkinson and Marshall, 1967). The traced circles get gradually smaller as the projectile continues in a forward motion, as does the frequency of the circles, evolving the traced pattern into a rosette pattern. This is known as nutation (Barach *et al.*, 1986) (Figure 2-7).

The presented cross-sectional area of a projectile is affected by its yaw before impact. The larger the yaw, the greater the cross-sectional area in contact with the target on impact. Considering eq. 2.7, this will mean a greater drag force will act on the projectile. Thus more energy is transferred at the point of impact (Adams, 1982; Cooper and Ryan, 1990). A contributing factor to yaw on impact is mass; projectiles of a lighter mass are less able to overcome yaw in air than heavier projectiles (Barach *et al.*, 1986). Variation in damage produced by the same projectile types may arise due to the angle of yaw at impact (Janzon, 1997). The effect of yaw after impact and through a target will be discussed further in wounding mechanisms (Section 2.2.3.1.2 *Yawing in tissue*).

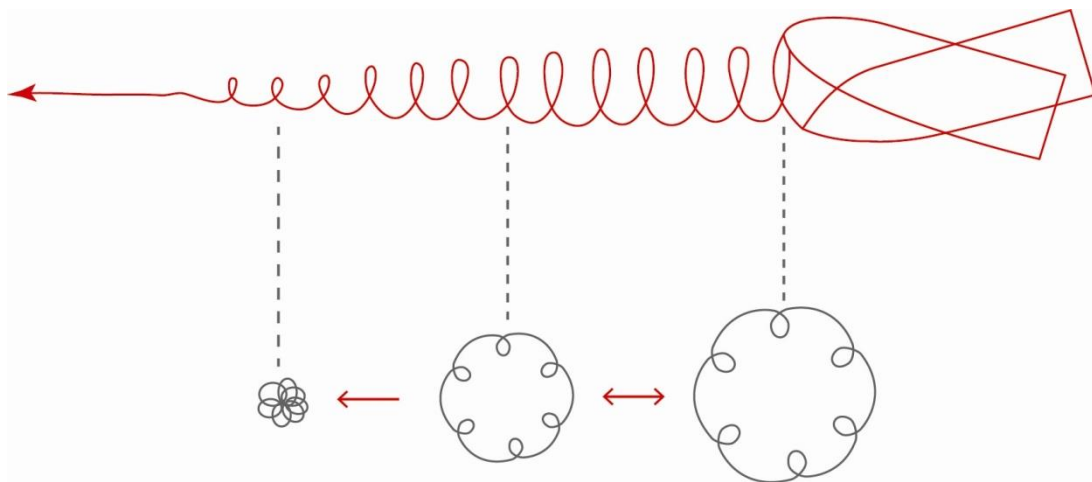


Figure 2-7: A spin stabilised projectile yawing from the stage of precession through to nutation.

2.2.2 Theories of wounding capability

Different theories have been proposed to explain the wounding capability of a projectile on impact. Each theory is concerned with the velocity (V , metres per second (m/s)) and mass (M , kilogram (kg)) of a projectile; they differ by the level of influence each factor has on wounding capability. Three of the most recognised are tabulated below with a brief description (Table 2-2).

Table 2-2: Theories of wounding capability of projectiles on impact

Theory	Formula	Description
Kinetic energy ¹	$KE = \frac{1}{2} M V^2, (J)$	<p>Most widely accepted theory. DeMuth (1966; 1968) claims it probably expresses wounding capability best, citing a large body of experimental and clinical information together with the fact that projectiles of relatively light mass and high velocity have been seen to produce deadly results. Doubling a projectile's mass will double the energy, while doubling the velocity will quadruple the energy.</p> <p>In order to obtain higher velocities, modern rifle ammunition is now lighter. For wounding capability, in theory, the loss in mass of the projectile is compensated for by the increase of velocity (Belkin, 1979). This highlights a greater dependency on velocity than mass (Adams, 1982).</p>
Momentum ¹	$p = MV, \text{kgm/s}$	<p>Equally reliant on both mass and velocity. Supporters of the momentum theory favoured the use of heavy bullets in order to increase wounding capability (DeMuth, 1966). This is particularly relevant when deep penetration is required, such as when hunting large thick-skinned game animals (DeMuth, 1968). Projectiles can travel in excess of 2600 ft/sec (~792m/s) and have a mass of 250 grains (16.2 g) or greater (DeMuth, 1968; Adams, 1982). DeMuth (1966) stated as a result of the deep penetrations characterised by these projectiles (typical depths not cited), it would be uncommon to recover such a projectile from a human target.</p>
Power ²	$P_W = MV^3, \text{kg m}^3/\text{s}^3$	<p>An even greater importance on velocity than the kinetic energy theory (DeMuth, 1968). Small increments in velocity produce vast increases in power and thus vast increases in the wounding capability of a projectile (DeMuth, 1966). Doubling a projectile's mass will double the power, while doubling the velocity will octuple the power.</p>

¹ Adams (1982), ² DeMuth (1968).

Which theory (if any) explains the wounding capability of a projectile best is still an ongoing point of contention amongst ballisticians. Adams (1982) suggested that these theories provide a working knowledge of the wounding capability of a projectile adequate for evaluating the damage produced. Due to misinterpretation, however, the theories have led to confusion, with velocity sometimes credited with being of sole importance in wound production. Cases have arisen where medical personnel have assumed the extent of a wound based on information received about the impact event, rather than investigating the actual damage (Besant-Matthews, 2000). Velocity is just one of many factors that must be considered when assessing injury capability or potential (Ryan *et al.*, 1997).

It must also be remembered that the severity and size of the damage produced is a function of the energy transferred to the target from the projectile (Vellema and Scholtz, 2005). As Barach *et al.* (1986) correctly state, the energy possessed by a projectile is irrelevant if it exits the body with the majority of it intact. Only the energy imparted to the body is energy used to damage tissue, and thus should be considered its wounding capability; not merely the total energy possessed by a projectile.

The location within and the material of the target are of importance when considering the energy transferred, as is a projectile's aspect change during penetration, as this will affect the (coefficient of) drag on the projectile. Determining wounding capacity should take into account the rate of energy transferred at different depths of penetration.

2.2.2.1 Expected Kinetic Energy (EKE)

Developing the theory that energy deposited is altered by: materials, and their respective thickness, as well as changes in the aspect of a projectile, Sturdivan quantified the expected kinetic energy (EKE) deposited by different projectiles in incremental sections of a human target. Sturdivan (1981) described EKE as the mean amount of energy which would be deposited in an average soldier by a large number of random impacts by identical projectiles.

Using data that was collected from a variety of ballistic projectiles into different tissues and tissue simulants, EKE is the experimentally determined incremental expected

kinetic energy deposited in a 20% gelatine target (Neades and Prather, 1991). The testing into 20% gelatine was carried out into blocks as large as 38 cm (380mm) and extrapolated if required to 45 cm (450mm), the theoretical maximum horizontal trajectory through a standing human (Neades and Prather, 1991). The output from Sturdivan's (1981) experimental work estimated the EKE, in joules (J):

$$EKE \approx \frac{m}{2} \sum_{i=1}^{45} P_i (v_{i-1}^2 - v_i^2), \quad (2.8)$$

where P_i is the probability of the projectile being within body tissue at depth i , v_i is the velocity at that depth in metres per second (m/s). The energy is measured in centimetre increments, while the probability of a projectile remaining within a target gradually falls from 1 (within the body) to 0 (exited the target) (Kneubuehl *et al.*, 2011). The probabilities of a projectile remaining within a human target were obtained from a number of random horizontal tracks through "computer man", with a set of probabilities calculated for six different body parts, including the thorax. The formula can be used to estimate the EKE of any projectile whose primary mechanism of causing damage is by the deposition of kinetic energy, provided the data is experimentally determined from measurements of energy deposited in gelatine (Sturdivan, 1981).

Kneubuehl *et al.* (2011) state NATO use EKE as a wounding criterion, though no references are provided to support this statement. Although much of the work surrounding EKE is classified (and thus cannot be discussed in this thesis), comparing the EKE in targets with and without armour could be potentially of benefit in assessing the effect armour has when it is overmatched.

2.2.3 Wounding mechanisms

When a projectile comes into contact with a live target, far too many variables exist to generalise the biophysical events that take place; there is no such thing as a typical ballistic wound (Ryan *et al.*, 1997). General observations have been, and can be, made of the passage of a projectile through living tissue, although many conflicting and controversial studies have led to misunderstanding and misinterpretation in this area (Ryan *et al.*, 1988).

2.2.3.1 Crushing and lacerating of tissue

Crushing and laceration of tissue, also described as rupturing, tearing, stretching, cutting and punching, occurs to tissue which is in the path of a projectile as it moves through a living target (Horsely, 1894; Hopkinson and Marshall, 1967; Bowyer *et al.*, 1997b; Janzon, 1997; Besant-Matthews, 2000). This is often considered the most direct method of inflicting damage to tissue (Adams, 1982). After the projectile passes through living tissue, three zones of wounding are broadly left (Bowyer *et al.*, 1997b). The zone left after the direct passage and contact with the projectile is called the central zone, or permanent cavity (Figure 2-8). It is called this because this cavity is what remains long after the ballistic event. The size of permanent cavity will depend on factors such as the size, shape, construction and stability of the projectile, together with the physical and mechanical properties of the tissues the cavity is created in (Di Maio, 1999; Besant-Matthews, 2000). These factors influence the rate of deceleration a projectile will experience travelling through a target.

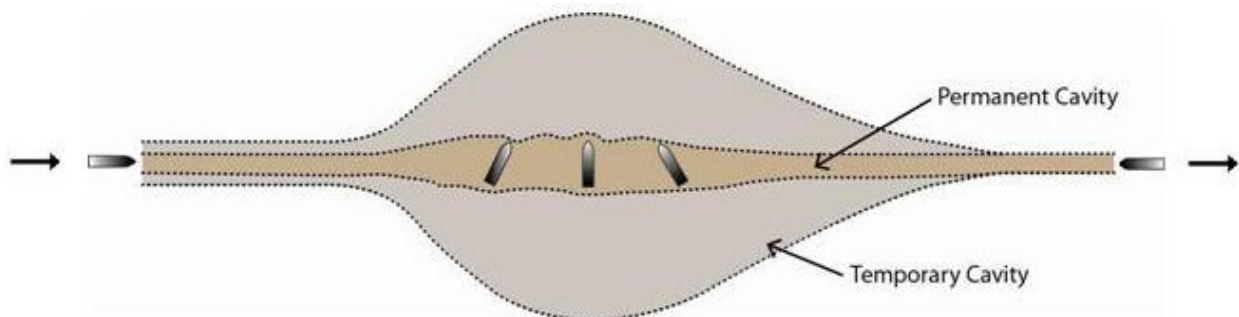


Figure 2-8: Schematic diagram illustrating the passage of a yawing projectile forming the permanent and temporary cavity. In this example the projectile exits the target backwards.

2.2.3.1.1 Deceleration in tissue

When a projectile hits tissue, it will decelerate. As this is occurring, energy is transferred to the tissue. The level of energy that is transferred as a projectile travels through tissue depends on the amount of drag (Ryan *et al.*, 1997). The level of drag is influenced by several factors, as shown from eq. 2.7. These include velocity squared: the greater the velocity a projectile penetrating tissue has, the greater the drag force on that

projectile. Tissues of greater density also cause greater drag. This is highlighted when the density of air is compared to the density of water using eq. 2.7. Water has an approximate density of 1000 kg/m^3 . Assuming all other factors remain unchanged (Appendix A), the drag force of a 9mm Luger projectile in water is 1507.90 N. The drag force on this projectile in water is over 850 times greater than the drag force acting on it in air (F_D in air was 1.76 N). Increased drag results in greater wounding.

The ratio of the density of a material to the density of water, known as the specific gravity (SG), is often used to characterise tissues of the human body:

$$SG = \frac{\rho_{sample}}{\rho_{water}}, \quad (2.9)$$

where ρ_{sample} is the density of the tissue (in kg/m^3) and ρ_{water} is the density of water (1000 kg/m^3). Table 2-3 summarises the specific gravities estimated by DeMuth (1966) of selected tissues of the human body. The estimates were derived from examination of an average of 4 specimens from fresh autopsy material, with no further details given. The location from which the striated muscle was collected was not stated. With respect to the specific gravity only, assuming the bullet does not deform and all other variables in both scenarios are constant, it can be deduced that a projectile that strikes bone ($SG = 1.11$) will be decelerated more, and therefore transfer more energy, than a projectile that strikes lung ($SG = 0.4 - 0.5$).

Cooper and Ryan (1990) state a larger presented cross-sectional area will cause greater drag in tissue, a claim backed up by eq. 2.7. The presented cross-sectional area could be increased by a projectile expanding, or by a projectile yawing within the tissue. In expanding projectiles, more mass means more available material to increase the cross-sectional area, increasing the projectile's diameter and thus the level of drag (Barach *et al.*, 1986). Projectiles of greater mass will also experience greater drag when compared to lighter projectiles.

Table 2-3: Specific gravities of selected tissues of the human body

Tissue	Specific gravity*
Lung	0.4 – 0.5
Fat	0.8
Liver	1.01 – 1.02
Striated muscle	1.02 – 1.04
Skin	1.09
Bone	1.11

*Data collected by DeMuth (1966) from an average of 4 specimens.

2.2.3.1.2 Yawing in tissue

Projectiles that have a greater degree of yaw on impact are more liable to yaw in tissue quicker than projectiles with lesser yaw striking a target. This is because the drag and angular momentum acting on the projectile cannot be overcome by the spin stabilisation that keeps the projectile stable in air. Progressive instability and greater angles of yaw are likely to occur as the projectile travels through a target (Cooper and Ryan, 1990; Janzon, 1997; Ryan *et al.*, 1997).

During the process of crushing and lacerating, the region of tissue damaged is the tissue that comes into contact with the projectile. That region is determined by the presented cross-sectional area of the projectile as it moves forward through the tissue. The largest presented area is typically achieved when a projectile yaws to 90 °, traveling perpendicular to the line of flight. The greater presented cross-sectional area means greater drag force is acting on the projectile and thus more energy is transferred. It also means a larger area of tissue is displaced.

The amount of tissue crushed may be up to three times greater when a projectile yaws at 90 ° compared to travelling nose first according to Hollerman and Fackler, (1995). No details are given as to which projectiles this may be the case for, nor any evidence provided to support this claim. Berlin *et al.* (1976) state that when a bullet tumbles within human tissue, the drag forces may be up to 10-20 times greater than the force that would have ensued if the projectile had maintained a head-on position. No information was provided about the projectile, nor the calculations involved in attaining these force

estimates. However, it can be shown that the estimated drag force of a cylinder³ (diameter 9mm, length 40mm) travelling through water side on is 13.24 times greater than the drag force of the cylinder travelling head on through water (Appendix A1).

Kneubuehl *et al.* (2011) stated that handgun bullets are substantially shorter than rifle bullets, with them being typically no more than twice as long as their own calibre. As a result the effect of yaw is considerably less. Comparing a cylinder once again, this time with a length of 15mm (15mm is the length of a 9mm Luger; a typical handgun round), it can be shown that the estimated drag force acting on the cylinder travelling sideways in water is 4.97 times greater than it travelling head on, adding support to Kneubuehl *et al.*'s evaluation. Spherical projectiles, such as ball bearings, are not affected by yaw and have been utilised for this reason in many ballistic trials (Sellier and Kneubuehl, 1994; Kneubuehl *et al.*, 2011).

The quicker a projectile reaches 90 ° inside a target, the earlier in the target greater damage is produced. Where a projectile yaws could mean the difference between causing a large surface wound with little internal damage, a wound with a small entry that causes large disruption internally, or even a through wound where the projectile has only marginally deviated from the line of flight and yaws after exiting the target (Rybeck and Janzon, 1976). A projectile will continue to yaw with the angle constantly changing as it passes through the varying densities of tissue in a human target (Adams, 1982), so a large enough target may witness a projectile rotating 180 ° before exiting backwards, or even fully rotating 360 ° during its passage (Figure 2-9). Projectiles of the same type, fired under identical conditions, seem to follow the same yawing sequence, albeit with different starting points, altered by different conditions at impact (Janzon, 1997). Due to the forces applied to a projectile yawing in tissue, the projectile may break up and/or deform (Ryan *et al.*, 1997). Hopkinson and Marshall (1967) state yaw is second only to velocity as a factor in determining the extent of tissue damage. As already mentioned, this would not appear to be the case for handgun projectiles.

³ Cylinder dimensions for the larger cylinder are 9 mm (d) x 40 mm (h). A known C_d for a cone (0.5) is used to calculate the drag force when the cylinder travels head on, a known C_d for a cylinder between two walls (1.17) is used to calculate the drag force when the cylinder travels side on. Assumptions that the velocities the cylinders are travelling at, are the same, and that the density of the medium they are travelling through remains the same are made.

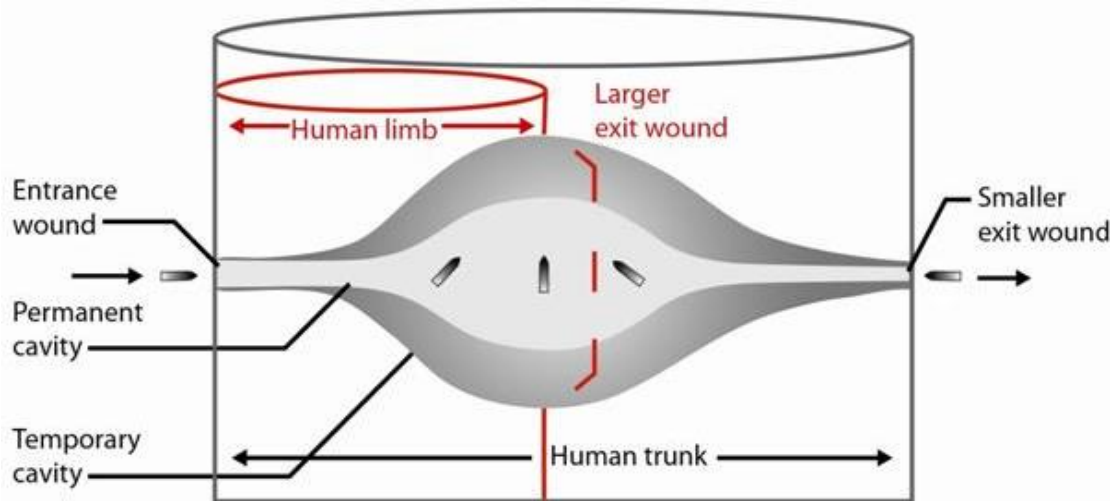


Figure 2-9: Schematic diagram highlighting the effect of target depth on where yaw occurs (adapted from Vellema and Scholtz (2005)).

Summarising the process by which the permanent cavity is formed; the crushing and laceration type of damage caused solely by the passage of a projectile is serious when a projectile comes into contact with vital organs and/or major blood vessels. The chances of this occurring increase if the presented cross-sectional area of the projectile increases; a process that in turn causes more energy to be transferred to the target. A zone of clotted blood and dead tissue is typically left as the permanent cavity in live tissue (Bowyer *et al.*, 1997b); Fackler (1996b) stated that no research had demonstrated a gunshot wound that could not be explained by either the mechanisms of tissue crush resulting from a direct hit by a penetrating projectile, or by tissue displacement caused by a process known as temporary cavitation.

2.2.3.2 Temporary Cavitation

Huguier proposed that the mechanism of destruction by which projectiles damage tissues involved a sudden catastrophic rise in pressure (Huguier, 1848, cited by Payne, 1997). Firing into both liver and muscle (projectile information unavailable), Huguier suggested that energy imparted by the moving projectile caused water present in these tissues to be dispersed in a hydrodynamic fashion. This was during a period of time when the notion of the use of ‘explosive bullets’ in the battlefield had been proposed (Besant-Matthews, 2000). According to Horsely (1894), the explosive effects that were seen could be explained by the fluidity of the particles in the impacted part of the body being

displaced. Horsley (1894) cited that work carried out by Kocher between 1874 and 1876 supported Huguier's original theory, with Kocher described by Wilson (1921) as the pioneer of accurate observations on the wounding effects of high velocity bullets. It was Woodruff (1898) however, who first coined the concept of cavitation (a hydrodynamic process) for wound ballistics (Wilson, 1977).

As already discussed, tissue that comes into contact with a moving projectile is damaged by crushing and lacerating. While a projectile is traversing living tissues, it also causes the tissues surrounding the projectile's path to accelerate away, due to high pressures created (Janzon, 1997). This results in the splashing and stretching of the margins of the tissues surrounding the projectile's path. This is the start of a temporary cavity formation (Besant-Matthews, 2000) (Figure 2-8).

The pressure imparts momentum to the tissues in both a forward and radial fashion; tissues that are pushed forward are accelerated by the bullet; tissues moved radially acquire approximately one tenth of the projectile's velocity (Belkin, 1979). As well as the propagation due to pressure, energy is transferred in the form of stored (potential) energy due to the elastic deformity of the tissues (Janzon, 1997). This explains why the particles in the tissue keep moving after the projectile has passed (Adams, 1982). Tissues are stretched and distorted, but because the tissues in a living target are neither wholly nor uniformly elastic, the extent of the damage is determined by the level of elasticity in combination with the tissue's respective density and air content. The energy that is imparted by the missile is also a determinant (Barach *et al.*, 1986).

Tissues with greater elasticity are better equipped at resisting the disruptive effects of the temporary cavity. Elastic tissue such as skeletal muscle, blood vessels and skin may rebound back after being pushed away during penetration (Jenkins and Dougherty, 2005). Tissues with little or no elasticity can be damaged in a method that is explosive in character (Adams, 1982). The effect of tissue density has been discussed; however, its effect is also important in temporary cavitation. Energy is absorbed by tissue in proportion to its density. Lung tissue is high in elasticity and low in density, and hence the temporary cavity effects are typically much smaller in size when compared to temporary cavities in organs such as the liver and spleen (Wilson, 1977). As previously stated, denser tissue causes greater drag on a projectile. Using Newton's third law, the forces acting on the tissues have to be equalled out by the tissues accelerating away with equal force. This

explains why the temporary cavity is usually largest when the projectile expands or is yawing at 90 °; these are instances where the drag and energy transfer is greatest.

Once the tissues have been extended up to and beyond their elastic limit, the cavity will reach its maximum size. Belkin (1979) stated this is 30 times or more the size of the permanent cavity, while Di Maio (1999) believes it is in the region of 11-12.5 times the diameter of the projectile. When at its maximum size, the cavity has a sub-atmospheric pressure present within it, sucking in air and matter from the outside environment through both the entry and exit wound (Adams, 1982; Janzon, 1997). Due to this sub-atmospheric pressure, the cavity collapses after a matter of milliseconds, setting up a positive pressure (Belkin, 1979; Adams, 1982). This causes a cycle of decreasing expansions and collapses of the cavity, the pulsations of which add to the disruption of the surrounding tissues (Belkin, 1979). The whole process of the temporary cavitation is in the order of 5-10 milliseconds from propagation to collapse (Krauss, 1957; Hiss and Kahana, 2000).

After the final pulsation, the permanent cavity will be what remains, with the evidence that there was a temporary cavity found in the 'zones of contusion' and 'concussion', the final two zones of a ballistic wound (Wang *et al.*, 1988). Although there is no clear-cut difference between the two zones, the borders will be irregular; the zone of contusion will contain areas of devitalised tissue together with haemorrhage within and between tissues. Conversely, the zone of concussion will contain wholly normal tissue, with microscopic evidence of damage, such as swollen myofibres and bleeding between fibres (Wang *et al.*, 1988; Bowyer *et al.*, 1997b). The shape of the temporary cavity will depend on the shape, presentation and yaw of the projectile, and generally mimics the shape of the permanent cavity (Belkin, 1979).

It had been claimed that low velocity projectiles (hand-gun rounds, less than 500m/s) did not cause a temporary cavity and that only high velocity impacts did, however, this is not the case, the temporary cavitation is just on a smaller scale in lower velocity impacts (Besant-Matthews, 2000; Hiss and Kahana, 2000).

The importance of the temporary cavitation is a debated subject. Some have considered it the most important factor in wounding mechanisms (e.g. Sellier and Kneubuehl, 1994; Janzon, 1997). Others have hypothesised that it is not as important as the permanent cavity and have questioned attempts that have been made to treat the temporary cavity effects, rather than actual injuries, believing this resulted in the

unnecessary removal of viable tissues (Lindsey, 1980; Fackler and Kneubuehl, 1990). This suggestion turned into advice from Cooper and Ryan (1990), who stated that not all tissue affected by the temporary cavitation process is necessarily damaged by it. Through cavitation can produce star-shaped damage radiating from the permanent track (Janzon *et al.*, 1997). The effect of cavitation will ultimately depend on the properties of the tissue in which the cavitation occurred.

2.2.3.3 Shock waves

It has been suggested that shock waves are a mechanism by which ballistic injury is caused (Rybeck and Janzon, 1976; Suneson *et al.*, 1990; Sellier and Kneubuehl, 1994). However, the physics of these wave effects are not well understood and it is a point of conjecture. It has been claimed that damage produced away from a projectile's track is the result of shock waves rather than temporary cavitation (Sellier and Kneubuehl, 1994) but Fackler (Fackler, 1987; Fackler and Peters, 1991; Fackler, 1996a; Fackler, 1996b) rebuffed this, claiming no physical evidence existed to support this idea, that did not take into account the effect of the temporary cavitation. This was further discussed by Kieser *et al.* (2013), who showed it was the process of temporary cavitation, rather than shock waves, that caused radial displacement that led to the indirect fracture of deer femur bones in 20% gelatine.

No further discussion of shock waves will take place in this thesis due to the lack of conclusive evidence to support them as a method of causing ballistic injury.

2.2.3.4 Bullet expansion and fragmentation

If a projectile expands or fragments while traversing a living target, the injury caused will often be more severe compared to that caused by a projectile that moves through a living target and does not deform or fragment. As discussed earlier, expansion of a projectile increases the cross-sectional area in contact with the tissue travelled through, an outcome that increases the level of drag. If expansion is desired it is often achieved by altering the design of the projectile (Section 2.1.2.1 *Expanding projectiles*), with an exposed nose deforming very soon after impact so long as the impact event generates enough pressure to deform the nose (Berlin *et al.*, 1988; Janzon, 1997).

Expansion can occur without design in instances where a projectile comes into contact with an intermediate target before entering the living tissue (Sellier and Kneubuehl, 1994), or when bone is struck inside a target (Ryan *et al.*, 1997).

Jacket design, projectile tip configuration, core material strength and impact velocity are all influences on a projectile's potential to fragment. The level of yaw a projectile experiences traveling through soft tissue is another factor. A high yaw angle on impact and a rapid yaw cycle within a target can cause fully jacketed projectiles that are designed to not fragment, to fragment (Janzon, 1997; Ryan *et al.*, 1997). If fragmentation does occur, the fragments produced are often irregular in size with large cross-sectional areas that can result in high drag forces (Janzon *et al.*, 1997). This causes a large transfer of energy. These irregular shapes of fragments are often sharp, causing tears and lacerations in tissues (Besant-Matthews, 2000; Hiss and Kahana, 2000). Multiple fragments will result in many tracks diverging from the projectile's direct path through a target. This will not only create many lacerations in the surrounding tissue, but also mean larger areas of the target are subjected to temporary cavitation. The outcome is often large areas of lacerated, non-viable tissue, complete with many metallic fragments (Janzon *et al.*, 1997).

2.2.3.5 Contamination

Contamination of tissue is a complication of wounding that could have immediate or delayed consequences for wound severity (Ryan *et al.*, 1997). Contrary to earlier beliefs, projectiles are not rendered sterile from the heat generated during the firing process (Hiss and Kahana, 2000), and are capable of carrying and spreading bacteria throughout a wound. This can be achieved by a projectile perforating fabric contaminated with bacteria or passing through a dispersed cloud of bacteria close to either the entry or exit site of a wound. Bacteria can even be drawn through a wound as a result of temporary cavitation pulsations (Thoresby and Darlow, 1967). Micro-organisms from perforated tissues inside the body can also be spread throughout a wound (Hiss and Kahana, 2000). Additionally, foreign bodies that may be contaminated with bacteria in the form of pieces of skin, fabric and other materials drawn in from the outside environment (or from contact with the projectile), often contaminate wounds (Ryan *et al.*, 1997; Bowyer *et al.*, 1997b).

Contamination is reportedly the principal threat to the health of a soldier who has survived their initial ballistic wound (Ryan *et al.*, 1997).

Debridement, derived from the French word *debrider*, is the laying open of the wound, before removing all non-viable tissue to leave a live and healthy surface to the wound (Janzon *et al.*, 1997). Before the action of debriding was used, wounds would putrefy, often leading to the injured patient dying from gas gangrene or cellulitis and septicaemia. Gas gangrene was first described as a complication of gunshot wounds by Fabricius of Hilden in 1593 (Mellor *et al.*, 1997).

Factors such as velocity, mass and shape of the projectile influence the pattern and amount of physical contamination to a wound (Bowyer *et al.*, 1997b). Typical wounds caused by handgun projectiles often result in the direct transfer of skin and fabric into the wound, often similar in size to the cross-sectional area of the projectile at impact (Mellor *et al.*, 1997; Ryan *et al.*, 1997). Ryan *et al.* (1997) state contamination is typically minimal and leads to little difficulty, while Mellor *et al.* (1997) claim fabric carried into a low velocity wound provides an excellent breeding ground for bacteria.

The high rates of energy associated with rifle projectiles cause fine shredding of both fabric and skin, which is then dispersed by the pulsating process of the temporary cavity. This leads to foreign materials being driven deep into the tissues of the wound, even into uninjured areas radiating from the permanent cavity. This makes removing the contamination complex. The effect of the contamination is made worse by the presence of devitalised tissue, which provides excellent conditions for bacterial replication as only a small inoculum of bacteria is required to cause an infection (Mellor *et al.*, 1997; Ryan *et al.*, 1997). The extent of foreign body and microbial contamination of these wounds is typically underestimated (Ryan *et al.*, 1997); tissues damaged and contaminated by high-energy projectiles must be debrided and excised (Janzon *et al.*, 1997).

Excision is the process by which foreign material and contaminants are removed from a wound (Janzon *et al.*, 1997). A surgeon must decide if the contaminants require removal, or if they are safe to remain *in situ* within the wound or surrounding tissues (Bowyer *et al.*, 1997b).

Not all wounds that are contaminated are infected. The foreign materials present may be sterile (Mellor *et al.*, 1997). That said, leaving metallic projectiles or projectile fragments within tissue can have adverse consequences in up to three ways: providing a

site of origin for infection, eroding neighbouring tissues, or releasing metal ions within the body. These potential effects must be weighed up against the level of difficulty and potential dangers associated with excision in that region of the body (Bowyer *et al.*, 1997b). Metallic fragments do not commonly become the source of septic difficulties, the exception being when they have passed through the gut. Although the majority of projectiles contain lead, lead intoxication (plumbism) is rare (Linden *et al.*, 1982), while small, sterile abscesses have been recorded when copper, a very common jacketing material, has been left within a body (Bowyer *et al.*, 1997b). A far greater threat than metallic fragments in tissues is the presence of fabric (Anonymous, 1944, cited by Bowyer *et al.*, 1997b).

The presence of fabric body armours, formed from materials including, but not limited to: para-aramids, ultra high molecular weight polyethylene (UHMWPE), silk, or a combination of the aforementioned, does not typically provide protection against rifle bullets. Penetration of these materials during a ballistic attack could not only lead to a projectile or multiple fragments of a projectile entering the body, but also widespread contamination of the wound by the armour and underlying clothing material.

2.2.5 Summary

There are many influences on injuries caused by gunshot. It is prevalently believed that the crushing and lacerating caused by direct contact with a projectile has the biggest influence, with the effect of the temporary cavity augmenting the trauma, particularly in non-elastic tissues. Factors such as the yawing or expanding will increase the presented area of the projectile, causing it to drag more within the target, transferring more energy to the tissues, increasing the damage produced. Where a projectile strikes is a key variable. Depending on the target material and its depth, it could be the difference between living and dying after being struck by a projectile. The estimated kinetic energy (EKE) takes into account these human target variables, and could be an ideal method by which to compare wounding for situations where armour is and isn't present.

2.3 Tissue simulants

Soft tissue simulants used in ballistic testing are substitutes for biological tissues such as skin, muscles and organs. Although previous studies have used human cadavers and animals (live, cadaver) for testing, many organisations consider it inhumane and unethical to test on live and/or deceased subjects (Berlin *et al.*, 1976; Berlin *et al.*, 1977; Tikka *et al.*, 1982; Breteau *et al.*, 1989; Gryth *et al.*, 2007; Breeze *et al.*, 2013; Breeze *et al.*, 2015b). Aside from ethical constraints, the inhomogeneity of both animal and human bodies implies that shooting channels will rarely resemble one another. Even minute differences in impact location can alter the damage profile, thus making statistical analysis complex (Sellier and Kneubuehl, 1994; MacPherson, 2005). As a result of this, there has been a longstanding desire to find a satisfactory non-biological homogeneous tissue that can act as a simulant for soft body tissue in the testing of projectile penetration and performance.

There have been many opinions as to what an ideal simulant should be composed of (Sellier and Kneubuehl, 1994; Jussila, 2004; MacPherson, 2005). Repeatability and reproducibility are imperative (material availability and costs are included within this). A simulant must produce similar forces on a projectile that soft tissue would do under the same conditions; this covers the level of deceleration and deformation a bullet will experience together with the dissipation of the kinetic energy. It has been described how different tissues of the human body react differently to a moving projectile in the previous section, thus finding a homogeneous simulant that behaves in an identical fashion to all these tissues is near impossible. Fackler (1987) stated that a frequently ignored requirement is that the projectile must stop at the same penetration depth in the simulant as it would in living animal tissue. A final requirement is to be able to either extrapolate or to produce both similar temporary and permanent cavities in the simulant comparable with cavities in soft tissue.

Trying to replicate the inhomogeneous nature of the human body with homogeneous materials has led to many materials being tested e.g. water, stacks of magazines, wet phone books, and newspapers (Fackler and Malinowski, 1985; Jussila, 2004). However, perhaps the most widely used simulants in ballistic testing are gelatine and glycerine soap, both of which have approximately the same density as muscle ($\rho =$

1.06 g/cm³) (Sellier and Kneubuehl, 1994). The development of polymer-based gels has also shown promise as an alternative simulant tissue (van Bree *et al.*, 2006; Mauzac *et al.*, 2010; Moy *et al.*, 2011).

2.3.1 Ballistic soap

Soap used in ballistic trials is formed from glycerine. The manufacturing process of the blocks is complex, but it ensures the soap blocks produced remain stable for a number of years, (Sellier and Kneubuehl, 1994). As a result, blocks are usually purchased and tested instead of being made in-house. For testing, soap blocks do not require preconditioning. When shot, glycerine soap displays almost complete plastic behaviour; it captures the temporary cavity during ballistic penetration, only contracting slightly (Sellier and Kneubuehl, 1994). This means that measurements of the temporary cavity can then be taken, either by cutting the block up or with the aid of X-rays (Kneubuehl, 2011).

There are however, limitations to the use of ballistic soap. One main problem is that because of its plastic nature, soap does not capture the permanent cavity that results from the collapsing of the temporary cavity (Janzon, 1997). The permanent cavity is the damage that remains after ballistic attack (Section 2.2.3.1 *Crushing and lacerating of tissue*). Without capturing this, the extent of the damage is hard to characterise. Other drawbacks of ballistic soap are that blocks are opaque and are not reusable. This means high speed imagery of ballistic impact is ineffective; while once blocks have been tested, they will need to be replaced if more shots are required. Although it has been used in ballistic trials previously (e.g. Berlin *et al.*, 1977; Janzon, 1982; Lanthier *et al.*, 2004), due to the limitations mentioned, ballistic soap will not be considered for this research and will not be discussed further.

2.3.2 Gelatine

Gelatine is a fibrous protein derived from collagen which is the major structural protein in the connective tissue of animal skin, bones and tendons. Depending on the method in which collagens are pre-treated, two different types of gelatine are produced;

Type A (produced from acid treated collagen), and type B (produced from alkali-treated collagen) (Totre *et al.*, 2011).

The gel (or jelly) strength of gelatine is traditionally referred to by *Bloom number*. To test the Bloom number, a 112 g sample of 6.67% w/w gelatine is prepared following a standardised time and temperature system. The sample is then brought to 10 °C before a plunger (12.5mm in diameter) is pushed 4mm into the gelatine. This is done by dropping shot into a cup until the plunger reaches the 4mm depth required. The mass (in grams) of the shot required to achieve the 4mm depth, is the Bloom number (Anon, 2011).

Gelatine is available in consistencies of between 50 and 300 Bloom, however for ballistic testing, type A with a Bloom number between 250 and 300 is usually used (Sellier and Kneubuehl, 1994). To form a gelatine block that can be used for testing, an appropriate quantity of gelatine is dissolved in water and allowed to solidify.

Early penetration studies found that using gelatine produced similar penetration depths to those observed in soft tissue whilst demonstrating the mechanics of the temporary and permanent cavities that resulted from an impact. These observations were the basis for the use of gelatine as a tissue simulant (Wilson, 1921; Krauss, 1957; Harvey *et al.*, 1962).

Once prepared, solid gelatine blocks are translucent, thus the behaviour of the projectile and the exact placement of bullet fragments can be easily viewed and measured. The use of high-speed imagery make it possible to view the formation and collapse of the temporary cavity, while x-rays and CT scans can aid the viewing of the permanent cavity (Fackler and Malinowski, 1985; Fackler *et al.*, 1988; Korać *et al.*, 2001a; Korać *et al.*, 2001b). Physical dissection can aid in the analysis of the permanent cavity, which is typically in the form of tears within the gelatine structure, called fissures (Ragsdale and Josselson, 1988; Jussila, 2005a). Once made, gelatine cannot be re-used. As it is produced from biological material, disposal of gelatine blocks is reportedly fairly simple (Sellier and Kneubuehl, 1994).

2.3.2.1 10% gelatine

The basic formula for 10% (by mass) gelatine is 90 parts water to 10 parts gelatine (Sellier and Kneubuehl, 1994). However, water temperature and post-manufacture conditioning reportedly affect the properties of gelatine blocks (Fackler and Malinowski,

1988; Cronin and Falzon, 2009). Due to the research carried out on wound ballistics and using gelatine, Col. Martin Fackler (Fackler *et al.*, 1984a; Fackler *et al.*, 1984b; Fackler and Malinowski, 1985; Fackler, 1987; Fackler *et al.*, 1988; Fackler and Malinowski, 1988) is often cited as the originator of the method many people use to make 10% gelatine (Jussila, 2004; Nicholas and Welsch, 2004; Cronin and Falzon, 2011).

Fackler claimed that the results obtained when two projectile types (5.56mm, 3.2g soft-point, 17mm long, manufactured by Hornady Manufacturing Co., Grand Island, NE and, 5.56mm, 3.1g, 19mm long solid brass bullet, machine made at the Letterman Army Institute of Research, San Francisco) were each fired three times into 10% gelatine blocks at 4°C reproduced the penetration depth measured in living swine leg muscle to within 3% (Fackler *et al.*, 1984b; Fackler *et al.*, 1984a). This conclusion was reached by comparing the penetration of projectiles in 10% gelatine blocks with a target formed of a single hind swine limb together with a 10% gelatine block placed against the skin of the swine at the predicted point of exit. A criticism of the use gelatine in these tests was, however, noted, in that the permanent cavities produced by fragmenting projectiles in muscle are not well reproduced in gelatine (Fackler and Malinowski, 1985). That limited original data was published and reference was made to unpublished data supporting the findings has also been previously noted (Nicholas and Welsch, 2004).

2.3.2.2 20% gelatine

It appears that gelatine blocks of 20% concentration were used first in ballistic testing, however, there is a difference of opinion as to when this was. Jussila (2004) claimed Harvey *et al.* (1962) were the first group to recommend the use of 20% gelatine blocks; whereas Lewis *et al.* (1982) correctly stated Wilson (1921) was the first to utilise cast blocks of 20% gelatine as a tissue substitute when he investigated gelatine blocks of 5, 10, 15 and 20% concentrations.

Formed of 80 parts water and 20 parts gelatine powder (Sellier and Kneubuehl, 1994), 20% gelatine blocks have continued to be used throughout the ballistic testing community. Often referred to as the 'standard' NATO gelatine (Knudsen and Vignaens, 1995; Nicholas and Welsch, 2004; Cronin and Falzon, 2011), although there is not a NATO standard from which this proclamation stems.

2.3.2.3 10% blocks vs 20% blocks – which blocks to use?

One of the major issues with ballistic gelatine blocks as a simulant is that there is no set standard procedure for its manufacture. As a result of this, different researchers favour different concentrations and different manufacturing techniques; but why has the ballistic testing community failed to agree which concentration to use exclusively?

A potential reason to favour 10% gelatine blocks over 20% blocks could be for cost reasons, as twice the amount of gelatine is required for 20%. However, 10% is more difficult to handle due to a lower stiffness. It has less strength; the higher the concentration the greater the gel strength (Osorio *et al.*, 2007; Rousselot, 2014). Whichever method researchers find simplest and/or less time consuming could also contribute to their decision of which concentration to manufacture.

Jussila (2005b) states an argument against the use of 10% gelatine is due to its “specific weight”. He writes that the specific weight of 10% gelatine is 1.03 (no units) before citing Janzon *et al.* (1997) for a figure of 1.06 (no units) for 20% gelatine; a closer match to muscle tissue. He then writes that the claim it is a closer match is wrong, as 1.06 is an approximation of thigh muscle tissue in swine, not human muscle. Finally he cites DeMuth (1966), and states values for human thigh are 1.02 - 1.04, thus a closer match to 10% gelatine. The current author believes Jussila (2005) was talking about specific gravity (equation 2.12, Section: 2.2.3.1.1 Deceleration in tissue), no units; not specific weight. No reference can be found for Janzon *et al.*, (1997) stating 20% gelatine has a specific density of 1.06, nor that it is a closer match for muscle tissue. From the same edited book, however, Janzon (1997) writes that soft tissue has a common density around 1050 kg/ m³, later mentioning 10% gelatine has a lower density of 1030 kg / m³. This would indeed give a specific gravity of 1.03. Eisler *et al.* (2001) state that 20% gelatine has a specific gravity of 1.05. Comparing these specific gravities to the specific gravities DeMuth (1966) achieved from an average of 4 samples, it can be seen 10% gelatine is within the range of muscle (1.02 - 1.04), while 20% gelatine lies just out of the range, but matches with the figure Janzon (1997) states as a common specific density for soft tissue of the body.

Several studies have been undertaken to measure the effect of strain rate on the mechanical properties of ballistic gelatine using a pendulum or drop tower for intermediate rates ($\approx 100 \text{ s}^{-1}$). However, these strain rates are slower than those produced

by ballistic ammunition and thus tests performed on the Split-Hopkinson Pressure Bar technique to achieve rates in the order of 1000 s^{-1} are more likely to be comparable to ballistic testing (Shepherd *et al.*, 2009; Cronin and Falzon, 2011).

Jussila (2005b) approached the subject of concentration by envisaging that it may be possible to use the differing nature of gelatine at various concentrations as an advantage. Stating that by altering the gelatine concentration together with incorporating air bubbles it should be possible to change the mechanical properties of the gelatine and thus replicate any soft tissue desired.

2.3.2.4 Temperature

Temperature during the mixing, storage and usage of gelatine plays a vital role in how it will behave during testing (Fackler and Malinowski, 1988; Jussila, 2004). The warmer the water that gelatine is mixed in, the quicker it will dissolve. Many temperatures have been used by researchers to prepare gelatine e.g. gelatine powder added to cold water ($7 \text{ }^{\circ}\text{C} - 10 \text{ }^{\circ}\text{C}$) and the solution heated to no higher than $40 \text{ }^{\circ}\text{C}$ (Fackler and Malinowski, 1985; Fackler and Malinowski, 1985; Cronin and Falzon, 2011; Schyma and Madea, 2012), gelatine powder added to distilled water at $85 \text{ }^{\circ}\text{C} - 90 \text{ }^{\circ}\text{C}$ (Berlin *et al.*, 1977) and water at $90 \text{ }^{\circ}\text{C} - 95 \text{ }^{\circ}\text{C}$ added to gelatine powder (Lewis *et al.*, 1982).

After heating gelatine solution to between $70 \text{ }^{\circ}\text{C} - 80 \text{ }^{\circ}\text{C}$, Fackler and Malinowski (1988) reported that the resulting gelatine block was “softer” than previous batches. How the mechanical properties were assessed is not stated. Although the softer gelatine block was not actually tested, later tests identified that abnormally large temporary cavities were produced in gelatine blocks prepared with boiling water. This led to the conclusion that excess heat had weakened the gelatine’s strength and it was thus less resistant to displacement by the temporary cavity. No measurements of the cavities, nor any of the details regarding the test method were released, nor was any statistical data to back up their observation that the gelatine blocks were “softer” when made with boiling water. After contacting their gelatine supplier, they were advised that gelatine’s gel strength and viscosity were steadily weakened when subjected to heating above 40°C while in solution (Fackler and Malinowski, 1988). If this is indeed the case, many experiments in which gelatine was subjected to such treatment may have skewed results, as pointed out by Fackler and Malinowski with reference to the work carried out by Berlin *et al.* (1977).

While investigating parameters which affect gelatine performance, Jussila (2004) tested the effect of water temperature (18.5 °C – 90.4 °C) during the manufacturing process of numerous gelatine blocks. Contrary to what Fackler and Malinowski (1988) were told, Jussila claims he was informed by Gelita (a gelatine manufacturer) that gelatine's gelling power did not significantly decrease after several hours exposure at 60 °C – 80°C (Jussila, 2004). Results from firing 4.5mm steel pellets (BB) into numerous gelatine blocks formed from solutions of different temperatures indicated that gelatine solutions with a temperature up to 58.5°C showed no significant effect to the gelatine's performance with regards to penetration depth, however, raising the gelatine solution to over 80°C appeared to cause significant changes to the level of penetration. The testing did not reveal what affect (if any), high solution temperatures had on the tensile strength or elasticity of gelatine blocks. These results did not disprove the research of Fackler and Malinowski (1988), but do provide a stricter temperature regime to follow during the manufacturing process.

Fackler and Malinowski (1988) claimed gelatine firmness varied greatly with temperature of the block during testing, while Nicolas and Welsch (2004) state temperature and composition are known to alter and affect gelatine consistency (firmness), however, firmness is not defined by a measurement in either case. The level of drag gelatine induces on projectiles also varies with usage temperature (Jussila, 2005b). Temperature affects the hardness and stiffness of gelatine and thus 10% gelatine blocks are commonly stored and tested at 4 °C, while 20% blocks are often stored and tested at 10 °C (Cronin and Falzon, 2011).

In order to achieve a constant temperature profile throughout, gelatine blocks must be kept at the required temperature over a long period of time (Sellier and Kneubuehl, 1994). Fackler and Malinowski (1988) suggested that once 10% gelatine blocks have been left to set at 7 °C – 10 °C overnight, they should be removed from their moulds and stored at 4 °C until at least 36 hours have elapsed from the time the gelatine solution was poured into their moulds. Testing should be conducted at the same temperature. No data as to why this method is best practice were presented. In comparison, Jussila (2004) recommended allowing 10% gelatine solution to be left to stand and solidify at room temperature for 24 hours before being transferred to a refrigerator at 4 °C for at least 24 hours.

Internal temperatures should be measured before and after testing at an approximate depth of 40mm to ensure block temperature is as expected (Jussila, 2004).

2.3.2.5 Block size

Standardisation of gelatine block size may also help the ballistic test community with comparing results (Jussila, 2004). Many block sizes have been reported e.g. 150mm (w) x 150mm (h) x 300mm (l) (Schyma, 2010), 5" x 6" x 14" (l) (127mm x 152.4mm x 355.6mm (l)) (which measurements are height and width are not clear from the paper) (Lewis *et al.*, 1982), 220mm (w) x 160mm (h) x 470mm (l) (Korać *et al.*, 2001b), 220mm (w) x 200mm (h) x 470mm (l) (The measurements that correspond to the width, height and length of the block are not stated in either paper, however, assumptions have been made after viewing figure 3 of Fackler *et al.* (1984b)) (Fackler *et al.*, 1984a; Fackler *et al.*, 1984b; Korać *et al.*, 2001a), 250mm (w) x 250mm (h) x 500mm (l) (details of which measurement is which is not stated, but are assumed with use of the diagrams in both papers) (Fackler and Malinowski, 1985), 200mm diameter with varying lengths (250 – 500mm) (Schyma and Madea, 2012) and cylindrical blocks with a diameter of 360mm and length of 700mm (Knudsen and Vignaes, 1995).

A block size of 150mm (w) x 150mm (h) x 400mm (l) was used by Jussila (2004), who noted that blocks this size did not easily accommodate more than two or three pistol shots and were “slightly thin” for high power rifle ammunition. Instead, Jussila recommended 200mm (w) x 200mm (h) x 250mm (l) as a replacement size suitable for all calibres and several shots with pistol ammunition. Fackler and Malinowski (1985) claimed blocks 250mm x 250mm x 500mm gave a “valid area”. Blocks this size were deemed suitable to capture the wound profile of high velocity ammunition without radial fissures reaching the blocks surface; a factor that deems the wound profile unsuitable for measurement (Fackler and Malinowski, 1985; Jussila, 2005b).

Gelatine blocks have been used end to end forming a “column” to collect the entire interaction of ammunition and gelatine (Fackler *et al.*, 1984b; Fackler and Malinowski, 1985). Although the gelatine is a homogeneous material, the act of exiting one block and entering another may produce different results (no matter how close together the blocks are) in comparison to a bullet penetrating through a single longer block.

2.3.2.5.1 Anthropometric measurements of the human torso

As this research is concerned with overmatching police armour that is typically used to protect the vital organs in the thorax, anthropometric data of this region could be of importance. Such measurements may also inform simulant block size. The chest depth, defined as the maximum horizontal distance from the vertical reference plane to the front of the chest (Pheasant, 1988), from different samples were compared (Table 2-4).

Table 2-4: Chest depths from different anthropometric studies

Population	Source	Chest depth (mm)		
		5%ile	50%ile	95%ile
Men aged 19-25	Stratified sample of households conducted in 1981. Population were British ¹ .	185	225	270
Women aged 19-25		190	235	275
Men aged 19-45		200	240	275
Women aged 19-45		195	240	285
Men aged 19-65		215	250	285
Women aged 19-65		210	250	295
New Zealand firefighters	691 male New Zealand Fire Service members from a sample of 750 (~7.5% of the total NZFS workforce) ² .	212	244	282
Europeans aged between 18-60	Jürgens, H. W., <i>et al.</i> , 1998 ³	170	215	250

¹(Pheasant, 1988), ²Laing, *et al.* (1999), ³In German, cited by British Standards Institution, 2004

2.3.2.6 Calibration

The credibility of scientific reports associated with the use of gelatine has been questioned due to the fact no agreed standards exist for preparing it (Jussila, 2004). MacPherson (2005) stated that due to the naiveté of quality control in preparation of gelatine, all test data from any source prior to the mid-1980s is suspect and should not be used in any application requiring precision.

Despite there not being a standard for manufacturing gelatine, a method for calibrating gelatine was proposed by Jussila (2004). Every batch of gelatine powder should be calibrated by firing nine pellets at a gelatine block at approximately three different velocities. The depth of penetration is compared with the values in Table 2-5. For every millimetre of penetration difference (short or long), 1% of gelatine should either be added or subtracted from the recipe used to make the remaining gelatine from that specific batch. Every block subsequently produced should have its depth of penetration verified. This is done by shooting two 4.5mm steel pellets (BB) at two different velocities (in the range 120-190m/s) into the gelatine blocks. Penetration (L_p) and impact velocity (V_i) are measured and compared to the minimum and maximum acceptable penetrations for different velocities (Table 2-5).

Table 2-5: The minimum and maximum acceptable penetrations for different impact velocities (Jussila, 2004).

V_i (m/s)	Minimum L_p (mm)	Maximum L_p (mm)
120	44	54
125	47	57
130	50	60
135	53	63
140	56	66
145	59	69
150	62	72
155	65	75
160	68	78
165	71	81
170	74	84
175	77	87
180	80	90
185	83	93
190	86	96

2.3.3 Polymer based gels

Due to the poor shelf life of gelatine and its storage requirements, alternative simulants have been sought. The development of polymer-based gels has led to optimism they could be an alternative tissue simulant (Moy *et al.*, 2011). SEBS gel and Slygard have both been used as an alternative to gelatine in the analysis of back face deformation and behind armour blunt trauma respectively (van Bree *et al.*, 2006; Mauzac *et al.*, 2010).

These products can be manufactured in-house and might be vulnerable to variation due to the manufacturing process used. Therefore, further discussion of these products is outside the scope of this thesis.

2.3.4 Perma-Gel™

Perma-Gel™ is a clear synthetic material manufactured by Perma-Gel Inc. (Patent pending) which was developed specifically as a soft tissue for the testing and comparison of different projectile types and is commercially available (Amick, 2006). Perma-Gel™ is a product of interest to the UK Home Office CAST. It was developed by Dr Darryl Amick in 2005 as a substitute for 10% ballistic gelatine (Boackle, 2011). Claims by the company include: storage at room temperature without decomposition problems, no need to condition, superior in clarity compared to chilled ballistic test gelatine, unaffected by water and being incapable of breeding bacteria (Amick, 2006). Independent validation appears lacking. A further claimed advantage of Perma-Gel™ is that it can be re-melted and reused, although the number of times this can be done before the gel loses its characteristics are unclear. Boackle (2011) claims Perma-Gel™ can be reused up to 12 times but after multiple reuses an amber/yellowish tint may form in the blocks. Another user of Perma-Gel™ claims that although ballistic properties supposedly do not change, blocks should not be re-melted more than 10 – 12 times, as after this the blocks are too yellow to see through (Tichler, 2012), with another opinion that Perma-Gel™ can be reused between 10 – 15 times although following repeated re-melts, the Perma-Gel™ gets softer and is more prone to breaking up (Holroyd, 2012). The chemical changes that are associated with re-melting Perma-Gel™ are not clear.

Perma-Gel™ has been used in a number of peer-reviewed studies e.g. simulant for brain tissue (Pervin and Chen, 2011), testing of mechanical responses of fully hydrated soft tissues under defined dynamic loading conditions (Kalcioğlu *et al.*, 2011) and the development of a shape memory alloy based tool for brachytherapy (Ho *et al.*, 2010). However, these research areas are outside the scope of this thesis and will not be discussed further.

Although limited in comparison to the use of gelatine, studies in the open source literature have used Perma-Gel™ as a ballistic test simulant. Boackle (2011) compared

the terminal performance of different pistol calibres using Perma-Gel™, while May (2010) reported a study comparing its wound ballistics performance against gelatine.

Boackle (2011) reported firing several pistols⁴ from 10 feet and measuring the depth of penetration into Perma-Gel™. The research focused on the performance of the individual bullets (number of shots per weapon not specified) rather than the Perma-Gel™. Limited detail regarding the wound profiles created was provided, and the only comparison to 10% gelatine blocks was for penetration depths reported by the FBI. Data was only provided for ammunition that displayed similar results in both simulants. These results do not support the author's claims that Perma-Gel™ is an adequate medium for testing terminal ballistic effects of different pistol ammunition.

The suppliers of Perma-Gel™ claim limited testing has been carried out on the material, although the details of these tests are not disclosed. They do report close similarities in the trajectory, deformation, and permanent wound cavities created by high-velocity (above approximately 1600 fps; 487.68m/s) expanding ammunition in Perma-Gel™ to those created in gelatine (concentration not given). It is also claimed that in tests using low-velocity ammunition (less than 1600 fps), Perma-Gel™ displayed less bullet expansion than in gelatine, while non-expanding ammunition (FMJ) showed more penetration (Amick, 2006). Specific details regarding penetration levels were not disclosed.

2.3.5 Summary

Table 2-6 summarises the advantages and disadvantage of the three simulant types discussed.

Table 2-6: The advantages and disadvantages of three tissue simulants

⁴Glock Model 27 .40 S&W pistol with following ammunition: Cor Bon 135 gr HP, Federal Hi Shock 180 gr JHP, Winchester Ranger 165 gr SXT, Remington 180 gr HP, Fiocchi 170 gr FMJ, and Winchester Black Talon 180 gr HP.

Sig Sauer p228 9 mm Luger pistol with ammunition: Winchester 147 gr SXT, Winchester 115 gr FMJ, Winchester 124 gr FMJ, Speer Gold Dot 124 gr HP, Remington 115 gr FMJ, Cor Bon 115 gr JHP, Golden saber 147 gr JHP, Federal Hydra Shok 147 gr HP, and Federal Hi Shok 115 gr JHP.

Smith & Wesson Model 686 revolver with ammunition: Fiocchi 142 gr FMJTC, Speer Gold Dot 158 gr HP, PMC Eldorado Starfire 150 gr JHP, Remington Express Lead 158 gr, Remington Express 125 gr SJHP, Remington Express 158 gr SJHP, and Federal 110 gr JHP.

Glock Model 21 .45 Auto with ammunition: Federal Hydra Shock 230 gr JHP, Remington Golden Saber 230 gr JHP, Remington 230 gr FMJ, Winchester Personal Protection 230 gr SXT, Winchester Silvertip 185 gr HP and, Speer Gold Dot 185 gr HP.

	Advantages	Disadvantages
Ballistic soap	<ul style="list-style-type: none"> -Can be stored for long durations prior to use. -No pre-conditioning required. -Captures the temporary cavity. 	<ul style="list-style-type: none"> - Complex Manufacturing process - Blocks purchased instead of being made in-house. -Does not capture the permanent cavity. -Opaque – difficulty recording ballistic event with high-speed video. - Not reusable.
Gelatine	<ul style="list-style-type: none"> - History of extensive testing using it. - Similar penetration depths to those observed in swine tissue. - Transparent. - Demonstrates the mechanics of the temporary and permanent cavities (with the aid of high-speed video). - Captures the permanent cavity. 	<ul style="list-style-type: none"> - Different Blooms of gelatine used. - No agreement on which concentrations to use. - No standardised method for manufacture. - Temperature dependant. - Not reusable. - Must be kept refrigerated. - Poor shelf life (2-3 days prior to use, refrigerated).
Perma-Gel™	<ul style="list-style-type: none"> - Clear and odourless. - Very good shelf life. - Sold as reusable. - No pre-conditioning required. - Displays the temporary cavity formation (with high-speed video). - Captures the permanent cavity. 	<ul style="list-style-type: none"> - Limited ballistic testing to confirm claimed performance. -Only comes in one block size/shape. - Difficulties with disposal as a synthetic polymer.

Tissue simulants that mimic the behaviour of live soft tissue have been used extensively in ballistic studies. Difficulties in simulating the inhomogeneous nature of the human body with a homogeneous material means there will never be a perfect resolution. That said, the use of gelatine in two different concentrations, and ballistic soap has been extensive, with the damage captured in these simulants succeeding in simulating certain features of a ballistic attack to a live target. Projectile depth of penetration in 10% gelatine

has been validated against live swine tissue, while the formation of both the permanent cavity and temporary cavity in both concentrations of gelatine follows the wounding mechanisms discussed in the previous section, unlike ballistic soap. Polymers and synthetic materials have not been extensively tested as tissue simulants for ballistic trails, thus judgement is reserved until this is the case. No standard simulant or even a standard method for the production of one of the simulants exists. This makes comparison of results gained from different users rely on assumptions that the simulants were made and thus behaved in the same way.

2.4 Body Armour

Body armour is a form of personal protective equipment that is worn all over the world in varying situations as a last defence mechanism. Specifically in the UK, Police officers, military personnel, and other individuals including some ambulance workers, fire-fighters, security guards and journalists are examples of professionals who don body armour to protect themselves as they carry out certain roles of their job. As a result, it is essential that modern body armour provides a range of users with protection against a vast range of specific ‘threats’ such as bullets and fragments as well as sharp and blunt objects (Tobin and Iremonger, 2006).

The primary role of body armour is to stop a penetrating injury to the wearer. This is usually achieved by the construction of the body armour deflecting or dissipating and partially absorbing the kinetic energy of a potentially lethal threat (Pinto *et al.*, 2012). The ability of a weapon (e.g. bullet, knife, spike, fragment) to defeat body armour depends on the weapon's characteristics i.e. velocity, size, shape, mass and how easily it deforms when it comes into contact with the body armour (Tobin and Iremonger, 2006). However, it is not viable for body armour to protect the wearer against all forms of attack. Consequently many different body armour solutions are available for a variety of specific threat levels (Watson *et al.*, 2010).

2.4.1 History

Although quoted as being as old as warfare itself (Dunstan, 1984), the first forms of body armour were most likely devised before this, for protection against wild animals whilst hunting (Woosnan-Savage and Hall, 2001). The materials used in body armour have changed dramatically over the centuries, ranging from utilisation of local resources to the manufacture of modern day composite materials (Dunstan, 1984).

The research described in this thesis focuses specifically on UK police body armour, therefore discussion of developments of military body armour throughout history are outside the scope of this topic. A brief history on the development of fibres used in soft body armour, together with an exploration of police body armour will be discussed further on in this section.

2.4.2 Forms of body armour

The tissues of the human body (e.g. skin, skeleton) provide protection to critical organs (e.g. heart, lungs). However, this natural protection is relatively easily overmatched resulting in a penetrating injury that could cause serious injury and/or death. Various types of personal armour exist to help increase protection to the body. Examples include body armour (fragment and bullet resistant torso covering vests / waistcoats), helmets (fragmentation and bullet resistant), face and eye protection (visors, glasses and goggles) and Explosive Ordnance disposal (EOD) suits (UK Ministry of Defence, 2005; Sakaguchi *et al.*, 2012). The coverage provided must not, however, hinder the wearer in such a way that they are not able to carry out their prescribed duties while wearing their body armour. Actions such as sitting, standing and changing between various body positions are made all the more difficult with increased coverage and the extra mass that comes with increased body armour (Brayley, 2011). Other issues that decrease the ergonomics of body armour include unbalanced weight distribution, chafing and overheating (Watson *et al.*, 2010; Carr and Lewis, 2014). For this reason, body armour worn is usually a compromise between the level of protection and extent of body coverage against ease of carrying out routine actions (Brayley, 2011).

There are two main types of body armour that are used to defeat ballistic threats: soft fabric body armour and hard plate body armour (Chen and Chaudhry, 2005; Tobin and Iremonger, 2006; Brayley, 2011; Prat *et al.*, 2012). Soft panels containing many layers of fabric provide the basis for the majority of all body armour, with hard plates added to increase protection of specific areas (Prat *et al.*, 2012). Hard plate body armour is inflexible; constructed of laminated materials such as ceramics and composites combined with ballistic fabrics (Brayley, 2011; Pinto *et al.*, 2012). Further discussion of hard plates is outside the scope of this research.

2.4.2.1 Soft body armour

Soft body armour is made from multiple layers of lightweight manmade polymeric fibrous materials (Chen and Chaudhry, 2005). These layers of fabric (often referred to as the ballistic panel or panel) are inserted into a 'carrier' manufactured from a polyester/cotton or nylon woven fabric to form a soft body armour pack (Pinto *et al.*, 2012). The panel may be encased in a UV- and light-, water-resistant fabric before being

inserted in the carrier. Soft body armour offers protection from a number of threats; typically armour worn by military personnel is designed to offer protection from fragments, while police are protected from the threat of sharp weapon (knife, spike) and hand-gun attacks (Tobin and Iremonger, 2006). The material(s) and the number of layers present in a pack will alter greatly depending on the protection that is required (Hewins, 2010).

Fibres used in soft armour systems include para-aramids (Kevlar®, DuPont and Twaron®, TeijinAramid), ultra-high molecular weight polyethylene (UHMWPE) (Dyneema®, DSM and Spectra®, Honeywell) and polyamides (Nylon®) (Chen and Chaudhry, 2005; Tobin and Iremonger, 2006). The fibres used can be in woven or nonwoven form (Prat *et al.*, 2012). A woven fabric consists of two sets of yarns interlaced at 90 ° to each other; weft yarns (horizontal yarns) are passed over and under warp yarns (lengthwise yarns) at points called crossovers. Non-woven fabrics are constructed from individual layers of parallel unidirectional fibres, with alternate layers positioned and adhered 90 ° to one another (Tobin and Iremonger, 2006).

2.4.2.1.1 Para-aramids

The term ‘aramid’ is short for ‘aromatic polyamide’. Aramid fibres are man-made synthetic-polymer high performance fibres which contain molecules that are characterised by relatively rigid polymer chains (Teijin Aramid, 2012). When these chains are orientated in a linear direction, strength is increased due to optimising the alignment of the chemical bonds.

Aramid fibres were discovered in 1965 when S. L. Kwolek synthesised a series of para-oriented aromatic polyamides. This led to DuPont de Nemours recognising that a rigid molecular chain and a fibre of ultra-high modulus could be made from a para-oriented symmetrical polymer; this fibre, originally named Fibre B, became known as Kevlar® (Yang, 1993) (Figure 2-10). The result is a combination of properties that include high tensile strength (>3 GPa), high modulus (>60 GPa) and medium strain to failure, hence high toughness (Chang, 2001; Chen and Chaudhry, 2005). With several grades of aramid fibres available, they have many applications e.g. tyres, ropes, space vehicles, boats and body armour (Magat, 1980; Tobin and Iremonger, 2006). Para-aramids were first used to make body armour for the police and military in the early

1970s. They are now the most common material used in soft body armours (Chen and Chaudhry, 2005). However, increasing competition from other fibre materials such as UHMWPE is challenging this (Tobin and Iremonger, 2006).

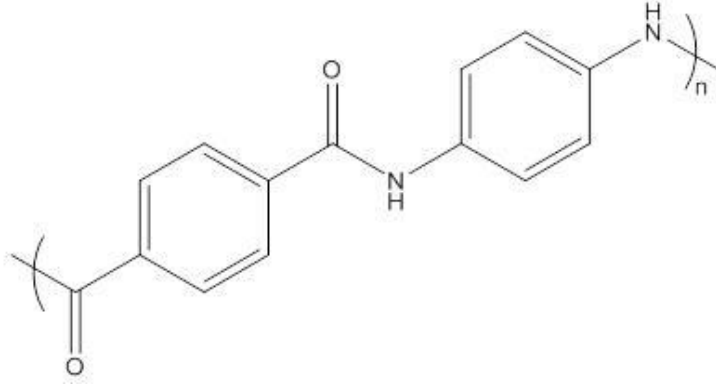


Figure 2-10: Molecular arrangement of a para-aramid

2.4.2.1.2 UHMWPE

UHMWPE contains orientated high-molecular weight molecules of polyethylene; its molecular formula is $-(C_2H_4)_n-$ (Figure 2-11), where n is the degree of polymerization; this can be as high as 200,000 (Kurtz, 2009). UHMWPE gives high material stiffness (>3 GPa) and high strength (>40 MPa) (Tobin and Iremonger, 2006). Dyneema® (DSM) has been in production since 1990, and is manufactured by a process of gel-spinning; very long molecules are first dissolved in a volatile solvent and then spun through a spinneret. In the solution, the molecules are disentangled, and remain so after cooling (van Dingenen, 1989). Spectra® fibre, by Honeywell, is another UHMWPE fibre that is produced using a gel-spinning process (Honeywell, 2012). UHMWPE fibres are used for medical sutures, ropes, sailcloth, fishing lines and nets, slings, cut-resistant gloves and apparel, as well as police and military personal and vehicle ballistic protection (DSM, 2012; Honeywell, 2012).

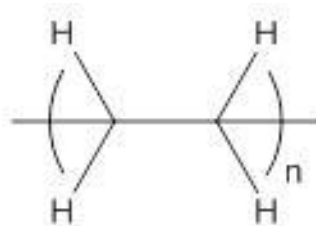


Figure 2-11: Molecular arrangement of polyethylene

2.4.2.1.3 Polyamides

Nylon® fibres are a type of polyamide. Developed in the 1930s by a team of scientists working for DuPont, Nylon® is the product of 2 monomers (DuPont, 2012) (Figure 2-12). Utilised up until 1972, Nylon® fibres were originally used to contain metal plates for body armour, before being used as ballistic protection in its own right. With a high degree of crystallinity and low elongation, all-nylon armoured vests started being produced by the end of the Second World War, although they were first used in service in the Korean War. Superior protection is offered by para-aramid and UHMWPE solutions. However, 'Ballistic' Nylon® (Nylon 6,6) is still used today in some armours and helmets as well as in other protective equipment such as motorbike apparel. This is due to its low cost compared to para-aramids and UHMWPEs (Chen and Chaudhry, 2005; Tobin and Iremonger, 2006).

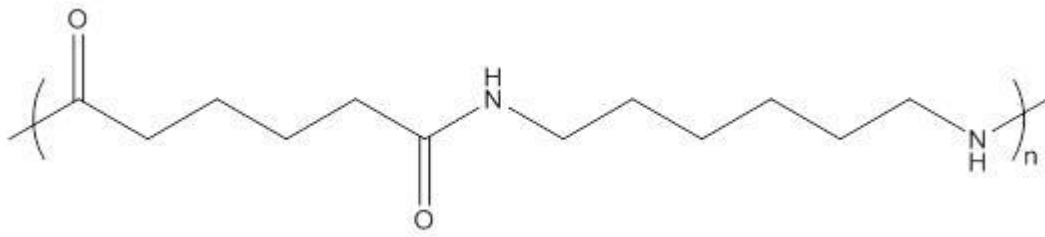


Figure 2-12: Molecular arrangement of Nylon 6,6

2.4.3 How does body armour work?

For body armour to protect the wearer, regardless of threat, it must create an interaction with that threat. This interaction must stop penetration by diminishing the threat's kinetic energy; dispersing it via means that do not cause injury to the wearer (Horsfall, 2012).

When a projectile strikes soft armour, it causes the layers at the impact location to accelerate in the line of travel of the projectile. Penetrating through the ballistic carrier, the projectile instantly encounters the ballistic panel, which will act like a mesh net and deform to try to stop further perforation (Brayley, 2011). Above a critical velocity, the contact load of the projectile will be too great for the first layers of the ballistic pack, causing the yarns to fail, while only reducing the projectile's energy slightly. As progressive deceleration of the projectile occurs, the subsequent layers of the body armour

pack are accelerated less, and thus a stage is reached where the yarn's strength and toughness means they no longer fail. A tensile wave spreads away from the point of contact along the yarns, reducing and absorbing the projectile's energy in the process. As this tensile wave moves along the yarns, a transverse wave is initiated through the pack, albeit at a slower rate of approximately one order of magnitude of the tensile wave (Horsfall, 2012). This process results in the deformation forming a pyramidal shape. Both waves are spread away by the primary fibres that come into contact with the projectile. In woven materials, stress waves are diverted to secondary fibres at crossovers, meaning that kinetic energy in theory is being transferred to secondary fibres away from the impact site. While these crossovers help to disperse the energy and prevent fibres and yarns moving away from the region of impact, reflected waves can cause energy to travel back in the direction it came from, increasing the chance of fibre failure and yarn pull-out, (Tobin and Iremonger, 2006; Carr *et al.*, 2012). A great degree of the surface area of fabric in soft body armour is used to slow down and defeat the impact of a projectile (Brayley, 2011).

In projectiles that deform, as the cross-sectional area of the projectile increases, larger areas of the next layers of the ballistic pack are loaded under tension meaning they are able to reduce the missile's velocity by dissipating and absorbing its kinetic energy (Brayley, 2011; Prat *et al.*, 2012). In non-deforming projectiles this is not the case, and although fabrics are good at dissipating and absorbing energy during impact, and the sheer volume of material involved in soft body armour helps to resist projectile penetration, this is only effective if the fibres engage the projectile (Tobin and Iremonger, 2006). Loosely woven yarns can be parted and penetrated through without fully engaging with the projectile; thus energy transfer is not effective (Horsfall, 2012). In a woven fabric, the fabric sett (number of yarns in both directions/10mm), fabric structure (e.g. plain woven, twill) and through fabric thickness will influence this occurrence (Tobin and Iremonger, 2006).

Multiple layers are often required in order to ensure the critical velocity is overcome, thus making sure the projectile is decelerated sufficiently (Horsfall, 2012). Although the number of fabric layers in a soft body armour pack and the level of protection it provides is not a linear relationship, understanding the interaction is crucial

for soft body armour design (Carr *et al.*, 2012). The inter-layer and inter-yarn interactions of projectile and soft armour are yet to be fully characterised (Horsfall, 2012).

2.4.4 Body armour failure mechanisms

If the body armour wearer is injured by a penetrating projectile, the body armour has failed i.e. it has been perforated. This happens as a result of one of the processes described above not occurring; the armour not engaging sufficiently with the threat or not removing and dispersing its kinetic energy. The energy of the threat divided by its contact cross-sectional area is termed the kinetic energy density (KED), and it is a good measure of penetration capability. For high KED, more penetration protection is required. Velocity is also an important factor; impact velocity squared influences the contact force (Horsfall, 2012).

As stated earlier, soft armours are worn by UK police officers to provide protection against the threat of handgun projectiles. They are effective against this threat because handguns tend to have low velocities ($< 450\text{m/s}$), as well as fairly low KED, which is decreased further in the case of deforming projectiles, i.e. .357" Remington. The soft armours not only have the strength required to halt the progress of this projectile-type during impact, they are also flexible, encouraging movement of the fabric layers during the event; increasing both the distance and time of the impact, and thus the deposition of impact energy. Horsfall (2012) states soft body armour formed from multiple layers of fabric is capable of stopping penetration occurring with KED levels of 20Jmm^{-2} ; a typical level for handgun projectiles.

Soft body armour solutions are not used to provide protection from rifle ammunition, unless they are combined with hard plates (Tobin and Iremonger, 2006). This is because rifle projectiles typically have a higher velocity than handgun projectiles ($> 600\text{m/s}$), together with a similar or higher level of KED, depending on the projectile type. Bullets with a KED of 30Jmm^{-2} against soft armour alone, cause shear failure of the fibres with penetration only stopped if enough layers are present (Horsfall, 2012). The need for increased layers means flexibility is lost, as is comfort. When not enough layers are present, rifle projectiles are able to penetrate against soft armour alone. This is because the yarns are impacted above their critical velocity and the contact load of the projectile is too great.

2.4.5 UK Police soft body armour

Police body armour in the UK is manufactured to meet one or more of seven levels of protection described in the *HOSDB Body Armour Standards for UK Police, Part 2: Ballistic Resistance* (Croft and Longhurst, 2007b). These levels are:

“**HG1/A:** Lightweight-flexible soft armour intended for use by the unarmed officer in very low risk patrolling situations. Suitable for both overt and covert use;

HG1: General Duty soft armour for low risk situations. May be overt or covert;

HG2: Special duty soft armour intended for use in firearms operations. Can be used in conjunction with RF1 and SG1 plates. Usually overt;

HG3: Heavy duty armour intended for use in firearms operations. Can be used in conjunction with RF and SG plates. Overt;

SG1: Offers protection from full-length shotguns at close range. Usually used in conjunction with HG2 armour;

RF1: Offers protection against soft-core ammunition fired from rifles. Usually used in conjunction with HG2 armour;

RF2: Offers protection against steel core high power ammunition fired from rifles. Intended for use in conjunction with HG2 or HG3 armour” (Croft and Longhurst, 2007b, p. 1).

In England and Wales there are 43 different territorial police forces. Police officers within each of these forces will be provided with body armour, albeit varying from one force to another. Deciding which specific armour a police force will wear is a job performed by procurement staff. The nature of a police officer’s job makes it difficult to predict day to day operational duties however, least of all predict potential day to day threats.

Protection to vulnerable areas of the body is paramount. Breeze *et al.* (2015a) have demonstrated the ability of military body armour to reduce wound incidence and severity. However, it is not possible to protect every part of the body while enabling military or police personnel to carry out their duties. As a result, vulnerable areas that are susceptible to fatal and serious injuries take precedence (Horsfall, 2000; Breeze *et al.*, 2015d; Breeze *et al.*, 2015c). These areas include the head and the torso. UK police body armour must provide coverage of the following 5 major organs: the heart, lungs, liver, kidneys and spleen (Figure 2-13).

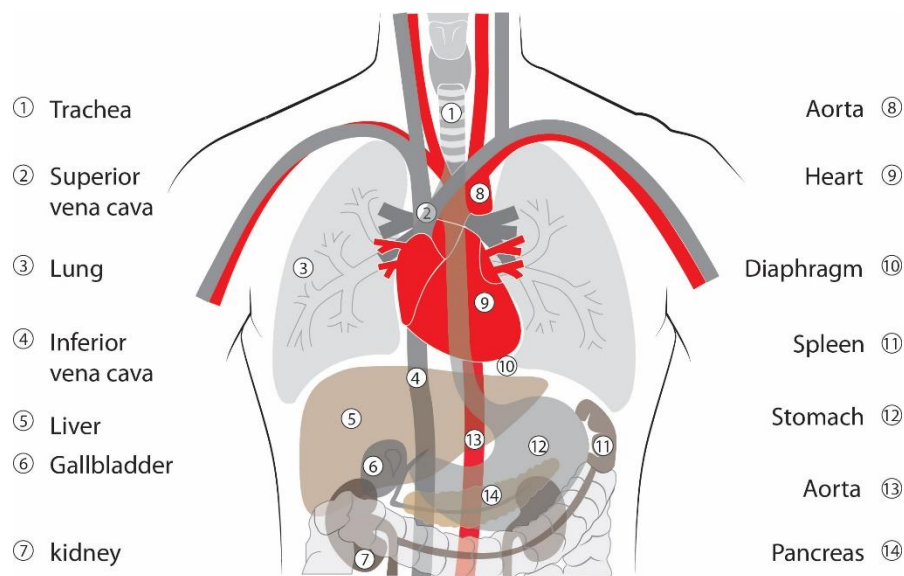


Figure 2-13: Schematic diagram showing the situation of the internal organs of a human torso. Police body armour must protect the heart (9), lungs (3), liver (5), kidneys (7) and spleen (11).

Bleetman and Dyer (2000) assessed the minimum skin-to-organ distances for the kidneys, spleen, pericardium and the minimum depth of the pleura and liver in twenty-five volunteers between the ages of 18 and 50. Ultrasounds were taken of the subjects in three positions and were carried out to aid developments in stab protection for UK police body armour. The measurements from the subjects in the standing position may be a useful for when assessing damage caused after overmatching armour, particularly as the subjects' age were typical of a UK police officer. The results are summarised below (Table 2-7).

Table 2-7: Anterior skin-to-organ distances when standing (Bleetman and Dyer, 2000)

Organ	Mean distance when standing (mm)
Left kidney	31
Right kidney	33
Spleen	22
Pericardium	25
Liver	21
Pleura	17

2.4.7 Summary

Body armour is primarily designed to protect the wearer from penetrating injury. As many threats occur in the form of ballistic projectiles, fragments and sharp weapons, many armour solutions exist. The principles of how to stop these threats are well understood. However, it is not possible to protect the wearer from all these threats with one solution; body armour must be worn and not hinder the wearers' ability to perform their duties. As a result, a compromise is reached, and thus armours are designed to protect from specified threats. Focusing on the identified threats, armours can be specifically engineered to stop the penetrating mechanisms associated with this threat, ensuring the correct protection level is achieved, while factors such as weight and discomfort are limited.

Problems occur when threats are greater than, or they are different (i.e. a ballistic threat against sharp-weapon protective armour), to what is expected. This often leads to the armour being defeated. What is not known however, is the effect armour has on this interaction, and the influence it has on the injury caused to the wearer.

2.5 Review of previous overmatching armour investigations

To overmatch is “to match with a superior opponent” (Allen, 2000, p. 995). With regards to body armour and ammunition, overmatching occurs when body armour that has been designed to defeat a specific threat, is challenged by a greater threat. An example would be an HG1/A armour (an armour designed to protect the wearer from lower velocity hand gun ammunition) being impacted by a rifle round, such as a 7.62 x 39mm round. Although the role of body armour is to protect the wearer from specified threats, there has been limited open source research into what happens should the body armour face a greater than expected threat. The opinions of authors who have carried out research in this area also vary. Due to the limited number of articles that do cover this topic area, this section of the literature review will now critically assess each research study individually.

2.5.1 The shielding capacity of the standard military flak jacket against ballistic injury to the kidney (O’Connell *et al.*, 1988)

A study that investigated the shielding capacity of body armour against direct ballistic injury to the kidneys evaluated shots ranging from low velocity handgun up to high velocity rifle shots (O’Connell *et al.*, 1988). Body armour, in the form of flak jackets constructed from 13 layers of 1500 denier weight Kevlar®, were placed onto both flanks of anaesthetised Yorkshire pigs (45 – 68 kg). Pigs were chosen as the anatomy of their urinary tract closely resembled a human both in terms of size and intrinsic anatomic protection. One shot was fired into each protected pig specimen (n=1) from a distance of 3 m. Only the tests that used M-14 (.308 calibre), M-16 (.223 calibre) and AK-47 (7.62mm) rifles will be discussed, as non-perforating shots are outside the scope of this research. Only one shot of each ammunition type was performed (n=1), but whether firing was carried out remotely or performed by an individual is not stated. The authors placed armour on both sides on the swine to mimic a human wearing body armour, as armour systems provide protection for both the anterior and posterior of the torso.

Post mortem trauma analysis was carried out on the targeted kidneys and the surrounding tissue. The .223 round perforated the anterior armour, but the projectile remained within the animal. In comparison the .308 round perforated both the anterior armour and the animal, but became lodged in the posterior armour. The 7.62 round

perforated the entire target. Autopsies were carried out on all three specimens, with severe external and internal injury discovered in each case. The authors suggested survival following an injury caused by any of the three rifle rounds tested would have been highly unlikely. Although this result is not unexpected, no comment can be made as to whether the body armour affected the level of wounding, as no baseline tests were conducted to compare. Confidence in the results can also be questioned, as only one shot of each ammunition type was conducted.

2.5.2 The personal protective equipment provided for combatants: The part played by wearing a protection vest in the behaviour of projectiles. Wounding outcomes (Breteau *et al.*, 1989)

The work carried out by Breteau *et al.* (1989) included investigating the effects of small calibre and high velocity projectiles on pigs protected by body armour vests that were used at the time by the French Army and law enforcement forces. The presentation of the results in the article is difficult to follow.

Bio-instrumented (instrument information not provided), anaesthetised, Large White pigs (90 kg) were the targets, with shots fired from either 3 m or 25 m, while some shots were also taken at simulated ranges of 50 m or 100 m. The number of shots taken at each distance was not stated. Vests that consisted of 24 layers of Kevlar®, sometimes with a 7mm ceramic plate (no further details provided), were placed on the pigs. Although a 24 layer vest was described in the method, analysis of results mentions vests of 20, 40 and 60 layers that were also tested; no further details of these other vests were given. Results from tests with ceramic plates present are outside the scope of this topic and will not be analysed. Several modern assault rifles were used to fire projectiles i.e. AK74, M193, M855, SS109 and FAMAS F1, although information regarding specific ammunition types was not disclosed. The number of shots fired from each weapon is not presented.

Results found that at all ranges and corresponding velocities (990m/s – 830m/s) all vests were perforated, regardless of a ceramic plate being present or not. Entrance wounds were reportedly larger for protected animals than those observed in animals with no protection, although measurements of the entrance wounds were not presented. X-rays of pigs protected by armour displayed an earlier and more extensive scattering of

fragments to the chest area when impacted with projectiles fired from FAMAS F1, M193, M855 or SS109. At shorter ranges (distance not specified), the more numerous the Kevlar® layers (20, 40, 60 layers), the higher the fragmentation rate of the projectile and the lung contusions were both more extensive and deeper. Details of fragment recovery and their respective size and mass were not given.

Discussing the results, Breteau *et al.* (1989) suggested that placing a body armour vest in front of a perforating round altered the behaviour of the bullet and thus the wound profile, commonly producing wounds with a shorter neck and earlier cavity. No data to support this theory is presented however. As the number of layers present in the armour was increased, the resistance on the bullet escalated during the process of perforation, slowing, destabilising and/or causing fragmentation of the bullet. Once bullet instability had been initiated, the authors hypothesised that it was exacerbated in the target, causing greater damage as a result of yawing and/or fragmentation (depending on ammunition type), when compared to a shot target with no armour. The scatter of fragmentation in the pigs also increased after perforation of armour, as did the presence of reportedly hard to recover fibres of Kevlar®.

2.5.3 Small Arms vs Soft Armour (Prather, 1994)

A pilot study carried out by Prather (1994) investigated the performance of body armour vests against small arms ammunition. The objective was to find out if there was a measurable difference in the wounding effect small arms projectiles caused as the number of layers of protective material was varied. The subject was of interest due to alleged stories regarding the performance of body armour vests (Personnel Armour System for Ground Troops (PASGT), used by US combat troops) that were designed to provide protection from fragmentation. When the vests came under attack from small arms munitions, one common belief was that the presence of the armour ameliorated wounding by reducing bullet impact velocity, while a conflicting story suggested the presence of the vest exacerbated wounding by destabilising the bullet, causing an earlier yaw-in-body motion. No evidence or references supporting either version of the vests' performance were presented.

Armours formed from either 8 or 28 plies of 1000 denier Kevlar® were tested against 7.62 bullets (AK47, 7.91 gram, no further information provided). Initial tests

measuring the retardation characteristics of the two armours were undertaken by measuring the impact and residual velocities of the projectiles (residual velocities were measured with the use of paper grid screens spaced 0.25 m behind the target. No comment was made regarding the method for capturing the impact velocity). Both target armours were set up to be struck at an angle of 0 °, while the 28 ply armour was also tested at a 45 ° angle. Impacts were carried out from ranges varying from 10 m up, while simulated ranges of up to 500 m were also tested. Information regarding simulation procedures was not presented. Distances tested other than the two limits were not clearly defined, nor were which shots were simulated and which were taken from the specified distances. The number of shots taken was also not reported.

Further trials utilised the same ammunition, fired from a Mann barrel secured to a fixed mount and fired remotely. Silver grid break screens spaced 0.5 m apart with a stop screen 50mm from the target were used to capture impact velocities. Gelatine blocks measuring 150mm (h) x 150mm (w) x 400mm (l), 20% in concentration at 10 ° C, were used as tissue simulant targets. Shots were fired into gelatine blocks and gelatine blocks with armour in front, although the number of times this was repeated is not stated. It is unclear whether both armour types were tested, or if just the 28-ply armour was used. Penetration-time measurements were obtained from analysis of high speed films taken. No further information about the high speed camera is given. Pictures and information on the post-firing analysis carried out on the targets is also lacking.

Results from the initial tests were presented in the form of a graph, with no corresponding tabulated data. Prather claims velocities that simulated ranges out to 500 m lost approximately 12 – 20m/s after perforation of the 28-ply sample (e.g. $V_i = 855\text{m/s}$, $V_r = 842\text{m/s}$; $V_i = 517\text{m/s}$, $V_r = 498\text{m/s}$). No comment is made on the performance of the 8-ply armour, although examining the graphical results suggests projectiles lost a similar rate of velocity as a result of perforating the armour. The velocity that is expected at 500 m is not stated, nor is it explained how this was known or tested for. The level of tension and support applied to the target armours is not provided, potential factors that may have influenced results. Examining the paper grid screens behind the target revealed instability of the projectiles did not occur at velocities above 430m/s. Below this, bullets yawed on exit, although whether this was the case after perforation of just one or both armour types

is not clear. Yawing was seen after perforation of the 28 ply armour at a 45° angle at velocities of 488m/s and below.

No results are presented from the tests that used gelatine as a tissue simulant. However, the probability of incapacitation, given a hit $P(I|H)$ is discussed. This is where bullet lethality is estimated by measuring the energy deposited by a projectile in gelatine before relating the kinetic energy deposited to a previously determined empirical relationship between energy and $P(I|H)$. Prather (1994) claims measuring kinetic energy enables the physical damage a projectile causes biological tissues to be quantified. This is done by correlating energy deposited in 20% gelatine to average wound tract volume, before correlating this result to incapacitation estimates. The energy deposited per unit length in 20% gelatine is then weighted by the probability of encountering tissue at that depth in a human, or a human body part e.g. thorax. The cumulative weighted energy deposit (for aimed fire) is designated ARRADCOM Kinetic Energy (AKE). AKE is equated to the $P(I|H)$ from previously determined results e.g. from ballistic trials and medical data.

For impact velocities simulating ranges of nearly 500 m (impact velocities not given), no significant differences were found between $P(I|H)_{\text{thorax}}$, in gelatine targets and targets of gelatine protected by. AKE values were approximately 10% lower for shots into armour-protected gelatine compared to just gelatine blocks, resulting in $P(I|H)_{\text{thorax}}$ values that varied by less than 1%. No data is provided to support this claim, nor is it stated that statistical analysis was carried out to validate the significant differences.

For impact velocities of 430m/s, the AKE value for targets of armour and gelatine was double that compared to the AKE value for gelatine targets. This led to a 7% increase in the $P(I|H)_{\text{thorax}}$, but again, presentation of data to support these claims was lacking. Increased instability exhibited by the bullet after penetrating the 28-ply sample was put forward as the reason for the increase seen, however, no comment on instability and the effect it had on the $P(I|H)_{\text{thorax}}$ was made.

Estimating bullet lethality and quantifying the physical damage a bullet can cause form a good basis for assessing whether the presence of soft armour affects injuries negatively. However, with no data or calculations presented, the eluded-to results carry little evidential strength. This is not helped by not knowing the number of shots that were carried out. Results from the initial trial showed that when armour was positioned at a 45°

angle, instability of the projectile occurred at higher velocities (488m/s compared to 430m/s); yet testing armour at a 45 ° angle with a backing simulant was not conducted. The second trial reportedly indicated that impact velocity played an important role increasing $P(I | H)_{\text{thorax}}$ by 7%, yet it was concluded that the armour did not significantly affect the wounding characteristics at realistic engagement distances (not further elaborated). An explanation of this conclusion was not provided, however a call for investigation into the effect other armours and projectiles have was requested.

2.5.4 Study on the wound ballistics of fragmentation protective vests following penetration by handgun and assault rifle bullets (Missliwetz *et al.*, 1995)

Missliwetz *et al.* (1995) reported that bullets would penetrate body armour vests, but that whether wounding would be exacerbated was not clear. The armours tested were those typically worn by military personnel (country not stated) to provide protection from fragments. Three different commercially available vest types were used: nylon vest (mass 4.340 kg; V_{50} 389m/s), Kevlar® vest (mass 4.406 kg; V_{50} 506m/s) and Kevlar® vest (mass 2.928 kg; V_{50} 413m/s). The number of layers of fabric in the body armours was not stated. The vests were tested with four ammunition types: 5.56 x 45mm (S-Patr StG 77; mass 3.61 g), 7.62 x 39mm (M-58-CSSR; mass 7.86 g), 7.62 x 51mm (S-Patr StG 58; mass 9.47 g) and 9mm Luger (S-Patr P 08; mass 7.98 g). The justification for the ammunition types used was that they represented a sample of common infantry weapon calibres together with the most common pistol ammunition for both the military and police in Europe.

Two trials were reported, the aims of which were: to examine the stability and deformation/fragmentation of the bullets, and to investigate the maximum temporary cavity size and the energy levels used to produce them. The first trial used ten waxed paper indicator disks arranged 0.5 m apart behind the body armours to record bullet stability after perforation of the vests. Fifty-six shots were taken in the first trial, at either a range of 10 m (n = 30) or 100 m (n = 26), although no information regarding the method of firing was given i.e. weapon or proof housing. The number of shots for each calibre varied (9mm Luger n = 19 shots; 7.62 x 39mm n = 14; 7.62 x 51mm n = 11 and .223 Remington n = 12). Analysis into the deviation of the circular form of the shot through

the indicator paper was used to judge instability. Although the instability of the bullets is captured in this trial, the influence dense tissues would have on the level of instability is not accounted for.

In the second trial, soap blocks (300mm in length, no further information given) were used to capture temporary cavities. A range of 100 m was used for this trial, no information was provided regarding firing method. The number of shots taken was not specified. Cavities produced after perforation of armour were compared to cavities produced in unprotected soap blocks, i.e. no armour was present. The use of soap blocks as a simulant was justified by claiming that according to both Sellier and Kneubuehl (1992, cited in Misliwetz *et al.*, 1995), and Tikka *et al.* (1982, cited in Misliwetz *et al.*, 1995), gelatine and soap produce comparable results. In light of this, soap was chosen as the authors' state it was easier to evaluate and document temporary cavities than in gelatine. The claim that both gelatine and soap produce comparable results is questionable. Gelatine is capable of capturing the permanent cavity due to its elastic nature, while the formation of the temporary cavity can be witnessed with the aid of high speed imagery. It is only possible to capture the temporary cavity in soap, which is often a lot larger than the permanent cavity. The gelatine concentration would also alter the cavities seen, with the concentration that is being compared to soap not specified.

Results from the first trial reported 18 out of the 56 shots (32%) fired at armours backed by paper indicator disks became unstable (Misliwetz *et al.* (1995) define instability as when the angle of bullet deviation exceeds 2 degrees) after perforation of the vest. Although a table of results breaks down under which parameters instability was witnessed (ammunition type, range, and vest type), no statistical analysis, nor comparison, of results was reported. Shot details and cavity measurements are tabulated from the second trial, with mean values from perforation of the 3 body armour types compared to the base line shots. Again, other than direct comparisons of means, no statistical analysis was presented.

Misliwetz *et al.* (1995) suggested that from the spread of their results from the first trial, bullet instability could not be assigned to a certain range or ammunition type, and that an undefinable feature could be a factor. They do, however, claim that it is probable that the material of the armour and how it is produced has an influence on instability. However, the results from any material analysis are not presented.

Analysis of the temporary cavities captured in soap suggested that in the majority of cases where armour was present, the initial channel of the damage was shorter. This was reported as a possible indication that bullet instability occurred earlier compared to when no protection was present, a result Misliwetz *et al.* describe as unfavourable as instability of a bullet results in quicker energy release. The other measurement that was taken, the temporary cavity diameter, was generally smaller when body armour was present. Perhaps not a surprising result as the bullets are slower and therefore have less kinetic energy after defeating the armour, however there were cases where the diameters were larger after perforation of the vests, namely when 5.56 x 45mm ammunition was used. The armour type also had an effect on diameter size, with the lightest Kevlar® vest on average causing diameters larger than shots when no vests were present. No potential reason for either of these observations was suggested; material analysis could have potentially provided an insight.

In summary, when armour was tested, a shorter channel which could potentially induce an earlier instability of the bullet was offset by a smaller temporary diameter due to the reduced bullet energy. An outcome such as this would mean a soldier and/or police officer wearing the vests tested would not necessarily come off worse than an unprotected individual, however, effects could occasionally be intensified. These results are based on empirical data only, from a handful of vest types and ammunition rounds, making an overall prediction unmanageable. Range is also a factor that would influence results, and when combined with both different ammunition and armour combinations, the degree of injuries produced can be hypothesised to be highly variable. Although the temporary cavities were compared, the use of gelatine would have given the option to compare permanent cavities, which are likely to have a greater effect on a human subject compared to the temporary cavity that only lasts a matter of milliseconds. The presence of fragments in the cavities produced was not commented on either, a factor that could greatly alter the amount of damage caused. Analysis into the failure of the materials in the vests may also have led to a greater understanding of the subject.

2.5.5 The destabilising effect of body armour on military rifle bullets (Knudsen and Sørensen, 1997)

This study investigated bullet behaviour after perforation of soft body armour. Using an AK-47 rifle mounted in a permanent stand and fired by remote control, 7.62 x 39mm (FMJ, LAPUA) rounds were fired at two types of soft body armour. Both armours were made from Kevlar® fibres, one of 14 layers with an areal density of 2.66 kg/m², the other of 28 layers with an areal density of 5.32 kg/m². Both armour types were fitted to frames without tension at angles of 60 ° and 90 °, 30 m down range. No tissue simulants or backing materials were used; instead, two techniques that utilised a shadowgraph or a Doppler radar were used to estimate the yaw of the bullets.

Initial tests reported that both energy and loss of spin rate decreased by less than 1% after perforation of both armour types, however, the data from these tests are not provided. Results of bullet yaw from ten reference shots were tabulated against ten shots into both body armours tested at both angles. Induced instability after perforation of both armour types was reported, with mean yaw angle smallest for the reference shots (1.04 °, range 0–2.62 °). Perforation of the 14 layer armour at 90 ° produced larger mean yaw angles (3.76 °, range 1.77–9.92 °), while the largest mean yaw angles occurred after perforation of the 28 layer armour at 60 ° (19.88 °, range 6.89–38.28 °).

Comparison of the yaw angle results with previous work led Knudsen and Sørensen (1997) to suggest that perforation of the armour formed from 14 layers of Kevlar® at both angles of impact would cause damage similar in nature to those produced by 7.62 NATO bullets at similar distances. However, when comparing results collected after perforation of the 28 layer armour, especially when the armour was at 60 °, it was hypothesised the damage seen would be far greater, as the yaw angle was far greater than any other shots they had tested. The authors suggested that as the thickness and/or angling of the soft armour were increased, destabilisation increased. Investigating a wider range of angles, particularly acute angles, would either provide further evidence to support the claim that bullet instability increases as the angle of the body armour increases, or disprove it, and highlight which angles cause the greatest instability.

A limitation of this study, by the authors' own admission, is the lack of tissue simulant. Yaw is defined as the total angle of incidence that a projectile makes with the line of fire (Textbook of ballistics and gunnery 1987, cited by Knudsen and Sørensen,

1997). If it is to be believed that a bullet striking a target at a greater yaw angle after perforation of body armour causes an earlier turning-over of the bullet in the target, and thus transfers greater energy, increasing the potential for damage; the behaviour of the bullet in a simulant must be captured. If the bullet continues to travel through air, the bullet will stabilise itself again by design, especially taking into consideration that loss of spin rate after perforation was claimed to be negligible. Therefore, measuring the yaw angle immediately after perforation of the armours may not give a representation of what would happen should a human target be struck. Breaking up of rounds after contact with a target (e.g. striking bone) is also a potential outcome that is not considered in this study.

2.5.6 Is the wounding potential of high velocity military bullets increased after perforation of textile body armour? (Lanthier, 2003; Lanthier *et al.*, 2004)

Lanthier (2003) and Lanthier *et al.* (2004) investigated whether injuries to the human body caused by high velocity bullets were exacerbated after perforation of body armour. AK-74 5.45 x 39mm bullets (600m/s and 900m/s) were fired at glycerine soap blocks fitted with and without armour from 10 m. The armour was constructed of 18 stitched layers of woven para-aramid fabric, with an areal density of 3.96 kg/m².

Initial tests investigated bullet velocity and yaw behaviour after perforation of the armour. Yaw increased after armour perforation, but little velocity was lost, a result that agreed with the findings of Knudsen and Sørensen (1997). A suggested reason for the lack of velocity loss was due to the bullets displacing the armour fibres and not breaking them. No images or any other means were presented in the paper to support this theory.

For the main trial, a new soap block (250mm x 250mm x 400mm) was used for each shot, while a soft capture system was placed behind every block for when the blocks were not large enough to capture the bullets. Five rounds were fired at approximately 900m/s at soap blocks, with a further five fired at armour plus soap blocks. Five further shots were taken using the 5.56 x 39mm round, but the propellant mass was reduced in order to get velocities of approximately 600m/s. Two shots were fired into soap blocks, with the other three into soap blocks complete with armour. Measurements of the entrance, exit, and diameter of the temporary cavities were taken, as was the volume by filling the cavity with water. Any debris present was noted.

T-tests were used to compare the data from soap blocks with and without armour and reportedly suggested there was “a low probability that the data sets had the same mean.” No further information is provided however and the results of the statistical analysis are not presented. Direct comparison of the two data sets indicated that the presence of armour resulted in the entry channel (also referred to as the ‘neck’) being narrower and longer, while also reducing the diameters and volumes of the temporary cavities. The authors suggested that the results demonstrated an injury reduction when body armour was overmatched compared to no body armour being present; a longer entry channel implies bullet stability while smaller diameters and volumes imply a reduction in energy transfer and transmitted shock. While a smaller volume may indicate a lower energy transfer rate, it does also reduce the risk of vital organs being struck, as a smaller cavity may mean certain organs avoid being affected.

The authors reported that the results indicated that soft textile armour may not exacerbate injuries after perforation of high velocity bullets. They did however, call for further research to consider other ammunition types and soft body armours. The use of a different tissue simulant that captures the permanent cavity may also be more advantageous for future research.

2.5.7 Miscellaneous

Fackler (1989) claimed research into a projectile’s capacity to wound after passing through protective equipment was both a pertinent question and a real concern.

The subject of overmatching was touched upon by Berlin *et al.* (1979). The question was raised regarding what effect body armour had on the ballistic behaviour of a bullet and whether any of the surgeons that were present had seen wound differences in casualties who had and hadn’t been wearing armour. One panel member (M. Owen-Smith) stated that in his experience, soft flexible armour did not influence penetrating chest injuries, particularly in shots that went through the heart or great vessels, as these injuries would ultimately be fatal regardless. Another member, B. Janson mentioned an investigation that involved soap blocks with 12 layers of nylon cloth placed 25mm in front of them being shot at with two different rounds (M193 bullets, no further information given, and 7.62mm bullets, no further information given). He stated an increased energy transfer was seen for both ammunition types, with the energy transfer

from the 7.62mm rounds approximately double that of when no armour was present. These results were interpreted as being caused by the body armour disturbing the bullet during its flight, before striking the simulant with a greater angle of yaw than normal. It would be unusual however, for someone wearing body armour to have the armour a distance of 25mm away from their body. A final comment on the subject was provided by W. Kokinakis, who claimed from investigations he had seen, large energy deposits and high yaws/overturning moments occurred early in targets, regardless of bullet calibre. Nylon vests with 11 or 12 layers were used in this study, however, information regarding the ammunition and target material was not discussed.

While investigating wounds to determine both entry and exit holes of gunshots, Stone and Petty (1991) claimed the striking of interposed targets could affect the stability of projectiles. Interposed targets were defined as objects or materials through which a projectile may pass after leaving the muzzle of a weapon before entering the target, to which body armour could be included. No cases of body armour as an interposed target were discussed; however, injuries caused by multiple projectiles were suggested as a possible consequence of striking interposed targets.

2.5.8 Case studies

Examples of military personal and police officers wearing body armour impacted by ammunition threats greater than expected may not provide any information on whether the presence of the body armour exacerbates the damage caused. This is because there is unlikely to ever be a case where identical shot parameters are duplicated, one into a target with body armour and one without. With that said, exploring that the topic is a real world issue is worthwhile, and may help to provide information on the types of scenarios where this issue may be encountered.

From a military perspective, fragmentation is the predominant threat to soldiers in modern conflicts; however, ballistic attacks are still common place (Lanthier *et al.*, 2004; White, 2013). Reviewing the fatalities that occurred during conflict in the West Bank between the 22nd of March and 30th April 2002, it was revealed that 22 soldiers (out of 26 cases examined) died while were wearing Kevlar® military personal armour system (MPAS) vests, with no added ceramic protection (Kosashvili *et al.*, 2005). The 26 fatalities suffered a total of 149 entrance wounds; 76 wounds (51%) were from fragments

and 73 (49%) were from bullets. Twelve fatalities (46%) were due to injuries from a combination of fragments and bullets, with 14 (54%) due to injuries solely from bullets. None of the fatalities were due to injuries caused purely by fragments.

Considering only round bullet entry holes, sixteen (49%) occurred in body regions that were covered by Kevlar® vests, and 17 (51%) occurred in uncovered regions. The locations of the remaining 40 irregular bullet entrance wounds were not given, without any reason provided for why they were excluded from the analysis. Injuries due to fragments in protected regions were very few, highlighting the protective effect of Kevlar® vests. However, very limited protection, if any, was offered against bullets. Statistical analysis of diameters of entry wounds in the covered versus uncovered regions revealed no significant differences (0.79 ± 0.42 cm vs. 0.73 ± 0.29 cm; $\rho = 0.11$), with the authors claiming the presence of armour did not seem to worsen the outcome of bullet injuries. Dimensions of the wounds other than the entrance diameters were not presented. Judging wounding outcomes solely on entrance diameters is not a fair representation of the damage produced by a bullet. This research provides evidence that the overmatching of armour is an issue, whilst also highlighting the role armour plays in protecting individuals from threats it is designed to defeat.

During conflict, instances can arise where weapon fire from one's own side can cause injury or death to one's team members. When these attacks are accidental, possibly caused by being caught in cross-fire, or by disorientated actions, it is called friendly fire (Pearsall, 1999). Instances can occur where these attacks are not accidental, and these instances are often termed green-on-green attacks, if it is a case of military personal firing at other military personal. Cases also arise where non-military members who are tasked to work alongside military forces, such as security forces and members of police forces, can open fire on military members, with these attacks often named green-on-blue. The issue is highlighted from casualty analysis from the conflict that began in 2001 in Afghanistan, with 21 deaths of coalition military members being a direct result of green-on-blue attacks (White, 2013), and with the United States of America Department of Justice stating 57 green-on-blue attacks have been recorded since 2007 (Marshall, 2012). As specific details into the attacks are often not available in the open source literature, analysis into the individual cases will not be carried out. Comment on whether victims were wearing protective clothing, or on whether the location on the victim was protected

cannot be made. Nonetheless, the figures highlight the need to ensure the level of protection provided takes into consideration the combination of both the weapon and ammunition type that will be used in conjunction with the armour worn. If it is not possible to ensure the level of protection is capable of protecting from the weapon/ammunition threat, ensuring the armour worn does not exacerbate the wounding potential is of paramount importance.

The threats faced by police differ greatly from those encountered by military personnel, although cases of over matching still occur. In the United States of America, between the years of 1991 and 2001, 21 deaths were caused by perforation of soft body armour from rifle fire (Federal Bureau of Investigation, 2001, cited by Wilhelm and Bir, 2003). From the period of 2003 to 2012, 321 law enforcement officers were feloniously killed due to ballistic attack (Federal Bureau of Investigation, 2012). Of these incidents, 21 (7%) were due to shots at the torso that used ammunition that was too powerful for the armour that was worn; with a further incident the result of a shot striking armour on the torso that failed. In all 21 cases, rifle ammunition, ranging in calibre size from .223 to 7.62 x 39mm, was used.

2.5.9 Summary

Studies that have been conducted in the area of overmatching are limited, especially considering the number of possible combinations that could be trialled using different ammunition types and different armour constructions. A potential reason why conflicting answers have been presented and that no definitive answer has been put forward can be put down to the fact many combinations are possible and that different combinations have been trialled in the previous research. Although this does suggest a definitive answer to the question of overmatching is unlikely, comparison to these results could help find patterns of when overmatching does and does not happen. Considering the real life case studies does however highlight that overmatching occurs, and the more understanding there is of the topic, the better.

2.6 Overall summary of literature review

Reviewing the literature of the four pivotal areas involved in this research question has uncovered many points from which this thesis will now develop.

Considering the limited work that has been done before within the area of overmatching, choice of ammunition should take into consideration projectiles that behave differently after impact i.e. a selection covering rounds that breakup and fragment, expand and remain intact would be ideal. The consideration of body armour should include armour that provides protection from knife and spike threats too, as not only does it not appear to have been investigated before, but knife and stab threats are the most prevalent to affect police officers in the UK; it's logical to believe these will be some of the most common armour types worn by patrolling officers.

A criticism of some of the literature that had studied overmatching before was the lack of tissue or tissue simulant used, so the damage was not captured. To assess whether damage has been affected by the presence of body armour, a tissue simulant is going to be required. The review of simulants shows many have been tried and tested, yet no standards exist to make them. The choice of a simulant that will be used throughout must be made, with the requirements that it is reliable and reproducible, as well as being able to capture the damage produced in a way that can be compared.

A final consideration is the method which characterises and compares any damage that is collected. Disagreements exist over which factor is most influential during the process of bullet penetration, the crushing and lacerating, or the temporary cavitation. This is not necessarily a point of contention this thesis is concerned with; being able to capture and compare both would be an advantage as the more information gathered, the stronger the evidence. Estimation of the amount of energy deposited should also be strongly considered.

The work presented in this thesis will aim to determine the effects of overmatching UK police body armour. Prior to that, an initial study investigating which tissue simulant would be best suited for this research will be presented.

Chapter 3 : EXPERIMENTAL SELECTION AND JUSTIFICATION OF A TISSUE SIMULANT

3.1 Introduction

As discussed in Chapter 2, many tissue simulants have been, and continue to be, used in the study of ballistics. That said, no internationally agreed standard exists for the preparation of such tissue simulants; a factor that has led to questions regarding reliability and reproducibility of results presented in the open literature (e.g. Jussila, 2004; MacPherson, 2005). In order to assess the overmatching of body armour, analysis of damage caused is essential, thus, a simulant that is both repeatable and reproducible is a vital part of the testing required.

Chapter 3 discusses work that was undertaken in order to select a simulant from those covered in the literature review, which would be used throughout the rest of this research into the overmatching of body armour. This chapter is split into three parts: *Part A – Depth of penetration of 5.5mm ball bearings*, *Part B – Baseline simulant tests* and *Part C – Ballistic testing of porcine samples*.

3.2 Part A – Depth of penetration of 5.5mm ball bearings

Part A describes preliminary experiments designed to test the repeatability and reproducibility of four different simulants by measuring the depth of penetration (DoP) of non-deforming projectiles (i.e. steel ball bearings, BBs) fired at various velocities (100m/s – 1050m/s). The simulants used were: 10% gelatine, 20% gelatine, Perma-Gel™ and re-melted Perma-Gel™. These gelatine concentrations were tested as they are very commonly used as simulants in wound ballistic studies though very little research has compared them. Perma-Gel™ was tested as it had the potential of being an ideal simulant, albeit though prior ballistic testing was limited.

BBs were used as they are not affected by yaw (2.2.3.1.2 *Yawing in tissue*) nor will deform on or after impact; by using them it was possible to study the effect of velocity on DoP, without any influence from projectile yaw and deformation. A wide range of velocities was used to cover the impact velocities of the ammunition of interest that was to be used later in the study (~420m/s and ~840m/s respectively), while also taking into

consideration that gelatine is strain rate sensitive (Shepherd *et al.*, 2009; Cronin and Falzon, 2011).

Other than the impact velocity and DoP, no further analysis on the simulants was carried out, as the aim of this trial was to assess the reliability and reproducibility of the simulants with respect to DoP, not the damage produced. There is currently no known conversion method to confidently compare results recorded in different concentrations of gelatine, as work in the open literature that has tested both concentrations is scarce (e.g. Bourget *et al.*, 2012; Mabbott *et al.*, 2013). Open-source literature that uses Perma-Gel™ as a simulant in ballistic testing is also lacking (Boackle, 2011; Ryckman *et al.*, 2011; Mabbott *et al.*, 2013).

3.2.1 Materials and methods

3.2.1.1 Simulants

3.2.1.1.1 Gelatine

Gelatine with Bloom strength 225-265 (Type 3 ballistic photographic grade gelatine (Gelita UK Ltd., 3 Macclesfield Road, Cheshire CW4 7NF, UK)) from a single batch (Appendix B) was used to manufacture all 10% and 20% gelatine blocks (e.g. Figure 3-1). In order for the blocks to set and then reach the required temperatures throughout, blocks were made two days prior to testing following methods developed during this research (Appendix C and D respectively). The literature review (2.3.2.5 *Block size*) was taken into account when considering block sizes. Blocks measuring 250mm (w) x 250mm (h) x 500mm (l) were chosen as they were capable of capturing wound profiles of multiple handgun shots and of single high velocity shots. To create blocks of this size, custom-made moulds were produced, which measured 250mm (w) x 250mm (h) x 500mm (l) at the base, with both longer sides tapered 1 ° to facilitate set gelatine removal (Figure 3-2).

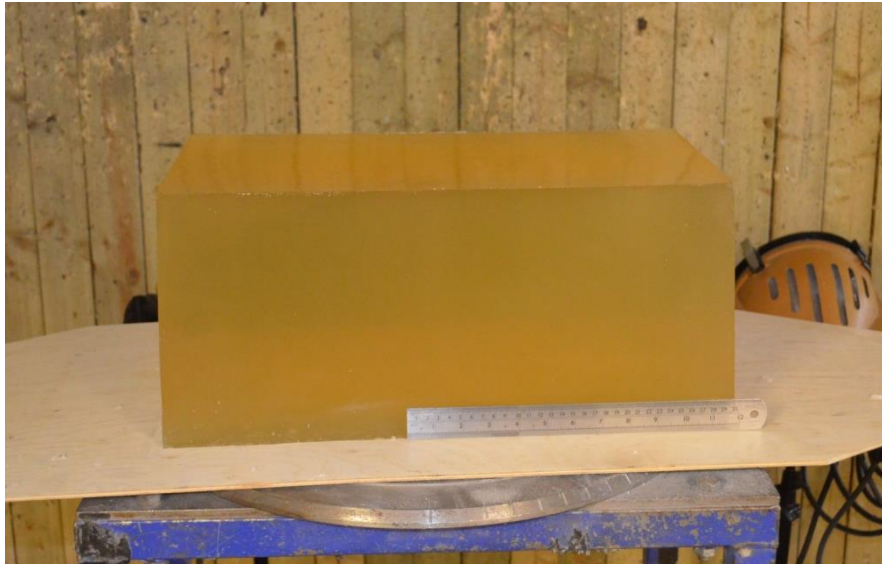


Figure 3-1: Typical example of the gelatine blocks produced



Figure 3-2: Moulds used for casting blocks

3.2.1.1.2 Perma-Gel™

Perma-Gel™ blocks were purchased (from USLACO, LLC, 2601 Cannery Avenue, Baltimore, MD 21226, USA) in the raw base media form. Blocks only came in one size; dimensions were approximately 295mm (w) x 100mm (h) x 445mm (l). These blocks were placed into a roaster oven (sourced from Midway UK Ltd, P.O. Box 4300, Warwick, CV34 9BR, UK) (Figure 3-3) and following the instructions provided with the Perma-Gel™, melted to form blocks ready for testing (Figure 3-4). Thus these blocks were smaller than the gelatine blocks.

When the Perma-Gel™ blocks had been used once, they were re-melted into blocks the same size as the gelatine blocks. This used approximately 26 Kg of Perma-Gel™. The Perma-Gel™ was melted in an environmental chamber set to 115 °C using a

sieving system (Figure 3-5) to filter out any debris from the blocks. Once melted down, the larger blocks were left at room temperature for at least 2 days before testing to ensure the internal temperature of the blocks was within the recommended range (55 – 75 ° F; 12.7 – 23.9 ° C) (Figure 3-6).



Figure 3-3: Roaster oven used for the melting of Perma-Gel™ raw base media



Figure 3-4: Example of a Perma-Gel™ block ready for testing

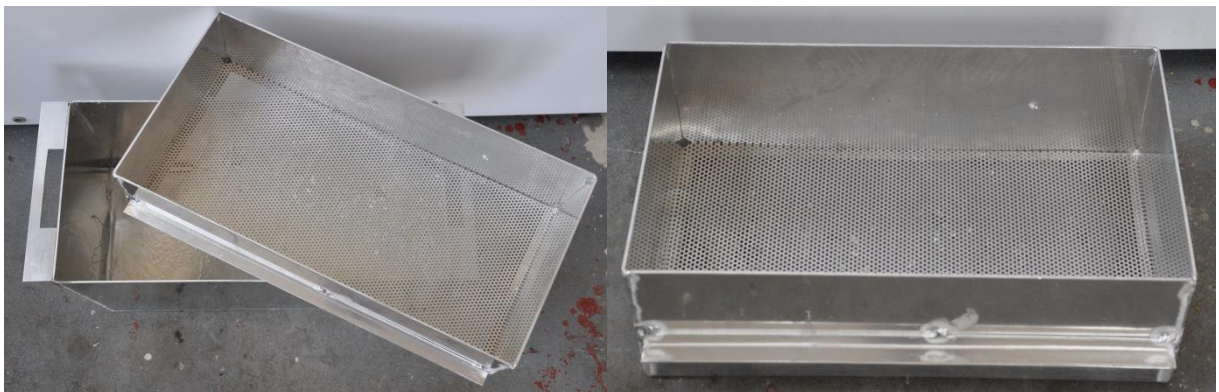


Figure 3-5: Sieving system used for the casting of larger Perma-Gel™ blocks



Figure 3-6: Perma-Gel™ block after being re-melted and cast into larger block

3.2.1.2 Ball bearings

Non-deformable 0.68 g stainless steel BBs 5.5mm in diameter were used (Atlas Ball & Bearing Co. LTD, Leamore Lane, Walsall, WS2 7DE, UK.). This diameter of ball bearing was used as they were of a similar diameter to ammunition of interest; mm .223 Remington (5.56 x 45mm) ammunition. A range of velocities were used for testing: 150m/s, 250m/s, 500m/s, 750m/s and 1050m/s. This was in order to test the simulants at impact velocities across both typical handgun and rifle impact velocities. Testing a large range of velocities could be important as it has been shown gelatine is strain-rate sensitive (Shepherd *et al.*, 2009; Cronin and Falzon, 2011).

3.2.1.3 Depth of penetration testing method

The BBs were secured in a polymeric sabot before being fitted into a 7.62 x 51mm cartridge case for firing (Figure 3-7). The cases were sourced from Sporting Services, Townhall Chambers, 148 High Street, Herne Bay, Kent, CT6 5NW, UK. Varying amounts of two types of propellant (N130 and N330) were used in order to achieve the desired impact velocities (Table 3-1).

The experimental set up is presented schematically below (Figure 3-8). The BBs were fired from an Enfield Number 3 Proof Housing (Figure 3-9) using a barrel of either 20" or 22" in length (from a GPMG and an FAL SLR respectively); different barrels were

required to achieve the range of velocities. The simulant targets were placed 10 m downrange from the end of the muzzle (Figure 3-10). Impact velocities were recorded using a Weibel W-700 Doppler radar (Manufactured by Weibel. Origin – Unknown.).

The impact events were recorded using a Phantom high-speed video camera (V12) (41,025 fps, 5 μ s exposure time and 512 x 256 frame resolution). The target block was illuminated from the rear and front using two Photon Beam lights. A scale was used in all impacts to allow the high-speed video footage to be calibrated. Depth of penetration into the simulants by the BBs was measured using a metal rod (1mm diameter) and a 1 m steel ruler (Figure 3-11). Neither the tract nor the permanent cavity of each individual shot came into contact with another shot. Testing into Perma-Gel™ blocks was limited by the original blocks not being long enough to capture the penetration of BBs over 1000m/s. Thus, velocity bins of 150m/s, 250m/s, 500m/s and 750m/s were used for raw base blocks; 1050m/s was added for re-melted blocks which were long enough to capture these BBs.



Figure 3-7: 7.56 x 51mm cartridge case, sabot and 5.5mm BB used for DoP testing

Table 3-1: Ballistic test variables

Desired impact velocity (m/s)	Type of propellant	Propellant mass (g)	Wad?	Type of barrel
150	N330	0.21	Yes	FAL SLR (20")
250	N330	0.30	Yes	FAL SLR (20")
500	N330	0.53	Yes	FAL SLR (20")
750	N130	2.70	No	FAL SLR (20")
1050	N130	3.00	No	GPMG (22")

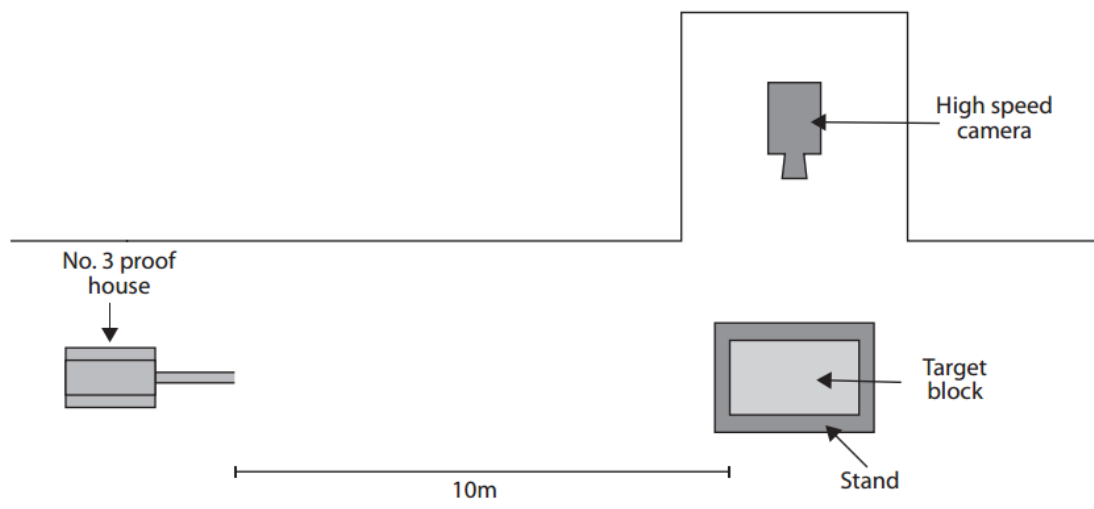


Figure 3-8: Schematic of the experimental setup for the depth of penetration testing of 5.5mm BBs.



Figure 3-9: Enfield Number 3 Proof Housing set up



Figure 3-10: Target set up complete with a 20% gelatine block

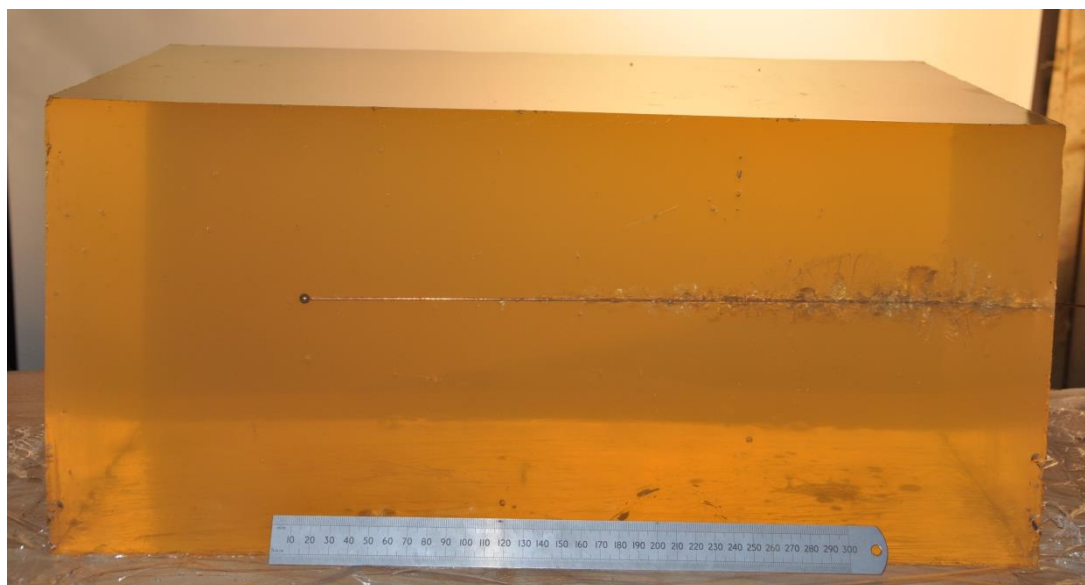


Figure 3-11: Penetration depth being measured with the use of a metal rod

3.2.1.4 Depth of penetration analysis

Summary statistics (mean (\bar{x}), standard deviation (s.d.) and coefficient of variation (CV)) were calculated for the DoP data. In order to do this, recorded impact velocities were grouped into bins (Table 3-2). Analysis of variance (ANOVA) and Tukey's HSD tests were used to determine when significant differences were present among velocity

bins (SPSS Statistics 22.0; a description of the statistical tests used can be found in Appendix E). ANOVA was used as it is a robust method for comparing three or more datasets which are normally distributed (Harraway, 1997). Normality of data and equality of variance were checked for each data set.

Table 3-2: Velocity bins used for data analysis

Velocity bins (m/s)	Velocity range for bins (m/s)
150	110 – 190
250	210 – 290
500	460 – 540
750	710 – 790
1050	1010 – 1090

3.2.2 Results

Figure 3-12 displays the impact velocities plotted against DoPs of 5.5mm BBs into the four simulants tested (10% gelatine, 20% gelatine, Perma-Gel™ and re-melted Perma-Gel™). The graph shows 10% and 20% gelatine following a similar pattern albeit with DoP greater in 10% gelatine. Perma-Gel™ and re-melted Perma-Gel™ follow a different pattern. DoP in both types of Perma-Gel™ is similar to 10% gelatine at approximately 400m/s however when compared to 10% gelatine against the range of velocities, DoP is shorter in both types of Perma-Gel™ at velocities less than 400m/s, and longer for velocities of 400m/s or more. The shortest DoP was in 20% gelatine, while the largest was in re-melted Perma-Gel™.

The mean impact velocities for each velocity bin plotted against mean DoP with standard deviations can be seen in Figure 3-13. As with Figure 3-11, the graph shows similar patterns for the two gelatine concentrations, with the two Perma-Gel™ simulant types having shorter mean DoP compared to 10% gelatine below 400m/s and greater at velocities over 400m/s.

Figure 3-14 is a graph of kinetic energy density plotted against DoP, which compares results from this research together with DoP data gathered from the open literature. The raw data for these graphs can be found in Appendix F. Results for 10% gelatine at the lower end of the velocities tested from this current study fit well with results from Jussila (2004). Comparing the current DoP results for 10% gelatine with

those produced by Bourget *et al.* (2012) revealed a pattern that followed the same configuration except for kinetic energy density values of approximately 3-4 J/mm². When comparing 20% gelatine the results followed the same formation, apart from DoPs at kinetic energy values between approximately 5 and 8 J/mm².

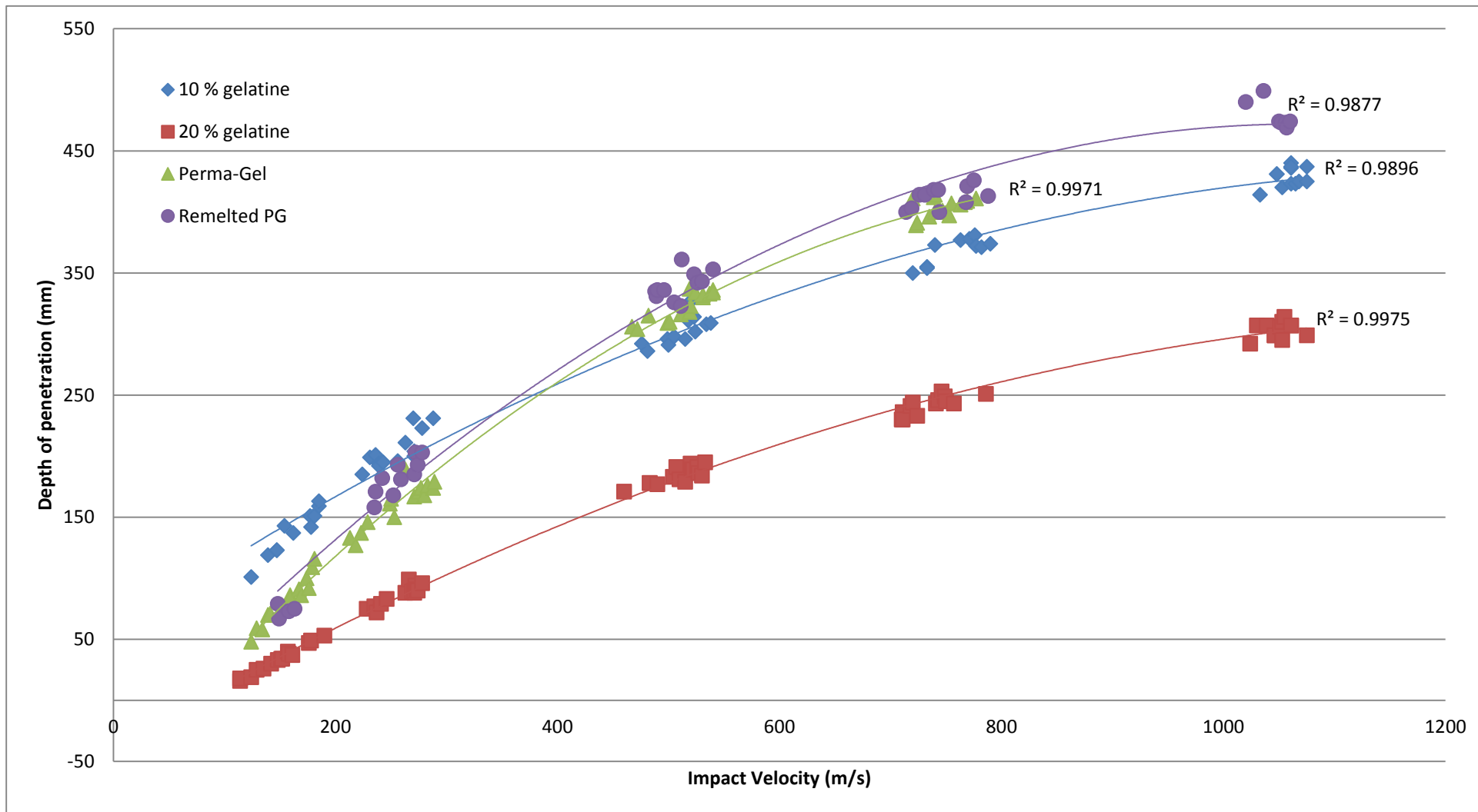


Figure 3-12: Graph of impact velocity vs. DoP for all simulants

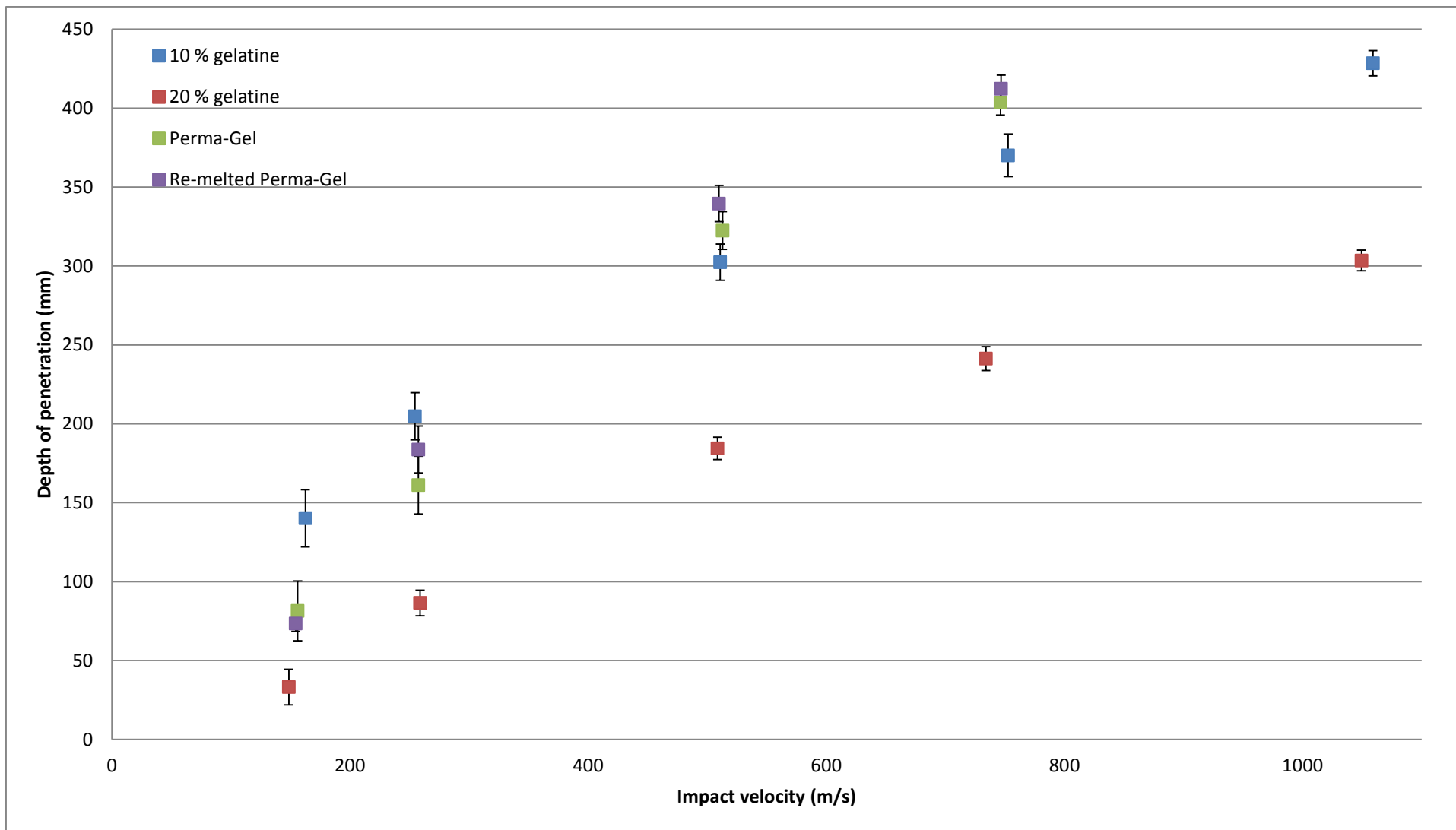


Figure 3-13: Graph showing mean impact velocity vs. mean (and s.d.) DoP for each velocity bin in all four simulants

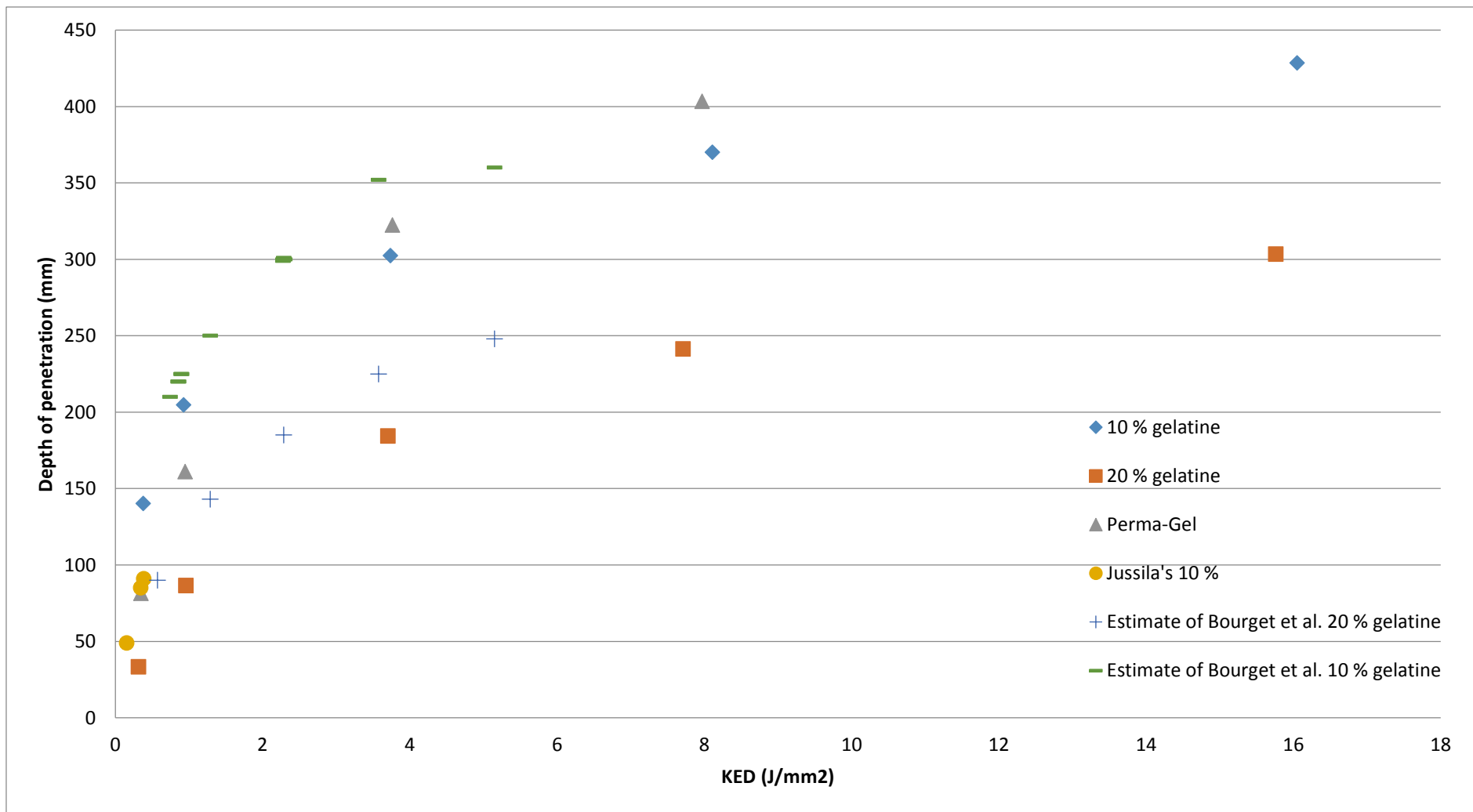


Figure 3-14: Graph showing kinetic energy density vs. mean velocity bins in all four tissue simulants, together with results from the open literature*

*Data from Bouget *et al.*, (2012) is an estimate due to the data being taken from a graph, not tabulated results.

DoP results are split into two parts: i) analysis of DoP in 10% gelatine, 20% gelatine and Perma-Gel™ across the velocity bins 150m/s – 750m/s, and ii) analysis of DoP in both 10% gelatine and 20% gelatine across all five velocity bins. This was due to the Perma-Gel™ blocks not being long enough to capture the whole DoP of the 1000m/s velocity bins, meaning a comparison of Perma-Gel™ DoP data with gelatine was only possible up to the 750m/s velocity bin. A section commenting on the performance of re-melted Perma-Gel™ during the DoP experiments is also included.

3.2.2.1 Depth of penetration results for 5.5mm BBs in 10% gelatine, 20% gelatine and Perma-Gel™

Analysis of 10% gelatine, 20% gelatine and Perma-Gel™ at velocity bins 150m/s – 750m/s showed that DoP varied significantly amongst velocity bins ($F_{3,157} = 3194.93, \rho \leq 0.001$) (Table 3-3b). Tukey's HSD multiple comparison test indicated that each velocity bin resulted in significantly different DoPs (Table 3-3c). In each tissue simulant the longest DoP occurred for the fastest velocity bin and the shortest DoP occurred for the slowest velocity bin.

Results also showed that the type of tissue simulant had a significant effect on DoP of 5.5mm BBs ($F_{2,157} = 1381.85, \rho \leq 0.001$) (Table 3-3b). Tukey's HSD multiple comparison test indicated that each simulant type resulted in significantly different DoPs (Table 3-3d). At 750m/s, the longest DoP was recorded in Perma-Gel™ (mean = 403.5mm, s.d. = 7.8mm), over 30mm longer than the next longest DoP which was in 10% gelatine (mean = 370.1mm, s.d. = 13.5mm), with 20% gelatine producing the shortest DoP at 750m/s (mean = 241.3mm, s.d. = 7.6mm). However, at 150m/s, the longest DoP was recorded in 10% gelatine (mean = 140.1mm, s.d. = 18.1mm), over 50mm longer than the next longest DoP which was in Perma-Gel™ (mean = 81.5mm, s.d. = 19.0mm), with 20% gelatine again producing the shortest DoP (mean = 33.3mm, s.d. = 11.3mm) (Table 3-3a). DoP in the simulants was more variable at the slower velocity bins, as indicated by the CV results.

DoP for velocity bins varied among the different tissue simulants, although weakly when compared to the main effects ($F_{6,157} = 70.85, \rho \leq 0.001$) (Table 3-3b); a significant interaction such as this indicates that the pattern of response for one factor differs among levels of the second factor.

Table 3-3: Depth of penetration in 10% gelatine, 20% gelatine and Perma-Gel™

a Selected descriptive statistics

Velocity bin (m/s)	n	Mean (mm)	s.d. (mm)	CV (%)
10% gelatine				
150	14	140.1	18.1	12.92
250	13	204.8	14.9	7.27
500	12	302.4	11.5	3.80
750	12	370.1	13.5	3.64
20% gelatine				
150	15	33.3	11.3	33.84
250	14	86.5	8.1	9.40
500	15	184.4	7.1	3.82
750	14	241.3	7.6	3.14
Perma-Gel™				
150	15	81.5	19.0	23.26
250	15	161.1	18.4	11.41
500	15	322.5	11.9	3.69
750	15	403.5	7.8	1.94

b Analysis of variance

Source of variation	SS	d.f.	Mean square	F	Sig.	$\rho \leq$
Main effects						
Simulant type	475949.69	2	237974.98	1381.85	0.000	0.001
Velocity bins	1650639.33	3	550213.11	3194.93	0.000	0.001
Interaction						
Simulant type*Velocity bins	73212.44	6	12202.07	70.85	0.000	0.001
Error	27037.68	157	172.22			

c Tukey's HSD multiple comparison test for velocity bin

Velocity bin (m/s)	Mean (mm)	n	Tukey groupings
150	83.7	44	
250	149.8	42	
500	267.4	42	
750	338.3	41	

d Tukey's HSD multiple comparison test for simulant type

Simulant type	Mean (mm)	n	Tukey groupings
20% gelatine	135.4	58	
Perma-Gel™	242.1	60	
10% gelatine	248.9	51	

3.2.2.2 Depth of penetration results for 5.5mm BBs in 10% and 20% gelatine

Analysis of 10% gelatine and 20% across all five velocity bins revealed that gelatine concentration had a significant effect on DoP of BBs ($F_{1,123} = 3703.45, \rho \leq 0.001$) (Table 3-4b). The longest DoP was recorded in 10% gelatine (mean = 428.5mm, s.d. = 8.1mm), over 100mm longer than the longest DoP in 20% gelatine (mean = 303.5mm, s.d. = 6.6mm) (Table 3-4a). The DoP varied significantly amongst velocity bins ($F_{4,123} = 2713.33, \rho \leq 0.001$). Tukey's HSD multiple comparison test indicated that each velocity bin resulted in significantly different DoPs (Table 3-4c). In both concentrations of gelatine, the fastest velocity bin (1050m/s) caused the longest DoP (10% mean = 428.5mm, s.d. = 8.1mm; 20% mean = 303.5mm, s.d. = 6.6mm) and the slowest (150m/s) velocity bins created the shortest DoPs (10% mean = 140.1mm, s.d. = 18.1mm; 20% mean = 33.3mm, s.d. = 11.3mm) (Table 3-4b).

The effect that gelatine concentration had on DoP varied according to impact velocity, although weakly compared to the main effects ($F_{4,123} = 3.76, \rho \leq 0.01$) (Table 3-4b). The result can be explained by the magnitude of difference there was between the lower velocity bins of the two gelatine concentrations. The respective CVs for the 150m/s and 250m/s velocity bins were larger for both gelatine concentration types (10% gelatine: 150m/s CV = 12.90%, 250m/s CV = 7.27%; 20% gelatine: 150m/s CV = 33.84%, 250m/s CV = 9.40%), compared to other velocity bins (e.g. 10% gelatine: 500m/s CV = 3.80%, 750m/s CV = 3.64%; 20% gelatine: 500m/s CV = 3.82%, 750m/s CV = 3.14%) (Table 3-4a).

Table 3-4: Depth of penetration in 10% and 20% gelatine

a Selected descriptive statistics				
Velocity bin (m/s)	n	Mean (mm)	s.d. (mm)	CV (%)
10% gelatine				
150	14	140.1	18.1	12.90
250	13	204.8	14.9	7.27
500	12	302.4	11.5	3.80
750	12	370.1	13.5	3.64
1050	12	428.5	8.1	1.88
20% gelatine				
150	15	33.3	11.3	33.84
250	14	86.5	8.1	9.40
500	15	184.4	7.1	3.82
750	14	241.3	7.6	3.14
1050	12	303.5	6.6	2.16

b Analysis of variance

Source of variation	SS	d.f.	Mean square	F	Sig.	$p \leq$
Main effects						
Gelatine concentration	470210.36	1	470210.36	3703.45	0.000	0.001
Velocity bins	1377997.20	4	344499.30	2713.33	0.000	0.001
Interaction						
Gelatine concentration*Velocity bins	1910.70	4	477.67	3.76	0.006	0.01
Error	15616.75	123	126.97			

c Tukey's HSD multiple comparison test for velocity bin

Velocity bin (m/s)	Mean (mm)	n	Tukey groupings
150	84.9	29	
250	143.4	27	
500	236.9	27	
750	300.7	26	
1050	366.0	24	

3.2.2.3 Depth of penetration results for 5.5mm BBs in re-melted Perma-Gel™

Figure 3-12 and Figure 3-13 display the DoP differences seen between Perma-Gel™ and re-melted Perma-Gel™. With such differences witnessed after just one melting process, the decision was taken to stop DoP testing in re-melted Perma-Gel™.

3.2.3 Discussion of depth of penetration testing

Figure 3-12 and Figure 3-13 support the ANOVA result that depth of penetration varied significantly amongst the tissue simulants considered in this work. Penetration into 10% and 20% gelatine blocks followed a similar polynomial curve, albeit with longer penetration depths in 10% gelatine blocks at comparable velocities (e.g. at velocity bin 500m/s: 10% gelatine mean DoP = 302.4mm; 20% gelatine mean DoP = 184.4mm). The BBs were slowed down and stopped quicker by the denser 20% gelatine blocks (1.05 g/cm³ for 20%, 1.03 g/cm³ for 10% (Janzon, 1997; Eisler *et al.*, 2001)).

The DoP results for BBs penetrating Perma-Gel™ did not follow the same pattern witnessed for either gelatine concentration. This was a surprising result considering Perma-Gel™ was marketed as a replacement for 10% gelatine (Amick, 2004). Comparison between

Perma-Gel™ and 10% gelatine revealed similar DoP at approximately 400m/s, however, at velocities below 400m/s DoP was observably less in Perma-Gel™, yet at velocities greater than 400m/s DoP was noticeably greater in Perma-Gel™. This result highlights the importance of testing tissue simulants at a range of velocities.

Figure 3-12 and Figure 3-13 illustrate the difference in DoP witnessed at comparable velocities between a new block of Perma-Gel™ and a block melted once. This again was surprising as Perma-Gel™ is advertised as reusable for numerous tests, without the characteristics of the tissue simulant being altered. This was clearly not the case for BBs over the velocity range considered. With such differences witnessed after just one melting process, questions regarding the repeatability of reused Perma-Gel™ arose. The fact DoP changed so much after just one melt meant testing of repeatedly melted versions was not carried out. The idea of these tests was to provide justification that the simulants would give reliable and reproducible results, in order to be used throughout the remainder of the research into the overmatching of armour. Continuing with DoP testing of Perma-Gel™ melted numerous times after witnessing a change after one re-melt would not have been of benefit.

Work in the open literature studying DoP into a selection of tissue simulants is limited. Bourget *et al.* (2012) presented DoPs for 5.5mm steel spheres in both 10% gelatine and 20% gelatine at a wide range of velocities, however the data was presented graphically, with the raw data not tabulated, making comparison of results difficult. Lack of information on the mass and the material of the BBs used also complicated trying to compare results.

Studying 10% gelatine only, Jussila (2004) investigated DoP of 4.5mm BBs at velocities of approximately 110m/s, 150m/s, 170m/s and 190m/s. For the current research, 5.5mm diameters BBs were used as they were a closer representation of the rifle ammunition of interest for the overall scope of this project (i.e. .223 Remington (5.56 x 45mm)). Also a much greater velocity range was tested; 500m/s is quoted as the upper limit of low velocity (handgun) ammunition (Tobin and Iremonger, 2006), and with rifle ammunition being of interest, it was felt testing gelatine blocks at velocities at which it was likely to be used was more beneficial, particularly as gelatine has been proven to be strain-rate sensitive (Shepherd *et al.*, 2009; Cronin and Falzon, 2011). The influence of gelatine's strain-rate sensitivity is emphasised by the CV results presented in this study; more variation was observed in the lower velocity bins, indicating the best repeatability was at high velocities. The importance of testing across a large range of velocities was also highlighted by the results produced by Perma-Gel™ and how they compared with 10% gelatine.

Figure 3-14 shows the kinetic energy density of the BBs plotted against the DoP results from the current study. Included on the graph are results from previous studies that also considered DoP, with the results estimated from the work by Bourget *et al.* (2012) due to them being presented graphically. Results produced by Jussila (2004) fit well with results from the present study when comparing 10% gelatine. However, Jussila's results were limited to the lower end of the velocity range considered in the current work. Comparing the current DoP results for 10% gelatine with those produced by Bourget *et al.* (2012) revealed a pattern that followed the same configuration except for kinetic energy density values of approximately 3-4 J/mm². When comparing 20% gelatine the results followed the same formation, apart from DoPs at kinetic energy values between approximately 5 and 8 J/mm². Reasons as to why the results differ include: different measuring techniques (measuring to the front of the BB, rather than the back), errors in the estimation of results from the graphs, or even due to differences in the gelatine used (e.g. bloom number).

One study that assessed the performance of BBs into Perma-Gel™ was found (Ryckman *et al.*, 2011). However, the BBs used were much larger (1/2 inch, 12.7mm diameter) and tested over a smaller velocity range (61m/s – 274m/s). No data on DoP was presented; however, remarks regarding the behaviour of Perma-Gel™, such as traces of BBs backtracking through the gel, and the permanent cavity collapsing leaving an incomplete wound tract behind were noted. Similar observations were made during the current study. The complete collapse of the wound tract did not occur in either concentration of the gelatine; the process of the temporary cavity subsiding to form the permanent cavity left a smaller cavity and tract. Conversely, the whole tract remained clearly visible, unlike in Perma-Gel™. The BBs backtracking through Perma-Gel™ (~ < 30mm) was witnessed with the aid of high-speed filming, this behaviour was also noticed in gelatine (~ < 15mm). The backtracking behaviour together with any potential optical influence witnessed from the high speed video footage meant measuring the resting DoP was more accurate and consistent.

The DoP study revealed that the processes by which 10% and 20% gelatine were made produced repeatable DoP results for impact velocities that were similar. This was a positive result, and supported Jussila's (2003) theory that consistent gelatine blocks are possible so long as the conditions of production and storage remain constant. After establishing that gelatine blocks performed better when it came to reproducibility and reliability, the next stage was to assess whether the damage produced by live ammunition was both repeatable and measurable. The success of using non-deforming projectiles not influenced by yaw was to be taken forward. The 5.5mm BBs were to be used as a quality

control check for the simulants, ensuring the reproducibility was maintained throughout testing.

3.3 Part B – Baseline simulant tests

Following on from the BB DoP experiments, *Part B* covers a series of baseline studies that were conducted into the different simulants using .223 Remington Federal Premium® Tactical® Bonded® and 9mm Luger DM11 A1B2 ammunition. The reason was twofold: i) to ensure the damage produced in the simulants would give results that could be collected, analysed and compared after a ballistic event, and ii) to collect data for comparison against results from when body armour has been defeated by projectiles (i.e. a baseline study).

As discussed in Chapter 2, there is no definitive answer as to what process has the most important role in causing a wound or damage during a ballistic event. As highlighted, many factors have been put forward as to having an influence, including the direct crushing and lacerating caused directly by a moving projectile and the process of temporary cavitation, (Horsely, 1894; Hopkinson and Marshall, 1967; Adams, 1982; Bowyer *et al.*, 1997b; Janzon, 1997; Besant-Matthews, 2000). While these baseline tests were a method to confirm analysis of the damage could be produced and collected from these tissue simulants, it was also an opportunity to gather data on the type of parameters that could be collected so as to be able to compare the damage seen when armour is and is not present on a target.

3.3.1 Materials and methods

3.3.1.1 Simulants

The simulants used in *Part A*, and the methods by which they were produced remained the same for the baseline simulant tests presented in Part B.

3.3.1.2 Ammunition

Two ammunition types of interest were provided by CAST and used throughout this study. They were:

- i) .223 Remington (62 grain; Federal Premium® Tactical® Bonded®)
- ii) 9mm Luger (124 grain; full metal jacket; DM11 A1B2) (Figure 3-15)

It was ensured every round of .223 Remington used in this study was from the same batch, batch No. 47V536N001. It was also ensured that every 9mm Luger round used was from the same batch, batch No. LOS DAG02K0956.



Figure 3-15: A .223 Remington (62 grain; Federal Premium® Tactical® Bonded®)(left) and a 9mm Luger (124 grain; full metal jacket; DM11 A1B2)

The .223 Remington Federal Premium® Tactical® Bonded® projectiles were of interest as they are a round that the UK Police firearms unit are interested in using. The .223 Remington Federal Premium® Tactical® Bonded® contains a tip that is open and as a result it expands on impact.

The 9mm Luger round was of interest as it is used in the HOSDB Ballistic Resistance Body Armour standard (Croft and Longhurst, 2007b). It is seen as a potential threat to UK police officers; certified armours (HG1/A up to HG2) must be able to protect against 9mm Luger projectiles from specified ranges and velocities. It is also a round that does not typically breakup or fragment, but does have a tendency to yaw within targets.

Three rounds of each ammunition type were pulled, mounted and sectioned (Figure 3-16), before elemental analysis and material hardness testing were carried out. A scanning electron microscope (SEM) was used to provide elemental composition information for the two projectile types. Backscattered EDX analysis/maps were undertaken using a JEOL 840A SEM and an EDAX Genesis microanalysis system with an accelerating voltage of 25 kV. Hardness-testing (using an Indentec Hardness Testing Machine HWDM-7) was carried out on three different locations within each different material type present (Figure 3-16). A load

of 100g was used during the hardness testing (unless otherwise stated), after which the indentation was measured to give a hardness result in Vickers (Hv).

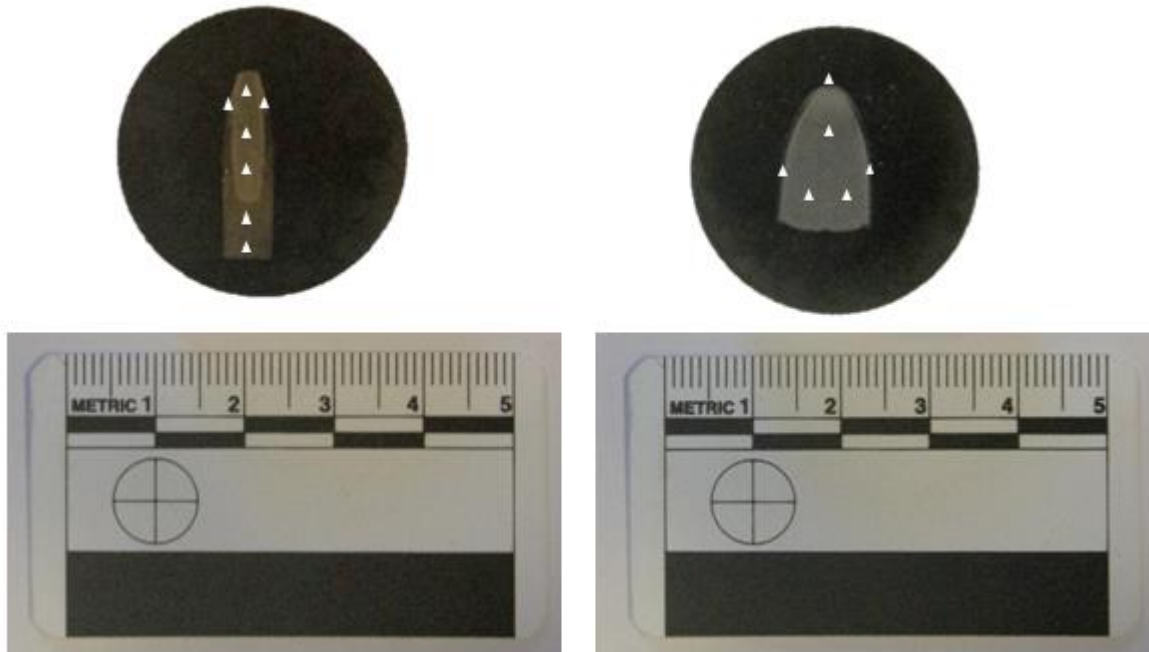


Figure 3-16: A mounted and sectioned .223 Remington Federal Premium® Tactical® Bonded®(left) and a 9mm Luger, complete with hardness testing locations.

3.3.1.3 Baseline simulant method

The target blocks were placed 10 m downrange from the end of the muzzle. An Enfield Number 3 Proof Housing, with the appropriate barrel fitted, was used to fire each ammunition type. A new tissue simulant target was used for every shot with the .223 Remington Federal Premium® Tactical® Bonded®, while 2 or 3 rounds of the 9mm Luger ammunition were fired at the simulant targets, ensuring the tracts did not overlay. Ten repeat shots were carried out for both ammunition types (n=10).

The .223 Remington Federal Premium® Tactical® Bonded® were fired as provided, however, the 9mm Luger ammunition rounds were uploaded with extra propellant in order to reach impact velocities required for testing HG2 level body armour (Croft and Longhurst, 2007b). This followed the directions provided by CAST. The impact velocities were recorded using a Weibel W-700 Doppler radar.

The tissue simulants were illuminated using Photon Beam lights, one from the front, and one from the rear, reflecting off a projection screen (Figure 3-10). This ensured that the impact events were captured when filmed with a Phantom high-speed video camera (V12). A scale was used in all impacts to allow the high-speed video footage to be calibrated during analysis.

Before each tissue simulant was fired at, a 5.5mm diameter steel BB was fired at \approx 750m/s into the top right of each target block. The velocity and depth of penetration of this shot was measured and compared with results collected from the depth of penetration testing, to ensure only consistent gelatine blocks were used for testing i.e. each block was quality control checked against a database produced from the DoP of simulants work (Appendix G).

3.3.1.4 Baseline simulants analysis

The tissue simulants were dissected after testing by cutting along the permanent tract using a knife (Figure 3-17). Lead debris present in the cavities was noted, photographed using a Nikon D90 (Nikon DX AF-S NIKKOR 18-105mm lens), removed and bagged for future analysis. Measurements of the permanent cavities produced in the gelatine blocks were taken, specifically: neck length, 'body' length, 'body' width, 'body' height and (when possible) distance to projectile (Figure 3-18). Table 3.5 gives a breakdown of why these measurements were taken.

Table 3-5: Measurements of permanent cavity and why they were taken.

Measurement	Description	Justification
Neck length	The point of entry up to the start of the permanent cavity expansion	The measurement of the projectiles initial channel entry before the permanent cavity begins. Important to measure as a shorter or longer entry channel could be the difference between a target experiencing the effects of cavitation and/or yawing or not.
Body length	The length of the permanent cavity expansion (not to include the neck length)	The distance over which permanent damage has been produced throughout the target. Longer body lengths mean more of the target through the line of flight has been damaged by the cavitation.
Body width	The longest part of the permanent cavity along the x axis (when looking at the target straight on)	The width over which permanent damage has been produced within the target. Wider widths mean cavitation expanded out further, damaging more of the target that was situated away from the project's path.
Body height	The longest part of the permanent cavity in the y axis (when looking at the target straight on)	The height over which permanent damage has been produced within the target. Larger heights mean cavitation expanded out further, damaging more of the target that was situated away from the projectile's path.
Ellipsoid volume	Formula 3.10 with the respective length, width and height measurements halved.	The estimated maximum volume of damage the projectile caused to the target. This would be the volume were the damage perfectly ellipsoid shaped, hence why it is an estimated maximum. All three prior measurements are taken into account for the volume and so give a better representation when comparing the damage of different shots.
Distance to projectile	(When possible) the distance from the point of entry up to touching the rear part of the projectile <i>in situ</i> .	The resting location of the projectile after travelling through the target. Of interest to compare what factors cause shorter or longer distances.

From the body dimensions, the formula for calculating the volume of an ellipsoid was used to calculate a representation of the maximal volume of the damage the permanent cavity created:

$$V_{ellipsoid} = \frac{4}{3} \pi lwh \quad (3.10)$$

where l, h and w are the length, height and width body dimensions, all halved. Length and height of fissures present in the gelatine blocks were also recorded (Figure 3-19). From these measurements, the area of each individual fissure was calculated using the formula for an ellipse, divided by two as a fissure was only half of an ellipse:

$$A_{ellipse} = \frac{\pi ab}{2} \quad (3.11)$$

where a and b are the respective length and height measurements of a fissure, halved. A total fissure area for each shot was calculated by adding together the areas of the individual fissures. Summary statistics (mean (x), standard deviation (s.d.) and coefficient of variation (CV)) were calculated for the fissure and the permanent cavity data sets. Analysis of variance (ANOVA) and Tukey HSD analysis were used to determine when significant differences between simulant types occurred (SPSS Statistics 22.0). ANOVA is a robust method for identifying whether there is variation between normally distributed data sets. It was selected instead of a t-test as the risk of getting a Type 1 error (an error of usually 5%) is mitigated (Harrway, 1997). Normality of data and equality of variance were checked for each data set.

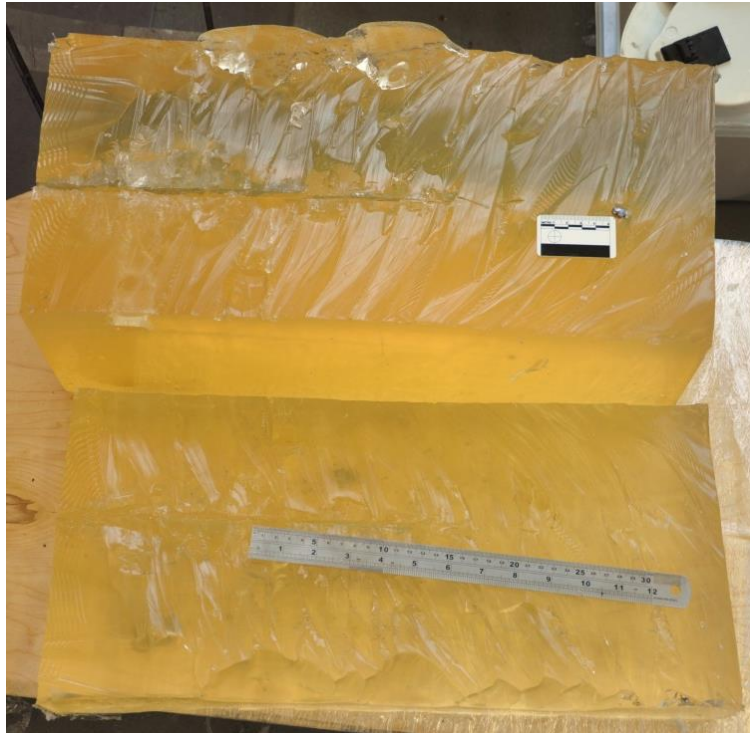
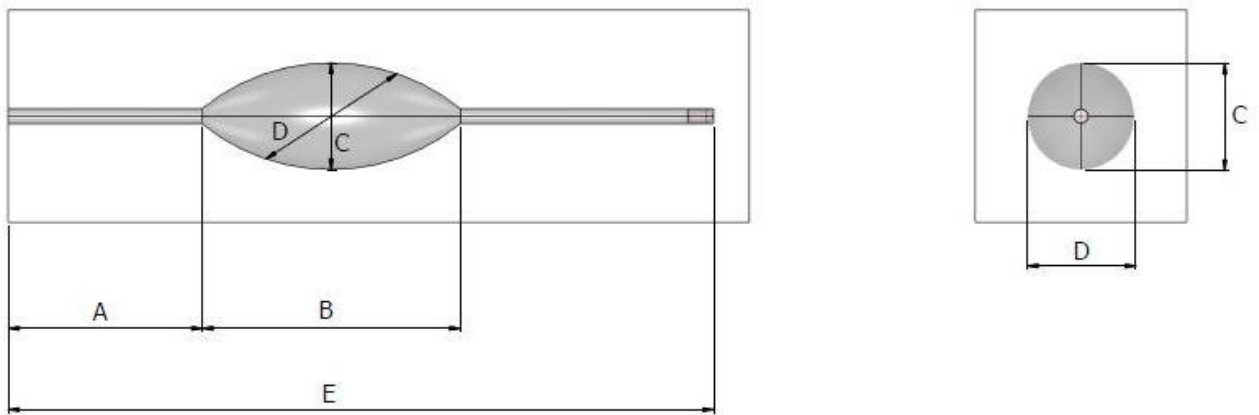


Figure 3-17: Gelatine block cut along the length of the tract to assess the permanent cavity damage



A - neck length, B - 'body' length, C - 'body' height, D - 'body' width and E - distance to projectile

Figure 3-18: Schematic diagram of the measurements taken of the permanent cavities



Figure 3-19: Measurement of fissures – length (left) and height measurements (right), with visible debris present highlighted.

3.3.1.4.1 High speed video analysis

Analysis of the high speed footage was carried out using Phantom software (Vision Research, Phantom Camera Control Application 2.5). Each file was calibrated by using a known length visible in the image e.g. a ruler or forensic scale, converting pixels present in the image to a dimension in mm. Once calibrated it was possible to take measurements that included: the diameter of the temporary cavity at its largest (Figure 3-20), and the distance (from the entry point of the projectile in the gelatine block) to where this occurred (Figure 3-21). Both these measurements were taken using the PCC 2.5 software, using the ‘instant measurement’ option. It was also possible to locate the position and the number of times the 9mm Luger rounds yawed within the target.

The same statistical analysis was carried out on these data sets to identify whether the different tissue simulants had a significant effect on i) the location where the temporary cavity was largest and on ii) maximum diameter reached.

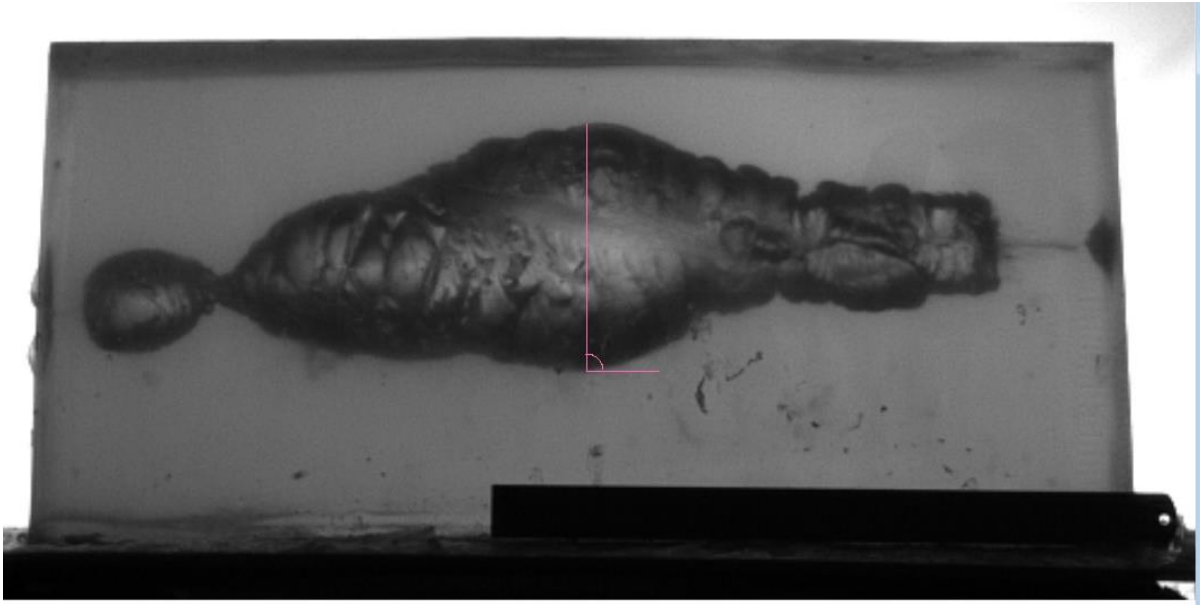


Figure 3-20: A still image of a typical 9mm Luger temporary cavity where the maximum diameter of the temporary cavity is being measured using the PCC 2.5 software

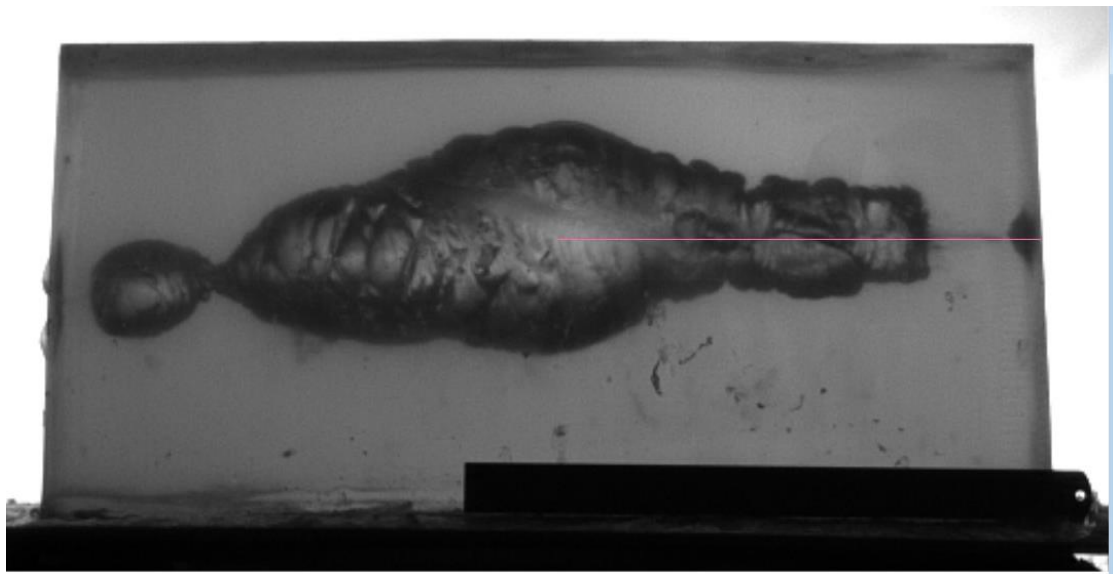


Figure 3-21: A still image of a typical 9mm Luger temporary cavity where the distance to the point of maximum expansion of the temporary cavity is being measured using the PCC 2.5 software.

3.3.2 Results

3.3.2.1 *Projectile construction*

The results from micro hardness testing are summarised in Table 3-6.

Table 3-6: Micro hardness results**a .223 Remington Federal Premium® Tactical® Bonded projectiles**

Sample	Core hardness (Hv)	Jacket hardness (bottom of projectile)(Hv)	Jacket hardness (Top of projectile)(Hv)
Projectile 1	6.1 (Bottom of core*)	74.3 (bottom of jacket)	115.9 (Top left)
	7.0 (Middle)	75.0 (Just above)	127 (Top right)
	6.6 (Top)		
Projectile 2	6.3	74.6	116.7
	7.1	74.3	115.9
	6.5		
Projectile 3	6.5	83.7	114.1
	5.9	75.6	115.6
	6.5		
Mean	6.50	76.25	117.53
s.d.	0.38	3.68	4.72
CV (%)	5.91	4.83	4.01
Min	5.9	74.3	114.1
Max	7.1	83.7	127.0

*See Figure 3-16 for hardness testing locations

b 9mm Luger projectiles

Sample	Core hardness (Hv)	Jacket hardness (Hv)	Inside Jacket hardness (Hv)^	Outside Jacket hardness (Hv)
Projectile 1	8.4 (Left*)	172.3 (Left)	69.7 (Left)	135.4 (Left)
	7.6 (Top)	166.2 (Top)	119.6 (Top)	85.2 (Top)
	7.1 (Right)	172.3 (Right)	51.6 (Right)	122.5 (Right)
Projectile 2	7.4	177.7	153.2	126.6
	7.5	144.6	71.5	117.4
	7.2	145.6	145.2	147.8
Projectile 3	7.0	185.1	106.4	98.8
	7.3	129.7	114.9	121.5
	7.4	183.9	147.8	145.2
Mean	7.43	164.16	108.88	122.27
s.d.	0.41	19.57	37.36	20.37
CV (%)	5.51	11.92	34.32	16.66
Min	7.0	129.7	51.6	85.2
Max	8.4	185.1	153.2	147.8

^ Inside and outside jacket hardness testing performed with a load of 10 g.

*See Figure 3-16 for hardness testing locations

Spectra from the SEM analysis of the .223 Remington Federal Premium® Tactical® Bonded projectiles revealed the core was constructed of lead (Appendix H). The surrounding jacket was made out of brass (Figure 3-22).

SEM analysis of the 9mm Luger revealed the core was constructed of lead, with the jacket made from steel. The jacket was coated, both inside and out, with brass. Figure 3-23 shows the different materials present.

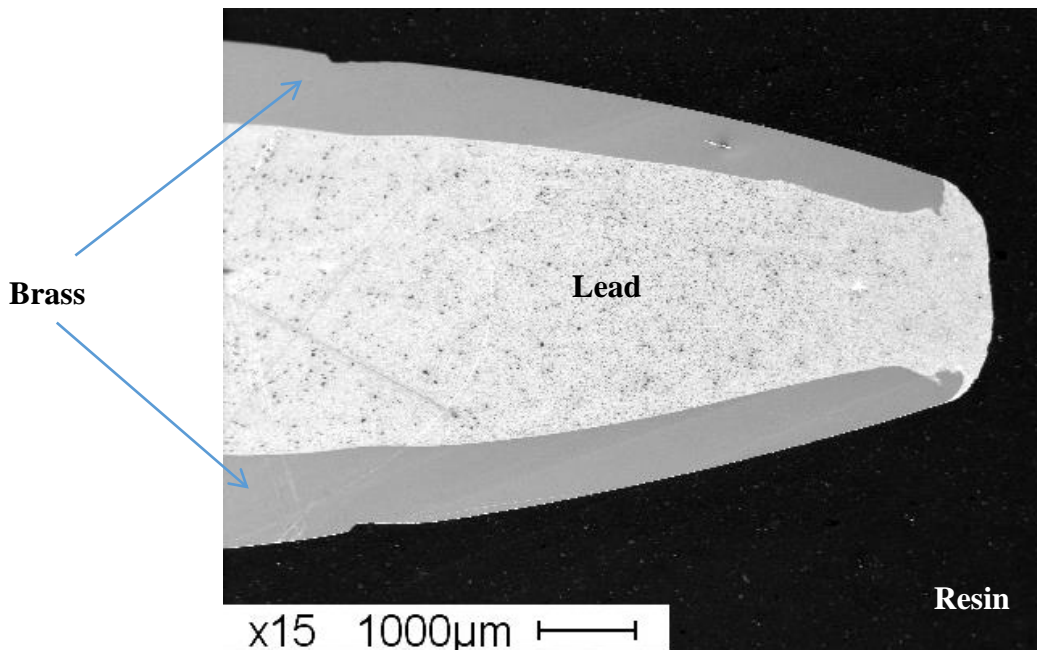


Figure 3-22: SEM analysis of a .223 Remington Federal Premium® Tactical® Bonded with composition labelled

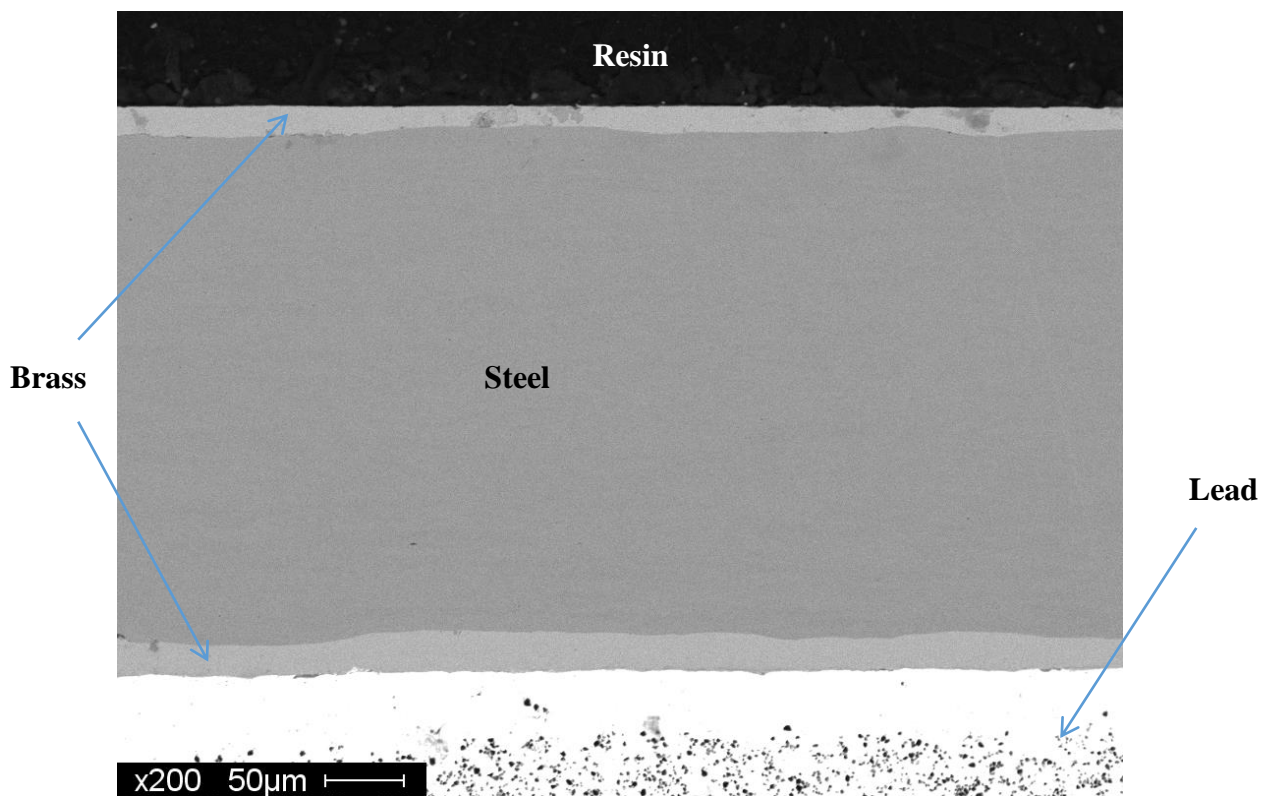


Figure 3-23: SEM analysis of a 9mm Luger with composition labelled

3.3.2.2 .223 Remington Federal Premium® Tactical® Bonded® results

Comparison of the results collected from tests with the .223 Remington Federal Premium® Tactical® Bonded® rounds revealed that the mean measurements of the permanent cavities in 10% gelatine were larger than those collected from cavities in 20% gelatine blocks (Table 3-7 and

Table 3-8). The spread of the data was also larger for the measurements collected from 10% gelatine. When measurements of fissures were compared, a similar result was seen; the area of the fissures was larger in 10% blocks, with the range also greater.

Analysis of the high speed video footage revealed temporary cavity formations were similar in both concentrations of gelatine (Figure 3-24 and Figure 3-25). No results for interactions with Perma-Gel™ will be presented, other than the series of pictures that capture the flash that was witnessed during penetration (Figure 3-26).

Table 3-7: Measurements collected from interactions of .223 Remington Federal Premium® Tactical® Bonded® with 10% gelatine blocks

a Shot information				
Shot	Impact velocity (m/s)	Fragments?	Distance to maximum expansion of temporary cavity (mm)	Maximum diameter of temporary cavity (mm)
Shot 1	843	In tract and fissures	85	178
Shot 2	844	In tract	91	180
Shot 3	842	In tract and fissures	75	177
Shot 4	852	In tract and fissures	77	171
Shot 5	853	No	100	174
Shot 6	852	In tract and fissures	99	182
Shot 7	853	In tract	102	179
Shot 8	839	In tract	85	178
Shot 9	844	In tract and fissures	93	184
Shot 10	854	In tract and fissures	75	173
Mean	847.6		88.7	178.1
s.d.	5.7		10.3	4.0
CV (%)	0.67		11.61	2.25
Min	839		75	171
Max	854		102	184

b Measurements of permanent cavities

Shot	Neck length (mm)	Body length (mm)	Body height (mm)	Body width (mm)	Distance to projectile (mm)	Total fissure area (mm ²)
Shot 1	0	300	95	105	454	47006
Shot 2	0	280	100	110	425	39977
Shot 3	2	260	100	115	425	45160
Shot 4	0	325	90	105	423	76223
Shot 5	0	330	105	105	423	81249
Shot 6	0	340	145	100	420	59337
Shot 7	0	290	140	95	402	84941
Shot 8	0	320	110	150	430	77480
Shot 9	0	315	110	130	428	67348
Shot 10	0	325	125	130	429	111252
Mean	N/A	308.5	112.0	114.5	425.9	68997.0
s.d.	N/A	25.3	18.7	17.1	12.7	21868.2
CV (%)	N/A	8.20	16.73	14.91	2.98	31.69
Min	0	260	90	95	402	39977
Max	2	340	145	150	454	111252

Table 3-8: Measurements collected from interaction of .223 Remington Federal Premium® Tactical® Bonded® projectiles with 20% gelatine blocks

a Shot information

Shot	Impact velocity (m/s)	Fragments?	Distance to maximum expansion of temporary cavity (mm)	Maximum diameter of temporary cavity (mm)
Shot 1	839	In tract	88	161
Shot 2	842	In tract and fissures	88	158
Shot 3	842	In tract	86	163
Shot 4	844	Yes, less than normal in tract, some early in fissures of body of wound	83	153
Shot 5	845	In tract and fissures	83	163
Shot 6	844	In tract and fissures	88	158
Shot 7	852	In tract and fissures	80	155
Shot 8	846	In tract and fissures	80	154
Shot 9	855	In fissures	90	155
Shot 10	841	In tract and fissures	84	156
Mean	845.0		85.03	157.6
s.d.	5.0		3.5	3.6
CV (%)	0.59		4.08	2.29
Min	839		80	153
Max	855		90	163

b Measurements of permanent cavities

Shot	Neck length (mm)	Body length (mm)	Body height (mm)	Body width (mm)	Distance to projectile (mm)	Total fissure area (mm ²)
Shot 1	5	240	95	85	315	57460
Shot 2	1	260	100	85	316	42097
Shot 3	1	270	115	110	306	36914
Shot 4	0	260	110	110	295	53329
Shot 5	1	275	115	100	287	49048
Shot 6	3	245	130	120	280	56549
Shot 7	1	260	110	120	289	37621
Shot 8	2	230	85	110	283	50030
Shot 9	0	260	115	95	299	57177
Shot 10	0	245	95	110	292	61850
Mean	1.4	254.5	107.0	104.5	296.2	50207.4
s.d.	1.6	14.0	13.2	12.8	12.7	8749.5
CV (%)	114.29	5.51	12.30	12.24	4.27	17.43
Min	0	230	85	85	280	36914
Max	5	275	130	120	316	61850

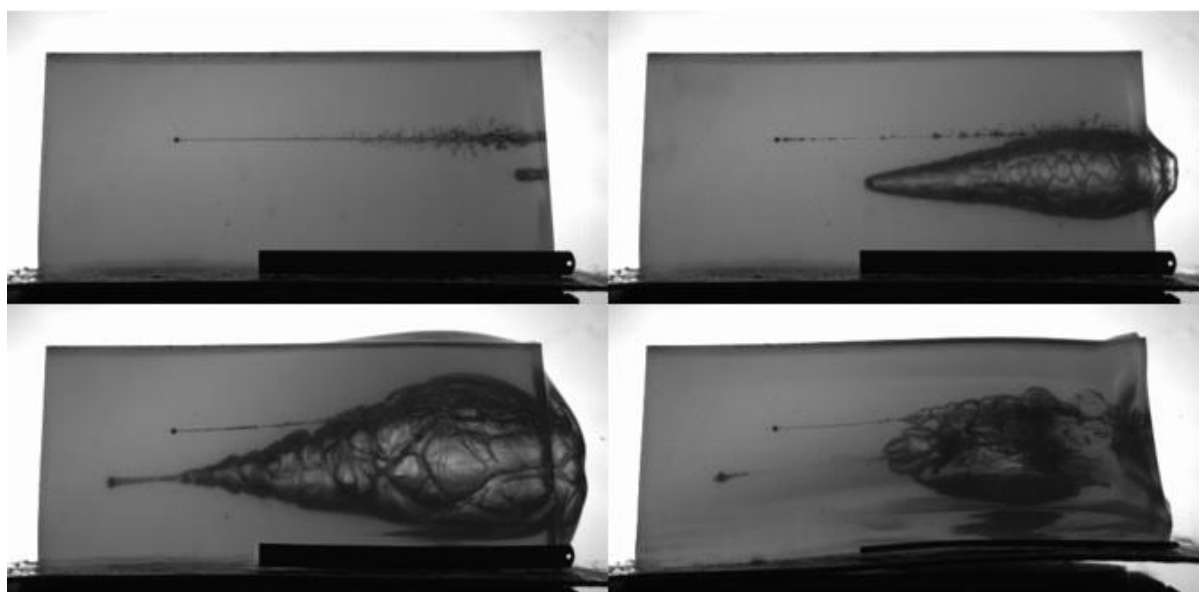


Figure 3-24: Stills from high speed footage showing the formation and collapse of a typical temporary cavity produced in 10% gelatine by a .223 Remington Federal Premium® Tactical® Bonded® projectile.

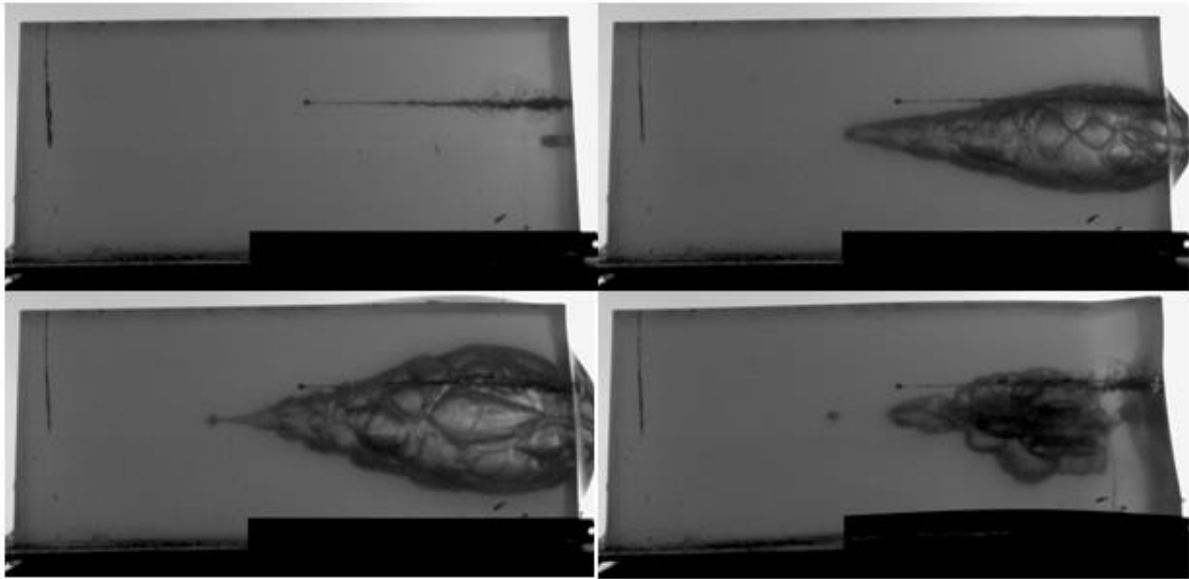


Figure 3-25: Stills from high speed footage stills showing the formation and collapse of a typical temporary cavity produced in 20% gelatine by a .223 Remington Federal Premium® Tactical® Bonded® projectile.

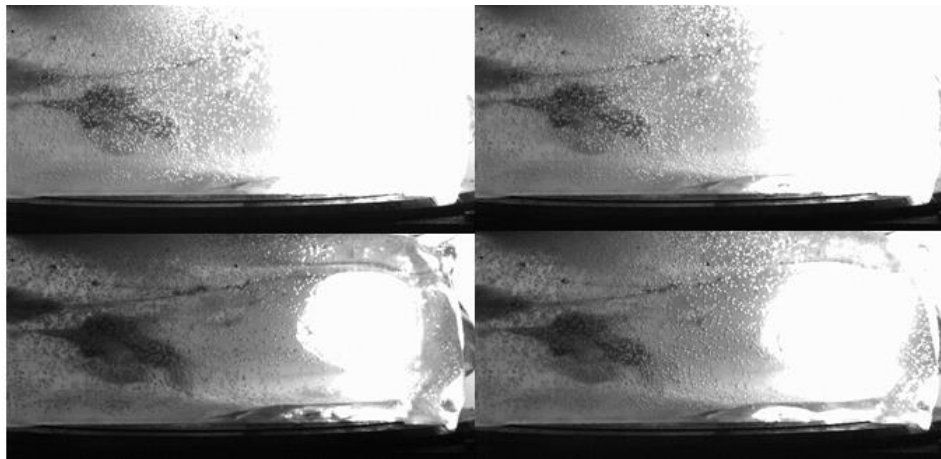


Figure 3-26: Example of the flash that propagates through a Perma-Gel™ block after impact with by a .223 Remington Federal Premium® Tactical® Bonded® projectile

3.3.2.2.1 ANOVA results

Neck length

Analysis of variance could not be carried out on neck length due to there being only one measurement in 10% gelatine; this was 2mm. Seven neck length measurements were taken in 20% gelatine blocks, ranging from 1mm - 5mm (mean = 1.4mm; s.d. = 1.6mm).

Body length

After being penetrated by .223 Remington Federal Premium® Tactical® Bonded® ammunition, gelatine concentration had a significant effect on the body length of the permanent cavity ($F_{1, 18} = 34.876, \rho \leq 0.001$) (Table 3-9b). The mean body length was 50mm longer in 10% gelatine (mean = 308.5mm, s.d. = 25.3mm) compared to 20% gelatine (mean = 254.5mm, s.d. = 14.0mm) (Table 3-9a).

Table 3-9: Body length after penetration with .223 Remington Federal Premium® Tactical® Bonded® projectiles

a Selected descriptive statistics						
Simulant type	Mean (mm)	s.d. (mm)	CV (%)			
10% gelatine	308.5	25.3	8.20			
20% gelatine	254.5	14.0	5.51			

b Analysis of variance						
Source of variation	SS	d.f.	Mean square	F	Sig.	$\rho \leq$
Gelatine concentration	14580.00	1	14580.00	34.876	0.000	0.001
Error	7525.00	18	418.06			

Representation of maximum ellipsoid volume

The representation of the maximum ellipsoid volume was significantly different in both concentrations of gelatine after penetration of the .223 Remington Federal Premium® Tactical® Bonded® ($F_{1, 18} = 9.079, \rho \leq 0.01$) (Table 3-10b). The mean volume was larger in 10% compared to 20% gelatine (10% gelatine mean = 2074000mm³, s.d. = 502200mm³; 20% gelatine mean = 1502000mm³, s.d. = 3312mm³) (Table 3-10a).

Table 3-10: Representation of maximum ellipsoid volume after penetration of .223 Remington Federal Premium® Tactical® Bonded® projectiles

a Selected descriptive statistics			
Simulant type	Mean (mm³)	s.d. (mm³)	CV (%)
10% gelatine	2074000	502200	24.21
20% gelatine	1502000	331200	22.05

b Analysis of variance						
Source of variation	SS	d.f.	Mean square	F	Sig.	$\rho \leq$
Gelatine concentration	1.643 x 10 ¹²	1	1.643 x 10 ¹²	9.079	0.007	0.01
Error	3.257 x 10 ¹²	18	1.810 x 10 ¹¹			

Fissure area

Concentration of gelatine significantly affected fissure area of the permanent cavity after penetration by a .223 Remington Federal Premium® Tactical® Bonded® projectile ($F_{1, 18} = 6.364, \rho \leq 0.05$) (Table 3-11b). The mean area in 20% gelatine (mean = 50210mm², s.d. = 8750mm²) was over 18000mm² less than the mean fissure area in 10% gelatine (mean = 69000mm², s.d. = 2187mm²) (Table 3-11a).

Table 3-11: Fissure area after penetration by .223 Remington Federal Premium® Tactical® Bonded® projectiles

a Selected descriptive statistics			
Simulant type	Mean (mm ²)	s.d. (mm ²)	CV (%)
10% gelatine	69000	2187	31.69
20% gelatine	50210	8750	17.43

b Analysis of variance						
Source of variation	SS	d.f.	Mean square	F	Sig.	$\rho \leq$
Gelatine concentration	1765295258	1	1765295258.0	6.364	0.021	0.05
Error	4992922352	18	277384575.1			

Distance to projectile

The distance of .223 Remington Federal Premium® Tactical® Bonded® projectiles was significantly different in 10 and 20% gelatine ($F_{1, 18} = 524.507, \rho \leq 0.001$) (Table 3-12b). The mean distance in 10% gelatine (mean = 425.9mm, s.d. = 12.7mm) was 129.7mm longer than the mean distance to projectile in 20% gelatine (mean = 296.2mm, s.d. = 12.7mm) (Table 3-12a).

Table 3-12: Distances .223 Remington Federal Premium® Tactical® Bonded® projectiles travelled within gelatine blocks

a Selected descriptive statistics

Simulant type	Mean (mm)	s.d. (mm)	CV (%)
10% gelatine	425.9	12.7	2.98
20% gelatine	296.2	12.7	4.27

b Analysis of variance

Source of variation	SS	d.f.	Mean square	F	Sig.	$\rho \leq$
Gelatine concentration	84110.45	1	84110.45	524.507	0.000	0.001
Error	2886.50	18	160.36			

Maximum temporary cavity analysis

The distance to the maximum temporary cavity expansion in both concentrations of gelatine was not significantly different ($F_{1, 18} = 1.119$, $\rho = NS$) (Table 3-13b). Mean distance was numerically greater in 10% gelatine (mean = 88.7mm, s.d. = 10.3mm) (Table 3-13a).

Conversely, the maximum expansion caused by the temporary cavity was significantly affected by gelatine concentration type ($F_{1, 18} = 144.253$, $\rho \leq 0.001$) (Table 3-14b). The mean temporary cavity was largest in 10% gelatine (mean = 178.1mm, s.d. = 4.0mm), over 20mm larger when compared to the mean temporary cavity diameter in 20% gelatine (mean = 157.6, s.d. = 3.6mm) (Table 3-14a).

Table 3-13: Distance to maximum expansion of temporary cavity caused by .223 Remington Federal Premium® Tactical® Bonded® projectiles in gelatine targets

a Selected descriptive statistics

Simulant type	Mean (mm)	s.d. (mm)	CV (%)
10% gelatine	88.7	10.3	11.66
20% gelatine	85.0	3.5	4.08

b Analysis of variance

Source of variation	SS	d.f.	Mean square	F	Sig.	$\rho \leq$
Gelatine concentration	66.53	1	66.53	1.119	0.304	NS
Error	1070.50	18	59.47			

Table 3-14: Maximum diameter of temporary cavity produced by .223 Remington Federal Premium® Tactical® Bonded® projectiles in gelatine targets

a Selected descriptive statistics

Simulant type	Mean (mm)	s.d. (mm)	CV (%)
10% gelatine	178.1	4.0	2.25
20% gelatine	157.6	3.6	2.29

b Analysis of variance

Source of variation	SS	d.f.	Mean square	F	Sig.	$\rho \leq$
Gelatine concentration	2095.20	1	2095.20	144.253	0.000	0.001
Error	261.44	18	14.524			

3.3.2.3 9 x 9mm FMJ results

The 9mm Luger rounds perforated the gelatine blocks, regardless of concentration. The tract left by the rounds was helical in shape; there was not a ‘body’ of damage left. As a result, the permanent cavity damage was only assessed by measuring the fissure area that was present. Results revealed fissure area measurements were on average greater in 10% gelatine, with the range also larger in 10% gelatine blocks. High speed video analysis provided comparable data on the temporary cavities produced in both concentration types, as well as information on when and how many times the 9mm Luger projectiles reached 90 ° yaw within the targets (Table 3-15 and Table 3-16) (Figure 3-27 and Figure 3-28).

Table 3-15: Measurements collected from interactions of 9mm Luger projectiles with 10% gelatine blocks

a Shot information			
Shot	Projectile mass (g)	Impact velocity (m/s)	Total fissure area (mm ²)
1	8.01	422	40841
2	7.99	429	36679
3	8.01	429	52700
4	8.00	429	59573
5	8.02	431	44728
6	8.00	433	41626
7	8.00	435	54193
8	8.02	427	59101
9	8.01	425	52818
10	8.01	432	46888
Mean	8.01	429.2	48915
s.d.	0.01	3.9	7919.4
CV (%)	0.12	0.90	16.19
Min	7.99	422	36678
Max	8.02	435	59573

b Temporary cavity analysis		
Shot	Distance to maximum expansion of temporary cavity (mm)	Maximum diameter of temporary cavity (mm)
1	276	113
2	314	80
3	277	118
4	247	116
5	225	117
6	212	100
7	252	125
8	235	106
9	281	120
10	226	104
Mean	254.6	110.0
s.d.	31.9	13.1
CV (%)	12.53	11.93
Min	212	80
Max	314	125

c Yaw analysis

Shot	Number of times 90 ° yaw reached	Distance within block (mm)		
1	3	243	301	466
2	2	318	367	-
3	2	265	485	-
4	3	266	311	475
5	2	215	402	-
6	3	216	449	474
7	2	241	476	-
8	3	223	275	448
9	2	298	348	-
10	3	231	277	451
Mean	2.5	251.4	369.1	462.7
s.d.	0.5	35.0	80.4	12.8
CV (%)	21.08	13.92	21.78	2.76
Min	2	215	275	448
Max	3	318	485	475

Table 3-16: Measurements collected from interactions of 9mm Luger projectiles with 20% gelatine blocks

a Shot information

Shot	Projectile mass (g)	Impact velocity (m/s)	Total fissure area (mm ²)
1	8.02	420	33890
2	8.01	434	30316
3	8.01	427	28628
4	8.00	427	38995
5	8.01	432	37660
6	8.00	427	37228
7	8.02	420	36246
8	8.00	422	31337
9	8.02	420	31691
10	8.01	427	24897
Mean	8.01	425.6	33089
s.d.	0.01	5.02	4512.12
CV (%)	0.10	1.18	13.64
Min	8.00	420	24897
Max	8.02	434	38995

b Temporary cavity analysis

Shot	Distance to maximum expansion of temporary cavity (mm)	Maximum diameter of temporary cavity (mm)
1	318	71
2	317	85
3	219	76
4	217	99
5	220	87
6	238	93
7	249	79
8	262	86
9	236	99
10	206	62
Mean	248.1	83.6
s.d.	39.9	12.1
CV (%)	16.09	14.42
Min	206	62
Max	318	99

c Yaw analysis

Shot	Number of times 90 ° yaw reached	Distance within block (mm)		
1	3	285	347	476
2	3	247	297	447
3	2	209	440	-
4	3	201	254	406
5	3	222	290	446
6	2	225	424	-
7	3	230	292	409
8	3	234	284	426
9	2	226	418	-
10	3	235	281	417
Mean	2.7	231.4	332.7	432.4
s.d.	0.48	22.9	69.5	25.3
CV (%)	17.89	9.89	20.88	5.86
Min	2	201	254	406
Max	3	285	440	476

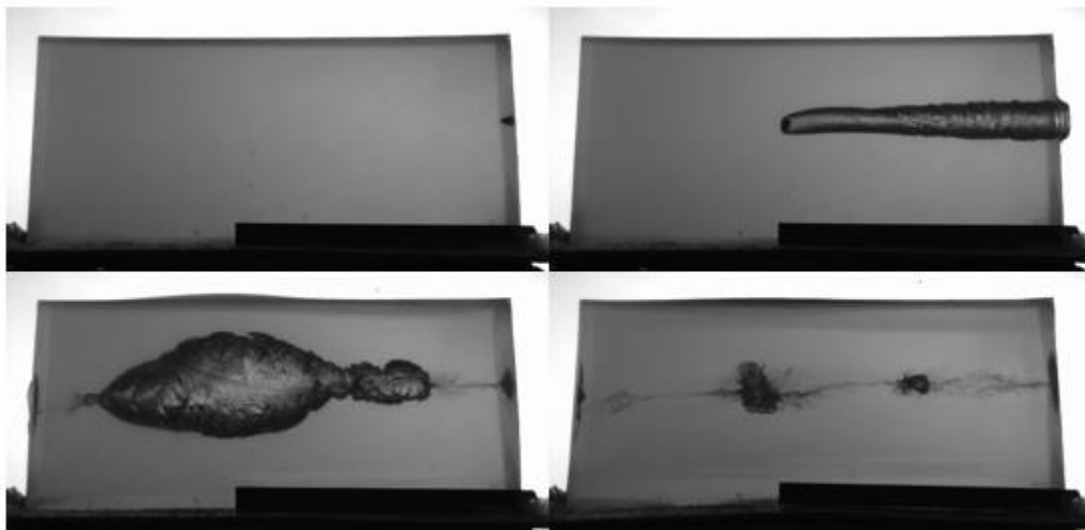


Figure 3-27: Stills from high speed footage showing the formation and collapse of a typical temporary cavity produced in 10% gelatine by a 9mm Luger projectile.

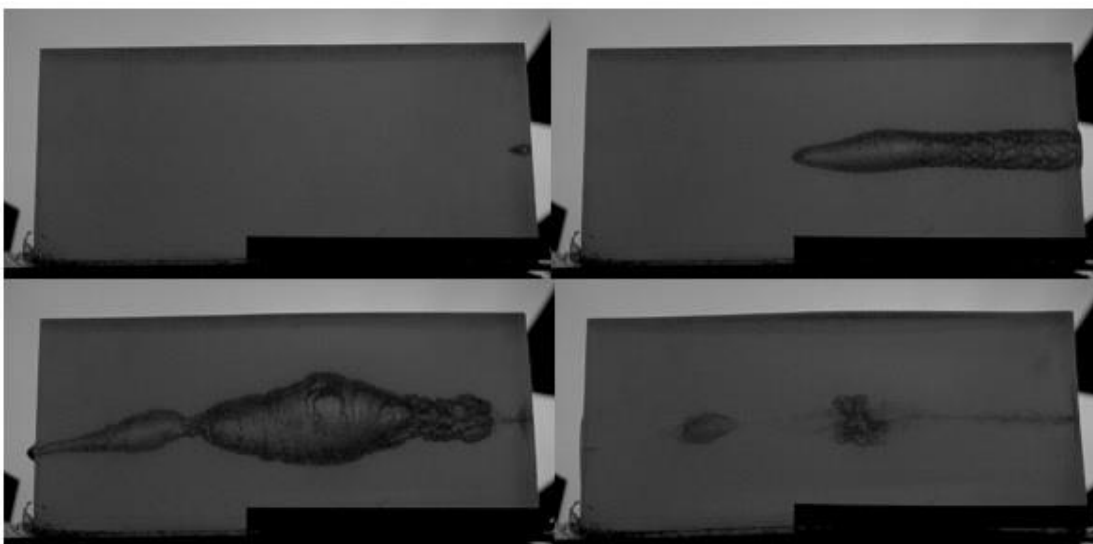


Figure 3-28: Stills from high speed footage showing the formation and collapse of a typical temporary cavity produced in 20% gelatine by a 9mm Luger projectile.

3.3.2.3.1 ANOVA results

Fissure area

The fissure area left in 10% gelatine and 20% gelatine blocks was significantly different after perforation by 9mm Luger DM11 A1B2 FMJ projectiles ($F_{1,18} = 30.148$, $p \leq 0.001$) (Table 3-17b). Mean area was less in 20% than in 10% gelatine (20% gelatine mean = 33100mm^2 , s.d. = 4510mm^2 ; 10% gelatine, mean = 48900mm^2 , s.d. = 7920mm^2) (Table 3-17a).

Table 3-17: Fissure area after perforation of 9mm Luger DM11 A1B2 FMJ projectiles

a Selected descriptive statistics			
Simulant type	Mean (mm²)	s.d. (mm²)	CV (%)
10% gelatine	48900	7920	16.19
20% gelatine	33100	4510	13.64

b Analysis of variance						
Source of variation	SS	d.f.	Mean square	F	Sig.	$\rho \leq$
Gelatine concentration	1252283368.00	1	1252283368.00	30.148	0.000	0.001
Error	747673144.30	18	41537396.90			

Temporary cavity analysis

The distance to the maximum expansion of the temporary cavity caused by 9mm Luger projectiles was not significantly affected by gelatine concentration ($F_{1, 18} = 0.159$, $\rho = NS$) (Table 3-18b). The mean distance was shorter in 20% gelatine blocks (mean = 248.1mm, s.d. = 39.9mm), although larger variability was also witnessed in the 20% gelatine blocks (Table 3-18a).

The size of the maximum diameter of the temporary cavity was significantly affected by gelatine concentration ($F_{1, 18} = 21.937$, $\rho = 0.001$) (

Table 3-19b). Mean cavity size was smaller in blocks 20% in concentration (mean = 83.6mm, s.d. = 12.1); temporary cavity size was over 35mm larger in 10% blocks (mean = 110.0mm, s.d. = 13.1mm). From the coefficient of variation results it was seen variability was greater in 20% gelatine blocks (

Table 3-19a).

Table 3-18: Distance to maximum expansion of temporary cavity caused by 9mm Luger projectiles in gelatine targets

a Selected descriptive statistics			
Simulant type	Mean (mm)	s.d. (mm)	CV (%)
10% gelatine	254.6	31.9	12.53
20% gelatine	248.1	39.9	16.09

b Analysis of variance						
Source of variation	SS	d.f.	Mean square	F	Sig.	$\rho \leq$
Gelatine concentration	207.15	1	207.15	0.159	0.695	NS
Error	23501.49	18	1305.64			

Table 3-19: Maximum diameter of temporary cavity produced by 9mm Luger projectiles in gelatine targets

a Selected descriptive statistics			
Simulant type	Mean (mm)	s.d. (mm)	CV (%)
10% gelatine	110.0	13.1	11.93
20% gelatine	83.6	12.1	14.42

b Analysis of variance						
Source of variation	SS	d.f.	Mean square	F	Sig.	$\rho \leq$
Gelatine concentration	3479.98	1	3479.98	21.937	0.000	0.001
Error	2855.38	18	158.63			

90 ° Yaw

The mean distance to where 9mm Luger yaws to 90 °, for the first and second time respectively, was not significantly affected by gelatine concentration ($F_{1, 18} = 2.294$, $\rho = NS$ (Table 3-20b); $F_{1, 18} = 1.173$, $\rho = NS$ (Table 3-21b)).

Gelatine concentration did however significantly affect the mean location of where 9mm Luger projectiles yawed to 90 ° for the third time ($F_{1, 10} = 0.015$, $\rho = 0.05$ Table 3-22b). Not all shots yawed three times; five shots did in 10% gelatine, and seven shots did in 20% gelatine. From those shots, the mean distance was longer in 10% gelatine (mean = 462.7mm, s.d. = 12.8mm) when compared to 20% gelatine (mean = 432.4mm, s.d. = 25.3mm) (Table 3-22b).

Table 3-20: Distance to first 90 ° yaw of 9mm Luger projectiles in gelatine targets

a Selected descriptive statistics						
Simulant type	Mean (mm)	s.d. (mm)	CV (%)			
10% gelatine	251.4	35.0	13.92			
20% gelatine	231.4	22.9	9.89			

b Analysis of variance						
Source of variation	SS	d.f.	Mean square	F	Sig.	p≤
Gelatine concentration	2005.16	1	2005.16	2.294	0.147	NS
Error	15736.22	18	874.24			

Table 3-21: Distance to second 90 ° yaw of 9mm Luger projectiles in gelatine targets

a Selected descriptive statistics						
Simulant type	Mean (mm)	s.d. (mm)	CV (%)			
10% gelatine	369.1	80.4	21.78			
20% gelatine	332.7	69.6	20.88			

b Analysis of variance						
Source of variation	SS	d.f.	Mean square	F	Sig.	p≤
Gelatine concentration	6619.69	1	6619.69	1.173	0.293	NS
Error	101565.32	18	5642.52			

Table 3-22: Distance to third 90 ° yaw of 9mm Luger projectiles in gelatine targets

a Selected descriptive statistics						
Simulant type	Mean (mm)	s.d. (mm)	CV (%)			
10% gelatine	462.7	12.8	2.76			
20% gelatine	432.4	25.3	5.86			

b Analysis of variance						
Source of variation	SS	d.f.	Mean square	F	Sig.	p≤
Gelatine concentration	2688.43	1	2688.43	5.977	0.035	0.05
Error	4497.68	10	449.77			

3.3.3 Discussion of baseline simulant tests

3.3.3.1 Baseline tests with .223 Remington Federal Premium® Tactical® Bonded® projectiles

The baseline simulant testing was performed in both 10% and 20% gelatine, using two types of ammunition. The results from hardness testing on both projectile types were supported by the SEM analysis. The .223 Remington Federal Premium® Tactical® Bonded® round is a soft point, designed to expand on impact. The exposed lead core, which had a lower Vickers result when compared to the partial brass jacket, facilitates expansion on impact.

The expansion of the .223 Remington Federal Premium® Tactical® Bonded® rounds occurred on impact with both concentrations of gelatine. This produced temporary cavities that expanded beyond the diameter of the projectile on initial penetration, with no initial channel present beforehand (Figure 3-24 and Figure 3-25). The formation of the temporary cavities in both concentrations followed the same pattern, supported by the result that there was no significant difference in the distance to the maximum point of temporary cavitation. The temporary cavities continued to grow as the projectile moved through the targets, with it reaching its greatest size towards the front, petering off as the projectile reached the end of the block; forming a funnel-like shape, with the mouth of the funnel towards the strike face. Every shot was captured completely in the block (for both concentration types) leaving a complete permanent cavity, from which analysis could be carried out, in order to compare the damage. The permanent cavity left in both concentrations of gelatine was reminiscent of an ellipsoid.

Both the permanent and temporary cavities produced by .223 Remington Federal Premium® Tactical® Bonded® projectiles were similar in shape and formation in both gelatine concentrations. However, greater damage was observed in 10% gelatine blocks; with both significantly larger temporary cavity diameters and significantly larger permanent cavity measurements recorded when compared to 20%. Although, as mentioned in the DoP testing, 20% gelatine has a higher density (1.05 g/cm³ compared to 1.03 g/cm³ (Janzon, 1997; Eisler *et al.*, 2001)), and materials of greater density absorb more energy and thus have a higher potential for sustaining damage (Belkin, 1979), the elasticity and gel strength also affects the level of damage. Blocks of 20% gelatine contain a higher concentration of gelatine and thus greater gel strength (Osorio *et al.*, 2007; Rousselot, 2014). The greater gel strength means the blocks are better at resisting the disruptive effects of the temporary cavity. As a result, blocks of 10% gelatine were less efficient at containing the expansion of the temporary cavity, with lesser gel

strength also having an effect on recovery, explaining why greater permanent damage was also produced in 10% blocks.

When measurements of fissures were compared, a similar result was seen; the areas of the fissures are larger in 10% blocks, with the range also greater. This could also be caused by the greater gel strength in 20% gelatine blocks being better at resisting the disruptive effects of the temporary cavity.

Apart from still images from high speed video footage, no results from baseline testing in Perma-Gel™ are presented. The reason for this is because of the inconsistencies witnessed when Perma-Gel™ was struck by a projectile. Three .223 Remington Federal Premium® Tactical® Bonded® rounds were fired into Perma-Gel™ blocks, all producing carbon filled cavities that were very small in comparison to gelatine, while the level of penetration depth varied drastically. These factors, together with problems that were encountered during the making of larger Perma-Gel™ blocks meant a decision was made that the required information from post firing analysis would not be achievable from Perma-Gel™ blocks. As a consequence, no further analysis of Perma-Gel™ blocks will be presented as they offer little benefit to the overall project aim.

3.3.3.2 Baseline tests with 9mm Luger projectiles

The presence of a brass coating on either side of the steel jacket of the 9mm Luger explains why softer areas were found on either side of the jacket during hardness testing. The 9mm Luger is not designed to expand on impact; the brass coated steel full metal jacket stops this from occurring, keeping the projectile intact as it continues through the target. In the baseline testing, this resulted in complete perforation of the 500mm target blocks, regardless of the concentration of gelatine.

During each shot of a 9mm Luger, the spin imparted to the individual projectiles designed to keep them stable during flight could be seen to fail during perforation of the gelatine targets, reaching 90 ° yaw within the 500mm blocks two or three times before exiting. This was not a surprising result considering the effect of density on projectile stability (Cooper and Ryan, 1990; Janzon, 1997; Ryan *et al.*, 1997). No significant difference in the locations of where 90 ° yaw occurred for the first and second time in both gelatine concentrations ties up with the fact that no significant difference was found between the locations where maximum temporary cavity expansion occurred. This is because the temporary cavity is usually largest when the projectile expands or yaws to 90 °; greater presented areas cause greater transfer of

energy to tissues (Berlin *et al.*, 1976). If the projectiles reached 90 ° yaw a third time, a significant difference in location was found between the two concentrations, possibly explained by the denser gelatine having a greater effect on bullet instability.

The permanent cavities left in both gelatine concentrations by the 9mm Luger rounds were vastly different in shape when compared to those left by the .223 Remington Federal Premium® Tactical® Bonded® rounds. Instead of an ellipsoid shape, a helical pattern was left. It can be hypothesised that the helical shape was a result of the spin present on the non-deformed projectile, with the larger areas of temporary cavity expansion a result of the projectiles reaching 90 ° yaw. As a result of the helical shape, a representation of an ellipsoid volume to measure the volume of damage could not be taken, however, fissure area analysis still revealed a similar pattern to that observed with the .223 Remington Federal Premium® Tactical® Bonded® projectiles; area of damage was significantly greater in 10% gelatine blocks compared to 20% gelatine blocks.

3.3.3.3 Overview of baseline tests

The results collected clearly display a difference occurred with regards to the permanent cavity size produced when the same ammunition was tested in different concentrations of gelatine. This result, although not unexpected, does not appear to have been discussed in the open literature before. It also confirmed both gelatine blocks produced permanent cavities that could be dissected, measured and qualitatively analysed.

In a gunshot wound in living tissue, three zones are used to describe the areas of the wound, the central zone, caused by the direct crushing and lacerating of tissue by the projectile, surrounded by the second and third zones, contusion and concussion respectively (Wang *et al.*, 1988; Bowyer *et al.*, 1997b; Ryan *et al.*, 1997). The outer two zones are believed to be the result of the temporary cavitation process, with the zone of contusion consisting of non-viable tissue, and the concussion zone showing damaged tissue capable of recovering (Janzon *et al.*, 1997).

The difference between the zones is not a factor in this discussion regarding gelatine, as the tissue was not living so its viability cannot be considered. However, the permanent cavity left in both concentrations of gelatine was equivalent to the central zone; the area damaged by the direct crushing and lacerating of tissue by both projectile types. Measuring the fissures present in both gelatine concentrations was a method by which this area could be calculated, from which comparison could also be performed between the two concentration types.

The suspected cause of the other two zones (the temporary cavity) was produced in both gelatine concentrations. With the use of high speed video analysis, it was possible to determine the location of where the temporary cavity formed. Measuring the maximum size the cavity reached, together with the location at which this happened, was a method from which comparisons could be drawn between target blocks. This information could then be used to work out where maximum cavitation might occur within a typical human target; it could be hypothesised which region within a human target would be affected given a specific entry location, and the effect this may have on certain organs.

Taking measurements from an estimated ellipsoid volume of damaged gelatine provided a method where comparison of the volume damaged could be achieved. The ellipsoid volume may not be an effective method for deciding the area of living tissue that should be debrided after a gunshot; that should be based on whether tissue is viable or not. However, it was a consistent method for estimating the volume that was damaged and comparing events to see where more damage was done.

The presence of debris was also an important analysis that could be used in assessing which situation's damage was worse. Contamination of tissue is a mechanism of wounding that could have immediate or delayed consequences for wound severity in living tissue (Ryan *et al.*, 1997) and is therefore an important consideration.

Both concentrations of gelatine were damaged in a way that enabled analysis to be carried out, giving results that could be statistically compared. The results that were collected also provided a method for comparison of whether the presence of armour altered the damage produced by the two different projectiles. Both concentrations of gelatine would be suitable to proceed with as a tissue simulant for the remainder of this study, however, a decision was required as to which simulant to use. A final testing method was planned, to see which simulant produced results most representative of porcine tissue.

3.4 Part C – Ballistic testing of porcine samples

Experimental data on how live rounds interact with living tissue is very limited in the open literature. Ethical constraints concerning testing on living tissue meant it was not feasible within the current research. However, with questions raised regarding what the damage recorded in tissue simulants meant in terms of both living tissue and specific areas of a human body, it was a subject that required exploration.

The questions asked are particularly pertinent to the current research topic; gelatine has been shown to be a close match for thigh muscle of both humans and pigs when comparing densities (Janzon *et al.*, 1997; Jussila, 2004), while Fackler produced depth of penetration results in 10% gelatine that were within 3% of living porcine muscle (Fackler *et al.*, 1984a; Fackler *et al.*, 1984b). However, the target area for this research is the thorax. The thorax is composed of many different materials (skin, muscle, bone, heart, lungs, blood vessels, fatty deposits, nerves etc.), and is thus very dissimilar to the composition of thigh muscle. Breeze *et al.* (2013) found significantly different depths of penetration were produced in the thorax and abdomen compared to 20% gelatine, when testing three different fragment simulating projectiles (FSPs). The outcome was attributed to the anatomical complexity and multiple tissue-air interfaces of the thorax and abdominal regions. But how would damage to a tissue simulant compare to damage seen in a thorax after ballistic attack? To try to formulate some answers, experiments were set up to mimic a thorax with the aid of a pair of porcine lungs, sandwiched between porcine ribs.

3.4.1 Materials and methods

3.4.1.1 Target materials

3.4.1.1.1 Porcine samples

Samples of porcine thoracic walls (consisting of the ribs, intercostal muscles, tissue and skin; vertebra and the sternum removed) (Figure 3-29) and sets of lung pairs complete with trachea (Figure 3-30) were collected (Andrews Quality Meats Ltd., 16 High Street, Highworth, Wiltshire, SN6 7AG, UK) and kept refrigerated one day prior to testing. Samples were brought up to room temperature for at least 12 hours before testing ($\approx 18^{\circ}\text{C} \pm 3^{\circ}\text{C}$). The samples used were all of food-grade standard and fit for human consumption, consequently there were no ethical concerns raised for this study (Appendix I).



Figure 3-29: A front and back view of a typical example of the porcine thoracic wall tested



Figure 3-30: A front and back view of a typical example of a set of lungs tested

3.4.1.1.2 Gelatine

Gelatine blocks (10% concentration by mass) were made following the method discussed in section 3.2.1.1.1 Gelatine.

3.4.1.2 Ammunition

The two rounds used in the baseline simulant tests were used for this study, namely the:

- i) .223 Remington (62 grain; Federal Premium® Tactical® Bonded®)
- ii) 9mm Luger (124 grain; full metal jacket; DM11 A1B2) (Figure 3-15, section 3.3.1.2 Ammunition).

3.4.1.3 Ballistic testing method

The porcine samples were arranged to simulate a thorax (Figure 3-31); a thoracic wall was placed as the anterior of the target (skin facing muzzle) (Figure 3-32), then a set of lungs positioned in relation to the thoracic wall as they would be anatomically in the body, followed by another thoracic wall (skin facing away from muzzle) (Figure 3-33). At the back of the simulated thorax, a 10% gelatine block was placed adjacent to and in contact with the back thoracic wall (Figure 3-34).

The target was placed 10 m away from the end of the muzzle. An Enfield Number 3 Proof Housing, with the appropriate barrel fitted, was used to fire each ammunition type. Each individual shot was aimed with the goal of striking: a rib within the front thoracic wall, either the left or right lung, and a rib in the rear thoracic wall, before capturing the rest of the tract in a gelatine block. Shots that were fired into the same thoracic sections were spread out to ensure damaged areas did not overlap. Ten shots in total were carried out (n = 7 for .223 Remington Federal Premium® Tactical® Bonded®; n = 3 for 9mm Luger).

The impact velocities were recorded using a Weibel W-700 Doppler radar. A Phantom high-speed video camera (V12) was used to record the impact events (28,070 fps, 5 μ s exposure time and 512 x 384 frame resolution). A scale was used in all impacts to allow the high-speed video footage to be calibrated during analysis. Digital photographs were also taken using a Nikon D90 complete with a Nikon DX AF-S NIKKOR 18-105mm lens.

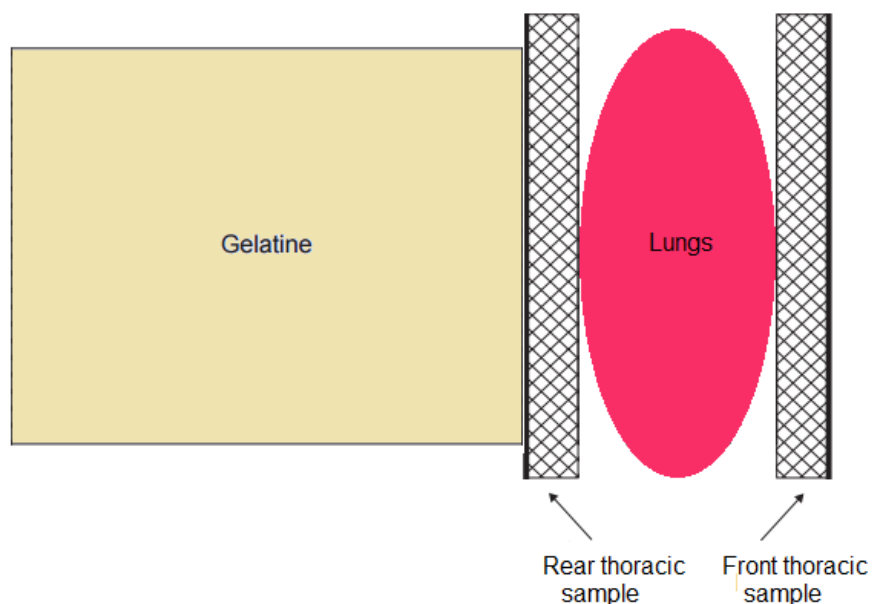


Figure 3-31: Schematic diagram showing the simulated thorax arrangement.



Figure 3-32: View of the typical set up from the front showing the front thoracic wall with the skin facing the muzzle



Figure 3-33: Typical set up showing the arrangement of the thoracic walls and lungs

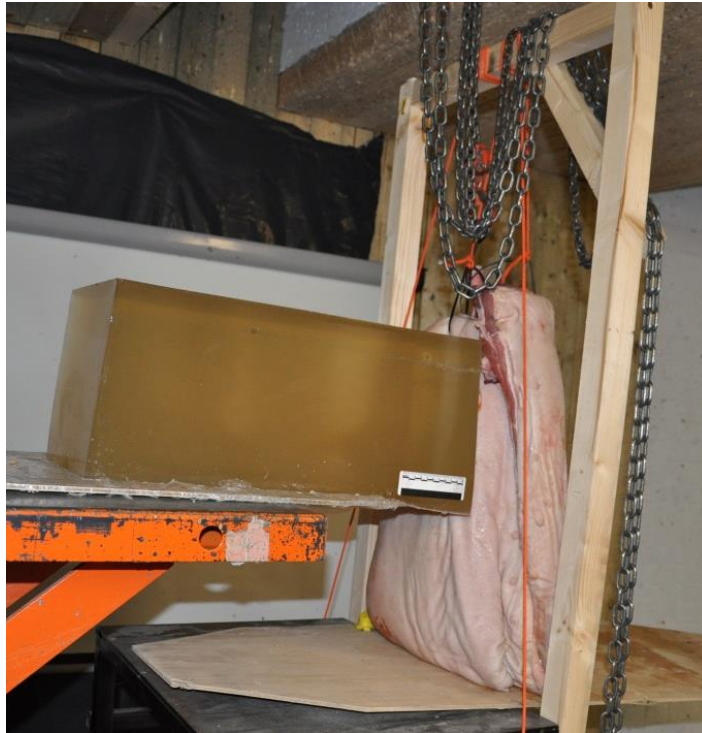


Figure 3-34: View of the set-up from the rear, with a 10% gelatine block placed adjacent to the porcine samples

3.5.1.4 Analysis

Post firing analysis of the thoracic walls and lungs was performed after all shots had been completed. Measurements of the entrance and exit wounds of each shot, together with photographs, were taken from every penetrated section of each simulated thorax (i.e. the front thoracic wall, the penetrated lung, and the rear thoracic wall) (Figure 3-35 - Figure 3-37). Any projectile and/or bone fragments found were photographed, recovered and then weighed (using an A2204 Oxford Balance; Analytical products Ltd, Oxford, England, OX3 8ST. Developed, manufactured and tested in compliance with ISO 9001), before dissection of the wounds took place (Figure 3-38 and Figure 3-39). Further fragments found from exploration of the damage were also photographed, recovered and weighed (Figure 3-40 and Figure 3-41).

Post firing analysis of the gelatine blocks consisted of cutting along the length of the permanent cavity, before measurements of the cavity were taken. When present, the projectile and any projectile and/or bone fragments were photographed, recovered and weighed.

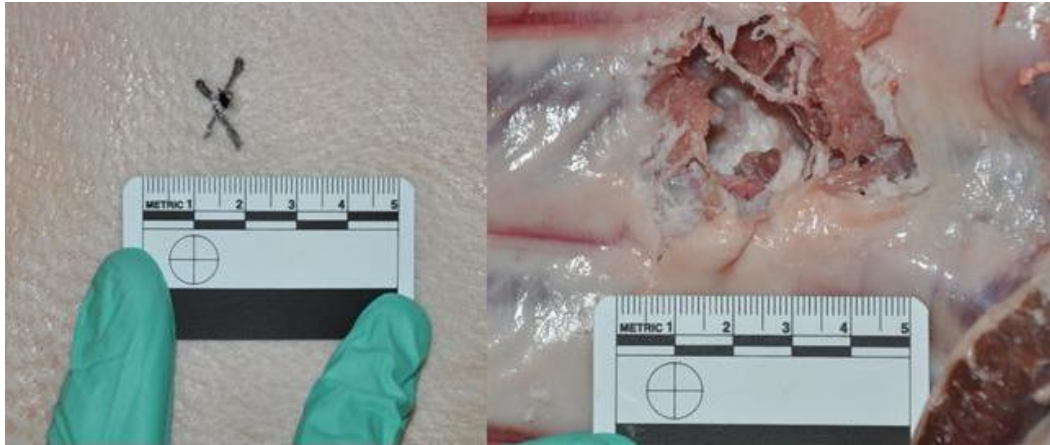


Figure 3-35: Typical example of an entrance (left) and exit (right) shot into the front thoracic wall. These examples are after perforation of .223 Remington Federal Premium® Tactical® Bonded® round

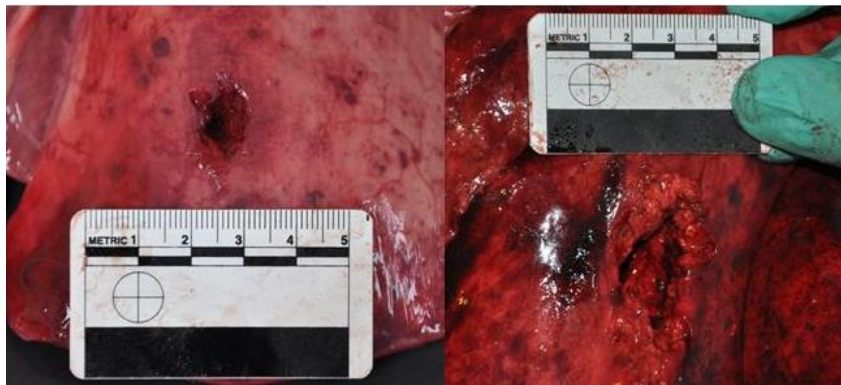


Figure 3-36: Typical example of an entrance (left) and exit (right) shot into the lung. This damage was caused by a .223 Remington Federal Premium® Tactical® Bonded® round

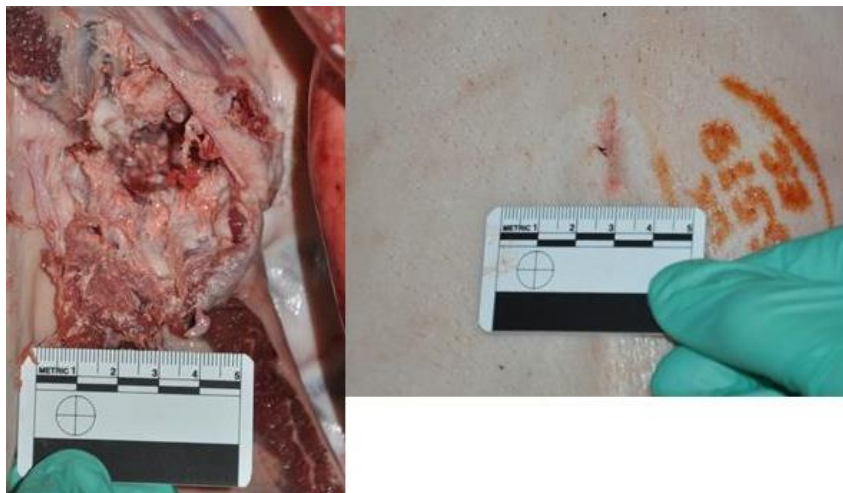


Figure 3-37: Typical example of an entrance (left) and exit (right) shot into the back (second) thoracic wall. These examples were caused by a .223 Remington Federal Premium® Tactical® Bonded® round

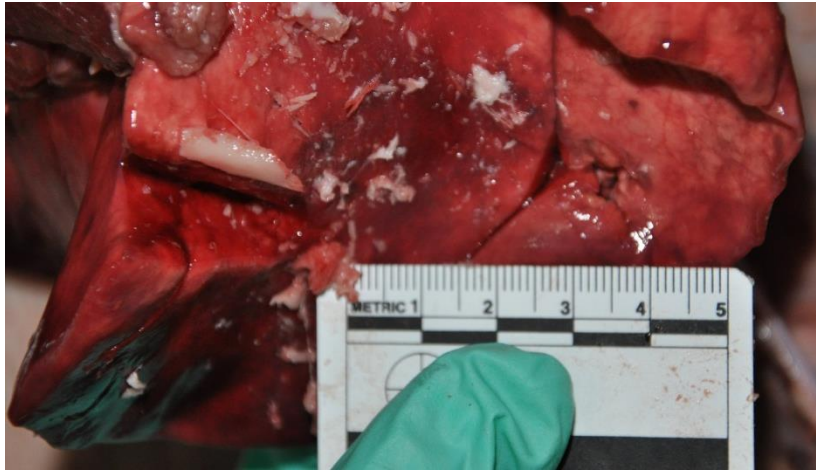


Figure 3-38: Typical example of the bone debris seen in lung. This example was after perforation of a .223 Remington Federal Premium® Tactical® Bonded® round

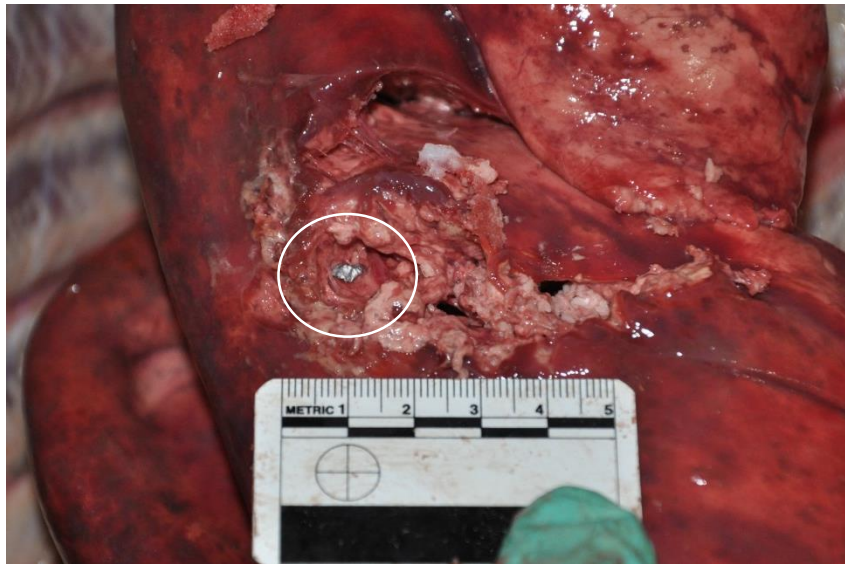


Figure 3-39: Example of the lead debris seen in the tract in the lung after the perforation of a .223 Remington Federal Premium® Tactical® Bonded® round

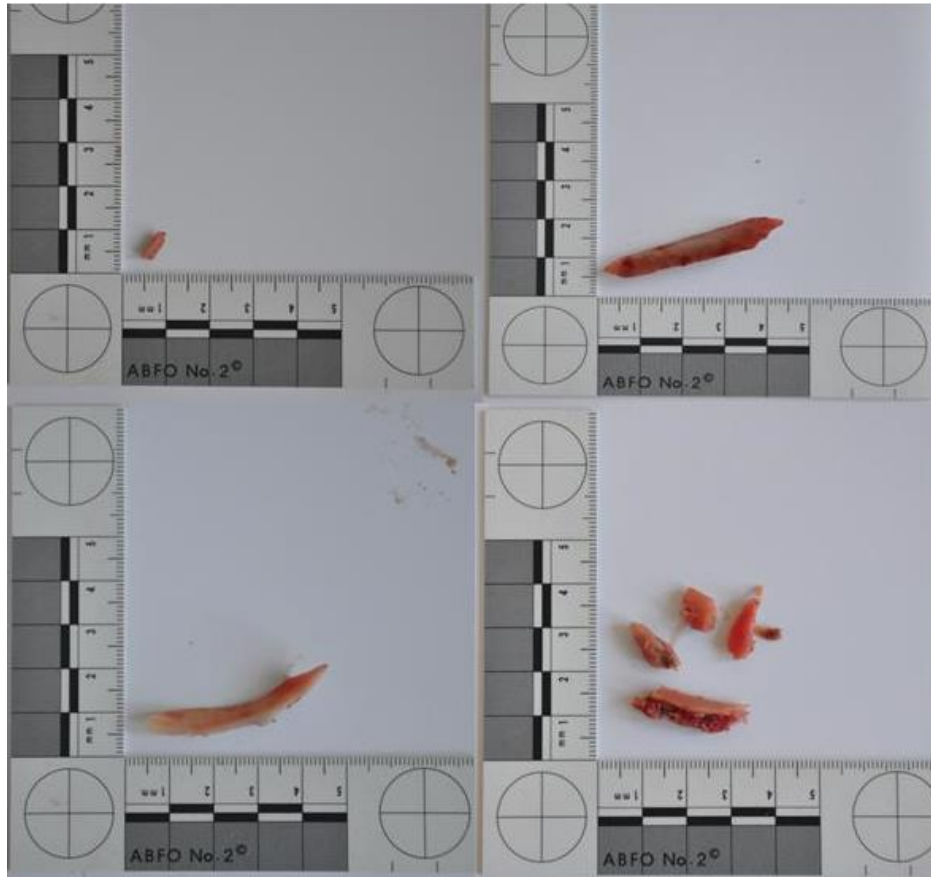


Figure 3-40: Typical examples of the of bone fragments recovered during dissection of the thoracic samples

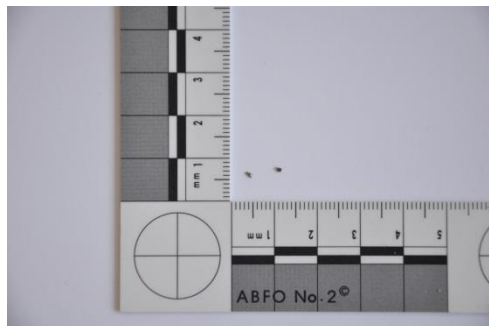


Figure 3-41: Typical examples of the lead debris recovered during the dissection of the thoracic samples

3.5.1.4.1 Comparison of results from porcine and baseline testing

Analysis of variance (ANOVA) and Tukey analysis were used to determine if there were significant differences among the distance to projectile data obtained from firing .223 Remington Federal Premium® Tactical® Bonded®mm projectiles at the porcine thoracic target arrangement, 10% gelatine targets and 20% gelatine targets (SPSS Statistics 22.0). Normality of data and equality of variance were checked for each data set.

3.4.2 Results

The raw data collected from firing .223 Remington Federal Premium® Tactical® Bonded® projectiles at simulated thoraxes is presented in the tables below (Tables 3-23 – 3-29). Every shot remained within the gelatine block placed at the rear of the simulated thoraxes. The results are then compared to the appropriate results from the baseline testing with the same ammunition.

Table 3-23: Thoracic sample details

Target number	Porcine sample	Mass (g)	Target depth (mm)*
1	Thoracic wall 1 anterior (right)	10074	177
	Thoracic wall 1 posterior (left)	9193	
	Lung 1	1080	
2	Thoracic wall 2 anterior (right)	9106	165
	Thoracic wall 2 posterior (right)	9484	
	Lung 2	1107	
3	Thoracic wall 3 anterior (right)	10327	170
	Thoracic wall 3 posterior (left)	7722	
	Lung 3	1589	

*Target depth was the distance from the front face of the anterior wall to the back face of the posterior wall

3.4.2.1 .223 Remington Federal Premium® Tactical® Bonded® results

Table 3-24: Shot details – .223 Remington Federal Premium® Tactical® Bonded®

Shot no.	Ammunition	Target set up	Impact velocity (m/s)
1	.223 Remington	Target 1 (right lung) with gelatine block 1	852
2	.223 Remington	Target 1 (left lung) with gelatine block 2	851
6	.223 Remington	Target 2 (left lung) with gelatine block 3	847
7	.223 Remington	Target 2 (right lung) with gelatine block 4	845
8	.223 Remington	Target 3 (right lung) with gelatine block 5	840
9	.223 Remington	Target 3 (left lung) with gelatine block 6	837
10	.223 Remington	Target 3 (left lung) with gelatine block 6	847

Table 3-25: .223 Remington Federal Premium® Tactical® Bonded® strike locations through target

Shot number	Entry location		
	Anterior thoracic wall	Lungs	Posterior thoracic wall
1	Nicked rib 5	Right lung, nicked the top of the inferior lobe	Hit rib 3
2	Hit rib 5	Left lung, top area of the inferior lobe	Hit rib 4
6	Hit rib 7	Left lung, middle area of the superior lobe	Hit rib 7
7	Hit rib 5	Right lung, nicked the top edge of the middle lobe	Between ribs 3 & 4
8	Hit ribs 5 & 6	Right lung, top area of the third inferior	Hit rib 5
9	Hit rib 7	Left lung, bottom area of the superior lobe	Hit rib 6
10	Hit rib 8	Left lung, middle area of the inferior lobe	Hit rib 8

Table 3-26: .223 Remington Federal Premium® Tactical® Bonded® entry and exit dimensions

Shot number	Anterior thoracic wall				Lungs				Posterior thoracic wall			
	Entry		Exit		Entry		Exit		Entry		Exit	
	Width (mm)	Height (mm)	Width (mm)	Height (mm)	Width (mm)	Height (mm)	Width (mm)	Height (mm)	Width (mm)	Height (mm)	Width (mm)	Height (mm)
1	4	3	22	24	16	18	22	32	31	23	5	5
2	3	4	41	42	18	20	23	21	28	25	3	5
6	4	3	35	22	40	37	19	8	19	31	4	3
7	3	3	36	33	N/A*	N/A	N/A	N/A	39	28	9	6
8	4	4	48	54	27	20	16	21	24	22	3	3
9	4	4	36	32	46	33	27	19	31	23	9	4
10	4	3	27	31	52	43	10	9	24	21	7	3

*Lobe was torn, so entry and exit measurements could not be taken

Table 3-27: Distance to .223 Remington Federal Premium® Tactical® Bonded® projectiles

Shot number	Distance through thoracic setup (mm)	Distance in 10% gelatine (mm)	Total distance (mm)
1	177	299	476
2	177	245	422
6	165	295	460
7	165	332	497
8	170	287	457
9	170	269	439
10	170	299	469

Table 3-28: Details of location and mass of fragments collected from samples after .223 Remington Federal Premium® Tactical® Bonded® shots

Shot number	Tract through anterior thoracic wall (g)	Front face of lung (g)	Tract through lung (g)	Back face of lung (g)	Tract through posterior thoracic wall (g)	Miscellaneous* (g)
1	0.0420				0.3293, 0.003[♠]	
2	1.2417	0.1153		0.0152	0.0216	0.03
6	0.0981				0.0020	
7	0.8323	0.2143			0.0467	
8	0.1025			0.0877	0.1055	1.5616, 0.1016
9	0.6787			0.3732, 0.0014		
10	0.0750	0.2276, 0.0252	0.0249	0.1530	0.0380, 0.0089	

* Collected from the range immediately after the shot

[♠]**Fragments in bold and italics were metal fragments.**

Table 3-29: Mass of .223 Remington Federal Premium® Tactical® Bonded® projectiles and fragments collected from 10% gelatine blocks

Shot number	Recovered projectile and fragment mass (g)
1	3.7933
2	3.8796
6	3.8291
7	3.7406
8	3.5363
9	3.2625
10	3.8206
9*	0.0318

* Bone fragment found in gelatine from shot 9

3.4.2.1.1 Distance to projectiles ANOVA

Results from the simulated thorax testing were compared with results from the baseline tests (Table 3-7b) in both 10% and 20% gelatine blocks 500mm in length. As only seven shots were carried out with the .223 Remington Federal Premium® Tactical® Bonded® rounds, only the first seven shot results collected from the baseline trials were used for the ANOVA to ensure equality of sample size.

The target material had a significant effect on the distance to .223 Remington Federal Premium® Tactical® Bonded® projectiles ($F_{2, 18} = 146.536, \rho \leq 0.001$) (Table 3-30b). Tukey's HSD multiple comparison test indicated the three target types resulted in three varying levels of distances travelled by the projectiles (Table 3-30c). Distance was greatest in the simulated thoraxes (mean = 460.0mm, s.d. = 24.5mm), closely followed by the distance in 10% gelatine (mean = 424.6mm, s.d. = 15.3). When standard deviations are considered, mean distance in simulated thoraxes and 10% gelatine overlap. Mean distance in 20% gelatine was over 160mm shorter compared to the simulated thoraxes (mean = 298.3mm, s.d. = 14.2mm) (Table 3-30a). Comparison of the respective CVs revealed the variability of the simulated thoraxes was similar to those produced in the gelatine targets.

Table 3-30: Distance to .223 Remington Federal Premium® Tactical® Bonded® projectiles

a Selected descriptive statistics						
Target material	Mean (mm)	s.d. (mm)	CV (%)			
Simulated thorax	460.0	24.5	5.33			
10% gelatine (500mm)	424.6	15.3	3.60			
20% gelatine (500mm)	298.3	14.2	4.76			

b Analysis of variance						
Source of variation	SS	d.f.	Mean square	F	Sig.	$\rho \leq$
Target material	101161.14	2	50580.57	146.536	0.000	0.001
Error	6213.14	18	345.18			

c Tukey's HSD multiple comparison test			
Target material	Mean (mm)	N	Tukey groupings
Simulated thorax	460.0	7	
10% gelatine (500mm)	424.6	7	
20% gelatine (500mm)	298.3	7	

3.4.2.1.2 Distance to .223 Remington Federal Premium® Tactical® Bonded® projectiles (non-rib striking shots removed) ANOVA

Studying the strike location through the simulated thoraxes revealed that shot 7, which resulted in the longest distance to the projectile, did not fully strike a lung (caught the top edge of the right middle lobe), while also exiting the posterior thoracic wall without hitting a rib (between ribs 3 and 4). Shot 1 also only nicked the top of a lung lobe (top of the inferior lobe), while not hitting a rib squarely when entering the anterior thoracic wall (nicked rib 5) (Table 3-25). Therefore, another ANOVA was run with these two shots removed along with the first five shots from the baseline work in the 10% and 20% gelatine (Table 3-7b).

Distance to .223 Remington Federal Premium® Tactical® Bonded® projectile was significantly affected by the target material ($F_{2, 12} = 135.094$, $p \leq 0.001$) (Table 3-31b). Tukey’s HSD multiple comparison revealed the existence of two differing levels of distances travelled by the projectiles; projectiles which struck the simulated thoraxes and 10% gelatine blocks in one level, shots into 20% gelatine blocks in the other (Table 3-31c). The simulated thoraxes produced the longest mean distances (mean = 449.4mm, s.d. = 18.8mm), 19.4mm greater in length than shots into 10% gelatine (mean = 430.0mm, s.d. = 13.5mm). Distances in 20% gelatine blocks were on average a further 126.2mm shorter (mean = 303.8mm; s.d. = 12.6mm) (Table 3-31a).

Table 3-31: Distance to .223 Remington Federal Premium® Tactical® Bonded® projectiles (non-rib striking shots removed)

a Selected descriptive statistics						
Target material	Mean (mm)	s.d. (mm)	CV (%)			
Simulated thorax	449.4	18.8	4.18			
10% gelatine (500mm)	430.0	13.5	3.13			
20% gelatine (500mm)	303.8	12.6	4.16			

b Analysis of variance						
Source of variation	SS	d.f.	Mean square	F	Sig.	$p \leq$
Target material	62503.60	2	31251.80	135.094	0.000	0.001
Error	2776.00	12	231.33			

c Tukey's HSD multiple comparison test

Target material	Mean (mm)	N	Tukey groupings
Simulated thorax	449.4	5	
10% gelatine (500mm)	430.0	5	
20% gelatine (500mm)	303.8	5	

3.4.2.2 9 x 9mm FMJ results

All 9mm Luger shots perforated both the simulated thoraxes and the 500mm gelatine block at the rear of the target. This result was the same as those produced in the baseline study with just gelatine blocks (10% and 20%) 500mm in length as the target. As a result, no analysis into the distance to the projectiles was carried out. However, the raw data collected from the interactions with the simulated thoraxes are presented below in tables 3-32 – 3-35.

Table 3-32: Shot details –9mm Luger DM11 A1B2

Shot	Ammunition	Target set up	Impact velocity (m/s)
3	9mm Luger	Target 1 (left lung) with gelatine block 2	413
4	9mm Luger	Target 1 (right lung) with gelatine block 1	420
5	9mm Luger	Target 2 (right lung) with gelatine block 3	410

Table 3-33: 9mm Luger strike locations through target

Shot number	Entry location		
	Anterior thoracic walls	Lungs	Posterior thoracic walls
3	Hit rib 8	Left lung, bottom area of the inferior lobe	Between ribs 7 & 8
4	Nicked rib 7	Right lung, bottom area of the inferior lobe	Between ribs 6 & 7
5	Between 7 & 8	Right lung, middle area of the inferior lobe	Between ribs 5 & 6

Table 3-34: 9mm Luger entry and exit dimensions

Shot number	Anterior thoracic walls				Lungs				Posterior thoracic walls			
	Entry		Exit		Entry		Exit		Entry		Exit	
	Width (mm)	Height (mm)	Width (mm)	Height (mm)	Width (mm)	Height (mm)	Width (mm)	Height (mm)	Width (mm)	Height (mm)	Width (mm)	Height (mm)
3	4	4	17	21	6	8	10	11	12	15	10	2
4	6	5	15	12	10	10	10	13	8	10	6	1
5	7	5	20	13	6	4	10	9	11	10	3	3

Table 3-35: Details of location and mass of fragments collected from samples after 9mm Luger shots

Shot number	Tract through anterior thoracic wall (g)	Front face of lung (g)	Tract through lung (g)	Back face of lung (g)	Tract through posterior thoracic wall (g)	Miscellaneous* (g)
3	0.1061					
4	0.0629	0.0392, <i>0.0009</i>				

*Fragments in bold and italics were metal fragments.

3.4.3 Discussion

The use of tissue simulants to represent the inhomogeneous nature of a living target is well documented, however a common question is “How would damage to a tissue simulant compare to damage seen in living tissue after ballistic attack?” With particular interest into the region of the thorax, this section considered the use of porcine tissue samples to see how damage compared to both 10% and 20% gelatine targets. Porcine samples have been used previously in ballistic testing; in the form of specific sections from whole cadavers (e.g. Breeze *et al.*, (2013): thigh, abdomen, thorax and neck; Breeze *et al.*, (2015b): thigh), as well as in similar form to the samples tested in this trial (Carr *et al.*, 2014; Mabbott *et al.*, 2014). Work conducted by Breeze *et al.* (2015) has shown that refrigerating or freezing porcine tissue followed by thawing had no effect on the level of retardation to FSPs. Although work comparing penetration depths of FSPs into 20% gelatine and porcine tissues has been carried out (Breeze *et al.*, 2013), it is believed that the current work is the first in the open literature to compare damage produced by live rounds in a simulated thorax formed of porcine samples to both 10% and 20% gelatine.

Comparing .223 Remington Federal Premium® Tactical® Bonded® baseline shots into porcine tissue and both 10% and 20% blocks of gelatine revealed significant differences between all three with respect to the distance to the projectile after penetration. However, when

shots which failed to strike all sections of a simulated thorax and/or ribs were removed, a significant difference was only apparent between the distances to projectiles in 20% gelatine (in one group) and distances in both 10% gelatine and the simulated thoraxes (both in the same group). The fact that the simulated thoraxes had a 10% gelatine block at the rear of the target and the measurement to the distance of the projectile included the distance travelled through this block is a point of discussion. The target design did however follow a similar setup to that used by Fackler *et al.* (1984a; 1984b), from which it was claimed penetration depth of 10% gelatine was measured to within 3% of the penetration depth in living porcine leg muscle, following three shots of two projectile types.

The two shots that were removed in order for no significant difference to be present between distance to the projectiles in the simulated thoraxes and the 10% gelatine was a result of the inhomogeneous nature of tissues which form living organisms. When bone was struck, no significant difference was observed. One of the recommended criteria for a tissue simulant is that it is homogeneous, so that factors such as location of shot do not have an effect on the results. This is why a simulant is required to simulate living tissue; a role which in this work 10% gelatine fulfilled with respect to the distance the projectile penetrated.

The damage produced in the simulated thoraxes was measured in terms of entry and exit dimensions, together with the collection of debris. The level of debris collected for the porcine specimens was far greater than that of the baseline simulant tests; the presence of solid materials (bone) in the target was the cause of this; not a surprising result. It did however demonstrate how the debris can spread when dense materials (such as bone) that are present within a target structure are involved in a gunshot incident. The production of secondary projectiles caused when a bullet strikes bone has been reported previously (e.g. Janzon *et al.*, 1997; Hiss and Kahana, 2000; Dodd, 2006). No exterior targets (e.g. clothing, body armour) were struck prior to entering the target, so there was limited chance of foreign debris being brought into the damaged region to cause contamination. However, Hiss and Kahana (2000) state that micro-organisms from perforated tissues of the target can be spread throughout a wound, causing contamination.

3.5 Discussion on the selection and justification of a tissue simulant

3.5.1 Perma-Gel™

Overall the performance of Perma-Gel™ did not meet the requirements of a tissue simulant needed for an investigation into the overmatching of UK police body armour. A summary of the reasons are:

- The ballistic performance of the blocks changed after melting, highlighted by the DoP results from testing 5.5mm BBs (Figure 3-12 and Figure 3-13).
- Difficulty in forming blocks large enough to capture a complete projectile tract, with issues including discolouration, presence of bubbles throughout the block that could not be removed and sinking occurring in the middle of the blocks.
- Inconsistencies in the damage produced when conditions were kept constant during testing.
- The damage produced after ballistic impact was contaminated with carbon, thus making it non-reusable.
- Large flashes occurring during ballistic penetration making high speed video analysis for section of the footage unmanageable.

3.5.2 Gelatine

Both 10% and 20% gelatine concentrations have been used by other researchers for ballistic testing, and both were considered in the current work (Fackler *et al.*, 1984a; Fackler *et al.*, 1984b; Fackler and Malinowski, 1985; Fackler, 1987; Fackler *et al.*, 1988; Fackler and Malinowski, 1988; Nicholas and Welsch, 2004; Cronin and Falzon, 2011).

The production of both concentrations followed guidelines used by CAST further developed in the current work, albeit altered to produce larger blocks. Although the work carried out by Jussila (2004) focused solely on 10% blocks, he reported that consistent quality gelatine blocks were “easy to make”, with variables such as temperature of the water having a far smaller effect than previously thought. The 10% and 20% blocks produced for both the DoP and baseline tests in the current work were of a consistent quality. This claim is supported by the confidence shots of 5.5mm BBs fired into every block tested, fitting the DoP results collected from the first trials completed (Appendix G). Although a standardised method is not currently available, the methods used in this work have been shown to produce repeatable blocks of a consistent nature.

These methods of making the blocks themselves were labour intensive; stirring the solution by hand, as well as requiring two people for efficient production times. However, this led to a gelatine solution with far less foam and bubbles when compared with solutions produced by other means (e.g. drill, cement mixer). The temperature of the water used for the production of both blocks was higher than that recommended by Fackler and Malinowski (1985), however, following the guidelines of Jussila (2004), temperatures of 80°C and above were avoided.

Block sizes of gelatine were another topic of debate amongst researchers, with no standardised size in existence. Jussila (2004) recommended 200mm (w) x 200mm (h) x 250mm (l) as a size suitable to capture all calibres while Fackler and Malinowski (1985) claimed blocks 250mm x 250mm x 500mm gave a 'valid area'. Blocks sizes 250mm (w) x 250mm (h) x 500mm (l) with tapered sides were selected. Ball bearings fired during DoP testing all remained in the gelatine blocks comfortably, unlike the standard Perma-Gel™ blocks. When it came to testing projectiles, the blocks of both concentrations captured the whole permanent cavities of the .223 Remington Federal Premium® Tactical® Bonded® rounds. Although the 9mm Luger rounds perforated both concentration types, cavities of the channel were still left leaving results for analysis, while imagery of the projectiles penetrating the blocks provided further data to analyse.

The overall performance of both 10% and 20% gelatine blocks were very good and from the baseline simulant tests there was little to decide between the two concentrations in terms of which to continue with. Testing of porcine samples arranged to simulate a thorax showed the distance to .223 Remington Federal Premium® Tactical® Bonded® rounds that struck ribs was not significantly different from distances captured in 10% gelatine blocks. Distances were significantly different to 20% gelatine blocks. This, together with the fact 10% gelatine has been validated against live tissue, albeit porcine thigh muscle, and 20% has not been, it was decided to use 10% throughout the remainder of this study. Other influences included less gelatine powder being required to make a 10% by mass concentration block, saving on the cost of materials. The process was also less labour intensive.

3.6 Chapter summary

The work described in Chapter 3 compared different simulants with respect to depth of penetration testing and the damage that could be collected, analysed and compared after a ballistic event. This work, together with the testing of porcine thoracic samples led to the justification and selection of 10% gelatine as the best simulant to use to assess how overmatching body armour affects the damage produced after a ballistic event. Blocks of 10% gelatine were taken forward and used to capture the damage produced after perforation of body armour. This work, together with the comparison of damage in baseline gelatine blocks and gelatine blocks with armour both in front and behind the target, is discussed in Chapter 4.

Chapter 4 : THE OVERMATCHING OF ARMOUR

4.1 Introduction

Chapter 4 discusses through the work that was carried out overmatching two types of UK police body armour (namely HG2 and KR1/SP1). The chapter is split into three parts: *Part A: Armoured gelatine blocks 500mm in length* which investigates the presence of these two armour types in front of 10% gelatine blocks, *Part B: Armoured gelatine blocks 250mm in length*, a section considering the role of armour that is overmatched both in front of and behind a 10% gelatine block, and finally *Part C: Armoured simulated thoraxes* which utilises the work of Chapter 3 Part C with the addition of armour panels on the front and back face of the target.

4.2 Part A: Armoured gelatine blocks 500mm in length

Gelatine blocks 10% by mass that were 500mm in length were used. Completed work from the previous chapter (*3.3 Part B – Baseline simulant tests*) showed that these blocks were large enough to capture the full damage of the .223 Remington Federal Premium® Tactical® Bonded® rounds, while also capturing a large damage profile for 9mm Luger projectiles. The aim was to capture as much of the damage profile as possible, regardless of the typical depth of the human body. Armour panels that met the compliance levels of HG2 and KR1/SP1 were placed on the front face of 10% gelatine blocks and impacted with .223 Remington Federal Premium® Tactical® Bonded® and 9mm Luger projectiles respectively. The results were then compared to the data collected from the baseline shots into not-armoured 10% gelatine blocks (*3.3.2 Results*), to assess the effect of overmatching armour.

4.2.1 Materials and methods

4.2.1.1 10% gelatine

The method for making 10% gelatine blocks was the same as the method described in Section *3.2.1.1.1 Gelatine*.

4.2.1.2 Body armour

Two levels of body armour protection were selected by The Home Office CAST. They were:

- i) HG2 (“Protection against standard ammunition fired from long-barrelled handguns” (Croft and Longhurst, 2007B)).
- ii) KR1/SP1 (Medium protection level from knife and spikes; “a general duty garment for extended wear and may be covert or overt” (Croft and Longhurst 2007C)).

The body armour was provided by CAST in the form of panels; HG2 panels were 250mm x 250mm in size and the KR1/SP1 were 400mm x 400mm (Figure 4-1). The HG2 armour was of particular interest as handguns were the most commonly used firearm in the UK after air weapons in 2013/2014 (Office for National Statistics, 2015). The HG2 specification was the highest level of protection specifically for the threat of handguns that was available to UK police officers. Thus, it was of interest to CAST to see the effect of overmatching such protection with rifle ammunition.

Patrolling police officers in the UK are under greater risk of coming up against a stab or slash threat (when compared to a ballistic threat) (Tobin and Iremonger, 2006), and as a result knife and spike protection is routinely available. In the topic of overmatching, what would happen if a ballistic threat in the form of a handgun was used against armour that was designed to protect against knives or spikes? The aim of using KR1/SP1 armour panels was to try to answer this question.



Figure 4-1: Typical examples of HG2 (Left) and KR1/SP1 body armour panels (right).

4.2.1.3 Ammunition

The ammunition used was the same as described in Section 3.3.1.2 *Ammunition*, namely the .223 Remington (62 grain; Federal Premium® Tactical® Bonded®) and the 9mm Luger (124 grain; full metal jacket; DM11 A1B2).

4.2.1.4 Ballistic testing method

Ballistic testing followed the same method that is described in Section 3.3.1.3 *Baseline simulant method*, with the following alterations. HG2 body armour panels were tested with .223 Remington Federal Premium® Tactical® Bonded® rounds, while the 9mm Luger rounds were used against KR1/SP1 panels. The respective armour panels were placed on the front face (i.e. impacted face) of the 10% gelatine blocks, making sure the two materials were in contact with no gap between them (Figure 4-2). For all shots it was ensured each armour panel was orientated in the correct way; the “body side” was placed against the gelatine blocks. Following the HOSDB ballistic testing standard, the position of each shot was marked out so that no armour panels were hit within 50mm to a previous shot or to the edge of the armour pack (Croft and Longhurst, 2007B). It was ensured that each projectile would strike the gelatine block as centrally as possible, encompassing the damage without interference from the edge of the block or from quality control check shots. No more than 3 shots were carried out on each individual HG2 250mm x 250mm armour panel, with no more than 6 shots on a single 400mm x 400mm KR1/SP1 panel. Ten replicate shots of both ammunition types against the respective protection levels present at the front of 10% gelatine blocks 500mm in length were performed (n=10).



Figure 4-2: Typical target set up of 10% gelatine block 500mm in length with a body armour panel (HG2) on the front face.

4.2.1.5 Analysis

Analysis of the tissue simulants post-firing followed the method described in Section 3.3.1.4 *Baseline simulants analysis*. Any debris (fibre, metal) present in the tract was photographed *in situ* before being collected. Additional physical analysis from this trial included collecting all the .223 Remington Federal Premium® Tactical® Bonded® rounds and photographing them to measure the level of expansion they went through. This was not possible with the 9mm Luger rounds as the projectiles were not recovered due to perforating all targets.

Summary statistics (mean (\bar{x}), standard deviation (s.d.) and coefficient of variation (CV)) were calculated for the fissure area for both projectiles. Summary statistics were also carried out on the permanent cavity data sets (neck length, ‘body’ length, ‘body’ width, ‘body’ height and (when possible) distance to projectile described and demonstrated in both Figure 3-18 and Table 3.5) produced by .223 Remington Federal Premium® Tactical® Bonded® projectiles, as was the level of expansion these projectile went through. Analysis of variance (ANOVA) was used to determine when significant differences between the shots from this trial and the baseline trial into 10% gelatine without armour occurred (SPSS Statistics 22.0). Normality of data and equality of variance were checked for each data set. In instances where an inequality of variance was present (i.e. Levene’s test was significant) that could not be explained, an unequal variance t-test (a Welch’s t-test) was carried out.

4.3.1.6 EKE deposited and high speed video analysis

The expected kinetic energy (EKE) deposited in each gelatine block from each shot was calculated following the method described in Appendix J. This was carried out on shots from this trial as well as the shots from the baseline trials. The values collected were then statistically analysed; summary statistics (mean (\bar{x}), standard deviation (s.d.) and coefficient of variation (CV)) were carried out on each data set before ANOVA was used to determine if the presence of armour produced significant differences in the EKE deposited (SPSS Statistics 22.0). Normality of data and equality of variance were checked for each data set.

As with the high speed analysis that was carried out on the baseline shots (3.3.1.4.1 *High speed video analysis*), the diameter of the temporary cavity at its largest, and the distance within the block where this occurred were taken for armoured block combinations. Summary statistics and ANOVA were used to compare these results with those collected from the baseline trial into 10% gelatine blocks to identify whether the presence of armour had a

significant effect on i) the location where the temporary cavity was largest and on ii) maximum diameter reached.

Finally, summary statistics and ANOVA was carried out on the respective distances collected for where 9mm Luger rounds yawed to 90 ° within the target.

4.2.2 Results from .223 Remington Federal Premium® Tactical® Bonded® rounds

The raw data collected from the interactions between .223 Remington Federal Premium® Tactical® Bonded® rounds and both baseline and armoured 500mm long 10% gelatine blocks are presented below in Table 4-1 and Table 4-2. The results revealed that the unprotected baseline gelatine block targets produced larger means in all physical measurements taken, apart from the calculated fissure area and neck lengths (comparison not possible due to lack of measureable data) (Table 4-3). From the high speed video analysis it was found mean maximum temporary cavity expansion was smaller and occurred earlier within HG2 protected targets (Figure 4-3), while mean projectile expansion was smaller within these targets too (Figure 4-4). Fabric and fibre debris was found and collected from nine out of the ten targets protected by HG2 armour (Figure 4-5).

Table 4-1: Measurements collected from baseline tests involving .223 Remington Federal Premium® Tactical® Bonded® projectiles and unprotected 10% gelatine blocks 500 mm in length

a Shot information				
Shot	Impact velocity (m/s)	Debris present	Total fissure area (mm ²)	Projectile expansion (mm ²)
Shot 1	843	Minute metal fragments in tract and fissures*	11750	109
Shot 2	844	Minute metal fragments in tract	9994	110
Shot 3	842	Minute metal fragments in tract and fissures	11290	116
Shot 4	852	Minute metal fragments in tract and fissures	19060	107
Shot 5	853	N/A	20310	112
Shot 6	852	Minute metal fragments in tract and fissures	14830	113
Shot 7	853	Minute metal fragments in tract	21240	113
Shot 8	839	Minute metal fragments in tract	19370	114
Shot 9	844	Minute metal fragments in tract and fissures	16840	111
Shot 10	854	Minute metal fragments in tract and fissures	27810	110
Mean	847.6		17250	111.7
s.d.	5.7		5467	2.7
CV (%)	0.67		31.69	2.45
Min	839		9994	107
Max	854		27813	116

*Metal fragments were not collected due to such small size (less than 0.5mm).

b Measurements of permanent cavities						
Shot	Neck length (mm)	Body length (mm)	Body height (mm)	Body width (mm)	Calculated ellipsoid volume (mm ³)	Distance to bullet (mm)
Shot 1	0	300	95	105	1567000	454
Shot 2	0	280	100	110	1613000	425
Shot 3	2	260	100	115	1566000	425
Shot 4	0	325	90	105	1608000	423
Shot 5	0	330	105	105	1905000	423
Shot 6	0	340	145	100	2581000	420
Shot 7	0	290	140	95	2020000	402
Shot 8	0	320	110	150	2765000	430
Shot 9	0	315	110	130	2359000	428
Shot 10	0	325	125	130	2765000	429
Mean	N/A	308.5	112.0	114.5	2075000	425.9
s.d.	N/A	25.3	18.7	17.1	502200	12.7
CV (%)	N/A	8.20	16.73	14.91	24.21	2.98
Min	0	260	90	95	1565560	402
Max	2	340	145	150	2765256	454

c Data collected from high speed videos

Shot	EKE deposited (J)	Distance to maximum expansion of temporary cavity (mm)	Maximum diameter of temporary cavity (mm)
Shot 1	958	85	178
Shot 2	958	91	180
Shot 3	1001	75	177
Shot 4	1005	77	171
Shot 5	1010	100	174
Shot 6	995	99	182
Shot 7	1006	102	179
Shot 8	953	85	178
Shot 9	991	93	184
Shot 10	1012	75	173
Mean	988.9	88.7	178.1
s.d.	23.3	10.3	4.0
CV (%)	2.36	11.66	2.25
Min	953.37	75	171
Max	1011.64	102	184

Table 4-2: Measurements collected from interactions of .223 Remington Federal Premium® Tactical® Bonded® projectiles with HG2 protected 10% gelatine blocks

a Shot information

Shot	Armour impact velocity (m/s)	Gelatine impact velocity (m/s)	Debris present	Total fissure area (mm ²)	Projectile expansion (mm ²)
Shot 1	855	617	Fibres throughout the tract of both carrier and armour pack	17150	99
Shot 2	846	626	Less than shot 1 but fibres still seen throughout block	18580	100
Shot 3	840	643	Similar to shot 2	17340	107
Shot 4	856	641	Similar to shots 2 and 3	21110	110
Shot 5	845	610	Minute metal fragments in tract	20180	105
Shot 6	846	621	Carrier case and armour fibres present in fissures.	17890	104
Shot 7	854	591	Lots of fibre debris in fissures	19020	113
Shot 8	849	617	Less than shot 7, but fibres still present	16370	113
Shot 9	835	609	Fibres present heavily at entrance; in fissures too.	15880	108
Shot 10	845	622	Fibres present heavily at entrance; in fissures too.	20310	105
Mean	847.1	619.7		18380.3	106.4
s.d.	6.7	15.2		1764.2	4.74
CV (%)	0.79	2.46		9.60	4.45
Min	835	591		15875	99
Max	856	643		21108	113

b Measurements of permanent cavities

Shot	Neck length (mm)	Body length (mm)	Body height (mm)	Body width (mm)	Calculated ellipsoid volume (mm ³)	Distance to bullet (mm)
Shot 1	0	349	125	110	2513000	408
Shot 2	0	320	105	95	1671000	400
Shot 3	0	313	125	90	1844000	374
Shot 4	0	321	130	110	2404000	389
Shot 5	0	245	100	115	1475000	375
Shot 6	0	275	95	105	1436000	385
Shot 7	0	280	130	135	2573000	385
Shot 8	0	270	90	130	1654000	375
Shot 9	0	302	90	120	1708000	375
Shot 10	0	310	100	90	1461000	375
Mean	0.0	298.5	109.0	110.0	1874000	384.1
s.d.	0.0	30.6	16.6	15.6	449200	11.9
CV (%)	N/A	10.26	15.26	14.21	23.97	3.11
Min	0	245	90	90	1436297	374
Max	0	349	130	135	2572964	408

c Data collected from high speed videos

Shot	EKE deposited [^] (J)	EKE deposited* (J)	Distance to maximum expansion of temporary cavity (mm)	Maximum diameter of temporary cavity (mm)
Shot 1	954	556	74	172
Shot 2	958	578	84	156
Shot 3	946	608	88	170
Shot 4	967	603	77	174
Shot 5	878	553	85	182
Shot 6	910	570	91	176
Shot 7	879	516	77	177
Shot 8	911	565	81	186
Shot 9	883	548	69	171
Shot 10	900	569	81	161
Mean	918.6	566.5	80.7	172.5
s.d.	34.5	26.43	6.6	8.9
CV (%)	3.75	4.67	8.17	5.17
Min	878.16	516.41	69	156
Max	966.63	607.57	91	186

[^]EKE calculated using the impact velocity of the projectile striking the front armour park, from the Weibel Doppler radar.

*EKE calculated using the impact velocity of the projectile striking the gelatine block, calculated using PCC 2.5 software.

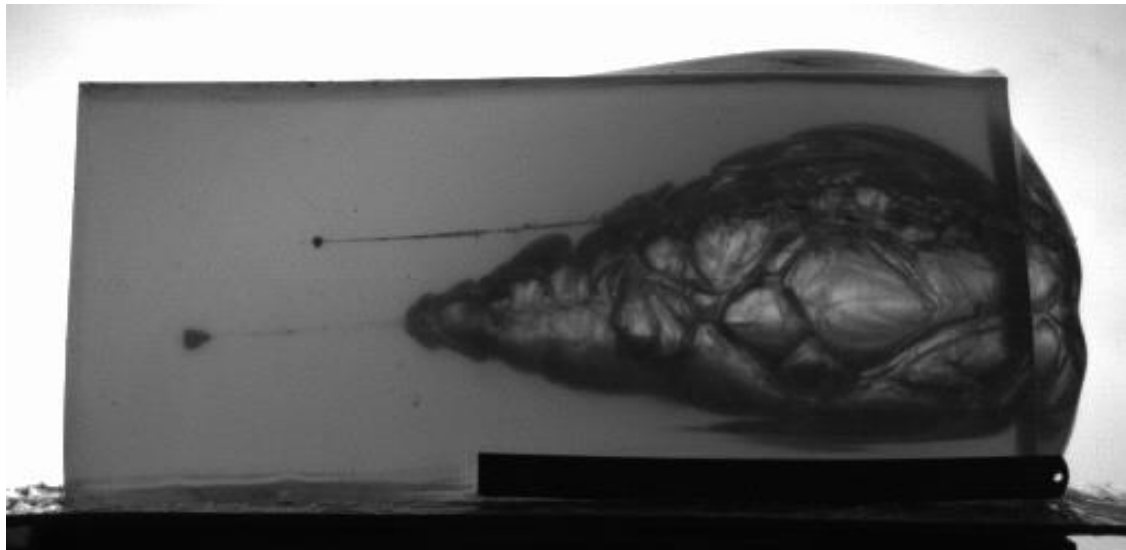


Figure 4-3: Typical example of temporary cavity expansion produced by .223 Remington Federal Premium® Tactical® Bonded® projectiles in (top) 10% gelatine blocks 500mm in length and (bottom) armoured 10% gelatine blocks.

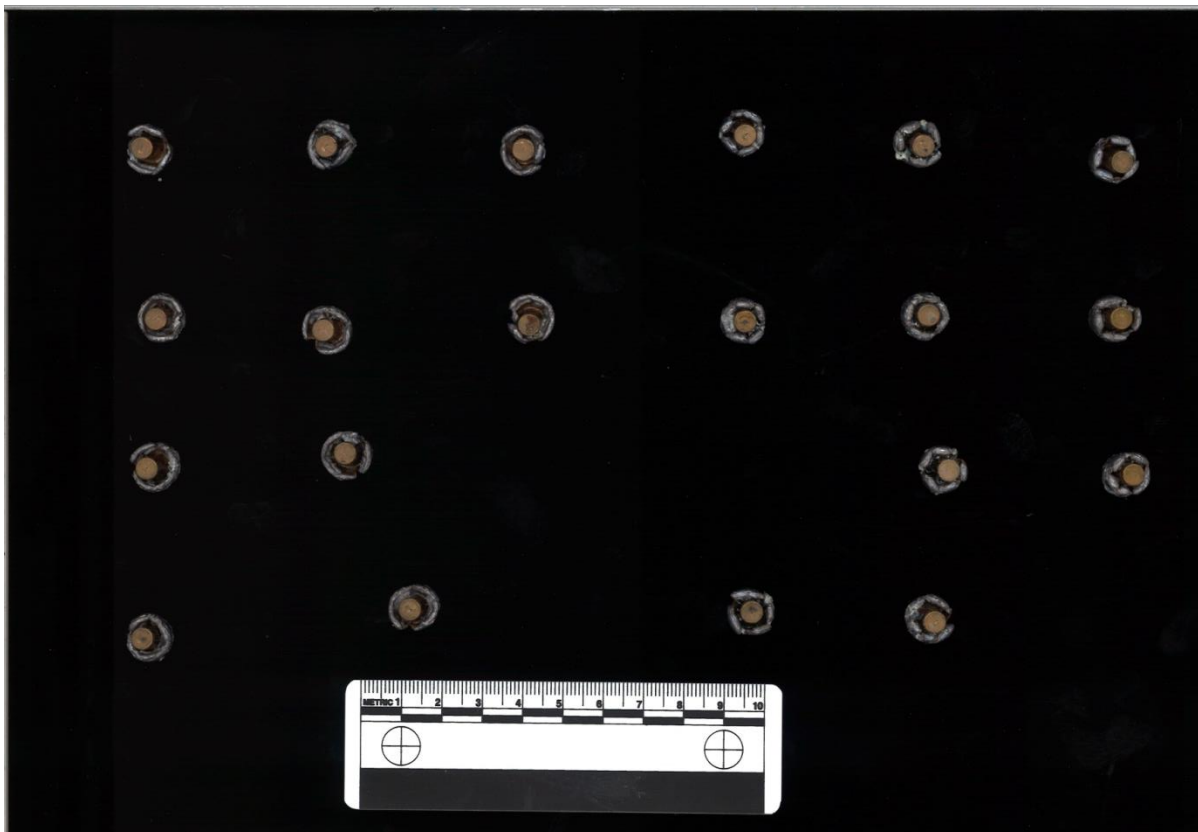
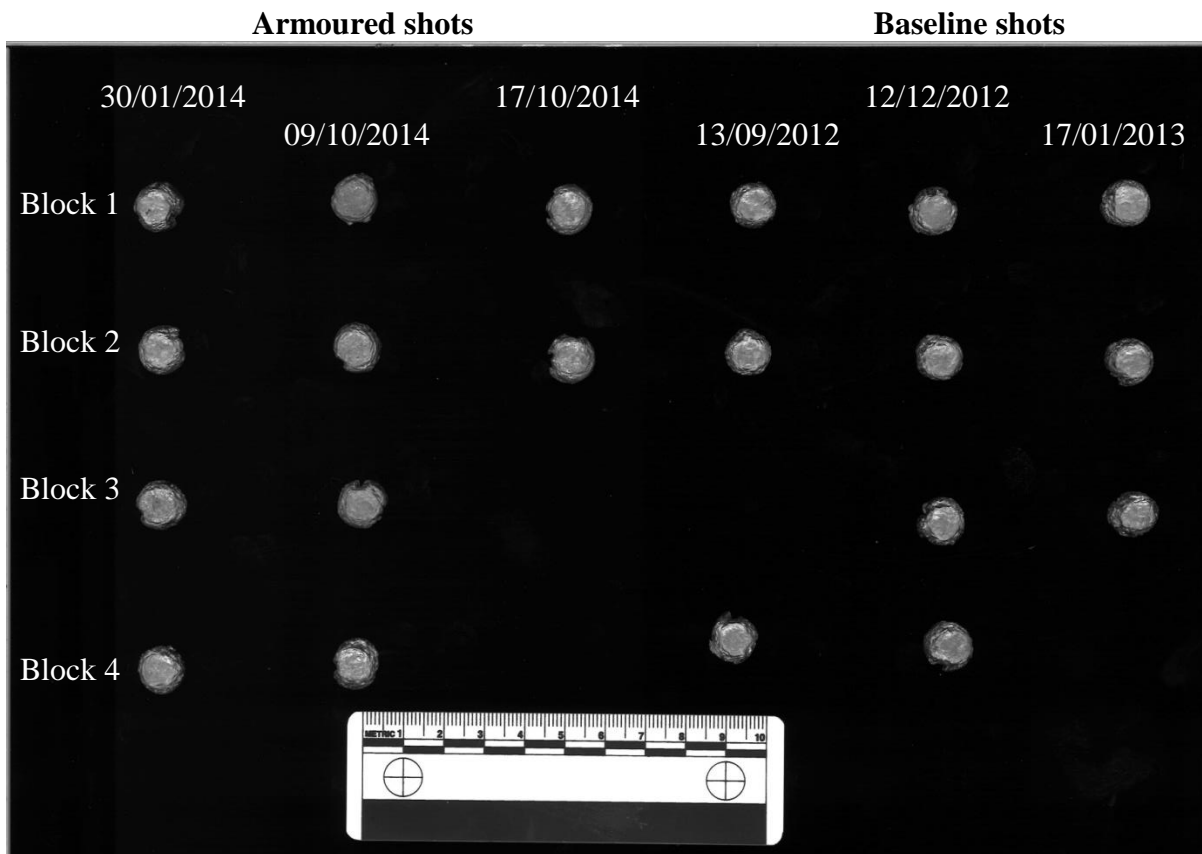


Figure 4-4: Expansion of .223 Remington Federal Premium® Tactical® Bonded® projectiles after penetration of armoured 500mm long gelatine blocks (left three columns) and after penetration of baseline 10% gelatine blocks (right three columns) from the front (top) and rear.

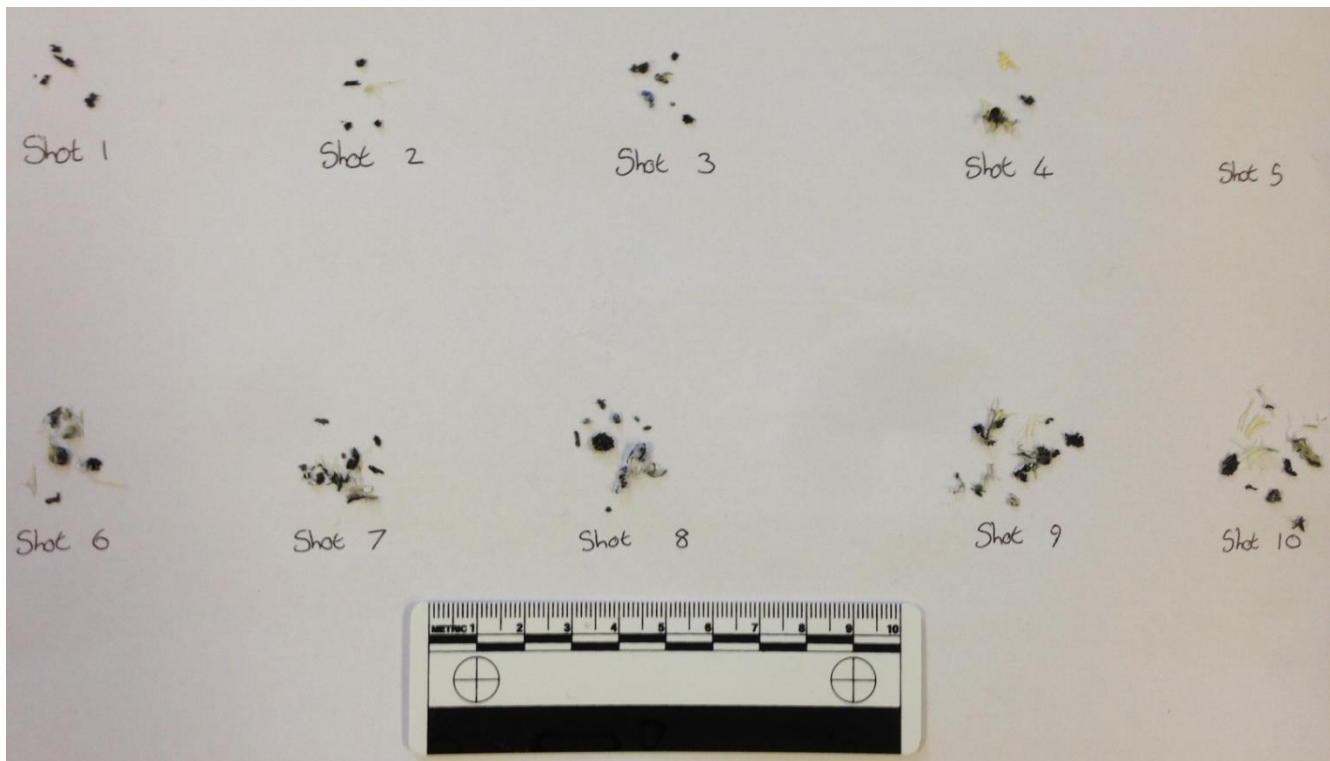


Figure 4-5: Fibre and fabric debris recovered from all ten .223 Remington Federal Premium® Tactical® Bonded® shots into armoured 10% gelatine blocks 500mm in length

Table 4-3: Summary of the mean results collected from protected and unprotected 10% gelatine blocks 500mm in length after penetration of .223 Remington Federal Premium® Tactical® Bonded® projectiles

Mean	Baseline blocks	HG2 protected gelatine blocks
Armour impact velocity (m/s)	847.6	847.1
Gelatine impact velocity (m/s)	847.6	619.7
Projectile expansion (mm ²)	111.7	106.4
Fissure area (mm ²)	17249.3	18380.3
Neck length (mm)	N/A	0.0
Body length (mm)	308.5	298.5
Body height (mm)	112.0	109.0
Body width (mm)	114.5	110.00
Calculated ellipsoid volume (mm ³)	2075000	1874000
Distance to bullet (mm)	425.9	384.1
EKE deposited in whole target (J)	988.9	918.6
EKE deposited in gelatine	988.9	566.5
Distance to maximum expansion of temporary cavity (mm)	88.7	80.7
Mean maximum diameter of temporary cavity (mm)	178.1	172.5

4.2.2.1 ANOVA results

4.2.2.1.1 Neck length

It was not possible to carry out analysis of variance for neck length as only one distance was recorded from the ten shots into the baseline blocks; while no neck length was recorded for any of the shots into HG2 protected blocks.

4.2.2.1.2 Body length

HG2 body armour panels in front of 10% gelatine blocks did not have a significant effect on the body length of the permanent cavity produced by .223 Remington Federal Premium® Tactical® Bonded® rounds ($F_{1,18} = 0.636$, $p = NS$) (Table 4-4b). The body length was typically shorter when HG2 body armour panels were present (mean = 298.5mm, s.d. = 30.6mm compared to the baseline results of mean = 308.5mm, s.d. = 25.2mm), though the spread of the data was larger (CV = 10.26% compared to CV = 8.16%) (Table 4-4a).

Table 4-4: Body length created by .223 Remington Federal Premium® Tactical® Bonded® projectiles

a Selected descriptive statistics						
Protection	Mean (mm)	s.d. (mm)	CV (%)			
None	308.5	25.2	8.16			
HG2 front panel	298.5	30.6	10.26			

b Analysis of variance						
Source of variation	SS	d.f.	Mean square	F	Sig.	$p \leq$
Protection	500.00	1	500.00	0.636	0.435	NS
Error	14143.00	18	785.72			

4.2.2.1.3 Representation of maximum ellipsoid volume

The calculated representation of the maximum ellipsoid volume was not significantly affected by the presence of HG2 body armour ($F_{1,18} = 0.889$, $p = NS$) (Table 4-5b). Larger volumes were created in gelatine blocks with no body armour (mean = 2075000mm³, s.d. = 502200mm³), over 200000mm³ larger in volume than when HG2 body armour panels were present (mean = 1874000.43mm³, s.d. = 449200.39mm³) (Table 4-5a).

Table 4-5: Representation of maximum ellipsoid volume after penetration of .223 Remington Federal Premium® Tactical® Bonded® projectiles

a Selected descriptive statistics			
Protection	Mean (mm ³)	s.d. (mm ³)	CV (%)
None	2075000	502200	24.21
HG2 front panel	1874000	449200	23.97

b Analysis of variance						
Source of variation	SS	d.f.	Mean square	F	Sig.	ρ≤
Protection	2.018 x 10 ¹³	1	2.018 x 10 ¹¹	0.889	0.358	NS
Error	4.086 x 10 ¹²	18	2.270 x 10 ¹¹			

4.2.2.1.4 Fissure area

Levene’s equality of variance test revealed there was a difference in the variability witnessed between the two target types when fissure area was considered (F = 8.110, ρ≤0.05) (Table 4-6b). The baseline gelatine blocks produced larger variance in fissure area (mean = 17249.3mm², s.d. = 5467.0mm²) when compared to the fissure area from HG2 protected 10% gelatine blocks (mean = 18380.3mm², s.d. = 1764.2mm²) (Table 4-6a). Welch’s t-test was then employed to test for any difference between the two group means since it allows for this unequal group variability. The measured fissure area was not significantly affected by the presence of HG2 body armour at the front of 10% gelatine blocks 500mm in length ($t_{10.9} = -0.623$, p = NS) (Table 4-6c).

Table 4-6: Fissure area after penetration by .223 Remington Federal Premium® Tactical® Bonded® projectiles

a Selected descriptive statistics			
Protection	Mean (mm ²)	s.d. (mm ²)	CV (%)
None	17249.3	5467.0	31.69
HG2 front panel	18380.3	1764.2	9.60

b Levene's test for equality of variances		
F	Sig.	ρ≤
8.110	0.011	0.05

c *t*-test for equality of means – equal variances not assumed

Source of variation	Mean difference	s.d. error difference	T	d.f.	Sig.	$\rho \leq$
Protection	-1130.97	1816.61	-0.623	11	0.546	<i>NS</i>

4.2.2.1.5 EKE

Comparing the EKE from the baseline trials in 10% gelatine, with the EKE calculated using the impact velocity of the projectile striking the gelatine block from high speed videos using PCC 2.5 software, revealed HG2 body armour present in front of 10% gelatine blocks had a significant effect on the EKE deposited by .223 Remington Federal Premium® Tactical® Bonded® projectiles ($F_{1, 18} = 1437.668$, $\rho \leq 0.001$) (Table 4-7b). The mean EKE deposited was over 400 J greater in the baseline blocks (mean = 988.9 J, s.d. = 23.3 J), when compared to the EKE deposited after perforation of an HG2 armour panel (mean = 566.5 J, s.d. = 26.4 J) (Table 4-7a).

Impact velocities are more accurate when recorded by Weibel Doppler radar than high speed video footage. However, when the target was an HG2 protected gelatine block, the impact velocities measured were for the impact into the armour, not into the gelatine blocks. The impact into the gelatine blocks would have been less than this, as the velocities of the respective projectiles would have decreased during perforation of the HG2 armour panels. The impact velocity of each shot into the gelatine blocks was calculated from the high speed videos of each individual shot using the PCC 2.5 software. However, when EKE was calculated using the impact velocities from the Weibel Doppler radar (into the armour panels), it was still shown that there was a significant difference between the EKE deposited when an HG2 armour panel was present ($F_{1, 18} = 28.550$, $\rho \leq 0.001$) (Table 4-8b). The mean EKE was once again greater in baseline blocks (mean = 988.9 J, s.d. = 23.3 J) compared to HG2 protected blocks (mean = 918.6 J, s.d. = 34.5 J) (Table 4-8a).

Table 4-7: EKE of .223 Remington Federal Premium® Tactical® Bonded® projectiles (EKE calculated using the impact velocity of the projectile striking the gelatine block, calculated using PCC 2.5 software)

a Selected descriptive statistics						
Protection	Mean (J)	s.d. (J)	CV (%)			
None	988.9	23.3	2.36			
HG2 front panel	566.5	26.4	4.67			

b Analysis of variance						
Source of variation	SS	d.f.	Mean square	F	Sig.	$\rho \leq$
Protection	892101.20	1	892101.20	1437.668	0.000	0.001
Error	11169.36	18	620.52			

Table 4-8: EKE of .223 Remington Federal Premium® Tactical® Bonded® projectiles (EKE calculated using the impact velocity of the projectile striking the front armour park, from the Weibel Doppler radar)

a Selected descriptive statistics						
Protection	Mean (J)	s.d. (J)	CV (%)			
None	988.9	23.3	2.36			
HG2 front panel	918.6	34.5	3.75			

b Analysis of variance						
Source of variation	SS	d.f.	Mean square	F	Sig.	$\rho \leq$
Protection	24710.81	1	24710.81	28.550	0.000	0.001
Error	15579.39	18	865.52			

4.2.2.1.6 Distance to projectile

Distance to the resting location of .223 Remington Federal Premium® Tactical® Bonded® rounds was significantly affected by the presence of HG2 body armour panels ($F_{1, 18} = 57.648, p = 0.001$) (Table 4-9b). The mean distance to the projectiles was shorter in gelatine blocks protected by HG2 armour panels (mean = 384.1mm, s.d. = 11.9mm) by over 40mm when compared to baseline gelatine blocks (mean = 425.9mm, s.d. = 12.7).

Table 4-9: Distance to .223 Remington Federal Premium® Tactical® Bonded® projectiles in 10% gelatine 500mm in length

a Selected descriptive statistics			
Protection	Mean (mm)	s.d. (mm)	CV (%)
None	425.9	12.7	2.98
HG2 front panel	384.1	11.9	3.11

b Analysis of variance						
Source of variation	SS	d.f.	Mean square	F	Sig.	$\rho \leq$
Protection	8736.20	1	8736.20	57.648	0.000	0.001
Error	2727.80	18	151.54			

4.2.2.1.7 Projectile expansion

The presence of an HG2 armour panel at the front of targets struck by .223 Remington Federal Premium® Tactical® Bonded® projectiles had a significant effect on the level of expansion of the projectiles ($F_{1, 18} = 9.162, \rho \leq 0.01$) (Table 4-10b). The mean expansion was larger in projectiles that stuck unprotected 10% gelatine blocks (mean = 111.7mm^2 , s.d. = 2.7mm^2), with the mean surface area over 5mm^2 smaller in projectiles that perforated HG2 armour panels (mean = 106.5mm^2 , s.d. = 4.7mm^2). The variation in surface area was larger in the projectiles that perforated HG2 armour panels, as shown by the coefficient of variance results (Table 4-10a).

Table 4-10: Surface area of .223 Remington Federal Premium® Tactical® Bonded® projectiles after recovery from targets

a Selected descriptive statistics			
Protection	Mean (mm^2)	s.d. (mm^2)	CV (%)
None	111.7	2.7	2.45
HG2 front panel	106.5	4.7	4.45

b Analysis of variance						
Source of variation	SS	d.f.	Mean square	F	Sig.	$\rho \leq$
Protection	137.10	1	137.10	9.162	0.007	0.01
Error	269.36	18	14.97			

4.2.2.1.8 Maximum temporary cavity location

The distance to the maximum temporary cavity location was not significantly affected by the presence of HG2 body armour on the front face of 10% gelatine blocks 500mm in length ($F_{1, 18} = 4.236$, $\rho = NS$) (Table 4-11b). When HG2 body armour panels were present, the mean distance to the location of the maximum size reached by the temporary cavity was 8.0mm shorter, with the variability of the data smaller (mean = 80.7mm, s.d. 6.6mm compared to mean = 88.7mm, s.d. = 10.3mm) (Table 4-11a).

Table 4-11: Distance to the location of the maximum temporary cavity produced by .223 Remington Federal Premium® Tactical® Bonded® projectiles

a Selected descriptive statistics						
Protection	Mean (mm)	s.d. (mm)	CV (%)			
None	88.7	10.3	11.66			
HG2 front panel	80.7	6.6	8.17			

b Analysis of variance						
Source of variation	SS	d.f.	Mean square	F	Sig.	$\rho \leq$
Protection	318.47	1	318.47	4.236	0.054	NS
Error	1353.39	18	75.19			

4.2.2.1.9 Maximum diameter of the temporary cavity

The size of the maximum diameter reached by the temporary cavity was not significantly affected by the presence of HG2 body armour panels ($F_{1, 18} = 3.302$, $\rho = NS$) (Table 4-12b). The mean maximum cavity diameter was larger in size in gelatine blocks with no protection (mean = 178.1mm, s.d. = 4.0mm). This was over 5mm longer compared to the mean maximum diameter created in blocks protected by an HG2 body armour panel, although comparing the CVs revealed a larger variability in results was observed with this target group (mean = 172.4mm, s.d. = 8.9mm).

Table 4-12: Size of the maximum temporary cavity diameter produced by .223 Remington Federal Premium® Tactical® Bonded® projectiles

a Selected descriptive statistics

Protection	Mean (mm)	s.d. (mm)	CV (%)
None	178.1	4.0	2.25
HG2 front panel	172.4	8.9	5.17

b Analysis of variance

Source of variation	SS	d.f.	Mean square	F	Sig.	$p \leq$
Protection	157.49	1	157.49	3.302	0.860	NS
Error	858.46	18	47.69			

4.2.3 Discussion of .223 Remington Federal Premium® Tactical® Bonded® results

Not all previous open source research that has investigated overmatching has provided specific details about ammunition tested; however, it appears work that utilises ammunition that has an exposed tip and typically expands on impact (as used in the current work) has not been previously reported (O'Connell *et al.*, 1988; Breteau *et al.*, 1989; Prather, 1994; Misliwetz *et al.*, 1995; Knudsen and Sørensen, 1997; Lanthier *et al.*, 2004).

During dissection, the main body of damage produced in both target types (10% gelatine with and without HG2 armour) occurred without a narrow entry channel in all but one gelatine block. The instance in which a narrow entry channel was present was when no armour was present, with the channel measuring only 2mm before the main body of damage was reached. This observation is different than previously reported work. Breteau *et al.* (1989) found that when body armour was overmatched (with non-expanding projectiles), the projectiles' behaviour was changed in a way that produced wounds with a shorter neck and an earlier cavity. Misliwetz *et al.* (1995) agreed, finding this to occur in the majority of cases when comparing damage between protected and unprotected ballistic soap with a range of ammunition. The reduced channel was reported as a possible indication that bullet instability had occurred earlier compared to when no protection was present, a result Misliwetz *et al.* (1995) described as unfavourable, as instability of a bullet would result in quicker energy release. Conversely, Lanthier *et al.* (2004) found the presence of armour resulted in longer and narrower entry channels. The .223 Remington Federal Premium® Tactical® Bonded® did not

typically produce neck lengths. This was not a surprising result considering the tip of the round is exposed, encouraging expansion immediately on impact irrespective of presence of armour.

A shorter entry channel was perceived to be a worst case scenario due to it indicating an earlier instability. This was not a primary effect observed with the .223 Remington Federal Premium® Tactical® Bonded® projectiles used in the current work. This was because after expansion, the projectiles travelled through the gelatine blocks head on with little evidence of yaw. However, the temporary cavity analysis revealed that maximum expansion of the temporary cavities occurred earlier in gelatine blocks protected by HG2 armour (this was a numerical difference not a statistical significant difference at $p \leq 0.05$). Although the projectiles may not behave the same in a human thorax, research from Chapter 3 (Section 3.4 Part C – *Ballistic testing of porcine samples*) demonstrated no significant difference between depths of penetration of .223 Remington Federal Premium® Tactical® Bonded® projectiles fired at thorax arrangements and 10% gelatine blocks 500mm in length. With that being the case, comparing distances to maximum temporary cavity expansions in both targets types to typical locations of organs susceptible to cavitation effects is worthwhile. The liver and spleen, are particularly vulnerable (Wilson, 1977), however, maximum temporary cavity expansion in both unprotected and HG2 protected 10% gelatine targets occurred past the typical depths of these organs (Bleetman and Dyer, 2000), and thus the presence of HG2 armour would not have exacerbated the damage experienced by them. However, the presence of HG2 armour may have caused expansion to occur inside a human target that otherwise may have perforated before reaching maximum expansion. The earlier occurrence of the temporary cavity agrees with the findings of Breteau *et al.* (1989) and Missliwetz *et al.* (1995).

Potential for greater damage in protected targets existed due to maximum temporary cavity occurring earlier. This contrasts to the numerically smaller temporary cavity diameters that were produced in HG2 protected 10% gelatine blocks. A reduced temporary cavity could mean a reduction in damage produced; less material would be disrupted. This is not an unexpected result, as the projectiles had less energy after overcoming the HG2 armour packs. Energy that is imparted by a projectile is a determinant in temporary cavitation effects; the greater the energy, the greater the tissues are stretched and the more drawn out the series of pulsations (Barach *et al.*, 1986). In a human target, in which temporary cavitation causes tissues to be stretched and distorted, a smaller cavity will affect less tissue and reduce the likelihood of susceptible areas being affected (Besant-Matthews, 2000).

The reduced temporary cavity diameters when HG2 armour was present agree with the findings of Lanthier *et al.* (2004) who reported reduced temporary cavity diameters in ballistic

soap blocks. Missliwetz *et al.* (1995) also found reduced temporary cavity diameters in some combinations of armour and ammunition tested, in particular when handgun projectiles were tested. However, when the 5.56mm S-Patr StG 77 was used, the temporary cavity diameters were smaller when no armour was used, compared to when three different variations of body armour were tested. This suggests that the characteristics of both the ammunition and armour used are paramount when determining the effects of overmatching.

When assessing body length, it is important to take into consideration the depth of the target. A longer body length would generally mean a larger area has been damaged; however, this is only the case if the damage is contained within the target. With police armour worn to protect the vital organs found in the human thorax, it is logical to assess anthropometric measurements of this area when reviewing body lengths produced. Comparing numerous sources, the chest depth for a 95th percentile human ranged from 250mm to 295mm, (Pheasant, 1988; British Standards Institution, 2004). The body lengths produced in both target types (which were not statistically different) were greater than 295mm, with the lengths greatest in gelatine blocks with no protection (308.50mm compared to 298.50mm). Comment cannot be made on how these measurements would alter with an inhomogeneous torso as a target, but using the measurements as a guide, the reduced body lengths when HG2 armour is present would not necessarily alter the damage produced, as the extended length would occur outside of a human sized target. A concern is that the presence of HG2 armour could reduce the body length to an extent where the damage produced is fully contained within a target, meaning all of a projectile's energy is deposited within that target. Results from testing blocks that were similar in depth to that of human chest depth are discussed in Section 4.3.3 *Discussion of .223 Remington Federal Premium® Tactical® Bonded® results.*

The measurements collected for the representation of maximum ellipsoid volume in 10% gelatine were numerically smaller in HG2 protected blocks. This is not surprising given that the temporary cavity diameters were numerically smaller in blocks protected by HG2 armour. This decrease in size of the temporary cavities could explain the reduction in size of the permanent damage left after the collapse of the temporary cavity, as after the final pulsation, the permanent cavity is what remains (Belkin, 1979).

A smaller volume indicated that the presence of HG2 armour reduced the damage produced in the gelatine block sizes tested when armour was overmatched. This is because a smaller volume would result in less disrupted material. However, this may not be the case for a human sized target, as it is once again important to take into consideration the length and depth of the target. Although a smaller volume would be less likely to come in contact with

and/or disrupt a vital structure/organ than a wound of larger volume, a smaller volume has more chance of being contained by the body. This would result in the entirety of the projectile's energy being deposited in the body, which could be more damaging than if a large wound volume had been produced, with only a portion of it occurring inside the target. Comparisons to other previous permanent cavity findings were not possible because no baseline shots were carried out in that study (O'Connell *et al.*, 1988) or no tissue simulant / simulant capable of capturing the permanent cavity was used (Misliwetz *et al.*, 1995; Knudsen and Sørensen, 1997; Lanthier *et al.*, 2004).

Within the estimated volumes of damage in both protected and unprotected gelatine target types, fissure area was larger in HG2 protected blocks, but more variable in unprotected blocks. Although smaller volumes were found in HG2 protected blocks, more damage in the form of fissures was present. These results do not appear to have been reported before. This is an important observation because fissures reflect the distribution of energy deposited by the projectile (Jussila, 2005a). Fissures were caused by the gelatine being strained to such an extent it fractured; more fissures indicated greater strain. A potential explanation for why HG2 protected blocks produced more fissures but a smaller volume of damage is that the energy deposited by the projectile was more concentrated. As the projectiles penetrated the body armour, they were slowed down sufficiently enough to cause more localised damage, compared to when the projectiles penetrated through the initial surface of the unprotected gelatine blocks with relative ease, and thus the projectiles were able to penetrate further. The presence of HG2 armour caused a change in the mechanism of damage production.

Work carried out by (Sturdivan, 1981) (although classified) made it possible to estimate the expected kinetic energy (EKE) of any projectile whose primary mechanism of causing damage was by the deposition of kinetic energy, provided the data was experimentally determined from measurements of energy deposited in gelatine. Calculating EKE to for both targets with and without armour was a useful tool in assessing the effect of police armour when it is overmatched. The initial analysis of variance used impact velocities for targets protected by HG2 armour that were collected from PCC 2.5 software. A limitation of using the software to estimate velocity was the projectiles not fitting in line with a pixel edge. Velocities collected are not typically as accurate as those recorded by the Weibel Doppler radar; however, statistical analysis on the velocities collected from the PCC 2.5 software gave confidence that they were true (i.e. small variation seen: mean = 619.7m/s, s.d. = 15.2m/s CV = 2.46% (Table 4-2a)). Regardless, it was demonstrated that the EKE deposited was significantly larger in unprotected blocks in both ANOVAs carried out, using impact velocities from both the PCC 2.5 software

and the impact velocities recorded by the Weibel Doppler radar of the armour packs being struck.

Although no results nor statistics are presented, Prather (1994) reported that 7.62 x 39mm AK47 projectiles fired at velocities that simulated ranges of nearly 500 m (velocities not given) produced no significant differences to the $P(I|H)_{\text{thorax}}$ in 20% gelatine targets and targets of 28-ply armour in front of 20% gelatine, though AKE (ARRADCOM Kinetic Energy) values were approximately 10% lower for shots into armour-protected gelatine compared to unprotected gelatine blocks. For impact velocities of 430m/s, the AKE value for armour-protected gelatine was double that of the unprotected gelatine targets. The current study's finding that measured the EKE to the area of a human thorax concurs with Prather's findings of kinetic energy levels being reduced by the presence of armour, though significantly so in the current study. The more energy present in a ballistic attack, the greater the potential for damage. The EKE results show the presence of HG2 body armour does not exacerbate energy deposited; rather, it significantly reduces it, and in doing so reduces the damage produced.

The result that distance to bullet was significantly less in HG2 armour-protected blocks is not a surprising result considering the reduced energy the projectiles had after perforating the HG2 armour, however it does not appear to have been reported previously. The outcome does not necessarily have a positive impact on the damage produced when considering a human sized target. A positive impact on the damage would be where the damage was reduced compared to baseline damage. Although the distances measured in 10% gelatine were greater than that of human chest depth, a concern is that reducing the distance a projectile travels increases the chances of the projectile penetrating a human target and depositing all its energy, rather than perforating and depositing only a portion of its energy within the target. The chances of a projectile remaining in a human target may also be increased if body armour was present on both the front and back faces, a setup explored in *Section 4.3 Part B: Armoured gelatine blocks 250mm in length*.

The scenario of a projectile remaining within a target would result in a contaminated wound. Not all wounds that have been contaminated become infected; the contaminant may be sterile (Mellor *et al.*, 1997). Contamination is reportedly the principal threat to the health of a soldier who has survived their initial ballistic wound (Ryan *et al.*, 1997), and thus would be a risk to a police officer who has survived the initial ballistic attack. Although comment on other contaminants (i.e. skin and micro-organisms from other organs within a living target (Hiss and Kahana, 2000)) being spread throughout a target cannot be made due to the target being homogeneous gelatine, targets that had HG2 body armour panels on the front face produced

fabric and fibre debris that was collected from 90% of the targets after dissection (Figure 4-5). This agrees with the findings of Breteau *et al.* (1989) who report the presence of hard-to-recover fibres of Kevlar® were observed after perforation of body armour by fragmenting rounds. Breteau *et al.* also found a greater scattering of projectile fragments after perforating armour when compared to shots that hadn't perforated armour. This result was not found in the current study as the round used does not have a tendency to break up. Lanthier *et al.* (2004) reported no aramid fibres were located in their overmatching experiments, claiming they were difficult to find in soap. They did however find signs of contamination which they linked to the projectile. No further comments on contamination were found from previous studies.

The finding that debris collected was spread throughout the permanent damage present in the gelatine agrees with the observation made by Meller *et al.* (1997): higher rates of energy associated with wounds produced by rifle projectiles cause fine shredding of both fabric and skin, which are then dispersed by the pulsating process of the temporary cavity. The presence of fabric in a wound provides a far greater threat of infection than metallic fragments (Anonymous, 1944, cited by Bowyer *et al.*, 1997b). This is made worse due to the complex problem of locating and removing all the contaminants, which are not identifiable by x-ray diagnostic procedures. Considering contamination alone, the damage caused when armour panels were overmatched was made worse when armour was present compared to when no armour is present.

There are many factors to consider in this case when determining the effects of overmatching HG2 UK police body armour with .223 Remington Federal Premium® Tactical® Bonded® rounds. Energy deposited into the target is a key factor, and finding that it is significantly reduced when HG2 armour is present indicated a positive influence on the damage produced (i.e. damage was reduced). However, the presence of HG2 armour not only creates a greater risk of infection for a human target via the introduction of fabric debris into the wounded area, but an earlier temporary cavity and an increased chance of the projectile remaining within smaller targets.

4.2.4 Results from 9mm Luger rounds

The data collected from the baseline and armoured gelatine blocks trials using 9mm Lugers are presented in Table 4-13 and Table 4-14. Comparing the data revealed mean -fissure area and -EKE deposited (when using the impact velocity from the PCC 2.5 software) was greater in unprotected blocks, while both the distance to and the diameter of the maximum

temporary cavity was also greater in these blocks (Figure 4-6). The 9mm Luger ammunition yawed in the blocks; distances to where 90 ° yaw was reached the first, second and third time were all shorter in blocks with KR1/SP1 armour panels on the front face. The mean data for all parameters collected in the two target types are summarised in Table 4-15.

Table 4-13: Measurements collected from interactions of 9mm Luger with 10% gelatine blocks 500mm in length

a Shot information			
Shot	Impact velocity (m/s)	Debris present	Total fissure area (mm ²)
1	422	No visible debris	10210
2	429	No visible debris	9170
3	429	No visible debris	13180
4	429	No visible debris	14890
5	431	No visible debris	11180
6	433	No visible debris	10410
7	435	No visible debris	13550
8	427	No visible debris	14780
9	425	No visible debris	13210
10	432	No visible debris	11720
Mean	429.2		12228.7
s.d.	3.9		1979.9
CV (%)	0.90		16.19
Min	422		9170
Max	435		14893

b Data collected from high speed videos			
Shot	EKE deposited (J)	Distance to maximum expansion of temporary cavity (mm)	Maximum diameter of temporary cavity (mm)
Shot 1	249	276	113
Shot 2	159	314	80
Shot 3	170	277	118
Shot 4	200	247	116
Shot 5	256	225	117
Shot 6	211	212	100
Shot 7	286	252	125
Shot 8	244	235	106
Shot 9	196	281	120
Shot 10	253	226	104
Mean	222.5	254.6	110.0
s.d.	41.2	31.9	13.1
CV (%)	18.50	12.53	11.93
Min	159.42	212	80
Max	286.04	314	125

c Yaw analysis

Shot	Number of times 90 ° yaw reached	Distance within block (mm)		
1	3	243	301	466
2	2	318	367	-
3	2	265	485	-
4	3	266	311	475
5	2	215	402	-
6	3	216	449	474
7	2	241	476	-
8	3	223	275	448
9	2	298	348	-
10	3	231	277	451
Mean	2.5	251.6	369.1	462.8
s.d.	0.53	34.9	80.4	12.7
CV (%)	21.08	13.89	21.77	2.70
Min	2	215	275	448
Max	3	318	485	475

Table 4-14: Measurements collected from interactions of 9mm Luger with KR1/SP1 protected 10% gelatine blocks 500mm in length

a Shot information

Shot	Armour impact velocity (m/s)	Gelatine impact velocity (m/s)	Debris present	Total fissure area (mm ²)
1	431	391	Armour carrier case debris present on front of block	7648
2	426	393	No visible debris	4683
3	432	390	Fibres on front of block	9788
4	438	373	No visible debris	9651
5	431	372	Fibres on front of block	9327
6	429	386	No visible debris	9798
7	431	374	Fibres present in first two fissures	7461
8	427	378	No visible debris	10900
9	427	382	Armour carrier case punch out recovered	8207
10	420	390	No visible debris	9376
Mean	429.2	382.9		8683.6
s.d.	4.71	8.16		1763.5
CV (%)	1.10	2.13		20.31
Min	420	372		4683
Max	438	393		10897

b Data collected from high speed videos

Shot	EKE deposited [^] (J)	EKE deposited* (J)	Distance to maximum expansion of temporary cavity (mm)	Maximum diameter of temporary cavity (mm)
Shot 1	210	201	249	92
Shot 2	154	149	273	63
Shot 3	267	247	237	107
Shot 4	226	209	250	101
Shot 5	244	220	230	121
Shot 6	232	218	234	122
Shot 7	269	245	212	113
Shot 8	233	216	212	121
Shot 9	213	205	259	107
Shot 10	254	242	218	119
Mean	230.0	215.1	237.5	106.8
s.d.	33.5	28.5	20.4	18.1
CV (%)	14.55	13.24	8.58	16.98
Min	154.27	149.35	212	63
Max	269.15	246.79	273	122

[^]EKE calculated using impact velocity of projectiles striking the front armour park, from the Weibel Doppler radar.

*EKE calculated using impact velocity of projectiles striking the gelatine block, calculated using PCC 2.5 software.

c Yaw analysis

Shot	Number of times 90 ° yaw reached	Distance within block (mm)		
1	3	240	294	450
2	2	288	327	-
3	2	222	431	-
4	2	246	456	-
5	3	232	278	455
6	3	229	289	454
7	2	207	430	-
8	3	224	271	448
9	3	204	265	421
10	2	207	433	-
Mean	2.5	229.9	347.4	445.6
s.d.	0.53	24.9	79.6	14.1
CV (%)	21.08	10.81	22.92	3.15
Min	2	204	265	421
Max	3	288	456	455

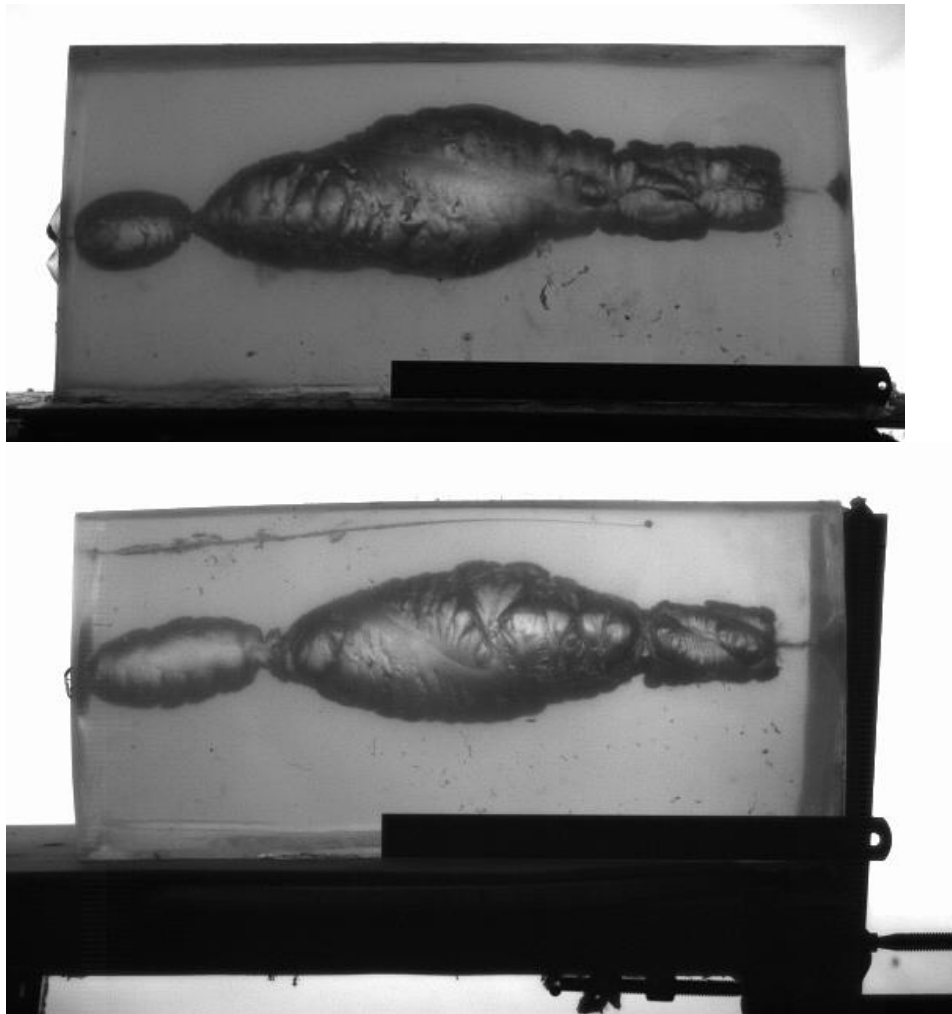


Figure 4-6: Typical example of temporary cavity expansion produced by 9mm Luger projectiles in 10% gelatine blocks 500mm in length (top) and armoured 10% gelatine blocks (bottom).

Table 4-15: Summary of the mean results collected from protected and unprotected 10% gelatine blocks 500mm in length after perforation of 9mm Luger projectiles

Mean	Baseline blocks			KR1/SP1 protected gelatine blocks		
Armour impact velocity (m/s)	429.2			429.2		
Gelatine impact velocity	429.2			382.9		
Fissure area (mm²)	12228.7			8683.6		
EKE deposited in target (J)	222.5			230.0		
EKE deposited in gelatine (J)	222.5			215.1		
Distance to maximum expansion of temporary cavity (mm)	254.6			237.5		
Mean maximum diameter of temporary cavity (mm)	110.0			106.8		
Yaw to 90 °	1 st	2 nd	3 rd	1 st	2 nd	3 rd
	251.6	369.1	462.8	229.9	347.4	445.6

4.2.4.1 ANOVA results

4.2.4.1.1 Fissure area

The fissure area produced in 10% gelatine- and KR1/SP1 protected 10% gelatine-blocks was significantly different after perforation by 9mm Luger projectiles ($F_{1,18} = 17.878$, $\rho \leq 0.001$) (Table 4-16b). The difference in mean area was over 3500mm², with the unprotected blocks producing larger areas (baseline mean = 12228.7mm², s.d. = 1979.9mm²; KR1/SP1 protected blocks mean = 8683.6mm², s.d. = 1763.5mm²) (Table 4-16a).

Table 4-16: Fissure area after penetration by 9mm Luger projectiles

a Selected descriptive statistics			
Protection	Mean (mm ²)	s.d. (mm ²)	CV (%)
None	12228.7	1979.9	16.19
KR1/SP1 front panel	8683.6	1763.5	20.31

b Analysis of variance						
Source of variation	SS	d.f.	Mean square	F	Sig.	$\rho \leq$
Protection	62838349.57	1	62838349.57	17.878	0.001	0.001
Error	63266949.68	18	3514830.54			

4.2.4.1.2 EKE

The EKE deposited by 9mm Luger projectiles, calculated using the impact velocity of the projectiles entering the gelatine blocks using PCC 2.5 software, was not significantly different when comparing protected and unprotected 10% gelatine blocks 500mm in length ($F_{1,18} = 0.216$, $\rho = NS$) (Table 4-17b). Although there was no significant difference, the mean EKE deposited was greater in blocks with no protection in front of the 10% gelatine blocks (mean = 222.5 J, s.d. = 41.2 J), 7.4 J greater than blocks with KR1/SP1 armour panels on the front face (mean = 215.1 J, s.d. = 28.5 J) (Table 4-17a).

Impact velocities were more accurate when recorded with the Weibel Doppler radar. However, when the KR1/SP1 armour panels were on the front face of the 10% gelatine blocks, the impact velocity measured by the Doppler was the impact into the armour panels, not the gelatine blocks. The impact velocities into the gelatine blocks would have been less than this;

velocities of the respective projectiles would have been reduced during the perforation of the armour panels. Using the high speed video footage and the PCC 2.5 software, it was possible to measure the impact velocities of each of the 9mm Luger shot entering the gelatine blocks. This gave the results discussed above.

Calculating the EKE using the impact velocities from the Weibel Doppler radar produced the same result; the presence of KR1/SP1 armour panels on the front face of 10% gelatine blocks 500mm in length did not significantly affect the amount of EKE deposited in the gelatine ($F_{1, 18} = 0.205$, $\rho = NS$) (Table 4-18b). However, the mean EKE was greater in blocks protected by KR1/SP1 armour panels (mean = 230.0 J, s.d. = 33.5 J), 7.5 J more than the mean EKE into the unprotected gelatine blocks (mean = 222.5 J, s.d. = 41.2 J) (Table 4-18a).

Table 4-17: EKE deposited by 9mm Lugers in 10% gelatine blocks 500mm in length (EKE calculated using the impact velocity of the projectile striking the gelatine block, calculated using PCC 2.5 software)

a Selected descriptive statistics						
Protection	Mean (J)	s.d. (J)	CV (%)			
None	222.5	41.2	18.50			
KR1/SP1 front panel	215.1	28.5	13.24			

b Analysis of variance						
Source of variation	SS	d.f.	Mean square	F	Sig.	$\rho \leq$
Protection	270.14	1	270.14	0.216	0.648	NS
Error	22544.21	18	1252.46			

Table 4-18: EKE calculated using the impact velocity of the projectile striking the front armour park, from the Weibel Doppler radar

a Selected descriptive statistics			
Protection	Mean (J)	s.d. (J)	CV (%)
None	222.5	41.2	18.50
KR1/SP1 front panel	230.0	33.5	14.55

b Analysis of variance						
Source of variation	SS	d.f.	Mean square	F	Sig.	$\rho \leq$
Protection	287.82	1	287.82	0.205	0.656	NS
Error	25325.07	18	1406.95			

4.2.4.1.3 Maximum temporary cavity location

The distance to the temporary cavity maximum produced by 9mm Luger projectiles was not significantly affected by the presence of KR1/SP1 body armour panels ($F_{1, 18} = 2.027$, $\rho = NS$) (Table 4-19b). The mean distance was shorter after the projectiles had perforated the body armour panels (mean = 237.5mm, s.d. = 20.4), while the CV results show more variability was observed from shots where no protection was present (mean = 254.6mm, s.d. = 12.5) (Table 4-19a).

Table 4-19: Distance to the temporary cavity maximum produced by 9mm Luger projectiles

a Selected descriptive statistics			
Protection	Mean (mm)	s.d. (mm)	CV (%)
None	254.6	31.9	12.53
KR1/SP1 front panel	237.5	20.4	8.58

b Analysis of variance						
Source of variation	SS	d.f.	Mean square	F	Sig.	$\rho \leq$
Protection	1452.05	1	1452.05	2.027	0.172	NS
Error	12896.29	18	716.46			

4.2.4.1.4 Maximum diameter of the temporary cavity

The maximum diameter of the temporary cavity was not significantly affected by the presence of KR1/SP1 body armour panels on the front face of target 10% gelatine blocks 500mm in length ($F_{1, 18} = 0.198$, $\rho = NS$) (Table 4-20b). The mean for unprotected blocks was larger (mean = 110.0mm, s.d. = 13.1mm) although only by 3.15mm (mean = 106.8mm, s.d. = 18.1mm) (Table 4-20a).

Table 4-20: Size of the maximum temporary cavity diameter produced by 9mm Luger projectiles

a Selected descriptive statistics						
Protection	Mean (mm)	s.d. (mm)	CV (%)			
None	110.0.	13.1	11.93			
KR1/SP1 front panel	106.8	18.1	16.98			

b Analysis of variance						
Source of variation	SS	d.f.	Mean square	F	Sig.	$\rho \leq$
Protection	49.63	1	49.63	0.198	0.662	NS
Error	4509.12	18	250.51			

4.2.4.1.5 90 ° Yaw

The mean distance to where 9mm Luger yaws to 90 ° for the first, second and third time respectively, was not significantly affected by the presence of a KR1/SP1 body armour panel on the front face of 10% gelatine block ($F_{1, 18} = 2.562$, $\rho = NS$ (Table 4-21b); $F_{1, 18} = 0.368$, $\rho = NS$ (Table 4-22b); $F_{1, 8} = 4.132$, $\rho = NS$ (Table 4-23b)). Only five out of the ten shots carried out into each target typed yawed to 90 ° three times, and thus only these 5 shots were compared for the distance to the third yaw ($n=5$).

With each respective yaw, the distance was closer to the front face of the gelatine in the gelatine blocks with a KR1/SP1 armour panel on the front face (first: mean = 229.9mm, s.d. = 24.9mm (Table 4-21a); second: mean = 347.4mm, s.d. = 79.6 (Table 4-22a) and third: mean = 445.6mm, s.d. = 14.1mm) (Table 4-23a).

Table 4-21: Distance to first 90 ° yaw of 9mm Luger projectiles in gelatine targets

a Selected descriptive statistics			
Protection	Mean (mm)	s.d. (mm)	CV (%)
None	251.6	34.9	13.89
KR1/SP1 front panel	229.9	24.9	10.81

b Analysis of variance						
Source of variation	SS	d.f.	Mean square	F	Sig.	$\rho \leq$
Protection	2354.45	1	2354.45	2.562	0.127	NS
Error	16543.3	18	919.07			

Table 4-22: Distance to second 90 ° yaw of 9mm Luger projectiles in gelatine targets

a Selected descriptive statistics			
Protection	Mean (mm)	s.d. (mm)	CV (%)
None	369.1	80.4	21.77
KR1/SP1 front panel	347.4	79.6	22.92

b Analysis of variance						
Source of variation	SS	d.f.	Mean square	F	Sig.	$\rho \leq$
Protection	2354.45	1	2354.45	0.368	0.552	NS
Error	115181.30	18	6398.96			

Table 4-23: Distance to third 90 ° yaw (when it occurs) of 9mm Luger projectiles in gelatine targets (n = 5)

a Selected descriptive statistics			
Protection	Mean (mm)	s.d. (mm)	CV (%)
None	462.8	12.7	2.70
KR1/SP1 front panel	445.6	14.1	3.15

b Analysis of variance						
Source of variation	SS	d.f.	Mean square	F	Sig.	$\rho \leq$
Protection	739.60	1	739.60	4.132	0.077	NS
Error	1432.20	8	179.00			

4.2.5 Discussion of 9mm Luger results

From the paucity of studies in the open-source literature that have investigated overmatching, the majority have approached the subject from a military perspective when considering both the armour and ammunition used. This is perhaps why only two studies have

used handgun rounds. As in the present study, Misliwetz *et al.* (1995) used a 9 x 19mm full-jacketed parabellum (S-Patr P 08, 7.98 g), citing the round as the most commonly used in European police and military pistols. O'Connell *et al.* (1988) fired a single shot from the following three handguns, providing only the ammunition mass and muzzle velocity as identifying features: 9mm pistol (115 grains; 1345 f/s /410m/s), .38-calibre revolver (158 grains; 920 f/s / 280m/s) and a .45-calibre pistol (230 grains; 820 f/s / 250m/s). Comparisons cannot be made between the present research and that conducted by O'Connell *et al.* as the armour tested by O'Connell was not perforated by the handgun ammunition used.

Investigations that have overmatched armour designed to provide protection against edged weapons (as in the current study) with ballistic impacts does not appear to have been previously reported. Attacks from edged weapons are more prevalent than ballistic attacks in the UK (25,972 offences involving a knife or sharp instrument were recorded by the police in 2013/2014 compared to 7,709 offences involving a firearm over the same time period (Office for National Statistics, 2015)); it is therefore logical to consider the occurrence of a patrolling police officer wearing a form of edged weapon projection coming up against the most common handgun threat in the UK. Thus, testing 9mm Luger rounds into both unprotected and KR1/SP1-protected 10% gelatine blocks 500mm in length was carried out to determine the effects of overmatching UK police body armour.

Maximum temporary cavities formed by 9mm Luger projectiles were reduced in size when KR1/SP1 armour was present; this result agreed with the finding of Misliwetz *et al.* (1995). From ballistic soap blocks that captured the temporary cavities of the 9 x 19mm projectiles, it was found that three different armour panels reduced the maximum diameter of the temporary cavity from 20mm to when no armour was present to 15mm, 12mm and 7mm respectively. Although a different tissue simulant and armour type was used in the current study, the result of a reduced diameter was the same, with the theory Misliwetz *et al.* put forward feasible in this instance also; the loss in velocity and thus energy the projectile loses when it perforates the KR1/SP1 armour ultimately reduces the projectiles damage potential once in the target.

Although reduced in size, the presence of KR1/SP1 armour caused the maximum expansion of the temporary cavities to occur earlier within the 500mm gelatine blocks. This could be potentially more harmful in a situation involving a human target, as an earlier expansion increases the likelihood of it occurring within the body. There is no reason to believe the locations of where maximum cavity expansion produced by 9mm Luger projectiles in 10% gelatine equate to equal distances within a human target; however, if that were the case, the

distances measured in KR1/SP1 armour-protected gelatine blocks would occur within the depth of an average human chest (Pheasant, 1988), whereas it would occur outside of that region when armour was not present. Considering the locations of the liver and spleen (Bleetman and Dyer, 2000); organs particularly susceptible to cavitation effects, the presence of armour would have no added influence, unless of course the maximum expansion only occurred in a human target with protection compared to one without. Results from testing blocks that were similar in depth to that of an average human chest are discussed in Section 4.3.5 *Discussion of 9mm Luger results*.

The shorter distances to maximum temporary cavity expansion may be related to the earlier yawing of the projectile. Numerically, the 9mm Luger projectiles yawed to 90 ° earlier in KR1/SP1 protected targets. Other open-source research has not discussed the number of times a projectile reached 90 ° yaw within a target. The reason why it was measured in this study was because greater damage is produced when a projectile yaws at 90 ° compared to travelling through nose first (Berlin *et al.*, 1976; Hollerman and Fackler, 1995). Although Kneubuehl *et al.* (2011) states the effect of yaw is considerably less in handgun projectiles due to them being typically no more than twice as long as their own calibre, investigating the effects of the 9mm Luger, which is prevalent to yawing (Nicholas and Welsch, 2004), was of interest in the current work. Results revealed the location of first yaw matched closely with the location of the maximum temporary expansion, supporting the concept that when a projectile yaws, greater damage is produced. Yaw occurred earlier in KR1/SP1 protected targets (as did the maximum expansion of the temporary cavity); this could be attested to the greater resistances the projectiles faced when they perforated the armour. This was Breteau *et al.*'s (1989) belief, who found the level of yaw in projectiles that did not typically fragment after impact (identified as AK74 and FAMAS tracer projectiles) increased as the number of layers of Kevlar® perforated, increased. The increased unsteadiness in the projectiles that could not be corrected, in addition to the sudden loss in velocity, led Breteau *et al.* to the conclusion that the wounding power of these projectiles was therefore increased. Knudsen and Sørensen (1997) had similar findings for 7.62 x 39mm AK-47 rifle rounds, as did Lanthier *et al.* (2004), particularly at reduced impact velocities (AK74 projectiles; 600m/s). Prather (1994) also tested reduced impact velocities to simulate longer distances, but only found an increase in projectile instability when testing the 7.62mm 7.91 g AK47 projectile at impact velocities of 430m/s and below, with tumbling noted after exiting the armour. Reduced spin rate was attested to play a role in the latter two studies. Though spin rate was not measured in this study, the 9mm Luger projectiles were not tested at reduced impact velocities, and thus were not more vulnerable to

instability due to out of proportion spin rates. Compared to previous results that overmatched handgun ammunition, Missliwetz *et al.* (1995) found projectile instability occurred in about one third of the shots that perforated armour (6/19 for 9 x 19mm). Yawing and thus instability was seen in all shots in the current study due to the use of a tissue simulant 500mm in length, though it was witnessed occurring earlier in KR1/SP1 protected targets.

Permanent damage in the gelatine blocks was measured by means of fissure area produced; KR1/SP1 armour on the front of blocks resulted in significantly smaller areas compared to blocks with no armour. This has not been previously reported. Smaller areas would indicate a reduction in damage produced, although location of where this damage occurs remains an important factor. As the 9mm Lugers fully perforated the 500mm gelatine blocks, the location was spread throughout the blocks. A human sized target would be shorter in depth, influencing the area that is damaged. Testing blocks similar in depth to that of a human is discussed in Section 4.3.5 *Discussion of 9mm Luger results.*

The more energy present in a ballistic attack, the greater the potential for damage. The EKE results show the presence of KR1/SP1 armour did not have a significant effect on the amount of energy deposited. This was the case when impact velocities were taken from both the PCC 2.5 software and Weibel Doppler radar. A potential reason for why the armour did not reduce the energy deposited was its make-up; the KR1/SP1 armour is designed to stop attack from sharp edged weapons, achieved by either catching the weapon before it reaches critical depths in a human, or by blunting the weapon. These mechanisms are not designed to stop a projectile of any form, hence why little energy was absorbed. Armour not engaging sufficiently with a threat with result in failure of the armour (Horsfall, 2012). Lanthier *et al.* (2004) also found little reduction in energy, a factor that tied in with yarns/fibres within the armours tested mostly being only displaced and not broken.

Debris was not found in the damage produced in unprotected gelatine blocks, but was found in 20% of the shots that perforated KR1/SP1 armour, in the form of a carrier case fabric 'punch out' and para-aramid fibres. The lack of debris could be linked to the KR1/SP1 armour not typically engaging with the projectiles, with the projectiles punching their way through. This could also explain why energy was not reduced after perforation of the KR1/SP1 armour packs. The presence of these contaminants would certainly have increased the risk of infection had the target been human, however in only 20% of the shots carried out was this a hazard. Previous studies have not commented on debris produced after overmatching armour with handgun ammunition.

Considering all the data collected to make a judgement, it is logical to conclude that the presence of KR1/SP1 armour in front of 10% gelatine blocks 500mm in length did not have detrimental effects on the damage produced. The significantly reduced fissure areas, as well as the reduced maximum expansion of the temporary cavity, were physical features that demonstrated a reduction in damage. The temporary cavity occurring earlier in protected blocks is not necessarily a more negative scenario; only if the presence of armour caused maximum cavitation to occur within a target that would have otherwise occurred outside the target would this be the case. Debris was not a key feature in the majority of shots.

4.3 Part B: Armoured gelatine blocks 250mm in length

The second series of shots carried out were on blocks of 10% gelatine that were 250mm in length. The length of 250mm was chosen with reference to the depth of the human torso (2.3.2.5.1 *Anthropometric measurements of the human torso*). Armour was placed on the front and back face of the gelatine block. The reason for this was to investigate the effect armour present on the back face of a target has on overmatching. This scenario is more realistic to a UK police officer wearing body armour coming up against an overmatched threat, as armour panels are worn on both the front and back of the torso. The 250mm length blocks were also tested with armour at the front, and with no armour. However, neither ammunition type stopped in either of these two types of targets, thus only three replicates of each were carried out.

4.3.1 Materials and methods

4.3.1.1 10% gelatine

The method for making 10% gelatine blocks was the same method described in Section 3.2.1.1.1 *Gelatine*. In order to create blocks 250mm in length, 500mm blocks were cast following this original method, but were cut in half using a de-boning knife after they were conditioned and had successfully met the quality control criteria after being penetrated by a 5.5mm BB in the top right corner of the block (Figure 4-7).



Figure 4-7: 10% gelatine block 250mm in length, cut to size after 5.5mm BB quality control check shot was carried out.

4.3.1.2 Body armour

The two levels of body armour protection used in *Part A* of this chapter were used again.

4.3.1.3 Ammunition

The ammunition used was the same as described in Section 3.3.1.2 *Ammunition*, namely the .223 Remington (62 grain; Federal Premium® Tactical® Bonded®) and the 9mm Luger (124 grain; full metal jacket; DM11 A1B2).

4.3.1.4 Ballistic testing method

Ballistic testing followed the same method as described in *Part A*, with the following alterations. Before cutting the 250mm blocks to size, the quality control check for gelatine constancy was performed. If the blocks met the required standard, they were then cut from 500mm to 250mm in length.

Prior to firing at the 250mm gelatine blocks, a metal picture-style frame was positioned at the rear of the target and was used as a support to the body armour panel that was placed at the rear face of the gelatine block (Figure 4-8). The armour panel at the front was placed against the front face of the gelatine block, sometimes with the aid of a Velcro strap to hold it in place so the correct shot position could be achieved. Shots to the front armour were at least 50mm away from previous shots and the panel edges; the utmost was done to ensure this was the case for the armour panels at the rear of the gelatine blocks too. Three shots were carried out on each HG2 250mm x 250mm armour panel and no more than 6 shots carried out on a single 400mm x 400mm KR1/SP1 panel. Ten replicate shots were carried out for both ammunition types against the respective protection levels front and back of gelatine blocks 250mm in length (n=10). Three replicate shots using each ammunition type were also carried out on 250mm gelatine blocks with no armour protection (n=3), with a further three replicate shots carried out with each ammunition type on 250mm blocks with an armour panel on the front face (n=3).



Figure 4-8: Typical target set up of HG2 armour panels on the front and back face of a 10% gelatine block 250mm in length.

4.3.1.5 Analysis

Analysis of the tissue simulants followed the method described in Section 3.2.4.2 *Baseline simulants analysis*. Any debris (fibre, metal) present in the tract were photographed *in situ* before being collected.

Summary statistics (mean (\bar{x}), standard deviation (s.d.) and coefficient of variation (CV)) were calculated for the fissure area for both projectiles. Summary statistics were also carried out on the permanent cavity data sets produced by .223 Remington Federal Premium® Tactical® Bonded® projectiles, as well as the level of expansion any recovered projectiles went through. Analysis of variance (ANOVA) and Tukey's HSD analysis were used to determine when significant differences between target types occurred (SPSS Statistics 22.0). Normality of data and equality of variance were checked for each data set.

4.3.1.6 Kinetic energy deposited and high speed video analysis

As the target length was chosen to represent the depth of a human torso, calculating the expected kinetic energy (EKE) was not carried out. Sturdivan's (1981) research took into account different body part estimates in order to calculate the EKE deposited. As the 250mm target block was set up to be the torso, no estimates of body size were required. Instead, using the mass of the respective projectiles, together with impact, and when penetration occurred, exit velocities, kinetic energy (J) deposited was calculated. These values were then statistically analysed; summary statistics (mean (\bar{x}), standard deviation (s.d.) and coefficient of variation

(CV)) were calculated for each data set before ANOVA and Tukey's HSD tests were used to determine if the presence of armour produced significant differences in the kinetic energy deposited (SPSS Statistics 22.0). Normality of data and equality of variance were checked for each data set.

From the high speed videos of every shot, the location (from the entry point of the projectile in the gelatine block) of where maximal temporary cavity occurred was measured and recorded. The size of this cavity at its largest was also taken. Both these measurements were acquired following the method described in section 3.3.1.4.1 *High speed video analysis*. The same statistical analysis was carried out on the temporary cavity data sets, with the aim of identifying whether the presence of armour had a significant effect on i) the location where the temporary cavity was largest and on ii) maximum diameter reached.

4.3.2 Results from the interactions of .223 Remington Federal Premium® Tactical® Bonded® rounds with 10% gelatine targets 250mm in length

The raw data collected from 10% gelatine targets 250mm in length with varying levels of protection are presented in Table 4-24 – Table 4-26. All .223 Remington Federal Premium® Tactical® Bonded® rounds perforated all targets without HG2 armour on the rear face, regardless of there being HG2 armour on the front face. A typical example of what occurred in three shots at 250mm gelatine blocks that were protected by HG2 armour on both the front and back face is also presented (Figure 4-9). The .223 Remington perforated the front HG2 armour before travelling through the gelatine, striking the rear armour pack, before then travelling back through the gelatine in the direction from which it came, exiting the front face of the gelatine.

A comparison of the data is discussed and presented in the next section, 4.3.2.1 *Order of magnitude*.

Table 4-24: Measurements collected from interactions of .223 Remington Federal Premium® Tactical® Bonded® projectiles with 10% gelatine blocks 250mm in length

a Shot information

Shot	Impact velocity (m/s)	Debris present	Total fissure area (mm²)
Shot 1	835	Minute metallic deposits at entry	23520
Shot 2	835	Minute metallic deposits at entry	21070
Shot 3	837	Minute metallic deposits at entry	25520
Mean	835.7		23370.0
s.d.	1.15		2229.0
CV (%)	0.14		9.54
Min	835		21066
Max	837		25516

b Measurements of permanent cavities

Shot	Neck length (mm)	Body length (mm)	Body height (mm)	Body width (mm)	Calculated ellipsoid volume (mm³)	Distance to bullet (mm)
Shot 1	0	250	120	115	1806000	N/A
Shot 2	0	250	140	115	2108000	N/A
Shot 3	0	250	155	110	2232000	N/A
Mean	N/A	250.0	138.3	113.3	2048700	N/A
s.d.	N/A	0	17.6	2.9	218700	N/A
CV (%)	N/A	0	12.69	2.55	10.68	N/A
Min	0	250	120	110	1806416	N/A
Max	0	250	155	115	2231840	N/A

c Data collected from high speed videos

Shot	Exit velocity (m/s)	Kinetic energy deposited (J)	Distance to maximum expansion of temporary cavity (mm)	Maximum diameter of temporary cavity (mm)
Shot 1	143	1360	81	170
Shot 2	158	1351	115	177
Shot 3	174	1347	94	173
Mean	158.3	1352.3	96.5	173.5
s.d.	15.5	6.7	16.9	3.6
CV (%)	9.79	0.49	17.51	2.10
Min	143	1346.62	81	170
Max	174	1359.64	115	177

Table 4-25: Measurements collected from interactions of .223 Remington Federal Premium® Tactical® Bonded® projectiles with HG2 on the front face of 10% gelatine blocks 250mm in length

a Shot information

Shot	Armour impact velocity (m/s)	Debris present	Total fissure area (mm ²)
Shot 1	836	Debris throughout fissures of whole block.	21340
Shot 2	840	Black carrier case, and fibres present throughout fissures.	15040
Shot 3	835	Black carrier case, and fibres present throughout fissures.	16980
Mean	837.0		17789.3
s.d.	2.7		3227.6
CV (%)	0.32		18.14
Min	835		15040
Max	840		21343

b Measurements of permanent cavities

Shot	Neck length (mm)	Body length (mm)	Body height (mm)	Body width (mm)	Calculated ellipsoid volume (mm ³)	Distance to bullet (mm)
Shot 1	0	245	140	110	1976000	N/A
Shot 2	0	250	80	125	1309000	N/A
Shot 3	0	250	110	110	1584000	N/A
Mean	N/A	248.3	110.0	115.0	1622800	N/A
s.d.	N/A	2.9	30.0	8.7	335000	N/A
CV (%)	N/A	1.16	27.27	7.53	20.64	N/A
Min	0	245	80	110	1308997	N/A
Max	0	250	140	125	1975538	N/A

c Data collected from high speed videos

Shot	Gelatine impact velocity (m/s)	Exit velocity (m/s)	Kinetic energy deposited (J)	Distance to maximum expansion of temporary cavity (mm)	Maximum diameter of temporary cavity (mm)
Shot 1	587	129	659	68	179~
Shot 2	563	131	602	82	197*
Shot 3	563	116	610	87	208*
Mean	571.0	125.3	623.6	78.9	194.6
s.d.	13.9	8.1	30.7	9.4	14.5
CV (%)	2.43	6.50	4.92	11.90	7.43
Min	563	116	602.31	68	179
Max	587	131	658.81	87	208

* Cavity expands past the limits of the gelatine block top surface

~ Presence of Velcro makes exact measurement difficult

Table 4-26: Measurements collected from interactions of .223 Remington Federal Premium® Tactical® Bonded® projectiles with HG2 on the front and back face of 10% gelatine blocks 250mm in length

a Shot information

Shot	Impact velocity (m/s)	Debris present	Total fissure area (mm²)	Projectile expansion (mm²)
Shot 1	835	Debris in fissures. Bullet found 1 m back, to the left.	18730	118
Shot 2	841	Debris in fissures. Bullet found 1 m back of the block.	18700	118
Shot 3	845	Debris throughout fissures, including a “punched out section” of fabric. Bullet recovered from under the testing table.	20710	126
Shot 4	840	Debris throughout fissures. Bullet recovered from in gelatine block.	20250	112
Shot 5	840	Debris throughout fissures. Bullet recovered from gelatine block.	20300	116
Shot 6	838	Debris in fissures, closer to entry and exit. Bullet came out of front of block	22450	116
Shot 7	841	Bullet recovered from gelatine block	20490	127
Shot 8	835	Debris in fissures, closer to the front of the block. Large lead sample collected.	20200	109
Shot 9	846	Lots of debris, deep in fissures. Bullet recovered from gelatine block.	20740	114
Shot 10	849	Lots of debris, deep in fissures. Bullet recovered from gelatine block.	18680	116
Mean	841.0		20126	117.1
s.d.	4.6		1172	5.7
CV (%)	0.54		5.82	4.84
Min	835		18683	109
Max	849		22453	127

b Measurements of permanent cavities

Shot	Neck length (mm)	Body length (mm)	Body height (mm)	Body width (mm)	Calculated ellipsoid volume (mm³)	Distance to bullet (mm)
Shot 1	0	245	125	100	1604000	N/A
Shot 2	0	250	100	110	144000	N/A
Shot 3	0	240	110	105	1451000	N/A
Shot 4	0	240	120	130	1960400	105
Shot 5	0	240	100	120	1508000	45
Shot 6	0	250	120	105	1649000	N/A
Shot 7	0	250	100	100	1309000	130
Shot 8	0	250	100	110	144000	N/A
Shot 9	0	245	110	75	1058000	60
Shot 10	5	235	90	90	996700	100
Mean	N/A	244.5	107.5	104.5	1441600	88.0
s.d.	N/A	5.5	11.4	15.2	280000	3.8
CV (%)	N/A	2.25	10.57	14.52	19.42	39.49
Min	0	235	90	75	996670	45
Max	5	250	125	130	1960354	130

c Data collected from high speed videos

Shot	Gelatine impact velocity (m/s)	Exit velocity (m/s)	Kinetic energy deposited (J)	Distance to maximum expansion of temporary cavity (mm)	Maximum diameter of temporary cavity (mm)	Comment on projectile behaviour
Shot 1	575	2	664	62	169 [~]	Strikes rear armour pack before exiting between the back armour and the gelatine block
Shot 2	566	Unknown	644	76	175	Strikes rear armour pack then not clear
Shot 3	585	6	688	86	178	Strikes rear armour pack before exiting the block from the front, striking the front armour pack on exit.
Shot 4	586	Did not exit	690	74	174	Strikes rear armour pack then not clear
Shot 5	560	Did not exit	630	79	179	Strikes rear armour pack then not clear
Shot 6	596	2	714	78	167 [~]	Strikes rear armour pack before exiting the block from the front, striking the front armour pack on exit.
Shot 7	625	Did not exit	785	77	181 [~]	Strikes rear armour pack then not clear
Shot 8	542	6	590	67	159	Strikes rear armour pack before exiting the block from the front, striking the front armour pack on exit.
Shot 9	568	Did not exit	648	88	203*	Strikes rear armour pack then not clear
Shot 10	580	Did not exit	676	80	216*	Strikes rear armour pack then not clear
Mean	578.3	4.0	672.8	76.8	180.2	
s.d.	22.4	2.3	52.6	7.8	17.0	
CV (%)	3.88	57.74	7.82	10.09	9.41	
Min	542	2	590.10	62	159	
Max	625	6	784.77	88	216	

* Cavity expands past the limits of the gelatine block top surface

[~] Presence of Velcro makes exact measurement difficult

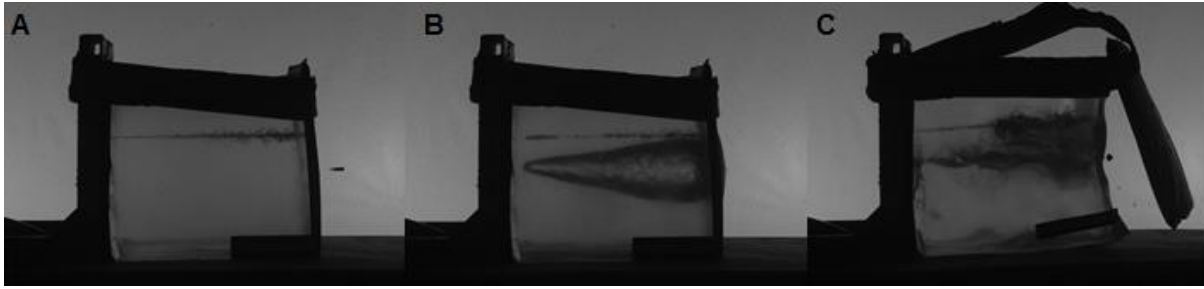


Figure 4-9: High speed footage stills showing the typical process of a .223 Remington Federal Premium® Tactical® Bonded® projectile (A) entering a 250mm 10% gelatine block protected by HG2 armour on both the front and back face before (B) reaching the rear face and then travelling back through the gelatine block and exiting via the front face.

4.3.2.1 Order of magnitude

All permanent cavity measurements taken were largest in the 250mm targets with no protection. The smallest measurements for all but fissure area were from targets with HG2 armour panels on the front and back face. The kinetic energy deposited was largest in the unprotected blocks, over double the kinetic energy that was deposited in the two protected target types. Maximum temporary cavity size was smallest in the unprotected blocks, while the mean distance to this location was longest. Maximum temporary cavity expansion happen earliest within targets with HG2 armour on the front and back face of the gelatine block, but the largest in actual size produced was in blocks with HG2 on the front face only (Table 4-27).

Table 4-27: Comparison of the summary statistics produced in all three 10% gelatine target types 250mm in length after impact by .223 Remington Federal Premium® Tactical® Bonded® projectiles

Parameter	Statistical description	No protection (n = 3)	KR1/SP1 front panel (n = 3)	KR1/SP1 front and back (n = 10)
Neck length	Mean (mm)	N/A	N/A	N/A
	s.d. (mm)	N/A	N/A	N/A
	CV(%)	N/A	N/A	N/A
Body length	Mean (mm)	250	248.3	244.5
	s.d. (mm)	0	2.9	5.5
	CV(%)	0	1.16	2.25
Ellipsoid volume	Mean (mm ³)	2049000	1623000	1442000
	s.d. (mm ³)	218700	335000	280000
	CV(%)	10.68	20.64	19.42
Fissure area	Mean (mm ²)	23368.2	17789.3	20125.8
	s.d. (mm ²)	2228.7	3227.6	1172.3
	CV(%)	9.54	18.14	5.82
Kinetic energy	Mean (J)	1352.3	623.6	672.8
	s.d. (J)	6.68	30.69	52.62
	CV(%)	0.49	4.92	7.82
Distance to maximum temporary cavity	Mean (mm)	96.5	78.91	76.76
	s.d. (mm)	16.9	9.4	7.75
	CV(%)	17.5	11.9	10.09
Diameter of maximum temporary cavity	Mean (mm)	173.5	194.6	180.2
	s.d. (mm)	3.6	14.5	17.0
	CV(%)	2.10	7.43	9.41
Projectile expansion (mm²) (n= 10)	Mean (mm ²)	111.7*	106.4*	117.1
	s.d. (mm ²)	2.7	4.7	5.7
	CV(%)	2.45	4.45	4.84

*These projectile expansions are from projectiles from were collected from testing 10% gelatine targets 500mm in length, as the projectiles perforated the 250mm targets and were not able to be recovered for analysis.

4.3.2.2 ANOVA results

In order to see if the patterns observed from comparing the means were statistically supported, ANOVA and Tukey's HSD analysis was carried out. To ensure equality of sample size, only the first three shots into 250mm 10% gelatine targets with HG2 armour on the front

and back face were used for the ANOVA. This meant the sample size for all three targets was three ($n = 3$), unless stated otherwise.

4.3.2.2.1 Neck length

No neck lengths were produced in any of the shots compared and thus ANOVA was not possible.

4.3.2.2.2 Body length

The presence of HG2 armour in any arrangement did not have a significant effect on the body length of the permanent cavity produced by .223 Remington Federal Premium® Tactical® Bonded® projectiles ($F_{2,6} = 1.750, \rho = NS$) (Table 4-28b). The mean body length was longest in unprotected targets (mean = 250.0mm, s.d. = 0.0mm), less than 2mm longer than the mean body length in targets that had HG2 on the front face (mean = 248.3mm, s.d. = 2.9mm). The shortest mean body lengths were produced in targets with HG2 on the front and back face (245.0mm, s.d. = 5.0mm) (Table 4-28a).

Table 4-28: Body length created by .223 Remington Federal Premium® Tactical® Bonded® projectiles in 10% gelatine targets 250mm in length

a Selected descriptive statistics						
Protection	Mean (mm)	s.d. (mm)	CV (%)			
None	250.0	0.0	0.00			
HG2 front panel	248.3	2.9	1.16			
HG2 front and back	245.0	5.0	2.04			

b Analysis of variance						
Source of variation	SS	d.f.	Mean square	F	Sig.	$\rho \leq$
Protection	38.89	2	19.44	1.750	0.252	NS
Error	66.67	6	11.11			

4.3.2.2.3 Representation of maximum ellipsoid volume

There was no significant difference between the ellipsoid volumes produced in all three target types by .223 Remington Federal Premium® Tactical® Bonded® projectiles ($F_{2,6} =$

4.450, $\rho = NS$) (Table 4-29b). The largest mean volume was in targets with no protection (mean = 2049000mm³, s.d. = 218700mm³), the smallest in targets with HG2 armour on the front and back face (mean = 1498000mm³, s.d. = 91330mm³) (Table 4-29a).

Table 4-29: Representation of maximum ellipsoid volume produced by .223 Remington Federal Premium® Tactical® Bonded® projectiles in 10% gelatine targets 250mm in length

a Selected descriptive statistics

Protection	Mean (mm³)	s.d. (mm³)	CV (%)
None	2049000	218700	10.67
HG2 front panel	1623000	335000	20.64
HG2 front and back	1498000	91330	6.09

b Analysis of variance

Source of variation	SS	d.f.	Mean square	F	Sig.	$\rho \leq$
Protection	5.00 x 10 ¹¹	2	2.50 x 10 ¹¹	4.450	0.065	<i>NS</i>
Error	3.37 x 10 ¹¹	6	5.61 x 10 ¹⁰			

4.3.2.2.4 Fissure area

There was no significant difference in the fissure areas produced in the three target types by .223 Remington Federal Premium® Tactical® Bonded® projectiles ($F_{2,6} = 4.451$, $\rho = NS$) (Table 4-30b). Targets with HG2 armour on the front face only produced the smallest mean fissure area (mean = 17790mm², s.d. = 3228mm²), followed by targets protected on both the front and rear face by HG2 armour panels (mean = 19380mm², s.d. = 1149mm²). The largest mean fissure area was in targets with no protection (mean = 23370mm², s.d. = 2229mm²) (Table 4-30a). Variation was greatest in targets with armour on both the front and back face (CV = 18.14%).

Table 4-30: Fissure area produced in 10% gelatine blocks 250mm in length after penetration by .223 Remington Federal Premium® Tactical® Bonded® projectiles

a Selected descriptive statistics

Protection	Mean (mm²)	s.d. (mm²)	CV (%)
None	23370	2229	9.54
HG2 front panel	17790	3228	18.14
HG2 front and back	19380	1149	5.92

b Analysis of variance						
Source of variation	SS	d.f.	Mean square	F	Sig.	$\rho \leq$
Protection	49568642.67	2	24784321.33	4.451	0.065	NS
Error	33408287.33	6	5568047.89			

4.3.2.2.5 Kinetic energy deposited

The presence of HG2 armour had a significant effect on the level of kinetic energy deposited into 10% gelatine targets 250mm in length when impacted by .223 Remington Federal Premium® Tactical® Bonded® projectiles ($F_{2,6} = 1026.540$, $\rho \leq 0.001$) (Table 4-31b). Tukey's HSD multiple comparison test indicated that mean kinetic energy deposited in unprotected blocks was significantly different to the kinetic energy deposited in the blocks with protection in both arrangements (Table 4-31c). The kinetic energy deposited in unprotected blocks was largest by a margin of over double the energy of the other two target types (mean = 1352.3 J, s.d. = 6.7 J; compared with (HG2 armour front and back) mean = 665.1 J, s.d. = 21.9 J; and (HG2 front panel) mean = 623.6 J, s.d. = 30.7 J) (Table 4-31c).

Table 4-31: Kinetic energy deposited in 10% gelatine blocks 250mm in length by .223 Remington Federal Premium® Tactical® Bonded® projectiles

a Selected descriptive statistics			
Protection	Mean (J)	s.d. (J)	CV (%)
None	1352.3	6.7	0.49
HG2 front panel	623.6	30.7	4.92
HG2 front and back	665.1	21.9	3.30

b Analysis of variance						
Source of variation	SS	d.f.	Mean square	F	Sig.	$\rho \leq$
Protection	1004871.24	2	502435.62	1026.540	0.000	0.001
Error	2936.68	6	489.45			

c Tukey's HSD multiple comparison test for kinetic energy deposited

Protection	Mean (mm)	N	Tukey groupings
None	1352.3	3	
HG2 front panel	623.6	3	
HG2 front and back	665.1	3	

4.3.2.2.6 Maximum temporary cavity analysis

The presence of HG2 armour in any arrangement had no significant effect on the distance to where the maximum temporary cavity was produced in any of the targets struck by .223 Remington Federal Premium® Tactical® Bonded® projectiles ($F_{2, 6} = 2.278$, $\rho = NS$) (Table 4-32b). Mean maximum temporary cavity was produced closest to the front face in targets protected by HG2 armour on the front and back face (mean = 74.7mm, s.d. = 12.1mm). The next mean longest depth was in targets with HG2 armour on the front face (mean = 79.0mm, s.d. = 9.9mm). The longest mean depth to where the maximum temporary cavity was recorded in unprotected blocks (mean = 96.7mm, s.d. = 17.2mm) (Table 4-32a).

The presence of HG2 armour did however, have a significant effect on the maximum diameter reached by the temporary cavity ($F_{2, 6} = 5.346$, $\rho \leq 0.05$) (Table 4-33b). However, Tukey's HSD multiple comparison test indicated no differentiation between the three target types (Table 4-33c). The mean maximum diameter was largest in targets with HG2 armour on the front face only (mean = 194.7mm, s.d. = 14.6mm), the smallest in unprotected blocks (mean = 173.3mm, s.d. = 3.5mm) (Table 4-33a).

Table 4-32: Distance to the location of the maximum temporary cavity in 10% gelatine blocks 250mm in length produced by .223 Remington Federal Premium® Tactical® Bonded® projectiles

a Selected descriptive statistics

Protection	Mean (mm)	s.d. (mm)	CV (%)
None	96.7	17.2	17.75
HG2 front panel	79.0	9.9	12.47
HG2 front and back	74.7	12.1	16.15

b Analysis of variance						
Source of variation	SS	d.f.	Mean square	F	Sig.	$\rho \leq$
Protection	814.89	2	407.44	2.278	0.184	NS
Error	1073.33	6	178.89			

Table 4-33: Size of the maximum temporary cavity diameter produced in 10% gelatine blocks 250mm in length by .223 Remington Federal Premium® Tactical® Bonded® projectiles

a Selected descriptive statistics			
Protection	Mean (mm)	s.d. (mm)	CV (%)
None	173.3	3.5	2.03
HG2 front panel	194.7	14.6	7.52
HG2 front and back	174.0	4.6	2.63

b Analysis of variance						
Source of variation	SS	d.f.	Mean square	F	Sig.	$\rho \leq$
Protection	882.67	2	441.33	5.346	0.046	0.05
Error	495.33	6	82.56			

c Tukey's HSD multiple comparison test for maximum temporary cavity diameter			
Protection	Mean (mm)	N	Tukey groupings
None	173.3	3	
HG2 front panel	194.7	3	
HG2 front and back	174.0	3	

4.2.2.2.7 Projectile expansion

The projectiles compared for when no protection and front HG2 armour panels were present are the projectiles from 4.2 Part A: *Armoured gelatine blocks 500mm in length*. This is because these projectiles were recovered, unlike the projectiles that perforated the equivalent target setups with 250mm length gelatine blocks.

The level of protection provided to targets of 10% gelatine had a significant effect on the level of expansion .223 Remington Federal Premium® Tactical® Bonded® projectiles experienced ($F_{2, 27} = 13.818$, $\rho \leq 0.001$) (Table 4-34b). Tukey's HSD multiple comparison test

indicated that three targets tested resulted in significantly different expansion of the projectiles (Table 4-34c). Expansion was greatest in projectiles that struck targets with HG2 armour panels on both the front and rear face of the 10% gelatine blocks (mean = 117.1mm², s.d. = 5.7mm²), while the smallest surface area was in projectiles that struck targets with an HG2 panel on the front face of 10% gelatine blocks (mean = 106.5mm², s.d. = 4.7mm²) (Table 4-34a).

Table 4-34: Expansion of .223 Remington Federal Premium® Tactical® Bonded® projectiles after striking the target

a Selected descriptive statistics

Protection	Mean (mm²)	s.d. (mm²)	CV (%)
None	111.7	2.7	2.45
HG2 front panel	106.5	4.7	4.45
HG2 front and back	117.1	5.7	4.84

b Analysis of variance

Source of variation	SS	d.f.	Mean square	F	Sig.	p≤
Protection	571.38	2	285.69	13.818	0.000	0.001
Error	558.23	27	20.675			

c Tukey's HSD multiple comparison test .223 Remington Federal Premium® Tactical® Bonded® projectile expansion

Protection	Mean (mm²)	N	Tukey groupings
None	111.7	10	
HG2 front panel	106.5	10	
HG2 front and back	117.1	10	

4.3.3 Discussion of .223 Remington Federal Premium® Tactical® Bonded® results

Many block sizes have been used in the study of ballistics (e.g. Lewis *et al.*, 1982; Fackler *et al.*, 1984a; Knudsen and Vignaes, 1995; Schyma and Madea, 2012). Blocks used in the current work that measured 250mm (w) x 250mm (h) x 500mm (l) were deemed suitable to capture the damage profile of high velocity ammunition (Fackler and Malinowski, 1985), supported by the work carried out in Part A of this Chapter. However, capturing a projectile's complete damage profile may not necessarily be the best method for assessing the effects of

overmatching armour. Target blocks with a depth more comparable to that of a human thorax (i.e. the targeted area of interest for this study) could be more valuable in assessing whether a protected or unprotected target is damaged more following ballistic attack. Previous studies that used tissue simulants have not tested different or altered blocks sizes.

Using 10% gelatine blocks 250mm x 250mm x 250mm to represent human chest measurements (Pheasant, 1988; Laing *et al.*, 1999; British Standards Institution, 2004), the effect of armour on both the front and back faces of targets, in addition to armour just on front faces, was investigated to discover the influence this had on overmatching. This is a more realistic setup when considering UK police officers, who would have armour protecting both the front and back of their thoraxes. O'Connell *et al.* (1988) conducted overmatching trials on anaesthetised pigs protected with armour on both flanks; however, no studies appear to have investigated the effect of armour on both sides of a tissue simulant.

The .223 Remington Federal Premium® Tactical® Bonded® projectiles perforated 10% gelatine targets without HG2 armour on the rear face, regardless of armour being present on the front face. This is not a surprising result given the penetration distances which were witnessed in Part A. However, an unexpected result that does not appear to have been reported before was the behaviour of the projectiles that struck targets with HG2 armour on both the front and rear faces. High speed video footage captured three of the five shots that exited the blocks; perforating the front armour before travelling through the gelatine, striking the rear armour pack, before then travelling back through the gelatine in the direction from which they came, exiting the front face of the gelatine, striking and bouncing off the front HG2 armour pack; these shots then exited the target setup (Figure 4.9). A similar phenomenon was seen in the five shots that remained in the gelatine targets; however, in these instances the projectiles remained within the gelatine blocks after bouncing off the rear armour pack, travelling back through the gelatine at least 120mm, but not striking the surface of the front armour. Of the remaining two shots where the projectiles exited; one exited between the rear face of the gelatine and rear armour pack after perforating the front armour and gelatine block, while it is unclear from the video how the other shot that exited the gelatine targets, exited.

O'Connell *et al.* (1988) tested nine ammunition types against anaesthetised pigs protected by armour on either flank; however, only three types perforated the front armour. Of those three, a .223 projectile (fired from an M16 rifle, 55 grains, 3240 f/s / 988m/s) remained within the animal. No comment was made regarding whether there was evidence to suggest the projectile had bounced off the rear armour and travelled back into the target. A .308 round (fired from an M14 rifle, 150 grains, 2820 f/s / 860m/s) perforated both the front armour and

the animal, but became lodged in the rear armour. No shots from the current study became lodged in the rear armour packs, with the only evidence of damage found to the carrier cases and not to the layers of para-aramid. The final round that perforated the front armour in the study by O'Connell *et al.* was a 7.62 round (fired from a AK-47, 180 grains, 2625 f/s / 800m/s) that perforated the entire target (i.e. armour/swine/armour).

Regardless of staying within a target, projectiles bouncing back off a rear armour pack have not been reported in the open source literature. That isn't to say it has never happened before in real life scenarios, such as in combat. It may have occurred, only without the benefit of high-speed video footage and transparent targets; witnessing a real life event such as this would be nearly impossible. Evidence may have been left in the form of a projectile taking multiple paths through a human body, but it has not been reported and/or published. Saving a patient's life of course takes much greater precedence over assessing a projectile's path through a target.

This demonstrates that armour present on the rear face of gelatine blocks increased the chance of .223 Remington Federal Premium® Tactical® Bonded® projectiles remaining within the target. In a human target, this is potentially very dangerous, not only because of contamination from the projectile that is still present, but because of the projectile travelling through more of the target, increasing the damage profile. This increases the chances of disrupting numerous tissues and organs, while potentially spreading micro-organisms and contaminating the wound (Hiss and Kahana, 2000). The gelatine blocks that were tested were homogeneous in nature, thus there was no effect of travelling through tissues of varying densities on the projectile. Materials of greater density present in a human (e.g. bone) may have an effect on not only the initial entry path of a projectile, but on its path back through if it were to bounce off a rear armour panel. The effect an inhomogeneous target has on projectiles bouncing back are discussed in section 4.4.2.2 *Discussion of .223 Remington Federal Premium® Tactical® Bonded® results.*

O'Connell *et al.* (1988) wrote that in the instance in which the front armour was perforated and the projectile remained within the target, more intensive surgery would have been required had the patient arrived at a hospital alive. As the gelatine blocks are not living, comment cannot be made on the need for surgery; however, if the projectiles remained within a human target as they did in 50% of tested blocks, the need for more intensive surgery would increase the risk faced by the patient.

The projectiles that remained within the target did not deposit the most kinetic energy, projectiles that perforated unprotected gelatine blocks did. The presence of the front armour

reduced the energy of the projectile, while the rear armour also absorbed some when the projectile struck, causing the projectile to either bounce back off and into the target, or exit the target setup. The energy absorbed by the front armour pack agrees with the findings of Misliwetz *et al.* (1995), while projectiles striking the rear pack and bouncing off does not appear to have been previously reported. That kinetic energy deposited was greatest in unprotected 250mm blocks agrees with the EKE findings when 500mm blocks were tested (*Section 4.2.3 Discussion of .223 Remington Federal Premium® Tactical® Bonded® results.*) The effect of overmatching armour with regards to kinetic energy deposited by .223 Remington Federal Premium® Tactical® Bonded® results was a reduction of damage for blocks 250mm in length.

Testing blocks the length of a typical human chest depth meant seeing the effect body armour has, if any, on offsetting where damage was produced within the targets. Maximum temporary cavity expansion occurred earliest in blocks with HG2 armour on both the front and back face, followed by blocks with armour on the front face only. A possible explanation for this occurrence is that the projectiles were slowed sufficiently by the front armour; therefore, the reduced velocity of the projectiles meant the projectiles traversed through less material before the largest temporary cavity expansion was produced. Although there were no statistical differences between the locations of temporary cavity expansion, numerically, HG2 armour caused expansion to occur earlier in armour-protected blocks. This agrees with the findings of both Breteau *et al.* (1989) and Misliwetz *et al.* (1995) as well as from Part A of this study (*Section 4.2.3 Discussion of .223 Remington Federal Premium® Tactical® Bonded® results.*). The diameters of the expansions were comparable to those from Part A too, indicating that all maximum expansions would occur inside a gelatine target this size, thus the presence of armour did not cause an expansion to occur that would have otherwise happened outside a target. As with targets 500mm in length, locations of maximum expansion were past the typical depths of both the liver and spleen (Bleetman and Dyer, 2000), indicating the effects of armour would not cause more severe cavitation effects in these organs.

Statistical analysis revealed maximum diameter of the temporary cavities was largest in blocks protected by armour on only the front face. The variance was largest in this target type as well, with the remaining two target types producing not only similar diameters but variances too. That the sample size was only three may be a factor here, as previously it was found that HG2 armour reduced temporary cavity expansion. Results from targets with no armour and armour on both faces were different by only 0.66mm. Although temporary cavity expansion was worse in terms of damage potential for blocks protected on the front face, all

results from permanent cavity analysis revealed the presence of armour would have a positive effect on the damage produced (i.e. less damage was produced). This is because body length, maximum ellipsoid volume and fissure area were all greatest in gelatine blocks with no protection. Comparison of permanent cavity data with previous studies is not possible.

In summary, the results from testing 10% gelatine blocks 250mm in length with different arrangements of HG2 protection agree with the findings of Missliwetz *et al.* (1995); positive factors incurred by the presence of armour (i.e. reduced permanent cavity damage) are offset by negative factors including an increased likelihood of a projectile remaining within a target that has armour on both the front and rear face. The effect of overmatching body armour in targets this size is to change the mechanism of inflicting damage.

4.3.4 Results from 9mm Luger rounds

The raw data collected from when 9mm Luger projects struck 10% gelatine targets 250mm in length with varying levels of protection are presented in Table 4-35 – Table 4-37. All shots that struck unprotected targets and targets with KR1/SP1 armour on the front face perforated the entire targets, with the projectiles not recovered. The 9mm Luger perforated targets with KR1/SP1 armour on the front and back panel four time (40%), remaining in the gelatine once (10%), being captured in the rear armour pack three times (30%) and in between the rear armour pack and the gelatine rear face twice (20%). Summary data is compared presented in the following section, 4.3.4.1 *Order of magnitude*.

Table 4-35: Measurements collected from interactions of 9mm Luger with 10% gelatine blocks 250mm in length

a Shot information			
Shot	Impact velocity (m/s)	Debris present	Total fissure area (mm ²)
1	423	No visible debris	5449
2	423	No visible debris	5841
3	420	No visible debris	6833
Mean	422.0	N/A	6041.0
s.d.	1.7	N/A	713.4
CV (%)	0.41	N/A	11.81
Min	420	N/A	5449
Max	423	N/A	6833

b Data collected from high speed videos

Shot	Exit velocity (m/s)	Kinetic energy deposited (J)	Distance to maximum expansion of temporary cavity (mm)	Maximum diameter of temporary cavity (mm)
Shot 1	296	365	233	87
Shot 2	295	368	230	89
Shot 3	278	397	242	98
Mean	289.7	376.4	235.0	91.3
s.d.	10.1	17.4	6.4	6.2
CV (%)	3.49	4.62	2.73	6.79
Min	278	365.25	230	87
Max	296	396.46	242	98

c Yaw analysis

Shot	Number of times 90 ° yaw reached	Distance within block (mm)	Comment on projectile behaviour
1	0	Over 250mm	Yawed after exit
2	0	Over 250mm	Yawed after exit
3	0	Over 250mm	Yawed after exit
Mean	N/A	N/A	
s.d.	N/A	N/A	
CV (%)	N/A	N/A	
Min	N/A	N/A	
Max	N/A	N/A	

Table 4-36: Measurements collected from interactions of 9mm Luger with KR1/SP1 body armour panels on the front face of 10% gelatine blocks 250mm in length

a Shot information

Shot	Impact velocity (m/s)	Debris present	Total fissure area (mm ²)
1	424	Minute metallic debris present at exit. Fibres present at entry	8296
2	427	Minute metallic debris present at exit. Fibres present at entry	7530
3	428	Minute metallic debris present at exit. Fibres present at entry	7972
Mean	426.3	N/A	7932.5
s.d.	2.1	N/A	384.4
CV (%)	0.49	N/A	4.85
Min	424	N/A	7530
Max	428	N/A	8296

b Data collected from high speed videos

Shot	Gelatine impact velocity (m/s)	Exit velocity (m/s)	Kinetic energy deposited (J)	Distance to maximum expansion of temporary cavity (mm)	Maximum diameter of temporary cavity (mm)
Shot 1	385	245	353	223	99
Shot 2	374	235	339	202	110
Shot 3	373	243	320	217	104
Mean	377.3	241.0	337.2	214.1	104.5
s.d.	6.7	5.3	16.3	10.6	5.3
CV (%)	1.76	2.20	4.83	4.95	5.11
Min	373	235	320.32	202	99
Max	385	245	352.80	223	110

c Yaw analysis

Shot	Number of times 90 ° yaw reached	Distance within block (mm)
1	1	219.9
2	1	212.5
3	1	219.9
Mean	1.0	217.4
s.d.	0.0	4.3
CV (%)	0.00	1.99
Min	1	212.45
Max	1	219.94

Table 4-37: Measurements collected from interactions of 9mm Luger with KR1/SP1 body armour panels on the front and back face of 10% gelatine blocks 250mm in length

a Shot information			
Shot	Impact velocity (m/s)	Debris present	Total fissure area (mm ²)
1	420	Minimal debris visible. Bullet retained in rear pack.	5419
2	421	Minimal debris visible. Bullet collected from in between rear pack and rear face of gelatine block.	6558
3	428	Minimal debris visible. Bullet exited target and not recovered.	6607
4	420	Minimal debris visible. Bullet exited target and not recovered.	5223
5	423	Debris present, located more towards the rear of the block, although very small in size. Bullet retained 165mm into gelatine block.	5812
6	420	Tiny debris in rear fissures. Bullet retained in rear pack.	5321
7	428	Tiny debris in rear fissures. Bullet not recovered	4781
8	420	Two 'punched' out carrier case debris sections in block. Bullet retained in rear pack.	6214
9	423	Bullet exited target and not recovered.	6057
10	423	Tiny debris in rear fissures. Bullet collected from in between rear pack and rear face of gelatine block	6273
Mean	422.3	N/A	5951.9
s.d.	3.9	N/A	733.0
CV (%)	0.91	N/A	12.32
Min	420	N/A	5223
Max	428	N/A	6607

b Data collected from high speed videos

Shot	Gelatine impact velocity (m/s)	Impact velocity into rear armour (m/s)	Kinetic energy deposited (J)	Distance to maximum expansion of temporary cavity (mm)	Maximum diameter of temporary cavity (mm)
Shot 1	396	247	383	211	94
Shot 2	375	255	302	193	112
Shot 3	393	287	288	226	79
Shot 4	373	253	301	199	113
Shot 5	371	268	263	214	102~
Shot 6	378	278	262	226	92
Shot 7	385	285	268	210	96
Shot 8	379	295	227	232	88
Shot 9	381	280	267	205	91~
Shot 10	381	244	343	194	101
Mean	381.2	269.2	290.4	211.0	96.8
s.d.	8.2	18.3	45.0	13.8	10.5
CV (%)	2.14	6.80	15.50	6.54	10.89
Min	371	244	226.46	193	79
Max	396	295	383.23	232	113

~ Presence of Velcro makes exact measurement difficult

c Yaw analysis

Shot	Number of times 90 ° yaw reached	Distance within block (mm)	Comment on projectile behaviour
1	1	229.2	
2	1	201.3	
3	0	Over 250mm	Yawed after exit
4	1	212.3	
5	1	219.0	
6	0	Over 250mm	Yawed after exit
7	1	241.3	
8	0	Over 250mm	Yawed after exit
9	1	214.1	
10	1	218.9	
Mean	0.7	219.4	
s.d.	0.5	12.8	
CV (%)	69.01	5.83	
Min	0	201.27	
Max	1	Over 250mm	

4.3.4.1 Order of magnitude

The mean fissure area was largest in targets with KR1/SP1 armour panels on the front face of gelatine blocks. The mean maximum diameter of the temporary cavity was also largest

in this target type. Kinetic energy deposited was greatest in unprotected blocks, with the least amount of kinetic energy deposited in targets with KR1/SP1 armour panels on the front and rear face. The location of where the maximum temporary cavity was formed was closer to the entry face in blocks protected on both faces.

Table 4-38: Comparison of the summary statistics produced in all three 10% gelatine target types 250mm in length after impact by 9mm Lugers

Parameter	Statistical description	No protection (n = 3)	KR1/SP1 front panel (n = 3)	KR1/SP1 front and back (n = 10)
Fissure area	Mean (mm ²)	6041.0	7932.7	5951.9
	s.d. (mm ²)	713.4	384.51	733.0
	CV(%)	11.81	4.85	12.32
Kinetic energy	Mean (J)	376.4	337.2	290.4
	s.d. (J)	17.4	16.3	45.0
	CV(%)	4.62	4.83	15.50
Distance to maximum temporary cavity	Mean (mm)	235.0	214.0	211.0
	s.d. (mm)	6.3	10.8	13.8
	CV(%)	2.66	5.06	6.54
Diameter of maximum temporary cavity	Mean (mm)	91.3	104.3	96.8
	s.d. (mm)	5.9	5.5	10.5
	CV(%)	6.42	5.28	10.89
Location of 1st yaw to 90 °	Mean (mm)		217.5	(n = 7) 219.4
	s.d. (mm)	N/A	4.5	12.8
	CV(%)		1.99	5.83

4.3.4.2 ANOVA results

In order to see if the patterns observed from comparing the means were statistically supported, ANOVA and Tukey's HSD analysis was carried out. To ensure equality of sample size, only the first three shots into 250mm 10% gelatine targets with KR1/SP1 armour on the front and back face were used for the ANOVA. This meant the sample size for all three targets was three (n = 3), in less stated otherwise.

4.3.4.2.1 Fissure area

The presence of KR1/SP1 armour had a significant effect on the fissure area produced in 10% gelatine targets 250mm in length by 9mm Luger projectiles ($F_{2,6} = 8.961, p \leq 0.05$) (Table 4-39b). Tukey's HSD multiple comparison test indicated that the fissure area produced in targets with KR1/SP1 on the front face was significantly different to the other two target types (Table 4-39c). Fissure area was largest in targets protected by KR1/SP1 on the front face (mean = 7932.7mm², s.d. = 384.5mm²), over 1700mm² larger than the fissure are in targets protected by KR1/SP1 armour on the front and rear face (mean = 6194.7mm², s.d. = 672.2mm²). The smallest mean area was in targets with no protection (mean = 6041.0mm², s.d. = 713.4mm²) (Table 4-39a).

Table 4-39: Fissure area in 10% gelatine blocks 250mm in length after penetration by 9mm Luger projectiles

a Selected descriptive statistics						
Protection	Mean (mm ²)	s.d. (mm ²)	CV (%)			
None	6041.0	713.4	11.81			
KR1/SP1 front panel	7932.7	384.5	4.85			
KR1/SP1 front and back	6194.7	672.2	10.85			

b Analysis of variance						
Source of variation	SS	d.f.	Mean square	F	Sig.	$p \leq$
Protection	6622660.22	2	3311330.11	8.961	0.016	0.05
Error	2217115.33	6	369519.22			

c Tukey's HSD multiple comparison test for fissure area			
Protection	Mean (mm ²)	N	Tukey groupings
None	6041.0	3	
KR1/SP1 front panel	7932.7	3	
KR1/SP1 front and back	6194.7	3	

4.3.4.2.2 Kinetic energy

There was no significant difference in the kinetic energy deposited in the three target types by 9mm Luger projectiles ($F_{2,6} = 2.058, p = NS$) (Table 4-40b). Energy deposited was

greatest in targets with no protection (mean = 376.4 J, s.d. = 17.4 J), over 39 J greater than the energy deposited in targets with KR1/SP1 on the front face (mean = 337.2 J, s.d. = 16.3 J). The least amount of kinetic energy deposited was in targets with KR1/SP1 armour panels on both the front and rear face (mean = 324.7 J, s.d. = 51.2 J), though the variation was over three times greater in this target type (CV = 15.78%) (Table 4-40a).

Table 4-40: Kinetic energy deposited by 9mm Lugers in 10% gelatine blocks 250mm in length

a Selected descriptive statistics			
Protection	Mean (J)	s.d. (J)	CV (%)
None	376.4	17.4	4.62
KR1/SP1 front panel	337.2	16.3	4.83
KR1/SP1 front and back	324.7	51.2	15.78

b Analysis of variance						
Source of variation	SS	d.f.	Mean square	F	Sig.	$\rho \leq$
Protection	4377.96	2	2188.98	2.058	0.209	NS
Error	6380.61	6	1063.43			

4.3.4.2.3 Maximum temporary cavity analysis

The presence of KR1/SP1 armour in any arrangement had no significant effect on the distance to where the maximum temporary cavity was produced in any of the targets struck by 9mm Luger projectiles ($F_{2,6} = 3.783$, $\rho = NS$) (Table 4-41b). Mean maximum temporary cavity was produced closest to the front face in targets protected by KR1/SP1 armour on the front and back face (mean = 210.0mm, s.d. = 16.5mm), with the mean distance in targets protected on the front face by KR1/SP1 4mm longer (mean = 214.0mm, s.d. = 10.8mm). The longest mean depth to where the maximum temporary cavity was recorded in unprotected blocks (mean = 235.0mm, s.d. = 6.3mm) (Table 4-41a).

The presence of KR1/SP1 armour also had no significant effect on the maximum diameter reached by the temporary cavity ($F_{2,6} = 1.197$, $\rho = NS$) (Table 4-42b). The mean maximum diameter was largest in targets with KR1/SP1 armour on the front face only (mean = 104.3mm, s.d. = 5.5mm), the smallest in unprotected blocks (mean = 91.3mm, s.d. = 5.9mm) (Table 4-42a).

Table 4-41: Distance to the temporary cavity maximum in 10% gelatine blocks 250mm in length produced by 9mm Luger projectiles

a Selected descriptive statistics

Protection	Mean (mm)	s.d. (mm)	CV (%)
None	235.0	6.3	2.66
KR1/SP1 front panel	214.0	10.8	5.06
KR1/SP1 front and back	210.0	16.5	7.87

b Analysis of variance

Source of variation	SS	d.f.	Mean square	F	Sig.	$\rho \leq$
Protection	1082.00	2	541.00	3.783	0.087	NS
Error	858.00	6	143.00			

Table 4-42: Size of the maximum temporary cavity diameter produced in 10% gelatine blocks by 9mm Luger projectiles

a Selected descriptive statistics

Protection	Mean (mm)	s.d. (mm)	CV (%)
None	91.3	5.86	6.42
KR1/SP1 front panel	104.3	5.5	5.28
KR1/SP1 front and back	95.0	16.5	17.39

b Analysis of variance

Source of variation	SS	d.f.	Mean square	F	Sig.	$\rho \leq$
Protection	269.56	2	134.78	1.197	0.365	NS
Error	675.33	6	112.56			

4.3.5 Discussion of 9mm Luger results

Only one previous study has tried to investigate the effects of overmatching armour present on both the front and back face of a target with handgun ammunition, and with all three ammunition types tested, perforation of the front armour was not achieved (O'Connell *et al.*, 1988). The current study is the first to overmatch 9mm Lugers against sharp edged (KR1/SP1) armour on both the front and back face of 10% gelatine with damage produced and analysed.

All shots at targets without KR1/SP1 armour on the back face perforated the gelatine blocks, regardless of any armour on the front face. This is not surprising given that all shots perforated larger gelatine blocks (500mm in length) even with KR1/SP1 armour on the front. Of the ten shots fired into gelatine blocks 250mm in length with armour on the front and back face, four shots perforated the target completely, with a further two shots exiting the target between the rear armour and the rear face of the gelatine block after impact had caused the two materials to separate. Of those that remained within the target, three were recovered from the rear armour pack, while one shot was found at a depth of 165mm into the gelatine. The presence of KR1/SP1 armour on both the front and back face increased the chance of 9mm Lugers staying within target. This has not been reported before. Though projectiles that remained within the rear pack would not necessarily increase damage, the projectile that stayed within the gelatine after striking the rear armour pack increased the damage potential. As was the case for the .223 Remington Federal Premium® Tactical® Bonded® projectiles tested against blocks protected on both faces, this would be more dangerous in a human target; a projectile staying within a target requiring surgical removal, as well as increased disruption due to the projectile travelling a greater distance within the target.

Although the chance of the projectiles remaining within the 250mm gelatine targets increased, this did not mean greater kinetic energy was deposited in these targets. Kinetic energy deposited was greatest in unprotected blocks, and although not significantly different, was smallest in blocks with armour on the front and back face. The rear armour was able to absorb a portion of the projectiles energy, reducing the projectiles ability to perforate the rear armour. The finding that kinetic energy deposited was reduced by the presence of armour agrees with the findings of Prather (1994). This indicated the armour had a positive effect in terms of damage produced, as the severity and size of the damage produced is a function of the energy transferred to the target (Vellema and Scholtz, 2005).

The presence of armour did however cause earlier instability of the 9mm Lugers. In the three targets with no armour, the projectiles did not reach a yaw of 90 ° before exiting the block. In all three shots at blocks with armour on the front face and 70% of the cases with armour on the front and back, a yaw of 90 ° was reached once before exiting. This earlier initiation of instability was a close match to Missliwetz *et al.* (1995) finding projectile instability occurring in about one third of the shots that perforated armour (6/19 for 9mm Luger), while agreeing with the concept that Breteau *et al.* (1989), Prather (1994), Knudsen and Sørensen (1997) and Lanthier *et al.* (2004) found; projectile instability increased after perforation of armour.

The fact that the 9mm Luger yawed in the majority of blocks with KR1/SP1 armour on the front face, and not in unprotected blocks corresponds with maximum temporary cavity expansion occurring earlier in these target types. The earlier onset of instability is potentially more damaging for a human target, especially as the maximum diameter of the temporary cavities was greatest in target types with armour on either the front or the front and back faces. This once again agrees with Breteau *et al.*'s (1989) belief that wounding power was increased by the presence of protective layers of armour.

The more damaging effects of the temporary cavities produced in blocks protected by KR1/SP1 armour led to larger fissure areas being left in protected blocks as well, particularly in blocks with armour on the front face only, which was significantly different to the other two target types. No other work has captured the permanent damage in a tissue simulant, other than the work carried out earlier in this study. However, results from the smaller blocks differ to those collected from blocks 500mm in length. From the earlier work, fissure area was greatest in unprotected blocks. This could be explained by the 9mm Lugers having deeper targets to perforate, meaning the projectiles yawed to 90 ° in the unprotected blocks that were 500mm, unlike the unprotected blocks 250mm in length. A greater fissure area means a greater area of the gelatine has been stretched and damaged; the presence of KR1/SP1 armour on the front face of 250mm gelatine blocks increases the damage produced.

Taking into account all factors that influence damage production, the reduced energy the 9mm Lugers deposited into armour-protected 250mm gelatine blocks is not reduced to a great enough extent to outweigh the results of the projectiles becoming unstable earlier. This is because the earlier instability caused earlier and larger temporary cavities that led to greater areas of permanent damage. Additionally, the likelihood of the projectiles remaining within the target increased with the presence of armour on the rear face. This leads to the conclusion that the presence of KR1/SP1 armour leads to greater damage being produced in gelatine blocks 250mm in length when compared to unprotected targets.

4.4 Part C: Armoured simulated thoraxes

Following the testing of 250mm gelatine blocks with armour on both the front and back face, a final trial was conducted that utilised porcine thoracic wall samples to mimic a thorax protected by body armour. Continuing on from the work that was presented in *Part C* of Chapter 3, body armour panels were placed in front and behind a simulated thorax that was formed from porcine thoracic walls placed either side of a 10% gelatine block (160 - 180mm in size). 10% gelatine was used instead of a pair of lungs so the interaction could be visualised by high-speed video.

4.4.1 Materials and methods

4.4.1.1 Porcine samples

Samples of porcine thoracic walls (consisting of the ribs, intercostal muscles, underlying tissue and skin; vertebra and the sternum removed) (Figure 4-10) were collected from Andrews Quality Meats Ltd. (16 High Street, Highworth, Wiltshire, SN6 7AG, UK) the day prior to testing, with each sample brought up to room temperature at least 12 hours before testing ($\approx 18^{\circ}\text{C} \pm 3^{\circ}\text{C}$). The mass, dimensions and number of ribs present in each sample were also taken and recorded prior to testing. The samples used were all of food-grade standard and fit for human consumption, consequently there were no ethical concerns raised for this study (Appendix I).



Figure 4-10: A front and back view of a typical example of the porcine thoracic walls tested

4.4.1.2 10% gelatine

The method for making 10% gelatine blocks was the same method described in Section 3.2.1.1.1 *Gelatine*. After the blocks were conditioned and had successfully met the quality control criteria, they were cut to size so as when placed in between two thoracic wall samples, the target was as close to 250mm in length as possible.

4.4.1.3 Ballistic testing method of protected simulated thoraxes

Facing the muzzle of the proof house, the front of the target was always a body armour panel (Figure 4-11). This was placed in contact with a thoracic wall sample (skin facing muzzle), with a 10% gelatine block (160 - 180mm (l) x 250mm (w) x 250mm (h)) positioned behind the front sample. In contact with the rear face of the gelatine block was another thoracic wall, with the skin facing away from muzzle. Completing the protected simulated thoraxes, a final body armour panel was placed against the skin of the posterior thoracic wall (Figure 4-12). In order to support the structure of the simulated thoraxes, each were placed between two picture frames that were clamped at both the front and back of the stand (Figure 4-13).

When HG2 body armour panels were the protection for the simulated thoraxes, .223 Remington Federal Premium® Tactical® Bonded® rounds were the ammunition type used. When KR1/SP1 panels were the protection, 9mm Luger rounds were used. The target was placed 10 m away from the end of the muzzle. An Enfield Number 3 Proof Housing, with the appropriate barrel fitted, was used to fire each ammunition type. Each individual shot was aimed to strike the target so the projectile would penetrate all materials if it was capable. Shots that were fired onto the same thoracic wall sections were positioned to ensure damaged areas did not overlap. No more than 3 shots were carried out on a single HG2 body armour panel, nor more than 6 shots carried out on a single KR1/SP1 panel. Three shots in total were carried out for each ammunition type (n = 3 for .223 Remington; n = 3 for 9mm Luger).

The impact velocities were recorded using a Weibel W-700 Doppler radar. A Phantom high-speed video camera (V12) was used to record the impact events (21005 fps, 5 μ s exposure time and 512 x 512 frame resolution). A scale was used in all impacts to allow the high-speed video footage to be calibrated during analysis. Digital photographs were also taken.



Figure 4-11: Typical front view of a protected simulated thorax

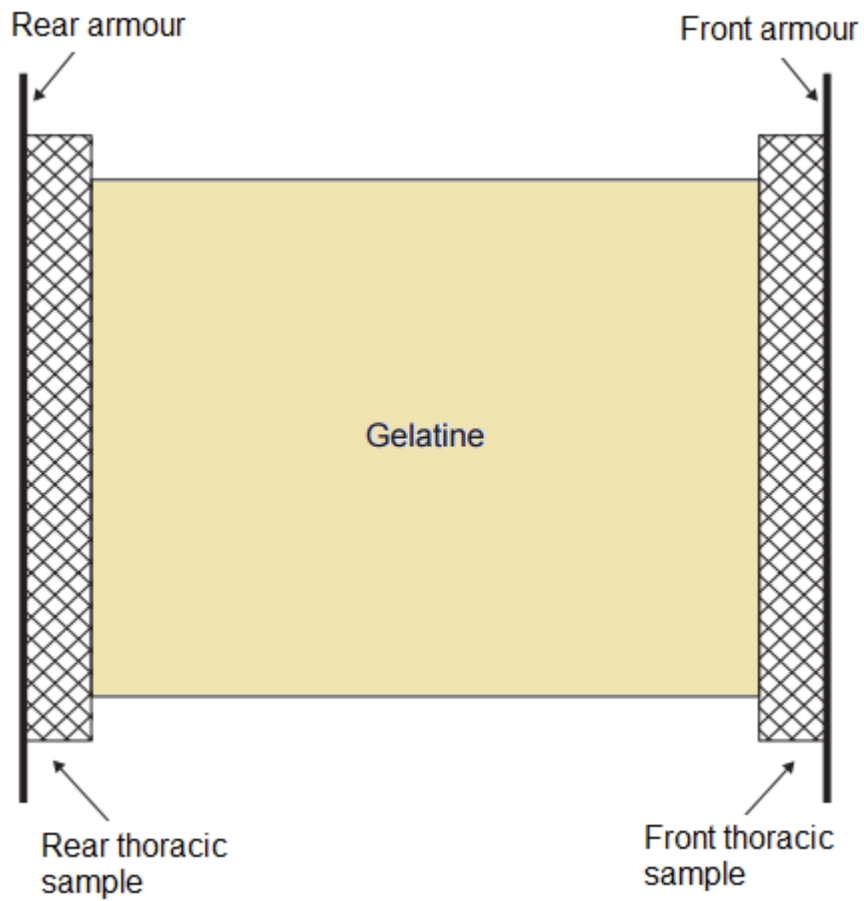


Figure 4-12: Schematic diagram of a protected simulated thorax arrangement.



Figure 4-13: Arrangement of the protected simulated thorax

4.4.1.4 Analysis

Post firing analysis of the thoracic walls was performed after all shots had been completed. Measurements of the entrance and exit wounds of each shot, together with photographs, were taken from every penetrated section of the thoracic walls (Figure 4-14). Any projectile and/or bone fragments found were photographed *in situ* (Figure 4-15 and Figure 4-16), weighed, and recovered, before dissection of the wounds took place. Further fragments found from exploration of the damage were also photographed, recovered and weighed (Figure 4-17).

Post firing analysis of the gelatine blocks that were present in between the thoracic walls consisted of cutting along the length of the permanent cavity, before measurements of the cavity were taken (Figure 4-18). This was done following the process described earlier in section 3.3.1.4 *Baseline simulants analysis*. When present, projectile and/or bone fragments were photographed, recovered and weighed (Figure 4-19 and Figure 4-20).



Figure 4-14: Measurement of a typical exit hole in the anterior thoracic wall caused by .223 Remington Federal Premium® Tactical® Bonded® rounds. Fabric debris visible.

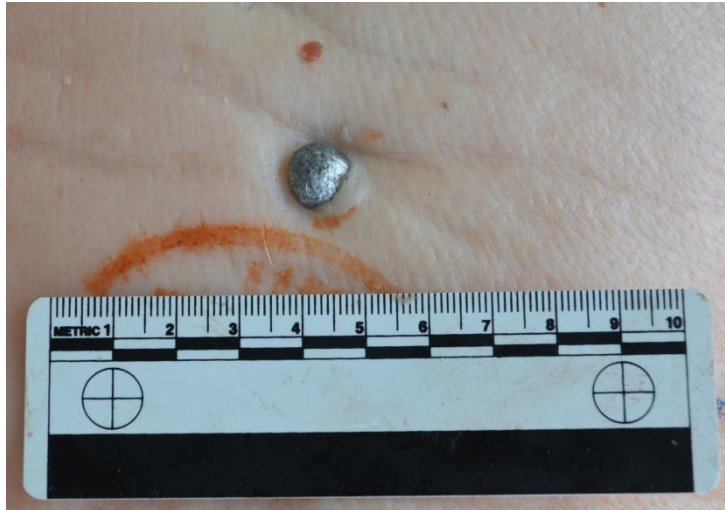


Figure 4-15: A .223 Remington Federal Premium® Tactical® Bonded® round *in situ* in a posterior thoracic wall.

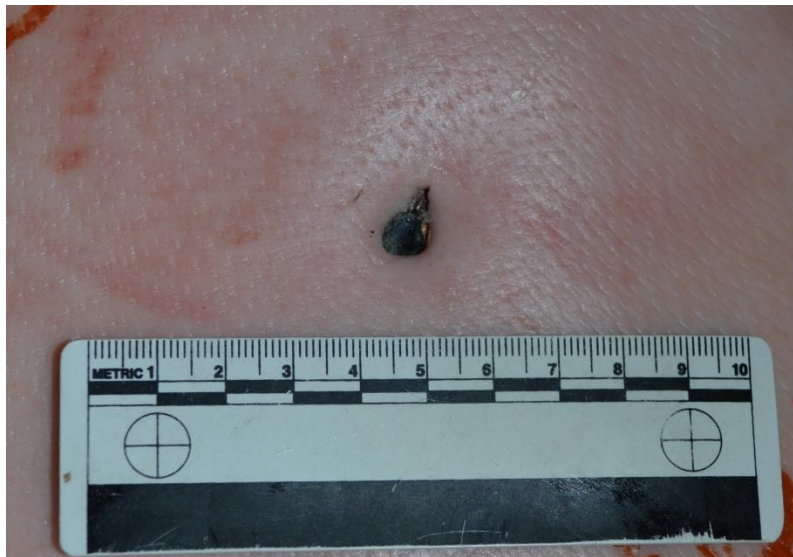


Figure 4-16: A 9mm Luger round recovered from *in situ* within a posterior thoracic wall.



Figure 4-17: A .223 Remington Federal Premium® Tactical® Bonded® round recovered from within a posterior thoracic wall during dissection.

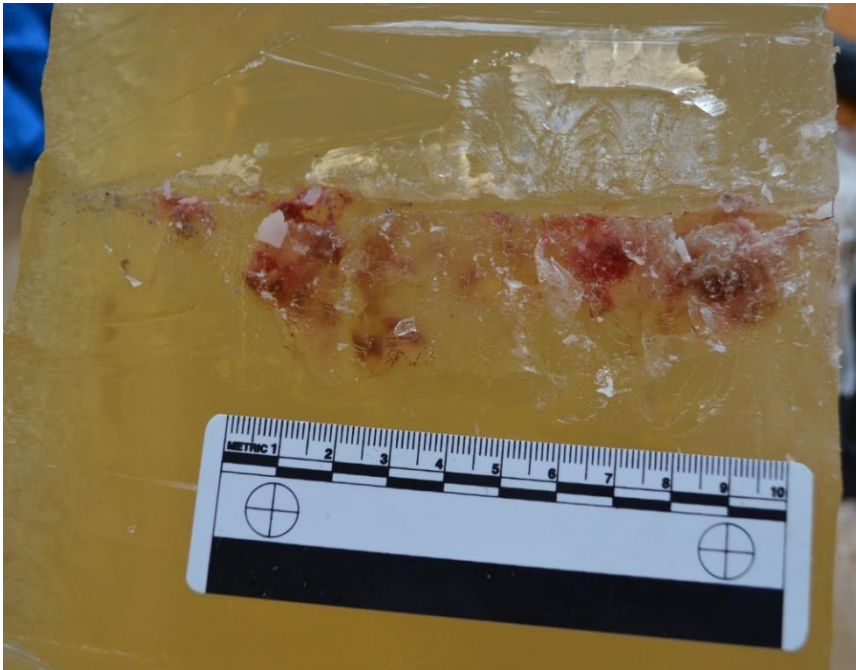


Figure 4-18: A typical permanent cavity complete with debris produced within 10% gelatine block that was situated in between two protected porcine thoracic walls after penetration of a .223 Remington Federal Premium® Tactical® Bonded® round.

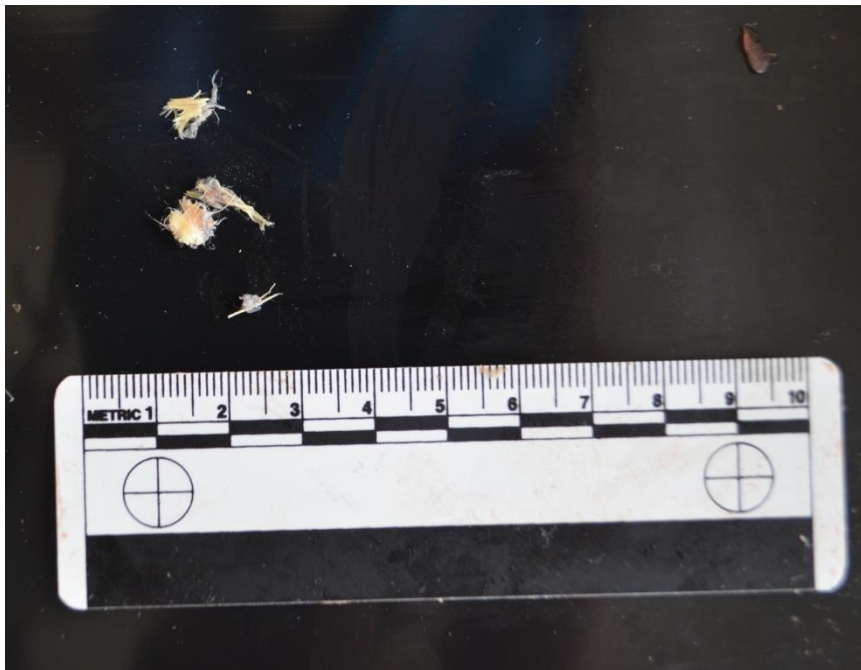


Figure 4-19: Typical fabric debris recovered from protected simulated thoraxes after perforation of 9mm Luger projectiles.



Figure 4-20: Typical tissue debris recovered from 10% gelatine blocks that was situated in between two protected porcine thoracic walls after penetration of a .223 Remington Federal Premium® Tactical® Bonded® round

4.4.2 Results

Table 4-43: Thoracic sample details

Thoracic sample	Mass (Kg)	Number of ribs
T1	3.609	11
T2	4.310	12
T3	4.347	12
T4	3.783	12
T5	4.039	12
T6	3.768	12
T7	3.785	11
T8	3.545	11

4.4.3 Results from .223 Remington Federal Premium® Tactical® Bonded® projectiles

The raw data collected from firing .223 Remington Federal Premium® Tactical® Bonded® projectiles at protected simulated thoraxes is presented below (Table 4-44 – Table 4-49). Every shot was recovered from within the posterior thoracic wall, with evidence that the projectile had travelled backwards after reaching a further point than the resting location evident in two of the three shots.

Table 4-44: .223 Remington Federal Premium® Tactical® Bonded® shot details

Shot number	Ammunition	Target set up	Impact velocity (m/s)
1	.223 Remington	HG2 panel, T1, gelatine section (B4a), T2, HG2 panel	852
2	.223 Remington	HG2 panel, T1, gelatine section (B1a), T2, HG2 panel	847
3	.223 Remington	HG2 panel, T3, gelatine section (B4b), T4, HG2 panel	850

Table 4-45: .223 Remington Federal Premium® Tactical® Bonded® strike location through target

Shot number	Entry location		
	Anterior thoracic sample	Complete perforation of gelatine block?	Posterior thoracic sample
1	Between 6 th and 7 th ribs (both broken)	Yes	Between 6 th and 7 th ribs (neither broken)
2	Between 4 th and 5 th ribs (4 th broken)	Yes	Hit 5 th rib (rib broken)
3	Hit 7th rib (rib broken)	Yes	Between 7 th and 8 th rib (neither broken)

Table 4-46: .223 Remington Federal Premium® Tactical® Bonded® entry and exit dimensions

Shot number	Anterior thoracic sample				Posterior thoracic sample			
	Entry		Exit		Entry		Exit	
	Width	Height	Width	Height	Width	Height	Width	Height
	(mm)	(mm)	(mm)	(mm)	(mm)	(mm)	(mm)	(mm)
1	5	4	50	40	10	7	4*	5*
2	4	6	50	35	10	9	9	8
3	6	4	30	45	4	5	-	-

*Damage was present but projectile did not exit.

-No hole present, an indent 3mm in width was.

Table 4-47: Distance to .223 Remington Federal Premium® Tactical® Bonded® projectiles

Shot number	Distance through anterior thoracic sample (mm)	Distance through 10% gelatine (mm)	Distance through posterior thoracic sample (mm)	Total target depth (mm)
1	44	160	41	245
2	40	165	46	251
3	44	180	36*	260

*Bullet tract reached end of posterior thoracic sample but did not perforate the skin.

Table 4-48: Mass of .223 Remington Federal Premium® Tactical® Bonded® projectiles and fragments collected from 10% gelatine blocks

Shot number	Projectile resting location	Projectile (and fragment) mass (g)	Total distance to bullet (mm)
1	In posterior thoracic wall, 19mm away from exit (rear of skin)	3.859	226
2	Remained in exit hole present in posterior thoracic wall	3.806	251
3	In posterior thoracic wall, 12mm away from exit (rear of skin)	3.978	248

Table 4-49: Details of location and mass of fragments collected from porcine samples after perforation by .223 Remington Federal Premium® Tactical® Bonded® projectiles

Shot number	Tract through anterior thoracic sample (g)	Gelatine	Tract through posterior thoracic sample (g)
1	Fibres – 0.023	Bone – 0.691 Tissue – 2.513	-
2	Punch out – 0.038	Bone – 1.399 Tissue – 0.348	Bone - 0.169
3	Bone – 0.475 Fibres – 0.017	Punch out – 0.005 Metal – 0.052 Bone – 1.459 Tissue – 0.897	-

4.4.3.1 ANOVA results

ANOVA analysis was carried out to investigate the presence of any significant differences between the data collected from shots into protected simulated thoraxes and shots into unprotected simulated thoraxes (*3.4 Part C – Ballistic testing of porcine samples*), that utilised porcine lung in between two porcine thoracic walls, backed up by a 10% gelatine block. The parameters compared were distance to projectile and the entry and exit sizes of both thoracic walls. To ensure equality of sample size, only the first three shots into unprotected simulated thoraxes were used for the ANOVA. This meant the sample size for all three parameters that were compared was three ($n = 3$).

4.4.3.1.1 Distance to projectile

The presence of HG2 armour on the front and back of a simulated thorax had a significant effect on the distance to .223 Remington Federal Premium® Tactical® Bonded®

projectiles ($F_{1,4} = 139.759$, $p \leq 0.001$) (Table 4-50b). Distance was greatest in the unprotected simulated thorax arrangement backed up by 10% gelatine (mean = 452.7mm, s.d. = 27.7mm). Mean distance in the protected thorax was shorter by over 200mm (mean = 241.7mm, s.d. = 13.7mm) (Table 4-50a). Comparison of the respective CVs revealed the variability was similar for both target types (CV (unprotected) = 6.13%, CV (protected) = 5.60%).

Table 4-50: Distance to .223 Remington Federal Premium® Tactical® Bonded® projectiles after penetration of simulated thorax

a Selected descriptive statistics			
Protection	Mean (mm)	s.d. (mm)	CV (%)
None	452.7	27.7	6.13
HG2 front and back	241.7	13.7	5.60

b Analysis of variance						
Source of variation	SS	d.f.	Mean square	F	Sig.	$p \leq$
Protection	66781.50	1	66781.50	139.759	0.000	0.001
Error	1911.33	4	477.83			

4.4.3.1.2 Entry dimensions in anterior thoracic walls

HG2 armour on the front and back of a simulated thorax had no significant effect on the entry width produced in the anterior thoracic wall after perforation by .223 Remington Federal Premium® Tactical® Bonded® projectiles ($F_{1,4} = 4.000$, $p = NS$) (Table 4-51b). Mean widths were larger in targets protected by HG2 armour (mean = 5.0mm, s.d. = 1.0mm), though with greater variability when compared to unprotected targets (mean = 3.7mm, s.d. = 0.6mm) (Table 4-51a). There was also no significant effect on the entry height produced in the anterior thoracic walls ($F_{1,4} = 3.200$, $p = NS$) (Table 4-52b). Mean entry height was greatest in anterior walls protected by HG2 armour (mean = 4.7mm, s.d. = 1.2mm) when compared to anterior walls with that had no protection (mean = 3.3mm, s.d. = 0.6mm) ((Table 4-52a). For both anterior entry measurements, variability was greatest when HG2 armour was present.

Table 4-51: Anterior thoracic wall entry widths after penetration by .223 Remington Federal Premium® Tactical® Bonded® projectiles

a Selected descriptive statistics

Protection	Mean (mm)	s.d. (mm)	CV (%)
None	3.7	0.6	15.75
HG2 front and back	5.0	1.0	20.00

b Analysis of variance

Source of variation	SS	d.f.	Mean square	F	Sig.	$\rho \leq$
Protection	2.67	1	2.67	4.000	0.116	NS
Error	2.67	4	0.67			

Table 4-52: Anterior thoracic wall entry heights after penetration by .223 Remington Federal Premium® Tactical® Bonded® projectiles

a Selected descriptive statistics

Protection	Mean (mm)	s.d. (mm)	CV (%)
None	3.3	0.6	17.32
HG2 front and back	4.7	1.2	24.74

b Analysis of variance

Source of variation	SS	d.f.	Mean square	F	Sig.	$\rho \leq$
Protection	2.67	1	2.67	3.200	0.148	NS
Error	3.33	4	0.83			

4.4.3.1.3 Exit dimensions in posterior thoracic walls

With only one shot creating an exit hole (from which it was recovered) when armour was present, ANOVA could not be carried out on the exit dimensions produced in the posterior thoracic walls.

4.4.4 Discussion of .223 Remington Federal Premium® Tactical® Bonded® results

Anaesthetised pigs were used in two previous studies that investigated overmatching (O'Connell *et al.*, 1988; Breteau *et al.*, 1989); however, the current study appears to be the first to utilise porcine thoracic samples. Arranged to simulate a thorax, the work continued on from the research carried out in Chapter 3: *3.4 Part C – Ballistic testing of porcine samples*, with the aim of exploring the effect armour has on a target that resembles a thorax in both size and inhomogeneous materials.

Comparing the two experiments from this thesis that have used simulated thoraxes revealed the presence of HG2 armour on both the front and rear face of the thorax arrangement drastically increases the chances of .223 Remington Federal Premium® Tactical® Bonded® projectiles remaining within the arrangement. Of seven shots fired at unprotected simulated thoraxes, all perforated the porcine thoracic walls which encompassed a pair of lungs, before penetrating a 10% gelatine block to at least 245mm. Of three shots which were fired at thorax arrangements constructed of porcine thoracic walls either side of a 10% gelatine block 160 – 180mm in depth, protected front and back by HG2 armour, all remained within the rear thoracic wall of the targets. This agrees with the findings from when 250mm gelatine blocks protected either side by HG2 armour were struck by .223 Remington Federal Premium® Tactical® Bonded® projectiles. This, as discussed when the projectiles remained within protected gelatine targets 250mm in length, is a more dangerous outcome for a living target.

Although one target type was a homogenous material while the other was formed of inhomogeneous materials, projectiles travelling backwards after striking the rear armour pack was a result seen in both protected 10% gelatine blocks 250mm in length and protected simulated thoraxes. It was not possible to view the .223 Remington Federal Premium® Tactical® Bonded® projectiles travelling backwards in the posterior thoracic wall; however, there was evidence in the form of damaged material in front of their respective resting locations in two out of the three shots. The distance the projectiles travelled backwards was less in the porcine thoracic wall when compared to 10% gelatine. This could be because of the thoracic wall material having a higher density than 10% gelatine, causing greater drag on the projectile, thus restricting movement. This is supported by the fact that the only shot not to produce evidence of travelling backwards struck a rib in the rear wall, the densest material tested (DeMuth, 1966). An alternative explanation is that the projectiles move back further in gelatine blocks due to the pulsations that occurred during the collapse of the temporary cavity, drawing

the projectiles back. This was less effective in the thorax arrangement than in the 250mm gelatine blocks. In the gelatine blocks the temporary cavity occurred in the one homogeneous material present, drawing the projectile that stayed within the block backwards as permanent cavity collapsed. In the thorax arrangement, the temporary cavity would have again been largest in the gelatine block (due to its elastic nature), but the projectile was in a separate material (i.e. the posterior thoracic wall) and thus the pulsations were less effective at drawing the projectile back. The backwards movement of the projectile would be a more damaging scenario for a living target, as it would cause more disruption to tissue. However, the disruption may not have been increased substantially because the movement backwards was limited to less than 20mm in the thoracic wall specimen. The projectile remaining within a thoracic wall in close proximity to the spinal column would be of greater concern, as this is an area that carries a great risk for surgical intervention. However, this would only be of concern should the original shot miss the spinal column avoiding damage to the central nervous system (CNS). If the original shot strikes the spinal column, the projectile remaining within the target may be irrelevant due to irreversible damage to the CNS.

Breteau *et al.* (1989) found the entrance wounds to the chests of anaesthetised pigs were always larger in specimens that were protected by armour than those not protected at all, though the extent of the difference was not presented. Entrance widths and heights were also larger in protected targets in the current study, though not at a statistical significance level at $p \leq 0.05$. Breteau *et al.* offer no hypotheses as to why entrance holes were larger, but one theory is that it is due to projectile instability. Stone and Petty (1991) found the presence of interposed targets (defined as any object or material which a projectile might pass after leaving the muzzle of a weapon and before entering the target) caused unusual entry injuries due to the stability of the projectiles being affected. As the .223 Remington Federal Premium® Tactical® Bonded® projectiles expanded on impact, the armour's effect on the level of expansion may have been a greater factor in the different sized entry dimensions found in the current study.

Exit wounds do not appear to have been commented on in previous studies. In the current study, they were found to be heavily influenced by the location of exit, with the presence or absence of bone (i.e. ribs) resulting in large variations in mean dimensions. As there was only one exit hole produced in the armour-protected targets, comment on the effect armour had on exit holes is not currently possible without further shots, with particular attention required on the effect of materials struck on exit.

The influence of HG2 armour on debris production in the simulated thoraxes was similar to its influence on gelatine blocks in both Part A and Part B of Chapter 4. The .223

Remington Federal Premium® Tactical® Bonded® projectiles deposited para-aramid fibres and sections from the armour carrier cases throughout the tract it produced up until the rear thoracic wall. In a living target this would once again increase the chances of infection (Mellor *et al.*, 1997). In both protected and unprotected targets, the presence of tissue spread along the tract was prominent; this highlights how micro-organisms present within certain organs of the body could be easily spread, regardless of any protection present.

Overmatching HG2 body armour that protected simulated thoraxes has provided more information about armour’s influence on damage production. The increased chances of .223 Remington Federal Premium® Tactical® Bonded® projectiles staying within the thorax setup agrees with the results from testing 10% gelatine blocks protected on both sides. As seen in previous experiments carried out in the current study, projectiles travelled backwards in two out of three shots after reaching the rear armour panel, though the distance travelled backwards was not as concerning as originally thought when the phenomena was first noticed in 250mm gelatine blocks. In a living target that has survived the initial ballistic attack, the final resting place of the projectile could be of concern. Foreign debris was still a common concern throughout the damage produced.

4.4.5 Results from 9mm Luger projectiles

The raw data collected from firing 9mm Luger projectiles at protected simulated thoraxes is presented in below (Table 4-53 – Table 4-58). Every shot was recovered; one from within the posterior thoracic wall, one from in between the carrier case of a rear KR1/SP1 armour pack and the first layer of protection, and one within a KR1/SP1 armour pack.

Table 4-53: 9mm Luger DM11 A1B2 shot details

Shot number	Ammunition	Target set up	Impact velocity (m/s)
1	9mm Luger	KR1/SP1 panel, T3, gelatine section (B1b), T4, KR1/SP1 panel	425
2	9mm Luger	KR1/SP1 panel, T5, gelatine section (B1c), T6, KR1/SP1 panel	430
3	9mm Luger	KR1/SP1 panel, T5, gelatine section (B1c), T6, KR1/SP1 panel	424

Table 4-54: 9mm Luger strike location through target

Shot number	Entry location		
	Anterior thoracic sample	Complete perforation of gelatine block?	Posterior thoracic sample
1	Between 4 th & 5 th ribs (4th broken)	Yes	Hit 5 th rib
2	Between 6 th & 7 th ribs (neither broken)	Yes	Hit 7 th rib
3	Between 4 th & 5 th ribs (4 th broken)	Yes	Nicked 4 th rib (broken)

Table 4-55: 9mm Luger entry and exit dimensions

Shot number	Anterior thoracic sample				Posterior thoracic sample			
	<i>Entry</i>		<i>Exit</i>		<i>Entry</i>		<i>Exit</i>	
	<i>Width (mm)</i>	<i>Height (mm)</i>	<i>Width (mm)</i>	<i>Height (mm)</i>	<i>Width (mm)</i>	<i>Height (mm)</i>	<i>Width (mm)</i>	<i>Height (mm)</i>
1	4	3	10	9	20	12	4	12
2	5	4	10	8	24	21	9	2
3	4	5	11	10	10	22	10	1

Table 4-56: Distance to 9mm Luger projectiles

Shot number	Distance through Anterior thoracic sample (mm)	Distance through 10% gelatine (mm)	Distance through posterior thoracic sample (mm)	Total distance (mm)
1	45	165	42	252
2	43	165	40	248
3	40	175	42	257

Table 4-57: Mass of 9mm Luger projectiles and fragments collected from 10% gelatine blocks

Shot number	Bullet resting location	Bullet (and fragment) mass (g)
1	In posterior thoracic wall, 4mm away from exit (rear of skin)	8.021
2	Between carrier case and first layer of protection in rear armour panel	7.990
3	Within rear armour panel layers	7.967

Table 4-58: Details of location and mass of fragments collected from porcine samples after 9mm Luger shots

Shot number	Tract through anterior thoracic sample (g)	Gelatine	Tract through posterior thoracic sample (g)
1	-	-	Bone – 0.230 Carrier case section – 0.007
2	-	Bone – 0.003	Bone – 0.341 Carrier case section- 0.004
3	Punch out section fibre – 0.005	Bone – 0.014	Bone – 0.016

4.4.5.1 ANOVA results

ANOVA analysis was carried out to investigate whether the entry and exit dimensions in each thoracic wall were significantly different between the data collected from 9mm Luger shots into protected and unprotected thoraxes (3.4 Part C – Ballistic testing of porcine samples), that utilised porcine lung in between two porcine thoracic walls, backed up by a 10% gelatine block.

4.4.5.1.1 Entry dimensions in anterior thoracic walls

KR1/SP1 armour on the front and back face of a simulated thorax had no significant effect on the entry width caused by 9mm Lugers in anterior thoracic walls ($F_{1,4} = 2.000$, $\rho = NS$) (Table 4-59b). Mean width was greatest in the unprotected targets (mean = 5.7mm, s.d. = 1.5mm), when compared to protected thoraxes (mean = 4.3mm, s.d. = 0.6mm) (Table 4-59a).

The entry height produced in anterior thoracic walls after impact by 9mm Lugers was also not significantly affected by the presence of KR1/SP1 body armour ($F_{1,4} = 1.000$, $\rho = NS$) Table 4-60. As with the mean width, mean height was greatest in unprotected simulated thoraxes (mean = 4.7mm, s.d. = 0.6mm), when compared to protected thoraxes (mean = 4.0mm, s.d. = 1.0mm) (Table 4-60a).

Table 4-59: Anterior thoracic wall entry widths after penetration by 9mm Luger projectiles

a Selected descriptive statistics						
Protection	Mean (mm)	s.d. (mm)	CV (%)			
None	5.7	1.5	26.95			
KR1/SP1 front and back	4.3	0.6	13.30			

b Analysis of variance						
Source of variation	SS	d.f.	Mean square	F	Sig.	$\rho \leq$
Protection	2.67	1	2.67	2.000	0.230	NS
Error	5.33	4	1.34			

Table 4-60: Anterior thoracic wall entry heights after penetration by 9mm Luger projectiles

a Selected descriptive statistics						
Protection	Mean (mm)	s.d. (mm)	CV (%)			
None	4.7	0.6	12.36			
KR1/SP1 front and back	4.0	1.0	25.00			

b Analysis of variance						
Source of variation	SS	d.f.	Mean square	F	Sig.	$\rho \leq$
Protection	0.67	1	0.67	1.000	0.374	NS
Error	2.67	4	0.67			

4.4.5.1.2 Exit dimensions in posterior thoracic walls

KR1/SP1 armour present on either side of a simulated thorax had no significant effect on the exit width of the hole produced by 9mm Luger projectiles in posterior thoracic walls ($F_{1,4} = 0.235$, $\rho = NS$) (Table 4-61b). Mean width was greatest in the protected simulated thoraxes (mean = 7.7mm, s.d. = 3.2mm), when compared to unprotected thoraxes (mean = 6.3mm, s.d. = 3.5mm) (Table 4-61a). There was also no significant effect on the exit height produced in the posterior thoracic walls by 9mm Luger projectiles ($F_{1,4} = 7.11$, $\rho = NS$) (Table 4-62b). Mean

height was greatest in protected targets (mean = 5.0mm, s.d. = 6.1mm), 3mm greater than in unprotected targets (mean = 2.0mm, s.d. = 1.0mm) (Table 4-62a).

Table 4-61: Posterior thoracic wall exit widths after penetration by 9mm Luger projectiles

a Selected descriptive statistics						
Protection	Mean (mm)	s.d. (mm)	CV (%)			
None	6.3	3.5	55.48			
KR1/SP1 front and back	7.7	3.2	41.92			

b Analysis of variance						
Source of variation	SS	d.f.	Mean square	F	Sig.	$\rho \leq$
Protection	2.67	1	2.67	0.235	0.653	NS
Error	45.33	4	11.33			

Table 4-62: Posterior thoracic wall exit heights after penetration by 9mm Luger projectiles

a Selected descriptive statistics						
Protection	Mean (mm)	s.d. (mm)	CV (%)			
None	2.0	1.0	50			
KR1/SP1 front and back	5.0	6.1	121.60			

b Analysis of variance						
Source of variation	SS	d.f.	Mean square	F	Sig.	$\rho \leq$
Protection	13.50	1	13.50	0.711	0.447	NS
Error	76.00	4	90.00			

4.4.6 Discussion of 9mm Luger results

Porcine thoracic samples have been used in combination with 9mm Luger projectiles previously (Carr *et al.*, 2014; Mabbott *et al.*, 2014); however, the current study appears to be the first to use both to investigate overmatching.

Comparison of shots into simulated thoraxes that were unprotected to those protected by KR1/SP1 armour revealed a vast difference in the level of penetration of 9mm Lugers. All three shots into thoraxes with no protection perforated not only porcine thoracic walls which

encompassed a set of lungs, but 10% gelatine blocks 500mm in length. When KR1/SP1 armour was introduced front and back to a thoracic set up that used 10% gelatine blocks in between the thoracic walls, the 9mm Luger projectiles did not exit the setup. One was recovered within the posterior thoracic wall, 4mm away from the skin, and the other two from the rear KR1/SP1 armour pack: one between the carrier case and the first layer of para-aramid, the other within the KR1/SP1 armour pack. The presence of KR1/SP1 armour increased the chances of the 9mm Luger projectiles remaining within the complete target. This has not been reported before.

When the projectiles remained within the rear armour panel, some of the projectiles' energy would have been absorbed. Therefore, not all of the projectiles' energy was deposited in the simulated thorax, potentially reducing the damage sustained. Thus the presence of armour in two thirds of the shots reduced the damage potential. However, the one projectile that remained within the thorax would have deposited all of its energy in the target, a scenario worse than when the projectile fully perforated the unprotected thoraxes without depositing all its energy.

The differing resting locations found in the protected simulated thoraxes agrees with data obtained when 250mm 10% gelatine blocks protected front and back were overmatched by 9mm Lugers. Although the number of repeats was less for the protected thoraxes, perhaps accounting for why no perforations were seen, one shot remained within the simulated area of both targets, while recovery from the armour pack was common.

The 9mm Luger projectile that remained within the protected simulated thorax showed evidence of travelling backwards in the posterior thoracic wall, as an exit hole was formed, while the projectile was recovered 4mm away from the rear face. This agrees with what was seen in the 9mm Luger projectile that remained within the 10% gelatine protected either side by KR1/SP1 armour, although the distance travelled backwards was much shorter in the thoracic wall. The difference could be explained by the projectile being subjected to greater drag by denser materials, particularly as the projectile struck a rib in the posterior thoracic wall. In a living target, greater disruption caused by the projectile travelling backwards is unlikely to exacerbate the damage due to the distance that was travelled back. However, a projectile remaining within a living target could be more dangerous than a perforating shot.

Entry dimensions in the anterior thoracic walls were found to be numerically greater when no armour was present, though the variation was greatest in unprotected targets. This finding agrees with the observations of Carr *et al.* (2014), who witnessed similar entry dimensions of 9mm Lugers in porcine thoracic walls that were either bare or mounted with common apparel fabrics (T-shirt, T-shirt plus hoodie and T-shirt plus denim jacket). Although

fabrics were tested and not armour, an observation of interest was that mean wound size was smaller as the fabric coverings became stiffer. The results from the current study are in contrast to the findings of Breteau *et al.* (1989), who found larger entrance wounds to the chests of anaesthetised pigs when armour was present, however this was with rifle projectiles. The altered entrance dimensions did not affect the level of damage that was produced.

Although only two shots exited the rear thoracic walls when armour was present, dimensions were larger when compared to unprotected targets, though not statistically at $p \leq 0.05$. The striking of bone in the posterior thoracic walls may have had more of an influence on this than the presence of armour. This may have also been the reason why debris throughout the tracts of shots into protected thoraxes was more prevalent than in unprotected targets. However, the presence of carrier case sections or para-aramid fibres was seen in all three shots, a definite result of armour being present. Mellor *et al.* (1997) claim fabric carried into low velocity wounds provides an excellent breeding ground for bacteria; in a living target, the presence of armour in an overmatching scenario would increase the chance of infection.

Although the effect of cavitation and yaw could not be analysed using porcine thoracic sections arranged to simulate a thorax, using an inhomogeneous target constructed of materials typically found in a thorax was of benefit in assessing the projectiles perforating capabilities. It revealed that 9mm Luger projectiles performed in a similar fashion to that witnessed when the target was formed of 10% gelatine 250mm in length protected by KR1/SP1, with increased chances of the projectile staying within the target with the presence of armour.

4.5 Summary of parts A, B and C of Chapter 4

Chapter 4 investigated the use two types of ammunition to overmatch two types of UK police body armour that were protecting different target types. The work involved a progression from large homogenous 10% gelatine blocks through to an original setup that placed armour on the front and back faces of targets first made out of 10% gelatine, and then porcine thoracic samples. This setup was based on a police officer wearing armour on both the front and back sides of their torso and produced a result that had not been reported before. Discussion of all three experiments carried out in Chapter 4 follows below, before the conclusions from the whole study are presented in Chapter 5. This is followed by a discussion of the limitations of this study before a final summarising of the thesis is presented.

4.6 Overall discussion on overmatching UK police armour

The three different trials completed in Chapter 4 investigating the effect of overmatching body armour have added to the knowledge on the subject, meeting the requests of Prather (1994), Knudsen and Sørensen (1997) and Lanthier *et al.* (2004) for further research to be conducted. The outcomes from testing two combinations of ammunition and armour with three different targets, revealed the effect of overmatching armour is not one that can be generalised and predicted for all overmatching scenarios, agreeing with the conclusions of Missliwetz *et al.* (1995).

4.6.1 Overmatching using targets of 10 % gelatine blocks 500mm in length

When 10% gelatine blocks 500mm in length were the targets, the presence of armour on the front face for both ammunition types revealed commonalities with respect to temporary cavity formation; maximum temporary cavity expansion occurred earlier within the blocks, while being reduced in diameter. Together, these results highlight the effect armour had was both a positive and negative influence on the damage produced. Positive in the form that reduced diameters meant less material was disrupted, negative in that the earlier cavitation in a human target could cause more disruption and damage to a more susceptible area. These findings agree with the observations Breteau *et al.* (1989) made from the overmatching ammunition/armour combinations they used, while also agreeing with the findings from when handgun ammunition was used by Missliwetz *et al.* (1995). The reduced size of the temporary cavities observed in armoured targets agrees with Lanthier *et al.* (2004), however, they noted longer entry channels were produced in the combination they tested. This adds weight to the argument that overmatching cannot be generalised for all overmatching scenarios.

In the current study, differences in the effect armour had when the two ammunition / armour combinations were trialled on 10% gelatine blocks 500mm in length included the area of fissure damage and the EKE deposited. When KR1/SP1 armour was overmatched with 9mm Luger projectiles, the fissure area produced was smaller than in unprotected blocks. However, when HG2 armour was perforated by .223 Remington Federal Premium® Tactical® Bonded® projectiles, the fissure area was larger in these protected targets than in unprotected blocks. The differences in the mechanisms by which the projectiles inflicted damage had could have an influence. The 9mm Luger projectiles perforated targets without breaking up, yawing numerous times, while the .223 Remington Federal Premium® Tactical® Bonded® projectiles

expanded on impact, remaining head on before coming to a stop within the target. Armour had greater influence on the projectile type that expanded (the .223 Remington Federal Premium® Tactical® Bonded® projectiles) than on the 9mm Luger projectiles that were unstable as they perforated the targets. Projectiles that expanded were slowed more by the armour and caused more localised damage when penetrating at reduced velocities, while the 9mm Lugers were not slowed to such an extent and thus localised damage was not increased. This also explains why the expected kinetic energy (EKE) results differed in the two combinations.

Testing of the .223 Remington Federal Premium® Tactical® Bonded® projectiles that expanded on impact resulted in significantly reduced EKE deposition when HG2 armour was present. The presence of the armour slowed the projectiles, and in doing so reduced the energy of the projectiles, subsequently reducing the energy deposited in the gelatine. No significant difference was found testing 9mm Lugers with or without KR1/SP1 armour. The velocity of the projectiles not being reduced by the armours resulted in the projectiles energy being largely unaltered and thus the EKE deposited in the gelatine targets was not reduced. However, Prather *et al.* (1994) found a reduced energy was deposited in targets protected by ballistic armour when testing rifle rounds that do not typically expand. An alternative explanation for the observations of the current study, is that the differences were because of the makeup and designs of the armours tested, with respect to the specific threats they were designed to protect against. Armour designed to protect from edged weapons such as KR1/SP1, combats the threat very differently from the way armour designed to stop ballistic attacks stops a penetrating projectile (Tobin and Iremonger, 2006; Horsfall, 2012).

Considering 10% gelatine blocks 500mm in length as targets, there was not enough substantial evidence to believe the presence of armour had a detrimental effect on the damage produced. Earlier temporary cavitation for both ammunition types was counteracted not only by reduced maximum cavitation diameters, but also by a significant reduction in the energy deposited by .223 Remington Federal Premium® Tactical® Bonded® projectiles and a reduced area of permanent damage in the form of fissure area by 9mm Lugers. Whether the earlier temporary cavity would be more damaging to a human was investigated with the use of smaller gelatine targets.

4.6.2 Overmatching using targets of 10 % gelatine blocks 250mm in length

Using 10% gelatine blocks 250mm in length was an ideal method to capture damage in a target that resembled human chest depth. In doing so, the effects of an earlier temporary

cavitation, witnessed from the trials with 500mm gelatine blocks, were investigated (i.e. would the armour cause a cavitation to occur inside the gelatine that otherwise would have occurred after perforation). Once again, the effect of the two ammunition and armour combinations tested to investigate overmatching had both consistencies and differences.

Targets of 10% gelatine 250mm in length that were protected by armour on both the front and rear face increased the chances of either one of the projectiles remaining within the gelatine. In these instances, the projectiles bounced off the rear armour pack back into the gelatine, with the .223 Remington Federal Premium® Tactical® Bonded® projectiles more prone to this behaviour. The travel back of the .223 Remington Federal Premium® Tactical® Bonded® projectiles was greater, with projectiles (30%) seen to exit the face from which they entered (i.e. travelling back greater than 250mm). These observations have not been reported previously, and are of concern when considering potential injury to a human target; a projectile entering and fully penetrating the body, before ricocheting back off rear armour through the body and either coming to a stop within the body or exiting from the side of entry. This would lead to greater disruption, increased risk of damaging a vital structure/organ and causing greater blood loss. If these injuries were survived, they would then be subjected to contamination from both the projectile itself and micro-organisms from the disrupted parts of the body.

The location of maximum temporary cavitation was earliest in 250mm gelatine blocks that were protected by armour on both front and back faces, with unprotected blocks the target responsible for the latest expansion. This matches what was found in 10% gelatine blocks 500mm in length, and is in agreement with the findings of Breteau *et al.* (1989) and Missliwetz *et al.* (1995). The earlier occurrence caused by the presence of armour would increase the risk of organs that are susceptible to temporary cavity being subjected to greater injury in a human target. Typically distances to the lung and spleen (Bleetman and Dyer, 2000) are however closer to the anterior of a human than where the expansions occurred in 10% gelatine blocks 250mm in length for both ammunition types.

A common feature in the 250mm gelatine blocks for both ammunition types was that the maximum diameter of the temporary cavity was smallest in unprotected blocks. The presence of armour did not have a positive effect on damage production. The result disagrees with earlier findings from gelatine blocks 500mm in length and is also different from what some previous overmatching studies found (e.g. Breteau *et al.*, 1989; Lanthier *et al.* 2004) with the presence of armour found to reduce the size of the temporary cavity. Conversely, when testing rifle ammunition, Missliwetz *et al.* (1995) reported an increase in the temporary cavity volume produced when armour was present, agreeing with the result found in 250mm gelatine

targets. In the current study, target size may have a factor for the difference seen between the two gelatine block sizes. Half the material was present in blocks 250mm in length when compared to the 500mm gelatine blocks. Temporary cavitation effects may have been influenced by this, while the presence of a firm armour pack on the front and the front and rear faces may have played a role too. The differences highlight the unpredictable nature of overmatching armour; with target size an additional factor to both ammunition and armour type.

Kinetic energy deposited by both projectile types to 10% gelatine targets 250mm in length was reduced when armour was present, agreeing with the observations of Prather (1994). Armour only on the front face was more effective than when armour was present on both the front and rear face for .223 Remington Federal Premium® Tactical® Bonded® projectiles. Conversely, 9mm Luger projectiles deposited least kinetic energy in targets with armour present on both faces. That armour reduced the deposited kinetic energy correlates with what occurred with .223 Remington Federal Premium® Tactical® Bonded® projectiles in gelatine blocks 500mm in length, but differs for what was seen with 9mm Luger projectiles in the larger gelatine blocks. The difference in 9mm Luger projectiles could be due to the differences in target length. In the 500mm gelatine blocks, the 9mm Luger projectiles perforated regardless of any protection present, while in the 250mm targets perforation did not always occur and the reduced distance of the targets, together with the presence of KR1/SP1 armour panels, could have influenced kinetic energy deposition.

The effect of armour on fissure area was different for the two armour and ammunition combinations when tested on 10% gelatine blocks 250mm in length. The .223 Remington Federal Premium® Tactical® Bonded® projectiles caused the largest fissure areas in blocks with no protection; smallest in blocks protected by front armour only. 9mm Luger projectiles produced the largest fissure areas in blocks protected by front armour only, while the smallest was in targets protected by armour on the front and back faces. Mechanisms of how the projectiles caused damage were altered, while the stability of the 9mm Luger projectiles was certainly affected; yawing to 90 ° was only seen in 250mm targets protect by armour.

Summarising the results from testing 10% gelatine blocks 250mm in length; the effect of armour on both the front and back face was one that increased the chances of the projectile remaining in the gelatine. Temporary cavitation occurred earlier when armour was present, as did the maximum diameter of the expansion. Although a limitation of the trial was that only three repeats were used for the means and statistical analysis (due to targets without armour on the rear face being perforated by both ammunitions types), these outcomes indicate that the

effect of overmatching armour in targets this size was a negative one, with an increase in the potential for greater destruction of material. A key influence was, however, that energy deposition was reduced, and thus a factor in considering the damage that would be seen in a human target protected both on the anterior and posterior of the body, would be the area that was impacted, and that area's vulnerability to the increased temporary cavitation effects and contamination.

4.6.3 Overmatching using simulated thoraxes as targets

To be able to comment on how an area of the body (the thorax) would respond in instances of overmatching, the final trial compared how unprotected and protected simulated thoraxes (utilising porcine thoracic walls) differed when shot at. Once again, the presence of armour on the front and rear face increased the chances of both projectile types remaining within the target. The distance projectiles travelled back through the simulated thoraxes after bouncing off the rear armour pack was however a lot shorter when compared to 10% gelatine. This was perhaps a result of the difference in tissue density of the targets, or because one target was formed of three separate materials, altering the influence the cavitation process had on drawing the projectiles back when compared to the influence of the cavitation process in the homogeneous elastic target that was a block of 10% gelatine. Although this was a damaging outcome, projectiles travelling back less in the posterior porcine thoracic walls compared to gelatine was a reduction in the potential for greater disruption; a more positive outcome of the effect of overmatching armour than originally thought. The resting location of the projectile being in close proximity to the spinal cord could still pose extreme consequences in a human target, so long as the original entry was survivable.

Comparing entry dimensions in the anterior porcine thoracic walls, the .223 Remington Federal Premium® Tactical® Bonded® projectiles that perforated HG2 armour created larger dimensions, agreeing with the observations of Breteau *et al.* (1989). The 9mm Luger projectiles, however, had larger entry dimensions in unprotected thorax arrangements compared to those protected by KR1/SP1 armour. Not enough .223 Remington Federal Premium® Tactical® Bonded® projectiles perforated the posterior thoracic wall to compare the effect of armour on exit dimensions, though 9mm Luger projectiles produced larger exit holes when KR1/SP1 armour was present. The location and more specifically the presence or absence of bone (ribs) had more influence on the dimensions recorded. Although only three

repeats were compared for each ammunition type, the variability in entry locations through the simulated thorax sections meant more repeats may not have necessarily been of benefit.

Trials using the inhomogeneous materials common to the region of the thorax demonstrated that observations that had been witnessed in 10% gelatine were not uncharacteristic of what happens when armour is overmatched. Although viewing the temporary cavitation process (including the influence of yaw) was not possible, and the permanent damage was not strictly comparable to the damage produced in gelatine (the spread of tissue and bones etc. was clearer in the thorax arrangements but the level of expansion and recovery of the target was less obvious in showing which regions had been affected by the ballistic event), the effect of materials of varying densities in a target similar in size and depth to that of the relevant area of a patrolling UK police officer uncovered further information on the effect of overmatching armour.

Chapter 5 CONCLUSIONS AND SUMMARY

5.1 Conclusions

The conclusions from this study are presented below, divided into the areas within this research from which they are drawn:

5.1.1 Tissue simulant comparison

- ❖ Depth of penetration of 5.5mm BBs at a range of velocities 150-1050m/s is repeatable in 10% gelatine, 20% gelatine and Perma-Gel™, with the level of penetration following a similar pattern for both concentrations of gelatine.
- ❖ The type of tissue simulant had a significant effect on depth of penetration of 5.5mm BBs while the depth of penetration varied significantly amongst velocity bins.
- ❖ Testing over a large range of velocities demonstrated gelatine is strain rate sensitive when impacted with BBs; therefore any calibration velocities should be tailored to the projectile that is to be tested.
- ❖ Depth of penetration of 5.5mm BBs in Perma-Gel™ is not the same as in 10% (except for approximately 400m/s) or 20% gelatine, even though it is marketed as a replacement for 10% gelatine.
- ❖ The characteristics of Perma-Gel™ change after it is re-melted making it unsuitable for use in numerous tests.
- ❖ The permanent cavities produced by both .223 Remington and 9mm Luger rounds are significantly larger in 10% gelatine blocks when compared to 20% gelatine blocks.

5.1.2 Conclusions from the study of overmatching HG2 protected 10% gelatine blocks 500mm in length with .223 Remington projectiles

- ❖ The presence of armour that met the compliance level of HG2 (Croft and Longhurst, 2007b) in front of 10% gelatine blocks 500mm in length had a significant effect on the expected kinetic energy deposited by .223 Remington Federal Premium® Tactical® Bonded® projectiles into blocks; less energy was deposited after perforation of the HG2 armour panels. This indicates a positive influence on the damage produced (i.e. damage was reduced).
- ❖ No other significant effects were found from the damage analysed between the two target types, though debris was found in shots that had perforated armour prior to the gelatine target.
- ❖ Estimated maximum ellipsoid volumes were typically larger in unprotected 10% gelatine blocks 500mm in length after penetration by .223 Remington Federal Premium® Tactical® Bonded® projectiles, however more damage in the form of fissures was typically present when the blocks were protected by HG2 armour on the front face.
- ❖ An earlier temporary cavity and an increased chance of the projectile remaining within smaller targets was witnessed when HG2 armour was on the front face of 10 % gelatine blocks 500mm in length.
- ❖ The presence of HG2 armour would create a greater risk of infection for a human target via the introduction of fabric debris into the wounded area after being struck by a .223 Remington.
- ❖ Overall, the presence of HG2 body armour panels did not significantly exacerbate the damage caused by .223 Remington Federal Premium® Tactical® Bonded® projectiles in 10% gelatine blocks 500mm in length.

5.1.3 Conclusions from the study of overmatching KR1/SP1 protected 10% gelatine blocks 500mm in length with 9mm Luger projectiles

- ❖ The presence of armour that met the compliance level of KR1/SP1 (Croft and Longhurst, 2007b) in front of 10% gelatine blocks 500mm in length had a significant

effect on the fissure area in the gelatine blocks; greater areas were produced in unprotected blocks. Of the other features of damage collected and compared, no significant differences were found. Following penetration of 9mm Luger projectiles, debris was not a key feature in the majority of 500mm gelatine blocks, regardless of KR1/SP1 armour being present on the front face.

- ❖ Overall, the presence of KR1/SP1 armour panels did not significantly exacerbate the damage produced by 9mm Luger projectiles in 10% gelatine targets of this size.

5.1.4 Conclusions from the study of overmatching HG2 protected 10% gelatine blocks 250mm in length with .223 Remington projectiles

- ❖ The presence of armour that met the compliance level of HG2 (Croft and Longhurst, 2007b) on the rear face of a 10% gelatine block 250mm in length, in addition to an HG2 armour pack on the front face, altered the mechanism by which damage was produced.
- ❖ The chance of the projectile remaining within a 10% gelatine target 250mm in length was increased with the presence of HG2 armour on both the front and rear face.
- ❖ The level of kinetic energy deposited in 10% gelatine targets 250mm in length with either HG2 armour panels on the front face, or the front and rear face, was significantly less than kinetic energy deposited into 10% gelatine blocks of this size with no protection.

5.1.5 Conclusions from the study of overmatching KR1/SP1 protected 10% gelatine blocks 250mm in length with 9mm Luger projectiles

- ❖ The presence of armour that met the compliance level of KR1/SP1 (Croft and Longhurst, 2007b) on the front face (and in cases where it was present on the rear face) of 10% gelatine blocks 250mm in length, increased the chance of the projectiles reaching 90 ° yaw within the gelatine target. The amount of kinetic energy deposited was still however greatest in unprotected blocks this size.

- ❖ The presence of KR1/SP1 armour panels on the rear face of 10% gelatine blocks 250mm in length increased the chance of the 9mm Luger projectiles remaining in the target.

5.1.6 Conclusions from the study of overmatching protected simulated thoraxes

- ❖ The use of porcine thoracic wall samples to produce a thorax arrangement ~ 250mm in length has been shown to support findings produced in 10% gelatine blocks 250mm in length.
- ❖ When testing .223 Remington Federal Premium® Tactical® Bonded® projectiles, the presence of armour panels that met the compliance level of HG2 on both sides of a thorax arrangement increased the chance of the projectile remaining within the target thoracic wall (n = 3).
- ❖ Evidence supporting the phenomenon of the projectiles moving back through the 10% gelatine blocks was found in the posterior thoracic walls.
- ❖ In thorax arrangements with no protection, complete perforation of the target occurred in every shot (n = 7).
- ❖ In thorax arrangements ~ 250mm in length protected by armour panels that met the compliance level of KR1/SP1 on the front and rear face, there was an increased chance of 9mm Luger projectiles remaining within the arrangement, unlike in unprotected simulated thoracic cavities in which each shot perforated the whole target (n = 3).

5.2 Limitations of this study on the overmatching of UK police armour

Using the research of Sturdivan (1981), EKE has been used as the NATO wounding criterion (Kneubuehl *et al.*, 2011). It is a useful mathematical description and was one of the parameters used in the current study to compare the damage produced in both protected and unprotected 500mm gelatine blocks. However, there were limitations to its use. Manually plotting a projectile's path through gelatine from high speed video footage occasionally led to velocity tables that did not make sense with respect to the laws of physics; i.e. a projectile's velocity fluctuating during early travel through a gelatine block. Resolution of the video footage and pixel edge effects not matching up with the location of the projectiles in the video

were the reasons why this occurred. This is why the equation of a polynomial curve that fitted the data best was used in EKE calculations. There were also difficulties in locating the precise moment a projectile entered the gelatine when armour packs were present on the front face. In order to minimise errors as much as possible, data collection was carried out by one person and a subset was repeated to check accuracy.

When analysing overmatching in 10% gelatine blocks 250mm in length, the kinetic energy deposited was calculated. This was because the research in EKE by Sturdivan (1981) took into account different body part estimates in order to calculate the EKE deposited. As the 250mm target block was set up to be the torso, no estimates of body size were required. In order to calculate the kinetic energy for each shot, entrance velocities were required from the high speed video footage. When armour panels were present, this was made difficult with the projectiles being lost from vision the frame before entering the gelatine. There were also issues when armour was present on the rear face. The kinetic energy measurement was for energy deposited in the gelatine block, not including the rear armour panel. In instances where the projectile remained in the rear armour pack and/or disappeared from view, an 'exit' velocity was collected using the two points before the respective projectiles disappeared from view, meaning the deposited kinetic energy that was calculated was for a target shorter than 250mm. One frame was not felt to significantly affect the results.

When utilising porcine thoracic walls for both protected and unprotected thorax arrangements, other than the presence or absence of armour, the two setups differed in the material located between the porcine thoracic walls. In the initial unprotected thorax arrangement (Section 3.4 Part C – *Ballistic testing of porcine samples*) porcine lungs were used and placed in the correct anatomical location with respect to the ribs. However, with a desire to witness events during the perforation of the thorax arrangement post perforation of armour, a gelatine block cut to size to make the whole target depth 250mm replaced the lungs in the protected thorax arrangement. The different materials used may have influenced the results. Lungs typically have a low specific gravity (0.4 – 0.5 (DeMuth, 1966)), and low water content unlike 10% gelatine, but both are elastic in nature with the lungs endowed with many elastic fibres (DeMuth, 1968). The lungs are not the only organ located in a human thorax however, and as it was shown earlier in the current study that 10% gelatine was not statistically different to porcine samples arranged to simulate a thorax, the influence of the change of material was not felt to compromise results.

5.3 Summary

Police officers and other personnel in the UK routinely wear body armour that provides protection from specific threats. Typically, 'soft' armours, usually formed from multiple layers of fabric, protect the wearer from fragmentation and low velocity (handgun) ballistic threats while 'hard' armours, formed from ceramic and composite plates, offer protection from high velocity (rifle) threats. The question has been raised however, of what would happen when armour is overmatched with a greater threat than it is designed to protect against.

The inconsistent results from the paucity of studies in the open literature concerned with the subject of overmatching soft armour, together with requests from researchers to explore further interactions of various ammunition and armour types, set the way for this current research. An initial investigation was carried out that led to the justification and selection of 10% gelatine as the tissue simulant that would be used throughout the study of overmatching. The effect of i) soft fabric body armour (HG2) protecting against the threat of high velocity rifle rounds (.223 Remington Federal Premium® Tactical® Bonded®) and ii) knife and spike resistant armour (KR1/SP1) protecting against the threat of low velocity handgun (9mm Luger) attack were then investigated.

The presence of HG2 soft body armour panels in front of 10% gelatine blocks 500mm in length did not exacerbate the damage produced by .223 Remington Federal Premium® Tactical® Bonded® projectiles compared to unprotected blocks. When the target size was reduced to resemble the depth of a human thorax, with HG2 protection on the front and back face of the target, the chances of the projectile remaining in the target were greatly increased, while the phenomena of the projectile bouncing off the rear armour panel back through the target was seen in 40% of shots (4/10). The kinetic energy deposited within the targets was not vastly greater than the energy deposited when compared to shots that had just perforated an armour panel on the front of the gelatine block and exited the target. Both of these scenarios deposited significantly less kinetic energy to the target than when no protection was present, however, the factor of the projectile bouncing back off the rear armour panel, either remaining in the target or exiting at the front, adds to the risk of greater disruption, particularly should this happen in a human target. This would result in a greater chance of vital organs and structures being disrupted by the projectile, as well as increasing the risk of infection due to contamination.

When the target was an arrangement that simulated a thorax (~ 250mm in depth, formed of porcine thoracic wall samples either side of a gelatine block), protected on either side by HG2

armour panels, the .223 Remington Federal Premium® Tactical® Bonded® projectiles remained in the target in all shots (n= 3). This was a different outcome from that seen when unprotected thoraxes (two porcine thoracic wall samples with porcine lung in between) were shot at by the same ammunition type; perforation of the complete thoracic sample occurred in each shot (n = 7).

Testing 9mm Luger projectiles against KR1/SP1 body armour panels on the front face of 10% gelatine blocks 500mm in length; no increase in damage was seen. In 10% gelatine targets that were 250mm in length, the kinetic energy deposited was greatest in unprotected blocks, followed by blocks with KR1/SP1 on the front face only and the least amount of energy was deposited in blocks with armour on both the front and rear face. The presence of a KR1/SP1 armour panel on the front face did increase the chance of 9mm Luger projectiles reaching 90 ° yaw within the target, as well as causing the maximum expansion of the temporary cavity to be greater in size and to occur earlier within the target. This was also true for thorax arrangements impacted by 9mm Lugers.

5.4 Recommendations

Suggestions for further work include:

5.4.1 The effect different impact angles for both projectile types has when fired into 10% gelatine targets 250mm in length protected by body armour panels on both the front and rear face to investigate if this stops or affects projectiles travelling back through the gelatine.

5.4.2 Testing different combinations that are yet to be tried, and within this the effect of chain mail armour designed to stop knife and spike threat on overmatching handgun rounds.

REFERENCES

- Adams, D. B. (1982), "Wound ballistics: A review", *Military Medicine*, vol. 147, pp. 831-834.
- Allen, R. (ed.) (2000), *The New Penguin English Dictionary*, Penguin books, Finland.
- Allsop, D. F. and Toomey, M. A. (1999), *Small arms*, Brassey's, UK.
- Amick, D. (2006), *Perma-Gel Product Overview*, available at: <http://www.perma-gel.com/overview.htm> (accessed March 2012).
- Anon, (2011), *Bloom*, available at: <http://www.sizes.com/indexes.htm> (accessed June 2012).
- Barach, E., Tomlanovich, M. and Nowak, R. (1986), "Ballistics: A pathophysiologic examination of the wounding mechanisms of firearms: Part I", *Journal of Trauma*, vol. 26, no. 3, pp. 225-235.
- Belkin, M. (1979), "Wound Ballistics", *Progress in Surgery*, vol. 16, pp. 7-24.
- Berlin, R., Blomqvist, G., Janzon, B., Kokinakis, W. and Sćepanović, D. (1979), "Various technical parameters influencing wound production", *Acta Chirurgica Scandinavica*, vol. Supplementum 489, pp. 103-120.
- Berlin, R., Gelin, L. E., Janzon, B., Lewis, D. H., Rybeck, B., Sandegård, J. and Seeman, T. (1976), "Local effects of assault rifle bullets in live tissue. Part I", *Acta Chirurgica Scandinavica*, vol. Supplementum 459, pp. 5-84.
- Berlin, R., Janzon, B., Rybeck, B., Sandegård, J. and Seeman, T. (1977), "Local effects of assault rifle bullets in live tissues. Part II", *Acta Chirurgica Scandinavica*, vol. Supplementum 477, pp. 5-48.
- Berlin, R. H., Janzon, B., Lidén, E., Nordström, G., Schantz, B., Seeman, T. and Westling, F. (1988), "Terminal behaviour of deforming bullets", *Journal of Trauma*, vol. 28, no. Supplement 1, pp. s58-s62.
- Besant-Matthews, P. E. (2000), "Examination and interpretation of rifled firearm injuries", in Mason, J. K. and Purdue, B. N. (eds.) *The Pathology of Trauma*, 3rd ed, Arnold, New York, USA, pp. 47-60.
- Bleetman, A. and Dyer, J. (2000), "Ultrasound assessment of the vulnerability of the internal organs to stabbing: determining safety standards for stab-resistant body armour", *International Journal of the Care of the Injured*, vol. 31, no. 8, pp. 609-612.
- Bleetman, A., Watson, C. H., Horsfall, I. and Champion, S. M. (2003), "Wounding patterns and human performance in knife attacks: optimising the protection provided by knife-resistant body armour", *Journal of Clinical Forensic Medicine*, vol. 10, no. 4, pp. 243-248.

Boackle, M. (2011), "The use of Perma-Gel testing medium for comparison of the terminal performance of different pistol calibres", *AFTE journal.*, vol. 43, no. 2, pp. 146-153.

Bourget, D., Dumas, S. and Bouamoul, A. (2012), "Preliminary estimate for injury criterion to immediate incapacitation by projectile penetration", *Proceedings of the Personal Armour Systems Symposium*, 16th–20th September, Nuremberg, Germany, The International Personal Armour Committee, pp. 449-456.

Bowyer, G. W., Payne, L., Mellor, S. G., Rhee, P. M. and Roberts, P. (1997a), "Historical overview and epidemiology", in Ryan, J. M., Rich, N. M., Dale, R. F., *et al.* (eds.) *Ballistic trauma - Clinical relevance in peace and war*, Arnold, pp. 9-29.

Bowyer, G. W., Ryan, J. M., Kaufmann, C. R. and Ochsner, M. G. (1997b), "General principles of wound management", in Ryan, J. M., Rich, N. M., Dale, R. F., *et al.* (eds.) *Ballistic trauma - Clinical relevance in peace and war*, Arnold, pp. 105-119.

Brase, C. H. and Brase, C. P. (2011), *Understandable statistics: Concepts and methods*, 10th ed, Brooks Cole, Boston, USA.

Brayley, M. J. (2011), *Modern body armour*, Crowood Press, Wiltshire, United Kingdom.

Breeze, J., Allanson-Bailey, L. S., Hepper, A. E. and Midwinter, M. J. (2015a), "Demonstrating the effectiveness of body armour: a pilot prospective computerised surface wound mapping trial performed at the Role 3 hospital in Afghanistan", *Journal of the Royal Army Medical Corps*, vol. 161, pp. 36-41.

Breeze, J., Carr, D. J., Mabbott, A., Beckett, S. and Clasper, J. C. (2015b), "Refrigeration and freezing of porcine tissues does not affect the retardation of fragment simulating projectiles", *Journal of Forensic and Legal Medicine*, vol. 32, pp. 77-83.

Breeze, J., Fryer, R., Lewis, E. A. and Clasper, J. (2015c), "Defining the minimum anatomical coverage required to protect the axilla and arm against penetrating ballistic projectiles", *Journal of the Royal Army Medical Corps*, vol. doi:10.1136/jramc-2015-000453.

Breeze, J., Hunt, N. C., Gibb, I., James, G. R., Hepper, A. E. and Clasper, J. C. (2013), "Experimental penetration of fragment simulating projectiles into porcine tissues compared with simulants", *Journal of Forensic and Legal Medicine*, vol. 20, pp. 296-299.

Breeze, J., Lewis, E. A., Fryer, R., Hepper, A. E., Mahoney, P. F. and Clasper, J. C. (2015d), "Defining the essential anatomical coverage provided by military body armour against high energy projectiles", *Journal of the Royal Army Medical Corps*, vol. 10.1136/jramc-2015-000431.

Bresin, G. (2011), *Collins English Dictionary*, 11th ed, HarperCollins, UK.

Breteau, J., Fackler, M., Sendowski, I. and Martin, P. (1989), "The personal protective equipment provided for combatants: the part played by wearing a protection vest in the

behaviour of projectiles wounding outcomes", *Proceedings of the 11th International Symposium on Ballistics*, Vol. 3, 9th – 11th May, Brussels, Belgium, pp. 9- 18.

British Standards Institution (2004), *Principles for selecting and using test persons for testing anthropometric aspects of industrial products and designs*, BS EN ISO 15537, CEN.

Byers, M., Ryan, J. M. and Mahoney, P. F. (2005), "Guns and bullets: Part 1 - How guns work", in Mahoney, P. F., Ryan, J. M., Brooks, A. J., *et al.* (eds.) *Ballistic trauma; A practical guide*, 2nd ed, Springer, USA, pp. 31-40.

Carr, D. J., Kieser, J., Mabbott, A., Mott, C., Champion, S. and Girvan, E. (2014), "Damage to apparel layers and underlying tissue due to hand-gun bullets", *International Journal of Legal Medicine*, vol. 128, no. 1, pp. 83-93.

Carr, D. J., Lankester, C., Peare, A., Fabri, N. and Gridley, N. (2012), "Does quilting improve the fragment protective performance of body armour?", *Textile Research Journal*, vol. 82, no. 9, pp. 883-888.

Carr, D. J. and Lewis, E. A. (2014), "Ballistic protective clothing and body armour", in Wang, F. and Gao, C. (eds.) *Protective clothing - Managing thermal stress*, Woodhead publishing, UK, pp. 146-170.

Chang, K. K. (2001), "Aramid fibers", in Miracle, D. B. and Donaldson, S. L. (eds.) *ASM Handbook, Volume 21 - Composites*, ASM International, USA.

Chen, X. and Chaudhry, I. (2005), "Ballistic Protection", in Scott, R. A. (ed.) *Textiles for protection*, Woodhead Publishing Limited, Cambridge, England., pp. 529-556.

Coolidge, F. L. (2006), *Statistics - A gentle introduction*, 2nd ed, Sage Publications, USA.

Cooper, G. J. and Ryan, J. M. (1990), "Interaction of penetrating missiles with tissues: Some common misapprehensions and implications for wound management", *British Journal of Surgery*, vol. 77, no. 6, pp. 606-610.

Croft, J. and Longhurst, D. (2007a), *HOSDB Body Armour Standards for UK Police (2007) Part 1: General Requirements*, Home Office Scientific and Development Branch, St Albans, UK.

Croft, J. and Longhurst, D. (2007b), *HOSDB Body Armour Standards for UK Police (2007) Part 2: Ballistic Resistance*, Home Office Scientific and Development Branch, St Albans, UK.

Croft, J. and Longhurst, D. (2007c), *HOSDB Body Armour Standards for UK Police (2007) Part 3: Knife and Spike Resistance*, Home Office Scientific and Development Branch, St Albans, UK.

Cronin, D. S. and Falzon, C. (2009), "Dynamic characterization and simulation of ballistic gelatin", *SEM annual conference and exposition on experimental and applied mechanics*, 1st - 4th June, Albuquerque, USA, pp. 856.

- Cronin, D. S. and Falzon, C. (2011), "Characterization of 10% ballistic gelatine to evaluate temperature, aging and strain rate effects", *Experimental Mechanics*, vol. 51, no. 7, pp. 1197-1206.
- Daintith, J. and Martin, E.A., (2010), *Dictionary of Science*, 6th ed., Oxford University Press.
- DeMuth, W. E. (1966), "Bullet velocity and design as determinants of wounding capability: An experimental study", *The Journal of Trauma*, vol. 6, no. 2, pp. 222-232.
- DeMuth, W. E. (1968), "High velocity bullet wounds of the thorax", *American Journal of Surgery*, vol. 115, no. 5, pp. 616-625.
- DeMuth, W. E. (1969), "Bullet velocity as applied to military rifle wounding capacity", *Journal of Trauma*, vol. 9, no. 1, pp. 27-38.
- Di Maio, V. J. M. (1999), *Gunshot wounds – Practical aspects of firearms, ballistics, and forensic techniques*, 2nd ed, CRC Press, Boca Raton.
- Dodd, M. J. (2006), *Terminal ballistics - A text and atlas of gunshot wounds*, CRC Press, Boca Raton.
- DSM (2012), *Dyneema - With you when it matters*, available at: <http://www.dyneema.com/emea/applications/life-protection/personal-protection.aspx> (accessed October, 2012).
- Dunstan, S. (1984), *Flak jackets: 20th Century military body armour*, Osprey, London, United Kingdom.
- DuPont (2012), *History of DuPont and the government*, available at: http://www2.dupont.com/Government/en_US/gsa_contracts/Government_Projects.html (accessed October 2012).
- Eisler, R. D., Chatterjee, A. K., Burghart, G. H. and O'Keefe, J. A. (2001), *Casualty assessments of penetrating wounds from ballistic trauma*, Technical report NATICK/TR-01/011, Mission Research Corporation, Costa Mesa CA.
- Fackler, M. C. (1996a), "A review of: Wound ballistics and the scientific background", *Journal of Forensic Sciences*, vol. 41, no. 2, pp. 327-328.
- Fackler, M. L. (1987), *What's wrong with the wound ballistics literature, and why*, 239, Letterman Army Institute of Research, Presidio of San Francisco, California.
- Fackler, M. L. (1989), "Effects of small arms on the human body", *Proceedings of the 11th International symposium on Ballistics*, Vol. 3, 9th - 11th May, Brussels, Belgium, pp. 1-7.
- Fackler, M. L. (1996b), "Gunshot wound review", *Annals of Emergency Medicine*, vol. 28, no. 2, pp. 194-203.

Fackler, M. L., Bellamy, R. F. and Malinowski, J. A. (1988), "The wound profile: Illustration of the missile-tissue interaction", *The Journal of Trauma*, vol. 28, no. 1 Supplement, pp. s21-s29.

Fackler, M. L. and Kneubuehl, B. P. (1990), "Applied wound ballistics: What's new and what's true", *Journal of Trauma (China)*, vol. 6, no. 2, pp. 32-37.

Fackler, M. L. and Malinowski, J. A. (1985), "The wound profile: A visual method for quantifying gunshot wound components", *Journal of Trauma*, vol. 25, no. 6, pp. 522-529.

Fackler, M. L. and Malinowski, J. A. (1988), "Ordnance gelatine for ballistic studies - detrimental effect of excess heat used in gelatine preparation", *The American Journal of Forensic Medicine and Pathology*, vol. 3, no. 3, pp. 218-219.

Fackler, M. L. and Peters, C. E. (1991), "The "shock wave" myth (and comment)", *Wound Ballistics Review*, vol. 1, pp. 38-40.

Fackler, M. L., Surinchak, J. S., Malinowski, J. A. and Bowen, R. E. (1984a), "Bullet fragmentation: A major cause of tissue disruption", *The Journal of Trauma*, vol. 24, no. 1, pp. 35-39.

Fackler, M. L., Surinchak, J. S., Malinowski, J. A. and Bowen, R. E. (1984b), "Wounding potential of the Russian Ak-74 assault rifle", *The Journal of Trauma*, vol. 24, no. 3, pp. 263-266.

Federal Bureau of Investigation (2012), *Law enforcement officers killed and assaulted*, available at: http://www.fbi.gov/about-us/cjis/ucr/leoka/2012/officers-feloniously-killed/felonious_topic_page_-2012 (accessed 11th November, 2013).

Greenwood, J. G., Gell, P. M., Longdon, L. w., Parks, P. C., Pennelegion, L., Tanner, F. J. and Weaver, A. K. (eds.) (1987), *Textbook of ballistics and gunnery: Volume 1*, HMSO, UK.

Gryth, D., Rocksen, D., Persson, J. K. E., Arborelius, W. P., Drobin, D., Bursell, J., Olsson, L. G. and Kjellstrom, T. B. (2007), "Severe lung contusion and death after high-velocity behind-armor blunt trauma: relation to protection level", *Military Medicine*, vol. 172, no. 10, pp. 1110-1116.

Haag, M. G. and Haag, L. C. (2011), *Shooting incident reconstruction*, 2nd ed, Academic Press, Oxford.

Harraway, J. (1997), *Introductory statistical methods for biological, health and social sciences*, University of Otago Press, New Zealand.

Harvey, E. N., McMillen, J. H., Butler, E. G. and Puckett, W. O. (1962), "Mechanism of Wounding", in Coates, J. B. (ed.) *Wound ballistics*, Medical department United States Army, Washington D.C., pp. 143-235.

Heard, B. J. (2008), *Handbook of firearms and ballistics*, 2nd ed, Wiley, England.

- Hewins, K. (2010), *Behind armour blunt trauma: The development of a thoracic and abdominal simulator rig* (PhD thesis), Cranfield University, UK.
- Hiss, J. and Kahana, T. (2000), "Modern war wounds", in Mason, J. K. and Purdue, B. N. (eds.) *The Pathology of Trauma*, 3rd ed, Arnold, New York, USA, pp. 89-102.
- Ho, S. C., Song, G. and Lim, G. (2010), "Development of an innovative shape memory alloy based tool for brachytherapy", *Proceedings of the 12th International Conference on Engineering, Science, Construction, and Operations in Challenging Environments - Earth and Space 2010*, pp. 1593.
- Hoerner, S. F. (1965), *Fluid-dynamic drag*, Hoerner, S.F., USA.
- Hollerman, J. J. and Fackler, M. L. (1995), "Gunshot wounds: Radiology and wound ballistics", *Emergency radiology*, vol. 2, no. 4, pp. 171-192.
- Home Office and May, T. (29 August 2014), *Threat-level from international terrorism increased*, available at: <https://www.gov.uk/government/news/threat-level-from-international-terrorism-increased> (accessed December, 2014).
- Honeywell (2012), *Honeywell advanced fibers and composites*, available at: <http://www51.honeywell.com/sm/afc/ind-apps-details/armor.html> (accessed October, 2012).
- Hopkinson, D. A. W. and Marshall, T. K. (1967), "Firearm injuries", *British journal of Surgery*, vol. 54, no. 5, pp. 344-353.
- Hornick, R. J., Hendrick, H. W. and Paradis, P. (2008), *Human factors issues in handgun safety and forensics*, CRC Press, Florida.
- Horsely, V. (1894), "The destructive effects of small projectiles", *Nature*, vol. 50, no. 1283, pp. 104-108.
- Horsfall, I. (2000), *Stab resistant body armour* (unpublished PhD thesis), Cranfield University, UK.
- Horsfall, I. (2012), "Key issues in body armour: threats, materials and design", in Sparks, E. (ed.) *Advances in military textiles and personal equipment*, Woodhead Publishing, pp. 3-20.
- Janzon, B. (1982), "Soft soap as a tissue simulant medium for wound ballistic studies investigated by comparative firings with assault rifles AK4 and M16A1 into live, anesthetized animals", *Acta Chirurgica Scandinavica*, vol. Supplementum 508, pp. 79-88.
- Janzon, B. (1997), "Projectile-material interactions: Simulants", in Cooper, G. J., Dudley, H. A. F., Gann, D. S., *et al* (eds.) *Scientific Foundations of Trauma*, Butterworth-Heinemann, Oxford, pp. 26-36.
- Janzon, B., Hull, J. B. and Ryan, J. M. (1997), "Projectile-material interactions: soft tissue and bone ", in Cooper, G. J., Dudley, H. A. F., Gann, D. S., *et al* (eds.) *Scientific Foundations of Trauma*, Butterworth-Heinemann, Oxford, pp. 37-52.

- Jenkins, D. and Dougherty, P. (2005), "Guns and bullets: Part 2 - The effects of bullets", in Mahoney, P. F., Ryan, J. M., Brooks, A. J., *et al* (eds.) *Ballistic trauma; A practical guide*, 2nd ed, Springer, USA, pp. 40-44.
- Jussila, J. (2005a), "Measurement of kinetic energy dissipation with gelatine fissure formation with special reference to gelatine validation", *Forensic Science International*, vol. 150, no. 1, pp. 53-62.
- Jussila, J. (2005b), *Wound ballistic simulation: Assessment of the legitimacy of law enforcement firearms ammunition by means of wound ballistic simulation* (PhD thesis thesis), Second Department of Surgery, University of Helsinki, Finland.
- Jussila, J. (2004), "Preparing ballistic gelatine—review and proposal for a standard method", *Forensic science international*, vol. 141, no. 2–3, pp. 91-98.
- Kalcioglu, Z. I., Qu, M., Strawhecker, K. E., Shazly, T., Edelman, E., Vanlandingham, M. R., Smith, J. F. and Van Vliet, K. J. (2011), "Dynamic impact indentation of hydrated biological tissues and tissue surrogate gels", *Philosophical Magazine*, vol. 91, no. 7-9, pp. 1339-1355.
- Kieser, D. C., Carr, D. J., Leclair, S. C. J., Horsfall, I., Theis, J. C. and Swain, M. V. (2013), "Gunshot induced indirect femoral fracture: Mechanism of injury and fracture morphology", *Journal of the Royal Army Medical Corps*, vol. 0, pp. 1-6.
- Kneubuehl, B. P. (2011), *Wound ballistics: Basics and applications*, Springer, Berlin.
- Kneubuehl, B. P., Coupland, R. M., Rothschild, M. A. and Thali, M. J. (2011), *Wound ballistics - Basics and applications*, Springer, New York.
- Knudsen, P. J. T. and Sørensen, O. H. (1997), "The destabilising effect of body armour on military rifle bullets", *International Journal of Legal Medicine*, vol. 110, no. 2, pp. 82-87.
- Knudsen, P. J. T. and Vignaes, J. S. (1995), "Terminal ballistics of 7.62mm NATO bullets: experiments in ordnance gelatine", *International Journal of Legal Medicine*, vol. 108, no. 2, pp. 62-67.
- Korać, Z., Kelenc, D., Baškot, A., Mikulić, D. and Hancević, J. (2001a), "Substitute ellipse of the permanent cavity in gelatin blocks and debridement of gunshot wounds", *Military Medicine*, vol. 166, no. 8, pp. 689-694.
- Korać, Z., Kelenc, D., Mikulić, D., Vuković, D. and Hancević, J. (2001b), "Terminal ballistics of the Russian AK 74 assault rifle: Two wounded patients and experimental findings", *Military Medicine*, vol. 166, no. 12, pp. 1065-1068.
- Kosashvili, Y., Hiss, J., Davidovic, N., Lin, G., Kalmovic, B., Melamed, E., Levy, Y. and Blumenfeld, A. (2005), "Influence of personal armor on distribution of entry wounds: lessons learned from urban-setting warfare fatalities", *Journal of Trauma*, vol. 58, no. 6, pp. 1236-1240.
- Krauss, M. (1957), "Studies in wound ballistics: Temporary cavity effects in soft tissues", *Military Medicine*, vol. 121, no. 4, pp. 221-231.

Kurtz, S. M. (2009), *UHMWPE Biomaterials Handbook - Ultra-High Molecular Weight Polyethylene in Total Joint Replacement and Medical Devices*, 2nd ed, Elsevier, USA.

Laing, R. M., Holland, E. J., Wilson, C. A. and Niven, B. E. (1999), "Development of sizing for protective clothing for the adult male", *Ergonomics*, vol. 42, pp. 1249-1257.

Lanthier, J.M. (2003), *The effects of soft textile body armour on the wound ballistics of high velocity military bullets* (unpublished MSc), Royal Military College of Science, Shrivenham, UK.

Lanthier, J. M., Iremonger, M. J., Lewis, E. A., Horsfall, I. and Gotts, P. L. (2004), "Is the wounding potential of high velocity military bullets increased after perforation of textile body armour", *Proceedings of the Personal Armour Systems Symposium*, 6th-10th September, The Hague, Netherlands, The International Personal Armour Committee, pp. 225-232.

Lewis, R. H., Clark, M. A. and O'Connell, K. J. (1982), "Preparation of gelatine blocks containing tissue samples for use in ballistic research", *The American Journal of Forensic Medicine and Pathology*, vol. 3, no. 2, pp. 181-184.

Linden, M. A., Manton, W. I., Stewart, R. M., Thal, E. R. and Feit, H. (1982), "Lead poisoning from retained bullets", *Annals of Surgery*, vol. 204, pp. 594-599.

Lindsey, D. (1980), "The idolatry of velocity, or lies, damn lies, and ballistics", *The Journal of Trauma*, vol. 20, no. 12, pp. 1068-1069.

Mabbott, A., Carr, D. J., Caldwell, E., Miller, D. and Teagle, M. (2014), "Bony debris ingress into the lungs due to gunshot", *28th International Symposium on Ballistics*, 22nd-26th September, Atlanta, USA, .

Mabbott, A., Carr, D. J., Champion, S., Malbon, C. and Tichler, C. (2013), "Comparison of 10% gelatine, 20% gelatine and Perma-Gel™ for ballistic testing", *27th International Symposium on Ballistics*, 22nd-26th April, Freiburg, Germany, pp. 648-654.

MacPherson, D. (2005), *Bullet penetration - Modelling the dynamics and incapacitation resulting from wound trauma*, 2nd ed, Ballistic Publications, United States of America.

Magat, E. E. (1980), "Fibres from extended chain aromatic polyamides", *Philosophical Transactions of the Royal Society of London, Series A, Mathematical and Physical Sciences*, vol. 294, no. 1411, pp. 463-472.

Marshall, T. C. (2012), *Most 'green-on-blue' attacks individually motivated*, available at: <http://www.defense.gov/News/NewsArticle.aspx?ID=116307> (accessed November, 2013).

Martin, E. A. (ed.) (1996), *Oxford concise colour medical dictionary*, Oxford University Press, UK.

Mauzac, O., Paquier, C., Debord, E., Barbillon, F., Mabire, P. and Jacquet, J. F. (2010), "A substitute of gelatine for the measurement of the dynamic back face deformation", *Proceedings of the Personal Armour Systems Symposium*, 13th-17th September, Quebec, Canada, The International Personal Armour Committee, pp. 99-108.

May, H. J. (2010), *The comparison of simulated wound ballistics using ballistic gelatine and Perma-Gel as simulated soft tissue* (unpublished Bsc thesis), Kingston University London, UK.

McCoy, R. L. (2012), *Modern exterior ballistics - The launch and flight dynamics of symmetric projectiles*, 2nd ed, Schiffer, Surrey, England.

Mellor, S. G., Easmon, C. S. F. and Sanford, J. P. (1997), "Wound contamination and antibiotics", in Ryan, J. M., Rich, N. M., Dale, R. F., *et al.* (eds.) *Ballistic trauma - Clinical relevance in peace and war*, Arnold, pp. 61-71.

Missliwetz, J., Denk, W. and Wieser, I. (1995), "Study on the wound ballistics of fragmentation protective vests following penetration by handgun and assault rifle bullets", *Journal of Forensic Sciences*, vol. 40, no. 4, pp. 582-584.

Morris, C. G. (1992), *Dictionary of Science and Technology*, 1st ed, Academic Press Limited, London, UK.

Moss, G. M. (1997), "Projectiles: Types and Aerodynamics", in Cooper, G. J., Dudley, H. A. F., Gann, D. S., *et al.* (eds.) *Scientific foundations of trauma*, Butterworth-Heinemann, pp. 12-25.

Moy, P., Foster, M., Gunnarsson, C. A. and Weerasooriya, T. (2011), "Loading rate effect on tensile failure behaviour of gelatins under mode I", *Conference Proceedings of the Society for Experimental Mechanics Series*, Vol. 1, June 7-10, Indianapolis, Indiana USA, SpringerLink, pp. 15.

Neades, D. N. and Prather, R. N. (1991), *The modelling and application of small arms wound ballistics*, BRL-MR-3929, Army Ballistic Research Laboratory, Aberdeen Proving Ground, MD.

Ness, L. S. and Williams, A. G. (2013), *IHS Jane's weapons - Ammunition 2013-2014*, Polestar Wheatons, UK.

Nicholas, N. C. and Welsch, J. R. (2004), *Ballistic gelatin*, Institute for non-lethal defence technologies, The Pennsylvania state University.

NRA (1970), *Firearms and ammunition - Fact book*, National Rifle Association, Washington DC, USA.

O'Connell, K. J., Frazier, H. A., Clark, M. A., Christenson, P. J., Keyes, B. T. and Josselson, A. (1988), "The shielding capacity of the standard military flak jacket against ballistic injury to the kidney", *Journal of Forensic Sciences*, vol. 33, no. 2, pp. 410-417.

Office for National Statistics (2015), *Crime Statistics, Focus on Violent Crime and Sexual Offences, 2013/14: Chapter 3: Violent Crime and Sexual Offences - Weapons*, UK Statistics Authority, London.

Osorio, F. A., Bilbao, E., Bustos, R. and Alvarez, F. (2007), "Effects of concentration, bloom degree, and pH on gelatin melting and gelling temperatures using small amplitude oscillatory rheology", *International Journal of Food Properties*, vol. 10, no. 4, pp. 841-851.

Payne, L. D. (1997), "Wound ballistics research before 1945", in Cooper, G. J., Dudley, H. A. F., Gann, D. S., *et al.* (eds.) *Scientific foundations of trauma*, Butterworth-Heinemann, Oxford, UK, pp. 3-11.

Pearsall, J. (ed.) (1999), *Concise Oxford English dictionary*, 10th ed, Oxford University Press, UK.

Pervin, F. and Chen, W. W. (2011), "Mechanically similar gel simulants for brain tissues", *Conference Proceedings of the Society for Experimental Mechanics Series*, Vol. 1, pp. 9.

Pheasant, S. (1988), *Bodyspace - Anthropometry, ergonomics and design*, Taylor and Francis, London.

Pinto, R., Carr, D. J., Helliker, M., Girvan, L. and Gridley, N. (2012), "Degradation of Military Body Armour due to Wear: Laboratory Testing", *Textile Research Journal*, vol. 82, no. 11, pp. 1157-1163.

Prat, N., Rongieras, F., Sarron, J. C., Miras, A. and Voiglio, E. (2012), "Contemporary body armor: technical data, injuries, and limits", *European Journal of Trauma and Emergency Surgery*, vol. 38, no. 2, pp. 95-105.

Prather, R. N. (1994), "Small arms vs. soft armour – A pilot study", Gotts, P. L. and Kelly, P. M. (eds.), in: *Proceedings of the Personal Armour Systems Symposium*, 21st-25th June, Colchester, UK, pp. 137-141.

Ragsdale, B. D. and Josselson, A. (1988), "Predicting temporary cavity size from radial fissure measurements in ordnance gelatin", *Journal of Trauma*, vol. 28, no. Supplement 1, pp. S5-S9.

Rousselot (2014), *Gelatine bloom*, available at: <http://www.rousselot.com/en/rousselot-gelatine/gelatine-characteristics/definitions/gelatine-bloom/> (accessed November 2014).

Ryan, J. M., Cooper, G. J. and Maynard, R. L. (1988), "Wound ballistics: Contemporary and future research", *Journal of the Royal Army Medical Corps*, vol. 134, pp. 119-125.

Ryan, J. M., Rich, N. M., Burriss, D. G. and Ochsner, M. G. (1997), "Biophysics and pathophysiology of penetrating injury", in Ryan, J. M., Rich, N. M., Dale, R. F., *et al* (eds.) *Ballistic trauma - Clinical relevance in peace and war*, Arnold, pp. 31-46.

Rybeck, B. and Janzon, B. (1976), "Absorption of missile energy in soft tissue", *Acta Chir Scand*, vol. 142, no. 3, pp. 201-207.

Ryckman, R. A., Powell, D. A. and Lew, A. J. (2011), "Ballistic penetration of Perma-Gel", *Proceedings of the 17th American Physical Society Topical Conference on Shock Compression of Condensed Matter*, 26th June–1st July, Chicago, Illinois, American Institute of Physics, pp. 143-148.

Sakaguchi, S., Carr, D. J., Horsfall, I. and Girvan, L. (2012), "Protecting the Extremities of Military Personnel: Fragment Protective Performance of one- and two-Layer Ensembles", *Textile Research Journal*, vol. 82, no. 12, pp. 1295-1303.

Schmidt, M. J. (1979), *Understanding and using statistics - Basic concepts*, 2nd ed, D. C. Heath and Company, USA.

Schwoeble, A. J. and Exline, D. L. (2000), *Current methods in forensic gunshot residue analysis*, CRC Press, Boca Raton.

Schyma, C. and Madea, B. (2012), "Evaluation of the temporary cavity in ordnance gelatine", *Forensic Science International*, vol. 214, no. 1-3, pp. 82-87.

Schyma, C. W. A. (2010), "Colour contrast in ballistic gelatine", *Forensic Science International*, vol. 197, no. 1-3, pp. 114-118.

Sellier, K. G. and Kneubuehl, B. P. (1994), *Wound ballistics and the scientific background* Elsevier, Netherlands.

Shepherd, C. J., Appleby-Thomas, G. J., Hazell, P. J. and Allsop, D. F. (2009), "The dynamic behaviour of ballistic gelatine", *Proceedings of the American Physical Society Topical Group on Shock Compression of Condensed Matter*, 28th June – 3rd July, Nashville (Tennessee), USA, American Institute of Physics, pp. 1399-1402.

Stone, I. C. and Petty, C. S. (1991), "Interpretation of unusual wounds caused by firearms", *Journal of Forensic Sciences*, vol. 36, no. 3, pp. 736-740.

Sturdivan, L. M. (1981), *Handbook of human vulnerability criteria, chapter 2. Spheres, cubes and fragments*", ARCSL-SP-81005, U.S. Army Chemical Systems Laboratory, Aberdeen Proving Ground, MD,.

Suneson, A., Hansson, H. A. and Seeman, T. (1990), "Pressure wave injuries to the nervous system caused by high-energy missile extremity impact: Part I. Local and distant effects on the peripheral nervous system-a light and electron microscopic study on pigs", *Journal of Trauma*, vol. 30, no. 3, pp. 281-294.

Teijin Aramid (2012), *Teijin Aramid, the global leader in aramid*, available at: <http://www.teijinaramid.com/> (accessed October, 2012).

Thomson, W. A. R. (ed.) (1981), *Black's medical dictionary*, 33rd ed, A. and C. Black Publishers, London, UK.

Thoresby, F. P. and Darlow, H. M. (1967), "The mechanisms of primary infection of bullet wounds", *The British Journal of Surgery*, vol. 54, no. 5, pp. 359-361.

Tichler, C., (2012), *Email communication with A. Mabbott regarding the use of Perma-Gel™*.

Tikka, S., Cederberg, A., Levänen, J., Lötjönen, V. and Rokkanen, P. (1982), "Local effects of three standard assault rifle projectiles in live tissue", *Acta Chirurgica Scandinavica*, vol. Supplementum 508, pp. 61-72.

Tobin, L. and Iremonger, M. (2006), *Modern body armour and helmets: An introduction*, Argos Press, Canberra, Australia.

Totre, J., Ickowicz, D. and Domb, A. J. (2011), "Properties and Haemostatic Application of Gelatin", in *Biodegradable Polymers in Clinical Use and Clinical Development*, John Wiley & Sons, Inc., pp. 91-109.

UK Ministry of Defence (2005), *Proof of Ordnance, munitions, armour and explosives, Part 2: Guidance*, Defence Standard 05-101 Part 2 Issue 1, Defence Procurement, Glasgow, UK.

van Bree, J. L. M. J., Volker, A. and van der Heiden, N. (2006), "Tissue simulant response at projectile impact on flexible fabric armour", Horn, R. and Gotts, P. (eds.), in: *Proceedings of the Personal Armour Systems Symposium*, 18th-22nd September, Leeds, UK., The International Personal Armour Committee, pp. 84-93.

van Dingenen, J. L. J. (1989), "High performance Dyneema fibres in composites", *Materials and Design*, vol. 10, no. 2, pp. 101-104.

Vellema, J. and Scholtz, J. (2005), "Forensic aspects of ballistic injury", in Mahoney, P. F., Ryan, J. M., Brooks, A. J., et al (eds.) *Ballistic trauma; A practical guide*, 2nd ed, Springer, USA, pp. 91-121.

Walter, E. (2008), *Cambridge advanced learner's dictionary*, 3rd ed, Cambridge University Press, UK.

Wang, Z. G., Tang, C. G., Chen, X. Y. and Shi, T. Z. (1988), "Early pathomorphologic characteristics of the wound track caused by fragments", *Journal of Trauma*, vol. 28, no. 1 Suppl, pp. s89-95.

Watson, C. H., Horsfall, I. and Fenne, P. (2010), "Ergonomics of body armour", *Proceedings of the Personal Armour Systems Symposium*, 13th-17th September, Quebec, Canada, The International Personal Armour Committee, pp. 360-369.

White, M. (2013), *Coalition deaths by nation*, available at: <http://icasualties.org/OEF/Nationality.aspx?hndQry=UK> (accessed November, 2013).

Wilhelm, M. and Bir, C. A. (2003), "Upper torso injuries to female law enforcement personnel due to firearm assaults", *Proceedings of the NATO AVT/HFM Specialists' Meeting*, Vol. NATO Technical Report RTO-MP-AVT-097, 19-23 May, Koblenz, Germany, pp. 1-8.

Wilson, J. (1977), "Wound ballistics (Trauma rounds)", *Western Journal of Medicine*, vol. 127, pp. 49-54.

Wilson, L. B. (1921), "Dispersion of bullet energy in relation to wound effects", *The Military Surgeon*, vol. 49, no. 3, pp. 241-251.

Woodruff, C. E. (1898), "The causes of the explosive effects of modern small-calibre bullets", *The New York Medical Journal*, vol. 67, pp. 593-601.

Woosnan-Savage, R. and Hall, A. (2001), *Body armour*, 1st ed, Brassey's, Virginia.

Yang, H. H. (1993), *Kevlar aramid fiber*, Wiley, New York, USA.

APPENDIX A – Ballistic calculations

A1 – Drag coefficient

Drag coefficient is a dimensionless quantity used to describe an objects ability to overcome drag in a fluid (Morris, 1992). To calculate the C_D of a projectile, two new equations must be utilised in addition to eq. 2.7. The first equation is a kinematic formula of motion which calculates final velocity squared (m/s):

$$V_2^2 = V_1^2 + 2as. \quad \text{A.1}$$

with initial velocity (V_1) in metres per second (m/s), acceleration (a) in metres per second squared (m/s^2) and the distance travelled, s , in metres (m). Rearranging eq. A.1 to acceleration the subject:

$$a = \left| \frac{V_2^2 - V_1^2}{2s} \right|. \quad \text{A.2}$$

Putting absolute values in the rearranged formula will give the scalar value of acceleration, ensuring when used later in the process, the drag force, and thus the drag coefficient is a positive number.

The next step is to use Newton's second law:

$$F_D = Ma \quad \text{A.3}$$

where M is mass (Kg), giving the drag force, F_D in Newtons (N). After calculating the force from the mass and the acceleration using eq. A.2, eq. 2.7 can be rearranged to make the drag coefficient the subject:

$$C_D = \frac{2 F_D}{\rho V^2 A}, \quad \text{A.4}$$

A worked example using the ballistic range data presented by Ness and Williams (2013) (Table A-1) for a 9mm Luger projectile (mass 7.45 g, length 15.58mm) traveling through air (1.2 kg/m³), with the assumption that the projectiles area is a circular (eq. 2.4) is:

$$a = \left| \frac{390^2 - 396^2}{2(10)} \right|$$

$$a = |235.8|$$

$$F_D = 7.45 \times 10^{-3} \times 235.8$$

$$F_D = 1.757$$

$$C_D = \frac{2 \times 1.757}{1.2 \times (393)^2 \frac{\pi(9 \times 10^{-3})^2}{4}},$$

$$C_D = 0.298$$

Table A-1: Ballistic table of a 9mm Luger parabellum (Ness and Williams, 2013)

Range (m)	Velocity (m/s)
0	396
10	390

Using the same method for a SS109 .223 Remington projectile (mass 4 g, diameter 5.7mm, length 23.98mm) with range data from Ness and Williams (2013), the drag coefficient can be calculated to be 0.352.

Table A-2: Ballistic table of a .223 Remington SS109 (Ness and Williams, 2013)

Range (m)	Velocity (m/s)
0	975
100	852

A2 – The drag force on a cylinder

As well as calculating the drag coefficient, estimates can be used for certain shapes thanks to experimental data. The estimated coefficient of drag for a cone is 0.5 and for a cylinder between two walls is 1.17 (Hoerner, 1965).

The effect of yaw and drag can be demonstrated using a scenario of a cylinder travelling both head- and side-on through a medium. Using the drag coefficient of a cone to represent the cylinder travelling head on, and the drag coefficient of a cylinder between two walls, the following ratio can be surmised:

$$\frac{F_{D\ cyl}}{F_{D\ Cone}} = \frac{\frac{1}{2} \rho V_{Cyl}^2 A_{Cyl} C_{D\ cyl}}{\frac{1}{2} \rho V_{Cone}^2 A_{Cone} C_{D\ Cone}}, \quad A.5$$

where $V_{Cyl} = V_{Cone}$:

$$\frac{F_{D\ cyl}}{F_{D\ Cone}} = \frac{A_{Cyl} C_{D\ cyl}}{A_{Cone} C_{D\ Cone}}, \quad A.6$$

The projected area of a cylinder (rectangle):

$$A_{Cyl} = d l, \quad A.7$$

while the projected area of a cone (circle) =

$$A_{Cone} = \frac{\pi d^2}{4}. \quad \text{A.8}$$

Inputting equations A.7 and A.8 into equation A.6, gives:

$$\frac{F_{D\ Cyl}}{F_{D\ Cone}} = \frac{4\ l\ C_{D\ Cyl}}{\pi d\ C_{D\ Cone}}. \quad \text{A.9}$$

Calculating the ratio of a cylinder sideways on to a cone head on with a diameter of 9mm and a length of 40mm:

$$\frac{F_{D\ Cyl}}{F_{D\ Cone}} = \frac{4 \times 40 \times 10^{-3} (1.17)}{\pi (9 \times 10^{-3}) (0.5)}$$

$$\frac{F_{D\ Cyl}}{F_{D\ Cone}} = \frac{0.1872}{1.41 \times 10^{-2}}$$

$$\frac{F_{D\ Cyl}}{F_{D\ Cone}} = 13.25.$$

Thus, the estimated drag force of a cylinder of these dimensions traveling sideways on is 13.25 greater than when travelling head on.

Following the same method, a cylinder of diameter 9mm, length of 15mm, has an estimated drag force 4.97 greater when travelling sideways when compared to travelling head on.

References

Hoerner, S. F. (1965), *Fluid-dynamic drag*, Hoerner, S.F., USA.

Morris, C. G. (1992), *Dictionary of Science and Technology*, 1st ed, Academic Press Limited, London, UK.

Ness, L. S. and Williams, A. G. (2013), *IHS Jane's weapons - Ammunition 2013-2014*, Polestar Wheatons, UK.

APPENDIX B – Gelatine data sheet

GELITA

ANALYTICAL REPORT

GELITA GELATINE TYPE BALLISTIC 3

Photographic Grade

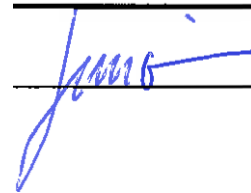
Batch No.: 07330

Size: 240KG

Customer: Home Office
Christopher Malbon
Hertfordshire, AL4 9HQ, Great Britain

Parameter Result	Test Method	Specification	Test	
Gel Strength	AOAC	255-265	265	g Bloom
Viscosity	6,67%; 60°C	3,40-4,60	4,03	mPa*s
pH	6,67%; 60°C	4,70-5,70	5,18	
Transmission 620 nm	6,67% ; 620 nm	93,00	95,61	%
Transmission 450 nm	6,67% ; 450 nm	83,00	87,01	%
Conductivity	1,00%; 30°C	300	190	J, S/cm
Moisture	16 h; 105°C	9,0-13,0	10,5	%
Total Aerob. Microb. Count	Ph. Eur./USP	< 1000	< 10	cfu / g

Eberbach, 23.03.2012



ANALYSER-1144.08.2008/ASW260/SIMON/175360/23.03.2012 11:22:51

GELITA AG-UferatraBe 7-D-6M12 Eberbach

APPENDIX C – Method for the preparation of 10% (by mass) gelatine

(32kg block)

Equipment required:

2 X 15 L buckets	Large spoon
2 X Large mixing bowls (40 L)	Silicone mould release spray
Temperature probe	Cinnamon oil
Type 3 ballistic gelatine (Gelita gelatine, photographic grade)	Arm length latex gloves
Water	8 Kettles / Urn
Mould (250mm x 300mm x 500mm)	Scales

Method

Make sure all apparatus is clean before use; especially mixing bowls and moulds. Fill up and turn on kettles / urn before starting and give adequate time for the water to get to 70°C.

1. In a well vented area apply a coating of silicone mould release spray to the mould.
2. In one of the mixing bowls weigh out 3.2 kg of gelatine powder.
3. Using the buckets weigh 14.4 kg of tap water. Ensure temperature is between 15 – 20°C. Pour water into the remaining mixing bowl.
4. Add 1/3 of the gelatine powder to the water and stir.
5. Once the gelatine has dissolved repeat step 4 a further 2 times (gelatine will swell),
6. Using the buckets weight out 14.4 kg of hot water. Ensure temperature is between 60 – 70°C.
7. Add the hot water to the gelatine solution and continue to stir. Gelatine should dissolve.
8. Two people are required to pour the gelatine solution into the mould.
9. To prevent the build-up of foam and inhibit microbial activity, add 3ml of cinnamon oil to the mixture.
10. Leave to stand for 12 hours.
11. Once left to stand, place in refrigerator (set at 4°C) and leave for 24 hours.

APPENDIX D – Method for the preparation of 20% (by mass) gelatine

(32kg block)

Equipment required:

2 X 15 L buckets	Large spoon
2 X Large mixing bowls (40 L)	Silicone mould release spray
Temperature probe	Cinnamon oil
Type 3 ballistic gelatine (Gelita gelatine, photographic grade)	Arm length latex gloves
Water	8 Kettles / Urn
Mould	Scales

Method

Make sure all apparatus is clean before use; especially mixing bowls and moulds. Fill up and turn on kettles / urn before starting and give adequate time for the water to get to 70°C.

1. In a well vented area apply a coating of silicone mould release spray to the mould.
2. In one of the mixing bowls weigh out 0.640 kg of gelatine powder.
3. Using the buckets weigh 2.56 kg of hot water. Ensure temperature is between 60 – 65°C. Pour water into the remaining mixing bowl.
4. Add the gelatine powder to the water and stir. Once gelatine is dissolved transfer the mixture into the empty mixing bowl.
5. Repeat steps 3 - 4 for a further 9 times. To prevent the build-up of foam and inhibit microbial activity add 2ml of cinnamon oil to the mixture after 5 mixtures have been completed.
6. Pour solution into the mould (two people required) and add a further 2ml of cinnamon oil to the mixture and stir.
7. Leave to stand for 12 hours.
8. Once left to stand, place in refrigerator (set at 10°C) and leave for 24 hours.

APPENDIX E – Explanation of statistical methods used.

Terms and statistical methods used in this research will be defined and explained first, before a worked example is explored in detail. The definitions below assume that a set of numerical data has been collected; this is referred to as ‘the sample’ below.

Mean - The sum of the sample, divided by the number of data points there were in the sample, n (Harraway, 1997).

The standard deviation (s.d.) – “Describes the distance on the measurement scale by which the typical group member differs from the mean” (Schmidt, 1979, p. 101). A large s.d. indicates a large range of data points, with a small s.d. meaning the data points are closer to the mean.

Coefficient of variation (CV) – The spread of the data in the sample relative to the mean. CV has no units, instead it usually expresses the s.d. as a percentage of the sample mean, allowing the variability between two data sets to be directly compared (Brase and Brase, 2011).

Analysis of Variance (ANOVA) – A group of tests for analysing data that involves separating a total sum of squares (see below) into bins associated with particular sources of variation. By comparing these bins, important sources of variation are detectable (Harraway, 1997). ANOVA can involve analysis of one factor or multiple factors.

Sum of squares (SS) – The sum of the squared deviation scores (Schmidt, 1979).

Degrees of freedom (d.f.) – A characteristic of the sample statistic that determines the appropriate sampling distribution (Schmidt, 1979).

Mean squares – Represent the mean variation resulting from different components (Harraway, 1997). They are the result of dividing the sum of squares by the degrees of freedom, and are the values which are compared when testing for significance.

F (- Test) – “A hypothesis test used in the analysis of variance. The observed statistic is a ratio made of two variances, each of which is computed from a different component of the total variation of the data” (Schmidt, 1979, p. 470).

Significance – A significant result is reported when the null hypothesis has been rejected (Coolidge, 2006).

Confidence levels / $p \leq$ – “A term used in constructing confidence-interval estimates of parameter values to specify the confidence that the interval includes the parameter value” (Schmidt, 1979, p. 473).

Tukey’s HSD multiple comparison test – A post hoc test performed after ANOVA has shown the null hypothesis has been rejected, which helps to determine the pattern of significant differences among the means. Each mean in the rejected null hypothesis is compared to every other mean (Coolidge, 2006).

Normality of data – A check to see that a sample of data is normally distributed; that is that the data set is spread so that few cases have a small amount of the dependant variable and a few cases will have a large amount of the dependant variable, while the majority will have a medium amount of the dependant variable. Approximated by a bell-shaped curve (Coolidge, 2006).

Normality of data (ANOVA) – For ANOVA, it is the residuals (the differences between each data point and its predicted mean) from the fitted model that are checked to see if they are normally distributed.

t-test (student’s test) – “A statistical examination of two population means” (Schmidt, 1979). t-tests are concerned with testing the difference between means and involve comparing a test statistic to the t distribution to determine the probability of that statistic if the study’s null hypothesis is true. There are different types of t-test, namely: one-sample t-test, two-sample t-test, repeated measures t-test and an unequal variance t-test (Boslaugh, 2012).

Welch’s t-test (Unequal variances t-test) - An adaptation of Student's t-test that can cope with two samples having unequal variances and unequal sample sizes. When the assumption that the two populations from which the samples are drawn have approximately equal variance is not met, an unequal variance t-test can be used (Boslaugh, 2012).

ANOVA

A sub-set of BB penetration data will now be analysed with each stage of the ANOVA analysis explored⁵. A two way analysis of variance will be carried out, with effect of simulant type (factor 1) on DoP and effect of velocity (factor 2) on DoP explored. For the purposes of this example, the velocity – simulant interaction is assumed to be zero.

Table E1: A sub-set of the DoP raw data collected

Velocity (m/s)	DoP in 10% gelatine (mm)	DoP in 20% gelatine (mm)	Mean DoP in both concentrations
150	101	16	58.5
150	119	18	68.5
150	123	19	71.0
150	123	25	74.0
150	155	26	90.5
500	286	77	181.5
500	296	72	184.0
500	291	79	185.0
500	298	83	190.5
500	296	88	192.0
Mean	208.8	50.3	129.55

Step 1: To start with the data from Table E1 can be split into the following components:

General level effect (common for all values)

+ velocity effect

+ simulant effect

+ experimental error (often called residual error)

Step 2: Estimates are then calculated for this effect:

The general level effect is taken as the overall mean = 129.55

The effects of velocity are the differences between the overall mean and the velocity means:

For Velocity = 150 $72.5 - 129.55 = -57.05$

For Velocity = 500 $186.6 - 129.55 = 57.05$

⁵ This data is only a sub-set of the data collected and is only being used to demonstrate the ANOVA technique. No conclusions will be drawn from the results the ANOVA produces.

The sum of these effects is equal to zero (expected, as they are deviations from their mean).

Step 3: The effects of simulant type, which also add to zero are:

$$\text{For DoP in 10\% gelatine} \quad 208.8 - 129.55 = 79.25$$

$$\text{For DoP in 20\% gelatine} \quad 50.3 - 129.55 = -79.25$$

Step 4: Estimates for the experimental error are obtained by subtracting the general level, velocity effect and simulant effect from each data value. Twenty partitions of the data values have been established, the residual values are the values used to complete the calculation:

$$101 = 129.55 - 57.05 + 79.25 - \mathbf{50.75}$$

$$119 = 129.55 - 57.05 + 79.25 - \mathbf{32.75}$$

$$123 = 129.55 - 57.05 + 79.25 - \mathbf{28.75}$$

$$123 = 129.55 - 57.05 + 79.25 - \mathbf{28.75}$$

$$155 = 129.55 - 57.05 + 79.25 + \mathbf{3.25}$$

$$286 = 129.55 + 57.05 + 79.25 + \mathbf{20.15}$$

$$296 = 129.55 + 57.05 + 79.25 + \mathbf{30.15}$$

$$291 = 129.55 + 57.05 + 79.25 + \mathbf{25.15}$$

$$298 = 129.55 + 57.05 + 79.25 + \mathbf{32.15}$$

$$296 = 129.55 + 57.05 + 79.25 + \mathbf{30.15}$$

$$16 = 129.55 - 57.05 - 79.25 + \mathbf{22.75}$$

$$18 = 129.55 - 57.05 - 79.25 + \mathbf{24.75}$$

$$19 = 129.55 - 57.05 - 79.25 + \mathbf{25.75}$$

$$25 = 129.55 - 57.05 - 79.25 + \mathbf{31.75}$$

$$26 = 129.55 - 57.05 - 79.25 + \mathbf{32.75}$$

$$77 = 129.55 + 57.05 - 79.25 - \mathbf{30.35}$$

$$72 = 129.55 + 57.05 - 79.25 - \mathbf{35.35}$$

$$79 = 129.55 + 57.05 - 79.25 - \mathbf{28.35}$$

$$83 = 129.55 + 57.05 - 79.25 - \mathbf{24.35}$$

$$88 = 129.55 + 57.05 - 79.25 - \mathbf{19.35}$$

Step 5: Separating the sum of squares is performed by:

$$\begin{aligned} \sum (\text{data values})^2 &= 101^2 + 119^2 + 123^2 \dots + 88^2 \\ &= 543387 \end{aligned}$$

$$\begin{aligned}\sum (\text{general values})^2 &= 20 (129.55)^2 \\ &= 335664.05\end{aligned}$$

$$\begin{aligned}\sum (\text{Velocity effects})^2 &= 10[(-57.05)^2 + (57.05)^2] \\ &= 65094.05\end{aligned}$$

$$\begin{aligned}\sum (\text{Simulant effects})^2 &= 10 (79.25)^2 + 10 (-79.25)^2 \\ &= 125611.25\end{aligned}$$

$$\begin{aligned}\sum (\text{Residual effects})^2 &= (-50.75)^2 + (-32.75)^2 \dots (-19.35)^2 \\ &= 17017.65\end{aligned}$$

It can be shown that:

$$\begin{aligned}\sum (\text{data values})^2 &= \sum (\text{general values})^2 \\ &+ \sum (\text{Velocity effects})^2 + \sum (\text{Simulant effects})^2 + \sum (\text{Residuals})^2 \\ 543387 &= 335664.05 + 65094.05 + 125611.25 + 17017.65\end{aligned}$$

Step 6: The degrees of freedom used to divide the sums of squares to produce the mean squares are:

- General level effect DF = 1 (since there is only one estimate for the general level effect)
- Velocity effect DF = 2 – 1 = 1 (as the velocity effects add to zero)
- Simulant effect DF = 2 – 1 = 1 (as the simulant effects add to zero)
- Residual DF = 20 – 1 – 1 – 1 = 17 (the number remaining)

Thus the mean squares are:

$$\text{Velocity effect: } 65094.05 \div 1 = 65094.05$$

$$\text{Simulant effect: } 125611.25 \div 1 = 125611.3$$

$$\text{Residual effect: } 17017.65 \div 17 = 1001.04$$

Step 7: Calculations of the F values

$$F \text{ for velocity effect} = 62094.05 \div 1001.04 = 65.02$$

$$F \text{ for simulant effect} = 125611.25 \div 1001.04 = 125.48$$

Step 8: Calculating significance is performed to see if the F statistic is large enough to indicate sample differences. This is done by comparing the observed F statistic with a critical value from an F table with a 5% level of significance. The number of d.f. for the numerator mean square (M_2) is ν_1 , while ν_2 is the number of degrees of freedom for the error mean square (M_e).

For velocity effect: $\nu_1 = 1$, and $\nu_2 = 17$, $\Pr(F_{1,17} = 4.451) = 0.05$. The F statistic (from the data) = 65.02, which is $>$ than 4.451 (from the F table), and therefore is significant at the 5% level.

For Simulant effect: $\nu_1 = 1$, and $\nu_2 = 17$, $\Pr(F_{1,17} = 4.451) = 0.05$. The F statistic (from the data) = 125.48, which is $>$ than 4.451 (from the F table), and therefore is significant at the 5% level.

From the stages above, the following analysis of variance table can be produced:

Table E2: Analysis of variance

Source of variation	SS	d.f.	Mean Square	F	Sig.	ρ
General level	335664.05	1				
Velocity effect	65094.05	1	65094.05	65.02	0.000	≤ 0.05
Simulant effect	125611.25	1	125611.25	125.48	0.000	≤ 0.05
Residual (error)	17017.65	17	1001.04			
Total	543387	20				

A typical method of describing the ANOVA results will now be presented:

Results showed that the type of tissue simulant also had a significant effect on DoP ($F_{1,17} = 125.48$, $\rho \leq 0.05$) (Table E2). This indicates that there is strong evidence that a difference between the data value means of the two velocity levels is present. This is the result of a hypothesis test; the null hypothesis (H_0) being that the two velocity means are equal, with the alternative hypothesis (H_A) that one of the velocity means is not equal to the other. A significant result indicates that there is evidence the H_0 should be rejected.

Analysis of 10% and 20% gelatine at velocity levels 150m/s and 500m/s showed that DoP varied significantly between the two velocity levels ($F_{1,17} = 65.02$, $\rho \leq 0.05$) (Table E2). This indicates that there is strong evidence that a difference between the data value means of the gelatine concentrations is present. This is the result of a hypothesis test; the null hypothesis

(H_0) being that the two gelatine concentration means are equal, with the alternative hypothesis (H_A) that one of the gelatine concentration means is not equal to the other. A significant result indicates that there is evidence the H_0 should be rejected.

Comparison of the respective F statistics for the main effects reveals the strength of the difference in the main effects. The F statistic value of 125.48 for tissue simulant is slightly larger than the F statistic for the velocity (65.02), indicating that the effect of tissue simulant is greater.

For a one way ANOVA a similar method to that presented above can be used. However, in a two way ANOVA, interactions can also be analysed; that is investigating the effect one factor has on another factor. In the above example an interaction of the effect of velocity could be investigated to see if the results varied among the tissue simulants. For example if an interaction was carried out that gave the following results⁶:

Table E3: Analysis of variance cont.

Source of variation	SS	d.f.	Mean Square	F	Sig.	$\rho \leq$
Interactions						
Simulant effect*Velocity effect	7215.00	1	7215.00	7.21	0.016	0.05

The result here shows that the effect velocity had on DoP varied between the two different tissue simulants ($F_{1,17} = 7.21, \rho \leq 0.05$). A significant interaction such as this indicates that the pattern of response for one factor differs among levels of the second factor. Comparison of the F statistic for the interaction with the F statistic for the main effects reveals the strength of the interaction. The result here of 7.21 is less than the F statistics for the main effects, meaning the effect of the interaction is weak compared to the main effects.

This analysis was conducted with reference to Harraway's (1997) textbook.

Welch's t -test

The fissure area data collected from 10 shots into both baseline and armoured blocks of 10% gelatine 500mm in length will now be analysed with each stage of the Welch's t -test explored.

⁶ The interaction has not been performed, the numbers are fictitious and are purely for demonstration purposes

Table E4: Measurements collected from baseline tests involving .223 Remington Federal Premium® Tactical® Bonded® projectiles and unprotected 10% gelatine blocks (left) and with HG2 protected 10% gelatine blocks (right)

Shot	Total fissure area (mm²)	Shot	Total fissure area (mm²)
Shot 1	11752	Shot 1	17151
Shot 2	9994	Shot 2	18575
Shot 3	11290	Shot 3	17338
Shot 4	19056	Shot 4	21108
Shot 5	20312	Shot 5	20175
Shot 6	14834	Shot 6	17887
Shot 7	21235	Shot 7	19016
Shot 8	19370	Shot 8	16366
Shot 9	16837	Shot 9	15875
Shot 10	27813	Shot 10	20312
Mean	17249.31	Mean	18380.28
s.d.	5467.04	s.d.	1764.17
CV (%)	31.69	CV (%)	9.60
Min	9994	Min	15875
Max	27813	Max	21108

A null hypothesis is set that there is no significant difference between the two data sets for fissure area. The alternative hypothesis is set that blocks with HG2 body armours present have a larger mean fissure area compared to the 10% gelatine blocks with no protection. A Welch’s test with a confidence level of 95% (0.05) is set.

Step 1: The t statistic is calculated first, using the following equation:

$$t = \frac{\bar{x}_1 - \bar{x}_2}{\sqrt{\frac{s_1^2}{n_1} + \frac{s_2^2}{n_2}}}$$

Where \bar{x}_1 and \bar{x}_2 are the sample means, s_1^2 and s_2^2 are the sample variances and n_1 and n_2 are the sample sizes. For the fissure area data, the t statistic is calculated as follows:

$$t = \frac{18380.28 - 17249.31}{\sqrt{\frac{5467.04^2}{10} + \frac{1764.17^2}{10}}}$$

$$t = 0.622576244$$

Step 2: The degrees of freedom for the Welch's test is calculated next by:

$$df = \frac{\left(\frac{s_1^2}{n_1} + \frac{s_2^2}{n_2}\right)^2}{\frac{s_1^4}{n_1^2(n_1 - 1)} + \frac{s_2^4}{n_2^2(n_2 - 1)}}$$

$$df = \frac{\left(\frac{5467.04^2}{10} + \frac{1764.17^2}{10}\right)^2}{\frac{5467.04^4}{10^2(9)} + \frac{1764.17^4}{10^2(9)}}$$

$$df = 10.85417561$$

Thus the degrees of freedom to the nearest whole number for fissure area are approximately 11.

Step 3: Using a table of critical t values, look up 11 df and a confidence level of 95% (0.05). This reveals $t_{11}(0.05) = 1.796$.

Step 4: The absolute value of the Welch t statistic (from the data) = 0.623, which is less than the critical value of 1.769 (from the t table), and therefore is not significant at the 5% level. So we accept the null hypothesis of no difference in the fissure area.

Reaching the conclusion that the result is not significant can be done using the t -tables (as above) or alternatively by comparing probabilities. SPSS uses the latter method of comparing the probabilities when running a Welch's t -test, and when reporting ANOVA output.

The probability is calculated by using the area under the curve for the sample value. For the above example: $t < -0.623$ and $t > +0.623$. That gives a probability of 0.546, which is greater than 0.05, and is not significant at the 5% level, again accepting the null hypothesis of no difference in the fissure area.

References

Brase, C. H. and Brase, C. P. (2011), *Understandable statistics: Concepts and methods*, 10th ed, Brooks Cole, Boston, USA.

Coolidge, F. L. (2006), *Statistics - A gentle introduction*, 2nd ed, Sage Publications, USA.

Harraway, J. (1997), *Introductory statistical methods for biological, health and social sciences*, University of Otago Press, New Zealand.

Schmidt, M. J. (1979), *Understanding and using statistics - Basic concepts*, 2nd ed, D. C. Heath and Company, USA.

APPENDIX F – Depth of penetration raw data

Simulant	Velocity Bin	Impact velocity (m/s)	Penetration (mm)
10% gelatine	150	124	101
10% gelatine	150	139	119
10% gelatine	150	147	123
10% gelatine	150	147	123
10% gelatine	150	153	155
10% gelatine	150	154	143
10% gelatine	150	162	137
10% gelatine	150	168	137
10% gelatine	150	175	158
10% gelatine	150	177	151
10% gelatine	150	178	142
10% gelatine	150	181	151
10% gelatine	150	185	159
10% gelatine	150	185	163
10% gelatine	250	224	185
10% gelatine	250	231	199
10% gelatine	250	236	201
10% gelatine	250	239	194
10% gelatine	250	239	192
10% gelatine	250	243	195
10% gelatine	250	256	196
10% gelatine	250	263	211
10% gelatine	250	270	231
10% gelatine	250	271	200

10% gelatine	250	271	204
10% gelatine	250	278	223
10% gelatine	250	288	231
<hr/>			
10% gelatine	500	476	292
10% gelatine	500	481	286
10% gelatine	500	499	296
10% gelatine	500	500	291
10% gelatine	500	505	298
10% gelatine	500	515	296
10% gelatine	500	518	311
10% gelatine	500	519	326
10% gelatine	500	523	314
10% gelatine	500	524	302
10% gelatine	500	534	308
10% gelatine	500	538	309
<hr/>			
10% gelatine	750	720	350
10% gelatine	750	724	359
10% gelatine	750	724	397
10% gelatine	750	733	355
10% gelatine	750	733	354
10% gelatine	750	740	373
10% gelatine	750	763	377
10% gelatine	750	771	378
10% gelatine	750	776	381
10% gelatine	750	777	372
10% gelatine	750	782	371

10% gelatine	750	790	374
<hr/>			
10% gelatine	1050	1033	414
10% gelatine	1050	1048	431
10% gelatine	1050	1048	431
10% gelatine	1050	1053	420
10% gelatine	1050	1061	440
10% gelatine	1050	1061	436
10% gelatine	1050	1061	437
10% gelatine	1050	1061	423
10% gelatine	1050	1065	423
10% gelatine	1050	1068	425
10% gelatine	1050	1075	437
10% gelatine	1050	1075	425
<hr/>			
20% gelatine	150	114	16
20% gelatine	150	114	18
20% gelatine	150	124	19
20% gelatine	150	129	25
20% gelatine	150	135	26
20% gelatine	150	142	30
20% gelatine	150	148	33
20% gelatine	150	151	34
20% gelatine	150	152	34
20% gelatine	150	157	40
20% gelatine	150	158	38
20% gelatine	150	161	37
20% gelatine	150	176	47

20% gelatine	150	178	49
20% gelatine	150	190	53
<hr/>			
20% gelatine	250	228	75
20% gelatine	250	235	77
20% gelatine	250	237	72
20% gelatine	250	241	79
20% gelatine	250	246	83
20% gelatine	250	263	88
20% gelatine	250	266	99
20% gelatine	250	269	89
20% gelatine	250	271	88
20% gelatine	250	271	90
20% gelatine	250	272	94
20% gelatine	250	273	91
20% gelatine	250	274	90
20% gelatine	250	278	96
<hr/>			
20% gelatine	500	460	171
20% gelatine	500	483	178
20% gelatine	500	483	178
20% gelatine	500	490	177
20% gelatine	500	504	183
20% gelatine	500	507	191
20% gelatine	500	510	181
20% gelatine	500	515	179
20% gelatine	500	520	194
20% gelatine	500	521	189

20% gelatine	500	522	189
20% gelatine	500	526	191
20% gelatine	500	527	186
20% gelatine	500	530	184
20% gelatine	500	533	195
<hr/>			
20% gelatine	750	710	230
20% gelatine	750	711	236
20% gelatine	750	711	234
20% gelatine	750	711	230
20% gelatine	750	718	241
20% gelatine	750	720	244
20% gelatine	750	724	233
20% gelatine	750	741	243
20% gelatine	750	743	246
20% gelatine	750	746	253
20% gelatine	750	749	249
20% gelatine	750	750	245
20% gelatine	750	757	243
20% gelatine	750	786	251
<hr/>			
20% gelatine	1050	1024	292
20% gelatine	1050	1030	307
20% gelatine	1050	1039	307
20% gelatine	1050	1046	299
20% gelatine	1050	1046	299
20% gelatine	1050	1051	306
20% gelatine	1050	1053	310

20% gelatine	1050	1053	295
20% gelatine	1050	1055	314
20% gelatine	1050	1061	307
20% gelatine	1050	1061	307
20% gelatine	1050	1075	299
<hr/>			
Perma-Gel™	150	124	48
Perma-Gel™	150	129	59
Perma-Gel™	150	134	58
Perma-Gel™	150	139	70
Perma-Gel™	150	141	71
Perma-Gel™	150	154	74
Perma-Gel™	150	155	78
Perma-Gel™	150	159	86
Perma-Gel™	150	159	84
Perma-Gel™	150	167	91
Perma-Gel™	150	169	86
Perma-Gel™	150	174	100
Perma-Gel™	150	176	92
Perma-Gel™	150	179	109
Perma-Gel™	150	181	116
<hr/>			
Perma-Gel™	250	213	133
Perma-Gel™	250	218	127
Perma-Gel™	250	223	137
Perma-Gel™	250	229	146
Perma-Gel™	250	249	161
Perma-Gel™	250	250	165

Perma-Gel™	250	253	150
Perma-Gel™	250	263	189
Perma-Gel™	250	271	167
Perma-Gel™	250	275	171
Perma-Gel™	250	277	174
Perma-Gel™	250	280	168
Perma-Gel™	250	283	176
Perma-Gel™	250	288	174
Perma-Gel™	250	289	179
<hr/>			
Perma-Gel™	500	467	306
Perma-Gel™	500	472	304
Perma-Gel™	500	482	315
Perma-Gel™	500	499	309
Perma-Gel™	500	501	310
Perma-Gel™	500	511	316
Perma-Gel™	500	519	337
Perma-Gel™	500	519	318
Perma-Gel™	500	520	323
Perma-Gel™	500	524	334
Perma-Gel™	500	531	330
Perma-Gel™	500	531	332
Perma-Gel™	500	537	333
Perma-Gel™	500	540	336
Perma-Gel™	500	540	334
<hr/>			
Perma-Gel™	750	720	411
Perma-Gel™	750	723	389

Perma-Gel™	750	724	391
Perma-Gel™	750	735	396
Perma-Gel™	750	739	412
Perma-Gel™	750	740	414
Perma-Gel™	750	740	400
Perma-Gel™	750	743	400
Perma-Gel™	750	747	401
Perma-Gel™	750	753	397
Perma-Gel™	750	755	407
Perma-Gel™	750	763	406
Perma-Gel™	750	767	408
Perma-Gel™	750	769	409
Perma-Gel™	750	777	411
<hr/>			
Re-melted Perma-Gel™	150	148	79
Re-melted Perma-Gel™	150	149	67
Re-melted Perma-Gel™	150	158	73
Re-melted Perma-Gel™	150	163	75
<hr/>			
Re-melted Perma-Gel™	250	235	158
Re-melted Perma-Gel™	250	236	171
Re-melted Perma-Gel™	250	242	182
Re-melted Perma-Gel™	250	252	168
Re-melted Perma-Gel™	250	256	193
Re-melted Perma-Gel™	250	259	181
Re-melted Perma-Gel™	250	271	185
Re-melted Perma-Gel™	250	272	203
Re-melted Perma-Gel™	250	274	193

Re-melted Perma-Gel™	250	278	203
Re-melted Perma-Gel™	500	488	335
Re-melted Perma-Gel™	500	489	331
Re-melted Perma-Gel™	500	490	336
Re-melted Perma-Gel™	500	496	336
Re-melted Perma-Gel™	500	505	326
Re-melted Perma-Gel™	500	511	323
Re-melted Perma-Gel™	500	512	361
Re-melted Perma-Gel™	500	523	349
Re-melted Perma-Gel™	500	526	342
Re-melted Perma-Gel™	500	530	343
Re-melted Perma-Gel™	500	540	353
Re-melted Perma-Gel™	750	714	400
Re-melted Perma-Gel™	750	719	403
Re-melted Perma-Gel™	750	726	414
Re-melted Perma-Gel™	750	731	414
Re-melted Perma-Gel™	750	739	418
Re-melted Perma-Gel™	750	743	418
Re-melted Perma-Gel™	750	744	400
Re-melted Perma-Gel™	750	768	408
Re-melted Perma-Gel™	750	769	421
Re-melted Perma-Gel™	750	775	426
Re-melted Perma-Gel™	750	788	413
Re-melted Perma-Gel™	1050	1020	490
Re-melted Perma-Gel™	1050	1036	499
Re-melted Perma-Gel™	1050	1050	474

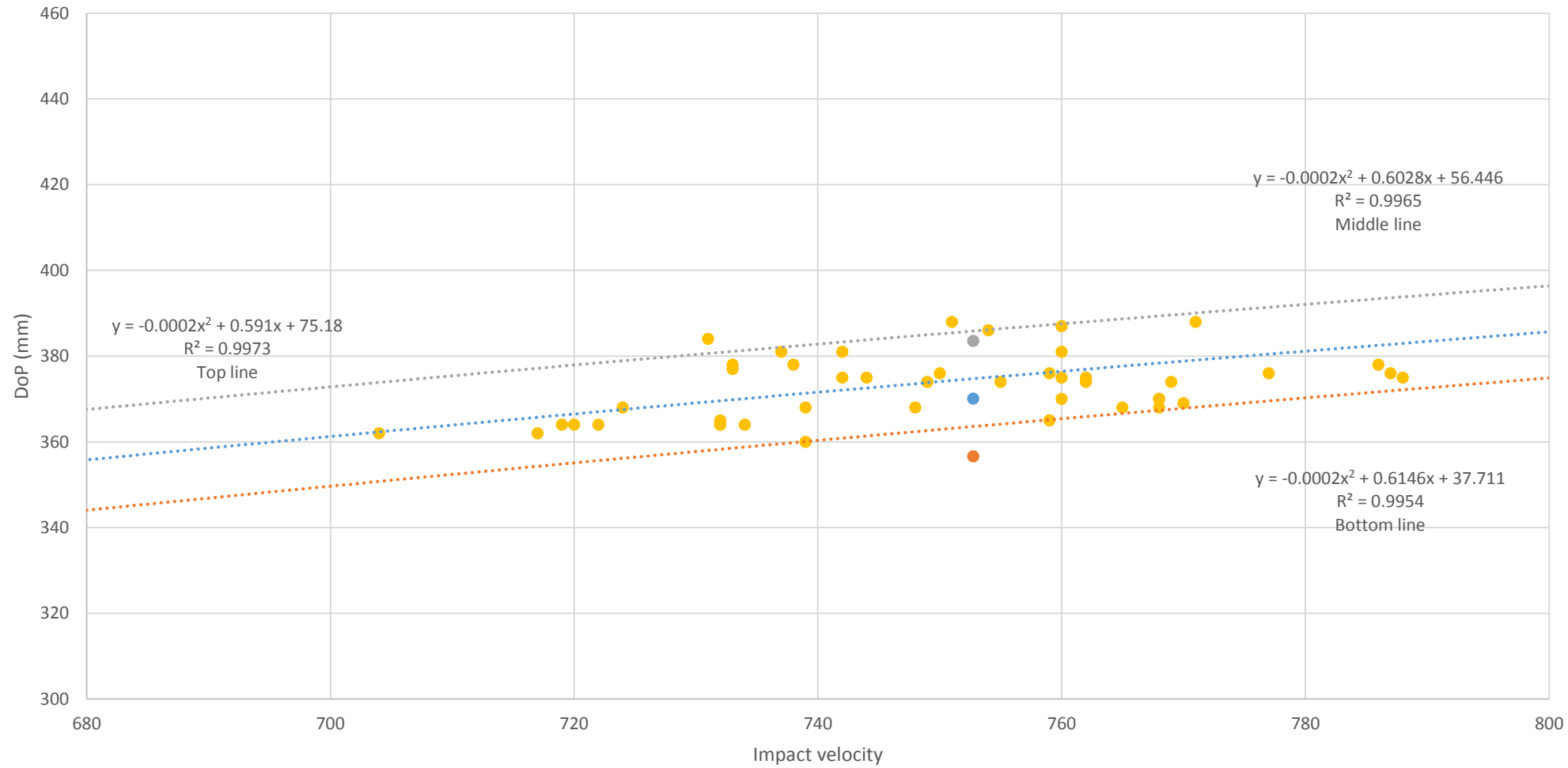
Re-melted Perma-Gel™	1050	1052	473
Re-melted Perma-Gel™	1050	1056	473
Re-melted Perma-Gel™	1050	1057	469
Re-melted Perma-Gel™	1050	1060	474

APPENDIX G – 10% gelatine quality control check

Date	Block no.	Gelatine concentration (%)	Impact velocity (m/s)	Penetration (mm)	Within s.d. (Y/N)
13th Sept 2012	Block 1	10%	744	375	Y
	Block 2	10%	724	368	Y
	Block 4	10%	731	384	N
Dec 13th 2012	Block 1	10%	733	377	Y
	Block 2	10%	742	375	Y
	Block 3	10%	704	362	Y
	Block 4	10%	734	364	Y
Jan 17th 2013	Block 1	10%	738	378	Y
	Block 2	10%	732	365	Y
	Block 3	10%	719	364	Y
18th Sept 2013	Block 5	10%	751	388	N
	Block 6	10%	742	381	Y
	Block 7	10%	737	381	Y
	Block 8	10%	733	378	Y
30th Jan 2014	Block 1	10%	749	374	Y
	Block 2	10%	732	364	Y
	Block 3	10%	739	368	Y
	Block 4	10%	760	387	Y
9th Oct 2014	Block 1	10%	720	364	Y
	Block 2	10%	754	386	Y
	Block 3	10%	760	381	Y
	Block 4	10%	759	376	Y
17th October 2014	Block 1	10%	777	376	Y
	Block 2	10%	759	365	Y
	Block 3	10%	748	368	Y
	Block 4	10%	770	369	Y
23rd Oct 2014	Block 1	10%	762	375	Y
	Block 2	10%	768	370	Y
	Block 3	10%	771	388	Y
	Block 4	10%	768	368	Y
7th Nov 2014	Block 1	10%	755	374	Y
	Block 2	10%	786	378	Y
	Block 3	10%	765	368	Y
	Block 4	10%	769	374	Y
	Block 5	10%	760	375	Y
	Block 6	10%	760	370	Y
12th Nov 2014	Block 1	10%	787	376	Y
	Block 2	10%	788	375	Y
	Block 3	10%	722	364	Y
	Block 4	10%	768	370	Y
	Block 5	10%	750	376	Y
23 rd April 2015	Block 1	10%	739	360	Y

Block 2	10%	732	364	Y
Block 3	10%	762	374	Y
Block 4	10%	717	362	Y

Calibration shots into 10% gelatine blocks

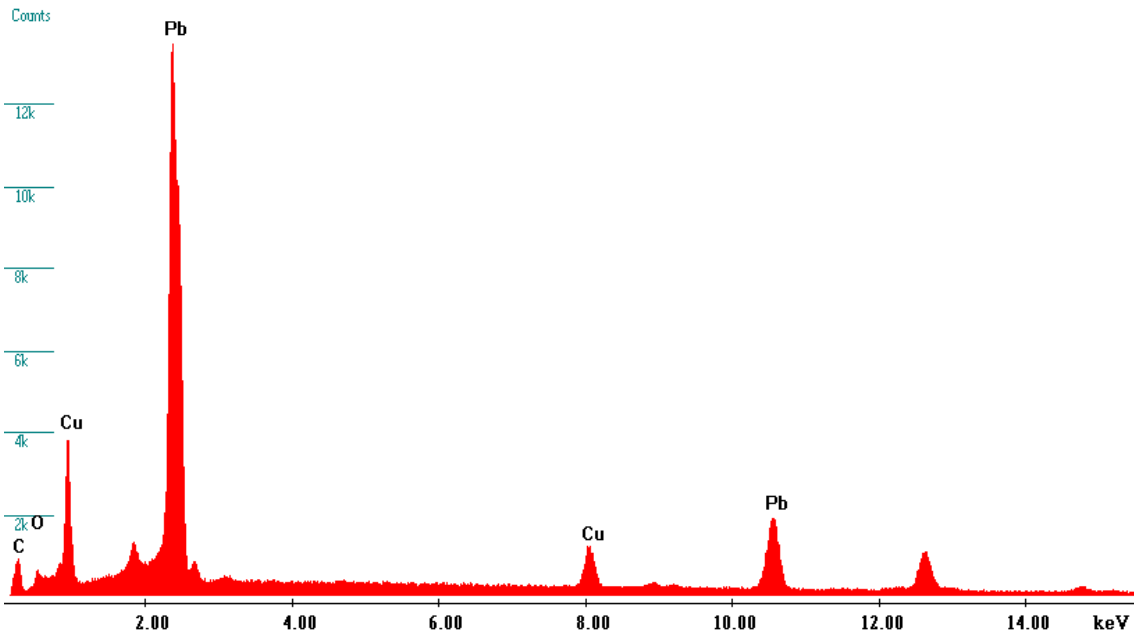


The coloured dotted lines are the mean DoP standard deviations +/- for 150, 250, 500, 750 and 1050m/s from the DoP work.

APPENDIX H – SEM spectra

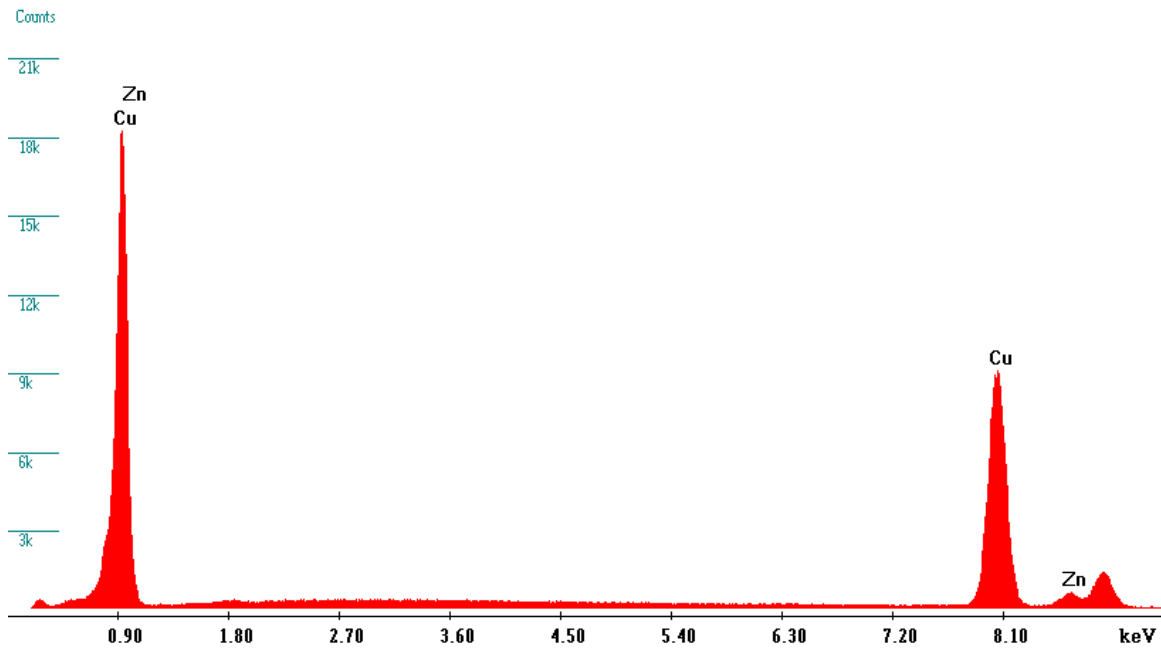
.223 Remington Federal Premium® Tactical® Bonded – Core

Label A:



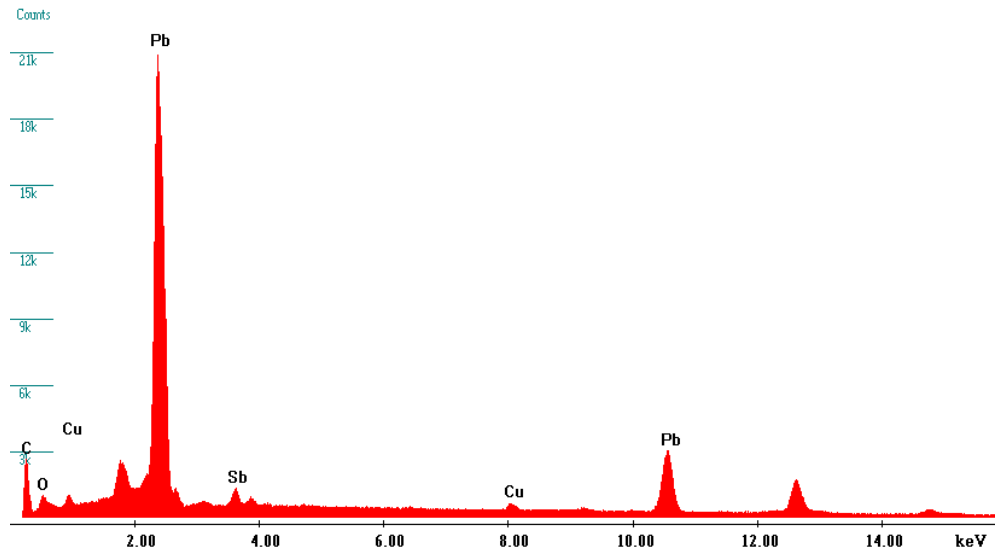
.223 Remington Federal Premium® Tactical® Bonded – Jacket

Label A:



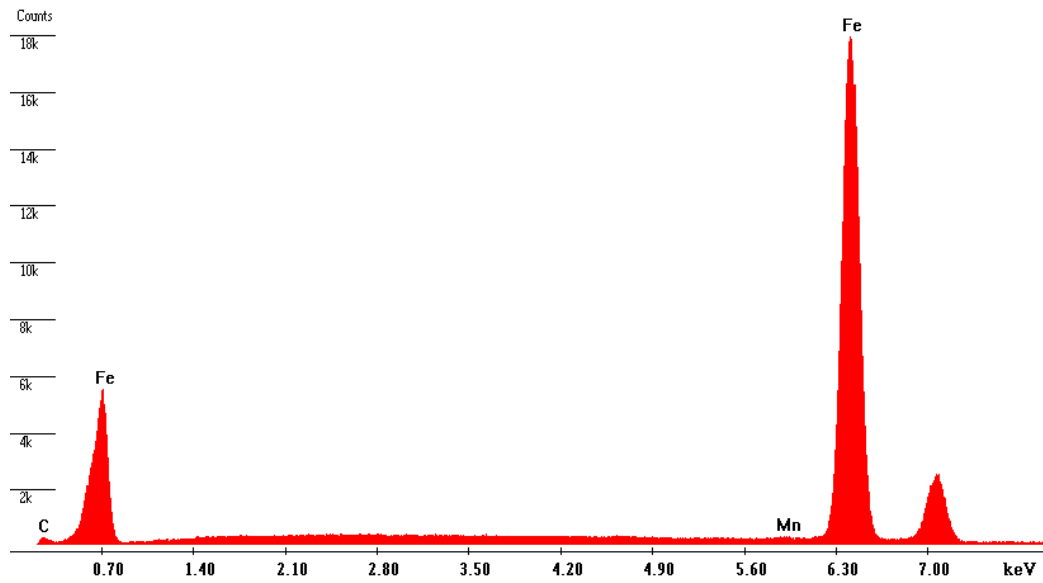
9mm Luger – core

Label A:



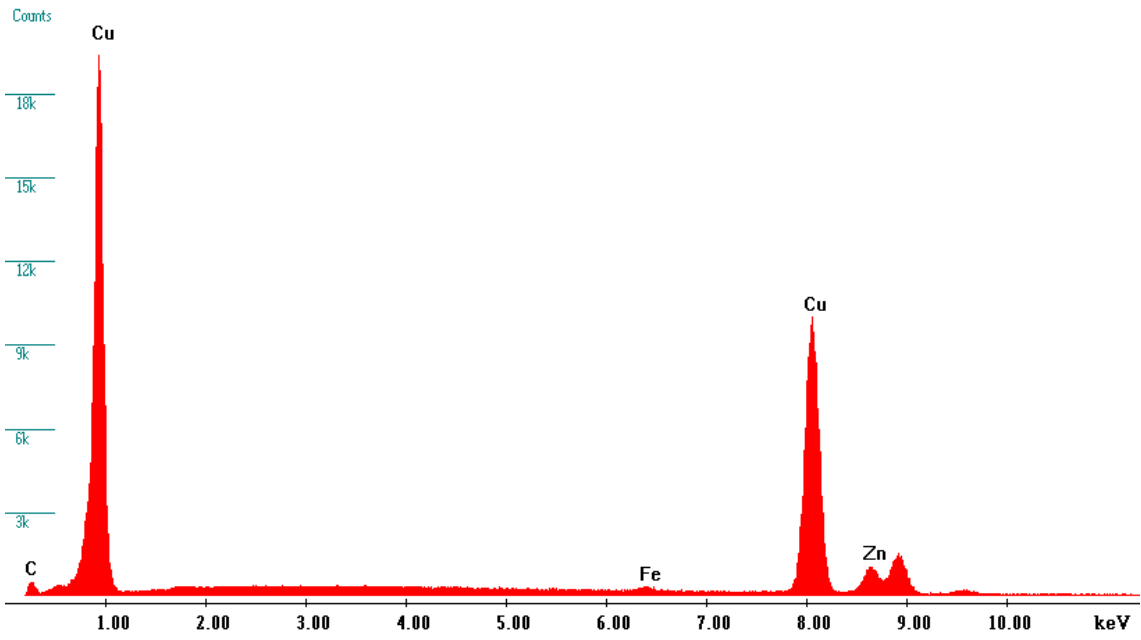
9mm Luger – Jacket

Label A:



9mm Luger – Jacket coating

Label A:



APPENDIX I – Ethics committee approval letter

Cranfield Health

Cranfield
UNIVERSITY

Vincent Building
Cranfield University
Cranfield
Bedfordshire
MK43 0AL
England
T: +44 (0)1234 758300
F: +44 (0)1234 758380
www.cranfield.ac.uk/health

25 September 2013

Wound ballistics investigations at Cranfield Defence and Security

Wound ballistics is an active research topic at Cranfield Defence and Security. Animal tissue sourced from a butcher or abattoir which is of food-grade and fit for human consumption is used during this testing. Typical examples include swine thoracic sections (skin, underlying tissue, rib) and lungs, sheep lungs and goat neck and thigh; occasionally eviscerated whole animals might be used, e.g. swine, deer.

Cranfield University Health Research Ethics Committee meets primarily to consider the use of human tissue and organs in experimental studies and also the use of animals when welfare issues are of concern. The Committee does not consider tests using animal tissue from the human food chain, such as those being proposed here, as being an ethical concern and it is therefore not necessary for ethical approval to be sought for studies of this kind.

Yours faithfully



Dr Ruth Bevan
Vice-Chair
Cranfield University Health Research Ethics Committee



APPENDIX J – Method for estimation of EKE

The estimation of EKE was calculated following the steps below:

1. Each high speed video was opened in Phantom PCC (Phantom Camera Control) 2.5.
2. Within the 'Play' tab, the 'Measurements' section was selected and calibration of each video performed by clicking 'Calibrate' and selecting two points of a known distance (e.g. a forensics scale (58mm or 109mm in total length) or a 300mm steel rule.)
3. Under the 'Axis' heading, the options to display an origin, with the coordinates in mm, were checked. Selecting the location of the origin on each video was done by locating a spot on the right hand side of the video (the side where the projectile enters the show from) before the gelatine block, below where the projectile enters the screen (Figure J-1).

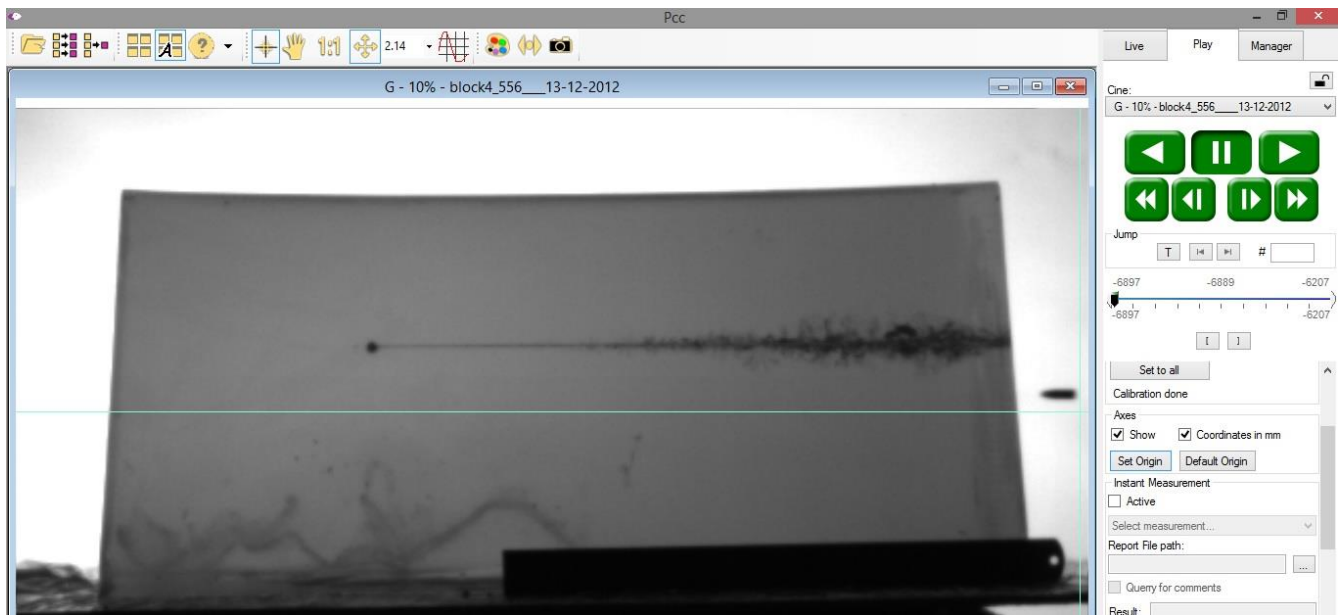


Figure J-1: Screenshot displaying the location of the axis for a video of a .223 Remington projectile.

4. Within the 'Collect Points' heading, a file path was started and opened; 1 point per frame (PPF) was inputted before the 'active' option was selected.
5. The Zoom function in PCC, as well as image tools to 'Sharpen' and adjust the sensitivity of the image were used in order to aid with the tracking of projectiles as they moved throughout respective video files. Once adjusted, the first point was selected by clicking on the projectile in flight before it entered the target (Figure J-2). Where this spot was selected on the projectile depended on the ammunition type. For videos

involving the .223 Remington Federal Premium® Tactical® Bonded® rounds, the front of the projectile was the location from which its movement was traced, as the round deformed on impact. For videos involving the 9mm Luger projectiles, the estimated location of the centre of mass was used as this projectile yaws but does not deform within gelatine blocks.

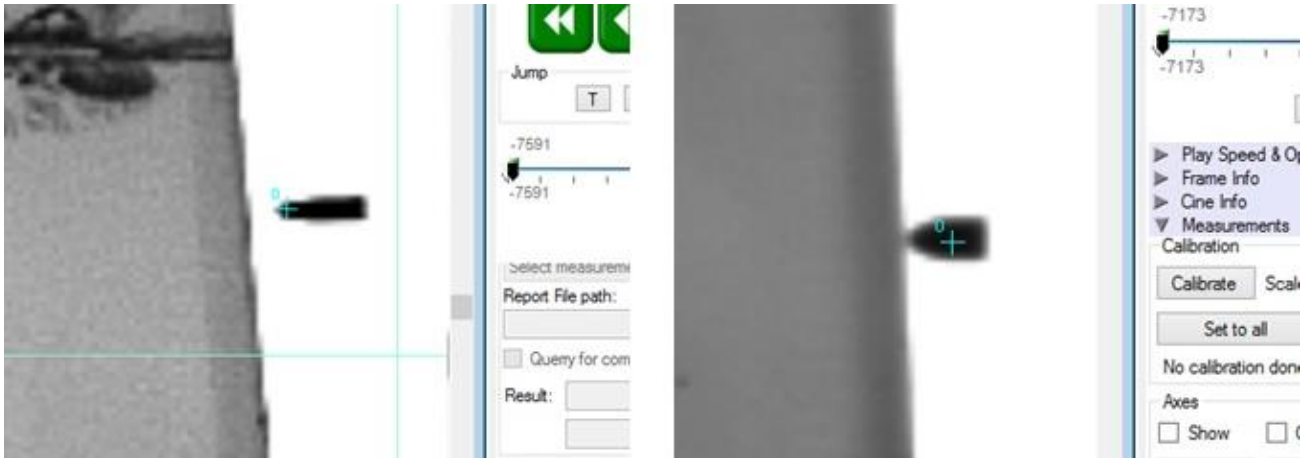


Figure J-2: (Left) the front location used to track a .223 Remington projectile and (right) the centre of mass location used to track a 9mm Luger projectile.

6. Tracking was manually continued (1 point per frame) as projectiles moved through the video. For the .223 Remington Federal Premium® Tactical® Bonded® rounds this was until the round reached the maximum depth of penetration before the first collapse of the temporary cavity, or when the rounds left the target block and/or screen. For the 9mm Luger rounds, tracking was continued until the target material was fully perforated.

7. Once the tracking of the projectile was finished, under the heading ‘Collect Points’, the save file button was used to ‘Save Points File’ which saved a document in the location previously set up in Step 4. Opening this document in Microsoft Excel opened a ‘Text Import Wizard’. ‘Delimited’ was selected on the first stage of the wizard, and by ticking the ‘Comma’ box in the second stage a spreadsheet was produced that contained four columns: frame numbers, time since the video was triggered and a column each for the x and y co-ordinates (in mm) of projectile.

8. From the inputted columns the following were calculated (Figure J-3):

- Time between points (seconds) – For a specific point, the time of the point since the video was triggered was taken and the previous cells time entry was taken away.

- Time since impact (seconds) - Starting with 0, time between points was cumulatively added for each frame.

- Distance between points (mm) – Using the x and y co-ordinates of two respective points together with Pythagoras theorem, distance between these two points in mm was calculated.
- Velocity (m/s) – The distance between points was divided by the time between those points.
- Normalised velocity – Each calculated velocity was divided by the first calculated velocity.

1	POSITION	1 D:\Users\Ale mm 508 145 1.19498										
2	ImageNr.	TimeFromTrig.	X0	Y0	Time between plots (S)	Time Since Impact (s)	normalised velocity	Distance between points (mm)	Velocity (mm/s)	Velocity (m/s)	normalised velocity	
3	-6888	-0.167893	-38.2394	9.55986		0	1					
4	-6887	-0.167868	-56.1642	10.7548	2.5E-05	2.5E-05	1	17.96458562	718583.425	718.583425	1	
5	-6886	-0.167844	-71.6989	10.7548	2.4E-05	4.9E-05	0.900771078	15.5347	647279.1667	647.2791667	0.900771078	
6	-6885	-0.16782	-87.2337	10.7548	2.4E-05	7.3E-05	0.900776877	15.5348	647283.3333	647.2833333	0.900776877	
7	-6884	-0.167795	-102.768	9.55986	2.5E-05	9.8E-05	0.867272507	15.58019121	623207.6483	623.2076483	0.867272507	
8	-6883	-0.167771	-117.108	9.55986	2.4E-05	0.000122	0.831497053	14.34	597500	597.5	0.831497053	
9	-6882	-0.167746	-131.448	9.55986	2.5E-05	0.000147	0.798237171	14.34	573600	573.6	0.798237171	
10	-6881	-0.167722	-143.398	8.36487	2.4E-05	0.000171	0.696370106	12.00960037	500400.0155	500.4000155	0.696370106	
11	-6880	-0.167698	-154.153	8.36487	2.4E-05	0.000195	0.62362279	10.755	448125	448.125	0.62362279	
12	-6879	-0.167673	-164.908	8.36487	2.5E-05	0.00022	0.598677878	10.755	430200	430.2	0.598677878	
13	-6878	-0.167649	-174.467	8.36487	2.4E-05	0.000244	0.554273384	9.559	398291.6667	398.2916667	0.554273384	
14	-6877	-0.167625	-182.832	8.36487	2.4E-05	0.000268	0.485039947	8.365	348541.6667	348.5416667	0.485039947	
15	-6876	-0.1676	-192.392	9.55986	2.5E-05	0.000293	0.536299415	9.634396769	385375.8708	385.3758708	0.536299415	
16	-6875	-0.167576	-199.562	9.55986	2.4E-05	0.000317	0.415748526	7.17	298750	298.75	0.415748526	
17	-6874	-0.167551	-207.927	9.55986	2.5E-05	0.000342	0.46563835	8.365	334600	334.6	0.46563835	
18	-6873	-0.167527	-216.292	9.55986	2.4E-05	0.000366	0.485039947	8.365	348541.6667	348.5416667	0.485039947	
19	-6872	-0.167503	-223.462	9.55986	2.4E-05	0.00039	0.415748526	7.17	298750	298.75	0.415748526	
20	-6871	-0.167478	-229.437	10.7548	2.5E-05	0.000415	0.339184921	6.093316552	243732.6621	243.7326621	0.339184921	
21	-6870	-0.167454	-236.606	10.7548	2.4E-05	0.000439	0.415690542	7.169	298708.3333	298.7083333	0.415690542	
22	-6869	-0.16743	-242.581	10.7548	2.4E-05	0.000463	0.346457105	5.975	248958.3333	248.9583333	0.346457105	
23	-6868	-0.167405	-248.556	10.7548	2.5E-05	0.000488	0.332598821	5.975	239000	239	0.332598821	

Figure J-3: Four columns produced from frame by frame analysis in PCC and the data produced from those columns.

9. The time since impact and normalised velocity columns for each shot were then inputted into Data Fit 9, which analyses and displays regression lines that fit the data. Of the regression lines produced, the equations of the best fitting polynomials were used.

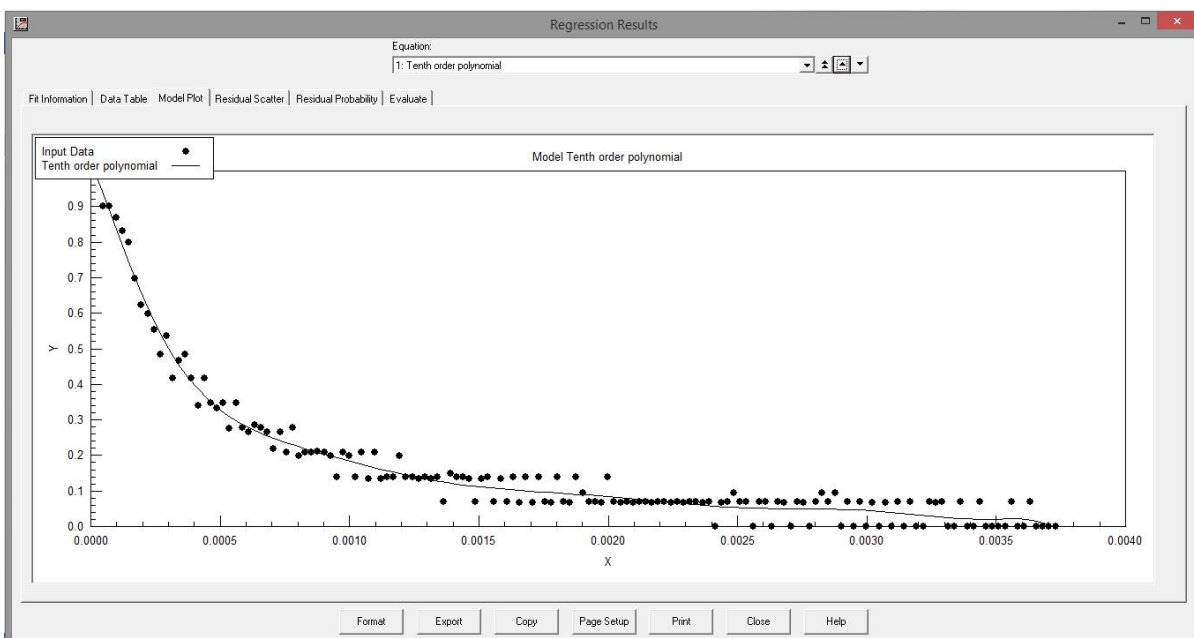


Figure J0-4: Typical example of a polynomial regression for a .223 Remington projectile that was fired into a block of 10% gelatine.

10. The numerical values from the equation of the line of the best fitting polynomial were then inputted into a Microsoft Excel spreadsheet, produced by Mr S. Champion (2015), utilising the work carried out by Sturdivan (1981) (Section 2.2.2.2 *EKE*) . The EKE value for the torso was the result of interest that was selected for each shot.

References

Champion, S. (2015), *Expected kinetic energy workbook*, unpublished data, Cranfield University, UK.
Sturdivan, L. M. (1981), *Handbook of human vulnerability criteria, chapter 2. Spheres, cubes and fragments*, ARCSL-SP-81005, U.S. Army Chemical Systems Laboratory, Aberdeen Proving Ground, MD, USA.

APPENDIX K – Publications generated from this research

Paper published in The International Journal of Legal Medicine

Comparison of porcine thorax to gelatine blocks for wound ballistics studies

A. Mabbott¹ & D. J. Carr¹ & S. Champion² & C. Malbon³

Received: 19 October 2015 / Accepted: 15 December 2015

© The Author(s) 2016. This article is published with open access at Springerlink.com

Abstract Tissue simulants are typically used in ballistic testing as substitutes for biological tissues. Many simulants have been used, with gelatine amongst the most common. While two concentrations of gelatine (10 and 20 %) have been used extensively, no agreed standard exists for the preparation of either. Comparison of ballistic damage produced in both concentrations is lacking. The damage produced in gelatine is also questioned, with regards to what it would mean for specific areas of living tissue. The aim of the work discussed in this paper was to consider how damage caused by selected pistol and rifle ammunition varied in different simulants. Damage to gelatine blocks 10 and 20 % in concentration were tested with 9 mm Luger (9 × 19 full metal jacket; FMJ) rounds, while damage produced by .223 Remington (5.56 × 45 Federal Premium® Tactical® Bonded®) rounds to porcine thorax sections (skin, underlying tissue, ribs, lungs, ribs, underlying tissue, skin; backed by a block of 10 % gelatine) were compared

to 10 and 20 % gelatine blocks. Results from the .223 Remington rifle round, which is one that typically expands on impact, revealed depths of penetration in the thorax arrangement were significantly different to 20 % gelatine, but not 10 % gelatine. The level of damage produced in the simulated thoraxes was smaller in scale to that witnessed in both gelatine concentrations, though greater debris was produced in the thoraxes.

Keywords Tissue simulants · Pistol · Rifle · 10 and 20 % gelatine

Introduction

Many tissue simulants have been and continue to be used in the study of ballistics as substitutes for biological tissues such as skin, muscles and organs, e.g. [1, 2]. Perhaps the most widely used simulants are gelatine and glycerine soap [3]. Gelatine is typically utilised in either a 10 %, e.g. [1, 2, 4–8] or 20 %, e.g. [9–11] (by mass) concentration, conditioned at 4 and 10 °C, respectively. Early studies found that using gelatine produced similar penetration depths for a range of ammunition to those observed in soft tissue, while demonstrating the mechanics of the temporary and permanent cavities that resulted from a ballistic impact [9, 12, 13]. Gelatine is translucent in nature meaning a projectile's behaviour and the exact path and placement of projectiles and/or fragments can be easily viewed and analysed [1, 7, 14, 15]. However, no agreement as to which gelatine concentration to utilise has been reached, nor a standard method for preparation [2, 16]. Work in the open source literature which uses and compares how both gelatine concentrations fare in ballistic testing is limited, e.g. [11, 12, 17]

Electronic supplementary material The online version of this article (doi:10.1007/s00414-015-1309-9) contains supplementary material, which is available to authorized users.

* D. J. Carr
d.j.carr@cranfield.ac.uk

¹ Impact and Armour Group, Centre for Defence Engineering, Cranfield University at the Defence Academy of the United Kingdom, Shrivenham SN6 8LA, UK

² Weapons and Vehicle Systems Group, Centre for Defence Engineering, Cranfield University at the Defence Academy of the United Kingdom, Shrivenham SN6 8LA, UK

³ Mechanical Engineering, Material Science and Civil Engineering, Centre for Applied Science and Technology, Home Office Science, Woodcock Hill, Sandridge, St Albans, Hertfordshire AL4 9HQ, UK

In a gunshot wound in living tissue, three zones are used to describe the areas of the wound, the central zone, caused by the direct crushing and lacerating of tissue by the projectile, surrounded by the second and third zones, contusion and concussion, respectively [18–20]. The outer two zones are believed to be the result of the temporary cavitation process, with the zone of contusion consisting of non-viable tissue, and the concussion zone showing damaged tissue capable of recovering [21]. Variables including shape, size, likelihood of fragmentation, mass, velocity and available kinetic energy of the projectile, together with the variable physical characteristics of the living target, all have an effect on the damage that is produced [20, 22–24].

Questions still remain regarding how damage recorded in tissue simulants compares to damage in living tissue and to specific areas of a human body. Although gelatine has been shown to be a close match for thigh muscle of both humans and pigs when comparing densities [2, 21, 25, 26], as well as 10 % gelatine being shown to produce depths of penetration that are within 3 % of living porcine muscle [4, 5], a typical priority area on a human target is not the thigh muscle. An area of the body that is more commonly targeted during a ballistic attack is the thorax, which is composed of many differing materials (skin, muscle, bone, heart, lungs, blood vessels, fatty deposits, nerves, etc.) and is thus very different to the composition of thigh muscle.

Breeze *et al.* [27] found significantly different depths of penetrations were produced in the thorax and abdomen of pig cadavers compared to 20 % gelatine, when testing three different fragment simulating projectiles (FSPs). The outcome was attributed to the anatomical complexity and multiple tissue interfaces of the thorax and abdominal regions.

The aim of the work discussed in this paper was to consider how damage to a tissue simulant compares to damage observed in a thorax after ballistic attack. Following previous work [28, 29], porcine thoracic walls were utilised either side of a pair of lungs to simulate a thorax, with results being compared to 10 and 20 % gelatine blocks.

Materials and methods

Materials

Gelatine from a single manufacturing batch and with a Bloom strength of 225–265 (type 3 ballistic photographic grade gelatine¹) was used to manufacture 10 and 20 % gelatine blocks. The moulds in which the gelatine blocks were manufactured measured 250 mm (w) × 250 mm (h) × 500 mm (l), with both longer sides tapered 1° to facilitate set gelatine block removal. Both gelatine concentrations

were left to set at room temperature ($\sim 18\text{ }^{\circ}\text{C} \pm 3\text{ }^{\circ}\text{C}$) for 24 h, before being placed in a refrigerator for a further 24 h; 10 % blocks at 4 °C, 20 % blocks at 10 °C prior to use.

Samples of porcine thoracic walls² (consisting of the ribs, intercostal muscles, underlying tissue and skin; vertebra and the sternum removed) and sets of porcine lung pairs complete with trachea were collected and kept refrigerated one day prior to testing. Samples were brought up to room temperature for at least 12 h before testing ($\sim 18 \pm 3\text{ }^{\circ}\text{C}$). The samples used were all of food-grade standard and fit for human consumption; consequently, there were no ethical concerns raised for this study

Two ammunition types were used for testing:

- (i) .223 Remington (5.56 × 45; 62 grain; Federal Premium® Tactical® Bonded®)
- (ii) 9 mm Luger (9 × 19 FMJ; 124 grain; DM11 A1B2) (Fig. 1)

The two types of ammunition cover both a rifle and a pistol round, both rounds are designed to interact differently with targets. The .223 Remington rifle round has an exposed tip and typically expands on impact, while the 9 mm Luger pistol round does not typically breakup or fragment, but does have a tendency to yaw within targets.

Methods—gelatine testing

All testing was performed at the Small Arms Experimental Range at Cranfield University. The targets were placed 10 m down range from the end of the muzzle. An Enfield Number 3 Proof Housing, with the appropriate barrel fitted, was used to fire each ammunition type. Ten shots with each ammunition type was carried out ($n = 10$). A new gelatine block was used for every shot with the .223 Remington ammunition, while two or three rounds of the 9 mm Luger ammunition were fired into each gelatine block, ensuring the tracts did not overlay. The impact velocities were recorded using a Weibel W-700 Doppler radar, and the impact event was recorded using a Phantom V12 high-speed video camera (41,025 fps, 5 μs exposure time and 512 × 256 frame resolution).

Prior to testing, a 5.5-mm-diameter steel BB was fired at $\sim 750\text{ m/s}$ from a distance of 10 m into the top right of each gelatine block. The velocity and depth of penetration of these shots were measured and compared with results collected from previously published depth of penetration testing to ensure only calibrated gelatine blocks were used for testing [17].

¹ Gelita UK Ltd., 3 Macclesfield Road, Cheshire CW4 7NF, UK.

² Andrews Quality Meats Ltd., 16 High Street, Highworth, Wiltshire, SN6 7AG, UK.



Fig. 1 .223 Remington (5.56 × 45; 62 grain; Federal Premium® Tactical® Bonded®) (left) and 9 mm Luger (9 × 19 FMJ; 124 grain; DM11 A1B2) (right)

Methods—porcine thorax testing

The porcine samples were arranged 10 m down range from the end of the muzzle to simulate a thorax; a porcine thoracic wall was placed as the anterior of the target (skin facing muzzle), then a set of lungs positioned in relation to the thoracic wall as they would be anatomically in a human, followed by another thoracic wall (skin facing away from muzzle) (Fig. 2). In order to ensure that a complete bullet tract was captured, a 10 % gelatine block 500 mm in length was placed adjacent to and in contact with the posterior thoracic wall. An Enfield Number 3 Proof Housing, with the appropriate barrel fitted, was used to fire each ammunition type. Each individual shot was aimed with the goal of striking: a rib within the anterior thoracic wall, either the left or right lung, and a rib in the posterior thoracic wall, before capturing the rest of the tract in a gelatine block (calibrated as above). Shots that were fired onto the same thoracic sections were located to ensure damaged areas did



Fig. 2 Typical set up showing the arrangement of the thoracic walls and lungs

not overlap. The impact velocities were recorded using a Weibel W-700 Doppler radar, and the impact event was recorded using a Phantom V12 high-speed video camera (21, 005 fps, 5 μs exposure time and 512 × 512 frame resolution). Ten shots in total were carried out (n = 7 for .223 Remington; n = 3 for 9 mm Luger).

Analysis

Gelatine blocks

Analysis of the high-speed footage was carried out using Phantom software (Vision Research, Phantom Camera Control Application 2.5) (Fig. 3). Each file was calibrated by using a known length visible in the image, converting pixels present in the image to a dimension in millimeters. Once calibrated, it was possible to take measurements that included the diameter of the temporary cavity at its largest, and the distance (from the entry point of the projectile in the gelatine block) to where this occurred. Both these measurements were taken using the PCC 2.5 software. It was also possible to locate the position and the number of times the 9 mm Luger rounds yawed within the target.

The gelatine blocks were dissected after testing by cutting along the permanent tract using a knife. Lead debris present in

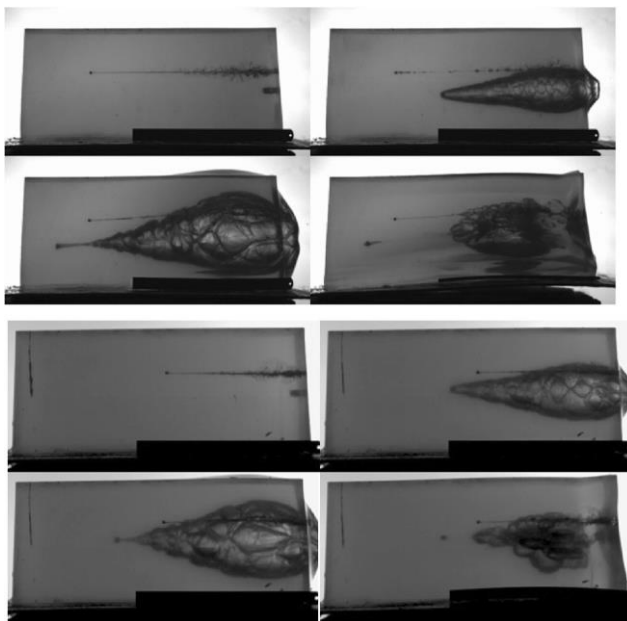


Fig. 3 High-speed stills of a typical .223 Remington impact into 10 % gelatine (top four images) and 20 % gelatine (bottom four images)

the cavities was noted, photographed,³ removed and bagged. Measurements of the permanent cavities (as indicated by damaged area / fissures) produced in the gelatine blocks were taken, specifically neck length, ‘body’ length, ‘body’ width, ‘body’ height and (when possible) distance to projectile. From the body dimensions, the formula for calculating the volume of an ellipsoid was used to calculate a representation of the maximal volume of the damage the permanent cavity created:

$$V_{\text{ellipsoid}} \approx \frac{4}{3} \pi lwh; \tag{3:1b}$$

where l, h and w are the length, width and height body dimensions, all halved. Length and height of fissures present in the gelatine blocks were also recorded. From these measurements, the area of each individual fissure was calculated using the formula for an ellipse, divided by two as a fissure was only half of an ellipse:

$$A_{\text{ellipse}} \approx \frac{\pi ab}{2}; \tag{3:2b}$$

where a and b are the respective length and height measurements of a fissure, halved. A total fissure area for each shot was calculated by adding together the areas of the individual fissures.

Summary statistics (mean (x), standard deviation (s.d.) and coefficient of variation (CV)) were calculated for the fissure and the permanent cavity data sets, as well as the data from the high-speed video analysis. Analysis of variance (ANOVA) was used to determine when significant differences between

the two gelatine concentrations occurred (SPSS Statistics

22.0). Normality of data and equality of variance were checked for each data set.

Porcine tissue

Post firing analysis of the porcine thoracic walls and lungs was performed after all shots had been completed. Measurements of the entrance and exit wounds of each shot were taken from every perforated section of each simulated thoracic cavity (i.e. the front thoracic wall, the lung and the rear thoracic wall). Any projectile and/or bone fragments found were photographed, weighed⁴ and recovered, before dissection of the samples took place. Further fragments found from exploration of the damage were also photographed, recovered and weighed.

Post firing analysis of the gelatine blocks located behind the porcine tissue consisted of cutting along the length of the permanent cavity, before measurements of the cavity were taken. When present, the projectile and any projectile and/or bone fragments were photographed, recovered and weighed.

ANOVA and Tukey analysis were used to determine if there were significant differences amongst the distance to projectile data obtained from firing .223 Remington projectiles at the porcine thoracic target arrangement, 10 % gelatine targets and 20 % gelatine targets (SPSS Statistics 22.0). Normality of data and equality of variance were checked for each data set.

Results

.223 Remington projectiles

Comparing the two gelatine concentrations revealed that the mean measurements of both the temporary and permanent cavities in 10 % gelatine were larger than those collected from cavities in 20 % gelatine blocks (Table 1). The spread of the data was also typically larger for the measurements collected from 10 % gelatine (Table 1). Metallic deposits were found within all targets, none greater than 0.5 mm in size.

Analysis of variance on the temporary cavity measurements revealed that the distance to the maximum expansion in both concentrations of gelatine was not significantly different ($F_{1, 18} = 1.12, p = NS$), though the mean distance was numerically greater in 10 % gelatine (Table 1). Conversely, the maximum expansion (diameter) reached by the temporary cavity was significantly affected by gelatine concentration ($F_{1, 18} = 144.25, p \leq 0.001$). The mean temporary cavity was larger in 10 % gelatine (mean = 178.1 mm, s.d. = 4.0 mm), when compared to the mean temporary cavity diameter in 20 % gelatine (mean = 157.6 mm, s.d. = 3.6 mm).

³ Nikon D90, Nikon DX AF-S NIKKOR 18–105 mm lens

⁴ A2204 Oxford Balance; Analytical products Ltd., Oxford, England, OX3 8ST. Developed, manufactured and tested in compliance with ISO 9001.

Table 1 Results collected from interactions between .223 Remington and (a) 10 and (b) 20 % gelatine

(a) 10 % gelatine									
Shot no.	Impact velocity (m/s)	Temporary cavity Distance to maximum expansion (mm)	Maximum diameter (mm)	Permanent cavity Neck length (mm)	Body length (mm)	Body height (mm)	Body width (mm)	Total fissure area (mm ²)	Distance to projectile (mm)
1	843	85	178	0	300	95	105	47,000	454
2	844	91	180	0	280	100	110	40,000	425
3	842	75	177	2	260	100	115	45,200	425
4	852	77	171	0	325	90	105	76,000	423
5	853	100	174	0	330	105	105	81,300	423
6	852	99	182	0	340	145	100	59,300	420
7	853	102	179	0	290	140	95	85,000	402
8	839	85	178	0	320	110	150	77,500	430
9	844	93	184	0	315	110	130	67,400	428
10	854	75	173	0	325	125	130	111,000	429
Mean	847.6	88.7	178.0	N/A	308.5	112.0	114.5	69,000	425.9
s.d.	5.7	10.3	4.0	N/A	25.3	18.7	17.1	22,000	12.7
CV (%)	0.7	11.7	2.2	N/A	8.2	16.7	14.9	31.7	3.0
Min	839	75	171	0	260	90	95	40,000	402
Max	854	102	184	2	340	145	150	111,000	454
(b) 20 % results									
Shot no.	Impact velocity (m/s)	Temporary cavity Distance to maximum expansion (mm)	Maximum diameter (mm)	Permanent cavity Neck length (mm)	Body length (mm)	Body height (mm)	Body width (mm)	Total fissure area (mm ²)	Distance to projectile (mm)
1	839	88	161	5	240	95	85	58,000	315
2	842	88	158	1	260	100	85	42,000	316
3	842	86	163	1	270	115	110	36,900	306
4	844	83	153	0	260	110	110	53,300	295
5	845	83	163	1	275	115	100	49,100	287
6	844	88	158	3	245	130	120	56,600	280
7	852	80	155	1	260	110	120	37,600	289
8	846	80	154	2	230	85	110	50,000	283
9	855	90	155	0	260	115	95	57,000	299
10	841	84	156	0	245	95	110	62,000	292
Mean	845.0	85.0	157.6	1.4	254.5	107.0	104.5	50,000	296.2
s.d.	5.0	3.5	3.6	1.6	14.0	13.2	12.8	8,800	12.7
CV (%)	0.6	4.1	2.3	112.7	5.5	12.3	12.2	17.4	4.3
Min	839	80	153	0	230	85	85	36,900	280
Max	855	90	163	5	275	130	120	62,000	316

From the permanent cavity data collected, analysis of variance could not be carried out on neck length due to there being only one measurement in 10 % gelatine. For body length, however, gelatine concentration had a significant effect ($F_{1, 18} = 34.88$, $p \leq 0.001$). The mean body length was longer in 10 % gelatine (mean = 308.5 mm, s.d. = 25.3 mm) compared to 20 % gelatine (mean = 254.5 mm,

s.d. = 14.0 mm). The representation of the maximum ellipsoid volume was significantly different in both concentrations of gelatine ($F_{1, 18} = 9.08$, $p \leq 0.01$). The mean volume was larger in 10 % compared to 20 % gelatine (10 % gelatine mean = 2,100,000 mm³, s.d. = 50,000 mm³; 20 % gelatine mean = 1,500,000 mm³, s.d. = 330,000 mm³). Concentration of gelatine also significantly affected fissure area of the permanent cavity

($F_{1, 18} = 6.36$, $p \leq 0.05$). The mean area in 20 % gelatine (mean = 50,000 mm², s.d. = 8700 mm²) was less than the mean fissure area in 10 % gelatine (mean = 69,000 mm², s.d. = 22,000 mm²).

The distance .223 Remington projectiles penetrated within the different gelatine concentrations was significantly different ($F_{1, 18} = 524.51$, $p \leq 0.001$). The mean distance in 10 % gelatine (mean = 425.9 mm, s.d. = 12.7 mm) was 129.7 mm longer than the mean distance to projectile in 20 % gelatine (mean = 296.2 mm, s.d. = 12.7 mm).

.223 Remington simulated thorax testing

Seven shots were carried out into the simulated thorax targets (Table 2). Tissue and metallic debris from all porcine samples was collected and weighed (see [electronic supplementary material](#)).

In order to compare the distances to which .223 Remington projectiles penetrated the simulated thoraxes with the distances produced in both gelatine concentrations, only the first seven shots into the respective gelatine blocks were used for ANOVA, ensuring equality of sample size. Target material had a significant effect on the distance to the projectiles travelled ($F_{2, 18} = 146.54$, $p \leq 0.001$). Tukey's HSD multiple comparison test indicated the three different target types resulted in three varying levels of distances travelled. Distance was greatest in the simulated thorax cavity arrangement (mean = 460.0 mm, s.d. = 24.5 mm); mean distance in 10 % gelatine was slightly shorter (mean = 424.6 mm, s.d. = 15.2). Mean distance in 20 % gelatine was over 160 mm shorter compared to the thoracic cavity (mean = 298.3 mm, s.d. = 14.2 mm) (Tables 1 and 2). Comparison of the respective CVs revealed that the variability of the thoracic cavity was similar to those produced in the gelatine targets.

Studying the strike location through the thoracic cavity targets revealed that shot 4, which resulted in the longest distance to the projectile, did not fully strike a lung (caught the top edge of the right middle lobe), while also exiting the posterior thoracic wall without hitting a rib (between ribs 3 and 4). Shot 1 also only nicked the top of a lung lobe (top of the right inferior lobe), while not hitting a rib squarely when entering the anterior thoracic wall (nicked rib 5). Therefore, a further ANOVA was run with these two shots removed. The remaining five shots were compared to the first five shots from the 10 and 20 % gelatine testing. For this data sub-set, mean distance to .223 Remington projectile was significantly affected by the target material ($F_{2, 12} = 135.09$, $p \leq 0.001$). Tukey's HSD multiple comparison revealed that two differing levels of distances travelled by the projectiles existed; projectiles which struck the simulated thorax and 10 % gelatine blocks in one level, and shots into 20 % gelatine blocks in the other. The longest mean distances were in the simulated thoraxes (mean = 449.4 mm, s.d. = 18.8 mm), ~ 19 mm greater in length

than shots into 10 % gelatine (mean = 430.0 mm, s.d. = 13.5 mm). Mean distance in 20 % gelatine blocks was a further 126.2 mm shorter (mean = 303.8 mm; s.d. = 12.6 mm).

9 mm Luger projectiles

The 9 mm Luger rounds perforated the gelatine blocks, regardless of concentration. The tract left by the rounds was helical in shape; there was not a 'body' of damage left. As a result, the permanent cavity damage was only assessed by measuring the fissure area that was present. The results revealed that fissure area measurements were typically greater in 10 % gelatine, with the range also larger in 10 % gelatine blocks (Table 3). No debris was found in any gelatine targets.

ANOVA identified that distance to the maximum expansion of the temporary cavity was not significantly affected by gelatine concentration ($F_{1, 18} = 0.16$, $p = \text{NS}$). The mean distance to maximum expansion was shorter in 20 % gelatine blocks (mean = 248.1 mm, s.d. = 39.9 mm), although larger variability was also witnessed in the 20 % gelatine blocks. The size of the maximum diameter of the temporary cavity was significantly affected by gelatine concentration ($F_{1, 18} = 21.94$, $p \leq 0.001$). Mean maximum diameter was smaller in blocks 20 % in concentration (mean = 83.6 mm, s.d. = 12.0); temporary cavity size was over 35 mm larger in 10 % blocks (mean = 110.0 mm, s.d. = 13.1 mm). Variability was greater in 20 % gelatine blocks.

The mean distance to where 9 mm Luger yawed to 90°, for the first and second time respectively, was not significantly affected by gelatine concentration ($F_{1, 18} = 2.29$, $p = \text{NS}$; $F_{1, 18} = 1.17$, $p = \text{NS}$). Not all shots yawed three times; five shots did in 10 % gelatine, and seven shots in 20 % gelatine. Using this sub-set of data, gelatine concentration significantly affected the mean location of where yaw for a third time occurred ($F_{1, 10} = 0.02$, $p \leq 0.05$). The mean distance to third yaw was longer in 10 % gelatine (mean = 462.7 mm, s.d. = 12.8 mm) when compared to 20 % gelatine (mean = 432.4 mm, s.d. = 25.3 mm).

ANOVA of the permanent cavity revealed that fissure area was significantly different ($F_{1, 18} = 30.15$, $p \leq 0.001$). Mean area was less in 20 % than in 10 % gelatine (20 % gelatine mean = 33,000 mm², s.d. = 4500 mm²; 10 % gelatine, mean = 49,000 mm², s.d. = 7900 mm²).

9 mm Luger simulated thorax testing

All 9 mm Luger shots perforated both the simulated thoracic cavity and the 500 mm gelatine block at the rear of the target. As a result, no analysis into the distance to the projectiles was carried out. Raw data collected from the interactions with the simulated thoracic cavities are presented in the [electronic supplementary material](#).

Table 2 Results collected from interactions between .223 Remington projectiles and simulated thoraxes

Shot no.	Impact velocity (m/s)	Entry location			Distance through thoracic samples (mm)	Distance in 10 % gelatine (mm)	Total distance (mm)
		Anterior thoracic walls	Lungs	Posterior thoracic walls			
1	852	Nicked rib 5	Right lung, nicked the top of the inferior lobe	Hit rib 3	177	299	476
2	851	Hit rib 5	Left lung, top area of the inferior lobe	Hit rib 4	177	245	422
3	847	Hit rib 7	Left lung, middle area of the superior lobe	Hit rib 7	165	295	460
4	845	Hit rib 5	Right lung, nicked the top edge of the middle lobe	Between ribs 3 and 4	165	332	497
5	840	Hit ribs 5 and 6	Right lung, top area of the inferior lobe	Hit rib 5	170	287	457
6	837	Hit rib 7	Left lung, bottom area of the superior lobe	Hit rib 6	170	269	439
7	847	Hit rib 8	Left lung, middle area of the inferior lobe	Hit rib 8	170	299	469

Discussion

Gelatine

The expansion of the .223 Remington rounds in both concentrations of gelatine produced temporary cavities that expanded beyond the diameter of the projectile on initial penetration, with no initial channel present beforehand (Fig. 3). The formation of the temporary cavities in both concentrations of gelatine followed the same pattern, supported by the result that there was no significant difference in the distance to the maximum point of temporary cavitation. Every shot was captured completely in the block (for both concentration types). The permanent cavity left in both concentrations of gelatine was reminiscent of an ellipsoid. Both the permanent and temporary cavities produced by .223 Remington projectiles were similar in shape and formation in both gelatine concentrations. However, greater damage was observed in 10 % gelatine blocks; with both significantly larger temporary cavity diameters and significantly larger permanent cavity measurements recorded when compared to 20 %. Although 20 % gelatine has a higher density (1.05 g/cm³ compared to 1.03 g/cm³) [25, 26], and materials of greater density absorb more energy and thus have a higher potential for sustaining damage [23], the elasticity and gel strength also affects the level of damage. Blocks of 20 % gelatine contained a higher concentration of gelatine and thus a greater gel strength [30, 31]. The greater

gel strength meant the blocks were better at resisting the disruptive effects of the temporary cavity. As a result, blocks of 10 % gelatine were less efficient at containing the expansion of the temporary cavity, with less gel strength also having an effect on recovery, explaining why greater permanent damage was also produced in 10 % blocks. When measurements of fissures were compared, a similar result was seen; the areas of the fissures were larger in 10 % blocks, with the range also greater. This can again be attributed to the 20 % gelatine having greater strength.

The 9 mm Luger is not designed to expand on impact; the brass-coated steel full metal jacket stops this from occurring, keeping the projectile intact as it continues through the target. This resulted in complete perforation of the 500 mm target blocks, regardless of the concentration of gelatine. The spin imparted to the individual projectiles designed to keep them stable during flight could be seen to fail during perforation of the gelatine targets, reaching 90° yaw within the 500 mm blocks between two or three times before exiting. This was not a surprising result considering the effect of density on projectile stability [20, 25]. No significant difference in the locations of where 90° yaw occurred for the first and second time corroborates with the fact that no significant difference was found between the locations where maximum temporary cavity expansion occurred and gelatine concentration. This is because the temporary cavity is usually largest when the projectile expands or yaws to 90°; greater projected area causes

greater transfer of energy to the tissues [22]. If the projectiles reached 90° yaw a third time, a significant difference in location was found between the two gelatine concentrations. A potential explanation for this is that the denser gelatine produced greater resistance on the projectiles, causing greater deceleration, which in turn led to the projectiles yawing for a third time earlier within the 20 % gelatine blocks.

Instead of an ellipsoid shape, a helical pattern was in 10 % gelatine blocks perforated by 9 mm Luger ammunition. It can be hypothesised that the helical shape was a result of the spin

Table 3 Results collected from interactions between 9 mm Luger and (a) 10 and (b) 20 % gelatine

(a) 10 % gelatine								
Shot no.	Impact velocity (m/s)	Temporary cavity Distance to maximum expansion (mm)	Maximum diameter (mm)	Yaw Number of times 90° reached	Location within block (mm)			Total fissure area (mm ²)
1	422	276	113	3	243	301	466	41,000
2	429	314	80	2	318	367	–	37,000
3	429	277	118	2	265	485	–	53,000
4	429	247	116	3	266	311	475	60,000
5	431	225	117	2	215	402	–	45,000
6	433	212	100	3	216	449	474	42,000
7	435	252	125	2	241	476	–	54,000
8	427	235	106	3	223	275	448	59,000
9	425	281	120	2	298	348	–	53,000
10	432	226	104	3	231	277	451	47,000
Mean	429.2	254.6	109.9	2.5	251.4	369.1	462.7	49,000
s.d.	3.9	31.9	13.1	0.5	35.0	80.4	12.8	8,000
CV (%)	0.9	12.5	11.9	21.1	13.9	21.8	2.7	16.2
Min	422	212	80	2	215	275	448	37,000
Max	435	314	125	3	318	485	475	60,000
(b) 20 % gelatine								
Shot no.	Impact velocity (m/s)	Temporary cavity Distance to maximum expansion (mm)	Maximum diameter (mm)	Yaw Number of times 90° reached	Location within block (mm)			Total fissure area (mm ²)
1	420	318	71	3	285	347	476	34,000
2	434	317	85	3	247	297	447	30,000
3	427	219	76	2	209	440	–	29,000
4	427	217	99	3	201	254	406	39,000
5	432	220	87	3	222	290	446	38,000
6	427	238	93	2	225	424	–	37,000
7	420	249	79	3	230	292	409	36,000
8	422	262	86	3	234	284	426	31,000
9	420	236	99	2	226	418	–	32,000
10	427	206	62	3	235	281	417	25,000
Mean	425.6	248.1	83.6	2.7	231.4	332.7	432.4	33,000
s.d.	5.0	39.9	12.1	0.5	22.9	69.5	25.3	4,500
CV (%)	1.2	16.1	14.4	17.9	9.9	20.9	5.9	13.6
Min	420	206	62	2	201	254	406	25,000
Max	434	318	99	3	285	440	476	39,000

present on the non-deformed projectile, with the larger areas of temporary cavity expansion a result of the projectiles reaching 90° yaw. As a result of the helical shape, only fissure area analysis was carried out on the permanent damage produced. However, this still revealed a similar pattern to that observed with the .223 Remington projectiles; area of damage was significantly greater in 10 % gelatine blocks compared to 20 % gelatine blocks.

The results collected clearly displayed that a difference occurred with regards to the permanent cavity size produced when the same ammunition was tested in

different concentrations of gelatine. This result, although not unexpected, does not appear to have been discussed in the open literature before. The permanent cavity left in both concentrations of gelatine was equivalent of the central zone of damage; the area damaged by the direct crushing and lacerating of tissue by both projectile types [18–20]. The calculation of the ellipsoid volume may not be an effective method for deciding the area of living tissue that should be debrided after a gunshot; that should be based on whether tissue is viable or not [21]. However, it was a consistent method for

estimating the volume that was damaged and comparing events to see where more damage was done.

Simulated torso

Porcine samples have been used previously in ballistic testing, in the form of specific sections from whole cadavers (e.g. thigh, abdomen, thorax and neck [27]; thigh [32]; as well as in similar form to the samples tested in this trial [28, 29]). Work conducted by Breeze *et al.* [32] showed that refrigerating or freezing porcine tissue followed by thawing had no effect on the level of retardation to FSPs. Although work comparing penetration depths of FSPs into 20 % gelatine and porcine tissues has been carried out [27], it is believed that the current work is the first in the open literature to compare damage produced by live rounds in a simulated thorax formed of porcine samples to both 10 and 20 % gelatine.

Comparing .223 Remington baseline shots into porcine tissue and both 10 and 20 % blocks of gelatine revealed significant differences between all three with respect to the distance to the projectile after penetration. However, when shots which failed to strike all sections of the simulat thoracic cavity and/or the ribs were removed, a significant difference was only apparent between the distances to projectiles in 20 % gelatine (in one group) and distances in both 10 % gelatine and the simulated thoracic cavity (both in the same group). The fact that the thoracic cavities had a 10 % gelatine block at the rear of the target and the measurement to the distance of the projectile included the distance travelled through this block is a point of discussion. This target design follows a similar setup used by Fackler *et al.* [4, 5], however, from which the basis of 10 % gelatine replicating the penetration depth of two projectile types to within 3 % of the penetration depth attained in living porcine leg muscle.

That two shots were removed in order for no significant difference to be present between distance to the projectiles in the simulated thorax, and the 10 % gelatine, was a result of the inhomogeneous nature of tissues which form living organisms. When bone was struck, no significant difference was observed. One of the recommended criteria for a tissue simulant is that it is homogenous, so that factors such as location of shot do not have an effect on the results.

Comment on the temporary cavitation formation in the thorax arrangements was not possible due to the porcine samples being opaque. Therefore, the measure used in this work to compare the two different concentrations of gelatine blocks and the thorax arrangement was depth of penetration, which is a widely accepted measurable criterion used in ammunition lethality studies. However, it should be noted that depth of penetration is not the only criterion considered in lethality studies. Alternatives include energy transfer. Therefore, a limitation of this study is that the energy transfer to tissue (important factor of wounding) could not be directly captured.

The permanent damage produced in the porcine specimens was smaller in scale than that produced in both gelatine blocks. Measurements of entry and exit holes in all porcine samples were the only physical measurements taken; damage in the lungs did not typically extend past the diameters of the penetrating projectiles.

The level of debris collected from the porcine specimens was far greater when compared with the gelatine targets; the presence of solid materials (bone) in the target was the cause of this; not a surprising result. It did, however, demonstrate how the debris can spread when dense materials (such as bone) are present within a target structure that is involved in a gunshot incident. The production of secondary projectiles caused after a bullet striking bone has been reported previously (e.g. [21, 24]). No exterior targets (e.g. clothing, body armour) were struck prior to entering the target, so there was limited chance of foreign debris being brought into the damaged region to cause contamination. However, Hiss and Kahana [24] state that microorganisms from perforated tissues of the target can be spread throughout a wound, causing contamination.

Conclusions

The damage produced in both concentrations of gelatine was similar in formation for both ammunition types tested, albeit with results on a smaller scaler in 20 % gelatine blocks. This is not a surprising result given the greater density and gel strength of the 20 % blocks. It is of importance, however, given that both concentrations of gelatine are used extensively as tissue simulants of the human body; which is more reminiscent of a human target? Experiments utilising porcine samples to simulate a thorax found depths of penetration to be significantly different to 20 % gelatine, but not 10 % gelatine for expanding rifle ammunition. The level of damage produced in the thoraxes was smaller in scale to the expansion witnessed in both gelatine concentrations, though greater debris was produced in the simulated thoraxes.

Acknowledgments The authors acknowledge the assistance of Mr D. Miller and Mr M. Teagle with ballistic testing. The support of EPSRC and The Home Office are also recognised.

Open Access This article is distributed under the terms of the Creative Commons Attribution 4.0 International License (<http://creativecommons.org/licenses/by/4.0/>), which permits unrestricted use, distribution, and reproduction in any medium, provided you give appropriate credit to the original author(s) and the source, provide a link to the Creative Commons license, and indicate if changes were made.

References

1. Fackler ML, Malinowski JA (1985) The wound profile: a visual method for quantifying gunshot wound components. *J Trauma* 25: 522–529
2. Jussila J (2004) Preparing ballistic gelatine—review and proposal for a standard method. *Forensic Sci Int* 141:91–98
3. Sellier KG, Kneubuehl BP (1994) *Wound ballistics and the scientific background*. Elsevier, Netherlands
4. Fackler ML, Surinchak JS, Malinowski JA, Bowen RE (1984) Bullet fragmentation: a major cause of tissue disruption. *J Trauma* 24:35–39
5. Fackler ML, Surinchak JS, Malinowski JA, Bowen RE (1984) Wounding potential of the Russian AK-74 assault rifle. *J Trauma* 24:263–266
6. Fackler ML (1987) What's wrong with the wound ballistics literature, and why. Letterman Army Institute of Research, Presidio of San Francisco, California
7. Fackler ML, Bellamy RF, Malinowski JA (1988) The wound profile: illustration of the missile-tissue interaction. *J Trauma* 28:s21–s29
8. Fackler ML, Malinowski JA (1988) Ordnance gelatine for ballistic studies - detrimental effect of excess heat used in gelatine preparation. *Am J Forensic Med Pathol* 3:218–219
9. Harvey EN, McMillen JH, Butler EG, Puckett WO (1962) Mechanism of wounding. In: Coates JB (ed) *Wound Ballistics*. Medical Department United States Army, Washington D.C., pp 143–235
10. DeMuth WE (1966) Bullet velocity and design as determinants of wounding capability: an experimental study. *Proc 11th Int Symp Ballist* 6:222–232
11. Knudsen PJT, Vignaes JS (1995) Terminal ballistics of 7.62 mm NATO bullets: experiments in ordnance gelatine. *Int J Legal Med* 108:62–67
12. Wilson LB (1921) Dispersion of bullet energy in relation to wound effects. *Mil Surg* 49:241–251
13. Krauss M (1957) Studies in wound ballistics: temporary cavity effects in soft tissues. *Mil Med* 121:221–231
14. Korać Z, Kelenc D, Baškot A *et al* (2001) Substitute ellipse of the permanent cavity in gelatin blocks and debridement of gunshot wounds. *Mil Med* 166:689–694
15. Korać Z, Kelenc D, Mikulić D *et al* (2001) Terminal ballistics of the Russian AK 74 assault rifle: two wounded patients and experimental findings. *Mil Med* 166:1065–1068
16. MacPherson D (2005) *Bullet penetration—modeling the dynamics and incapacitation resulting from wound trauma*. Ballistic Publications, United States of America
17. Mabbott A, Carr DJ, Champion S, *et al.* (2013) Comparison of 10 % gelatine, 20 % gelatine and Perma-Gel™ for ballistic testing. In: 27th Int Symp Ballistics. International Ballistics Society, Freiburg, p 648–654
18. Wang ZG, Tang CG, Chen XY, Shi TZ (1988) Early pathomorphologic characteristics of the wound track caused by fragments. *J Trauma* 28:s89–s95
19. Bowyer GW, Ryan JM, Kaufmann CR, Ochsner MG (1997) General principles of wound management. In: Ryan JM, Rich NM, Dale RF, *et al.* (eds) *Ballist trauma - Clin Relev peace war*. Arnold, New York, p 105–119
20. Ryan JM, Rich NM, Burris DG, Ochsner MG (1997) Biophysics and pathophysiology of penetrating injury. In: Ryan JM, Rich NM, Dale RF, *et al.* (eds) *Ballist trauma - Clin Relev peace war*. Arnold, New York, p 31–46
21. Janzon B, Hull JB, Ryan JM (1997) Projectile-material interactions: soft tissue and bone. In: Cooper GJ, Dudley HAF, Gann DS *et al* (eds) *Sci Found Trauma*. Butterworth-Heinemann, Oxford, pp 37–52
22. Berlin R, Gelin LE, Janzon B, *et al.* (1976) Local effects of assault rifle bullets in live tissue. Part I *Acta Chir Scand Suppl* 459:4–48
23. Belkin M (1979) Wound ballistics. *Prog Surg* 16:7–24
24. Hiss J, Kahana T (2000) Modern war wounds. In: Mason JK, Purdue BN (eds) *Pathol Trauma*. Arnold, New York, pp 89–102
25. Janzon B (1997) Projectile-material interactions: simulants. In: Cooper GJ, Dudley HAF, Gann DS *et al* (eds) *Sci Found Trauma*. Butterworth-Heinemann, Oxford, pp 26–36
26. Eisler RD, Chatterjee AK, Burghart GH, O'Keefe JA (2001) Casualty assessments of penetrating wounds from ballistic trauma. Mission Research Corporation, Costa Mesa
27. Breeze J, Hunt NC, Gibb I *et al* (2013) Experimental penetration of fragment simulating projectiles into porcine tissues compared with simulants. *J Forensic Leg Med* 20:296–299
28. Carr DJ, Kieser J, Mabbott A *et al* (2014) Damage to apparel layers and underlying tissue due to hand-gun bullets. *Int J Legal Med* 128: 83–93
29. Mabbott A, Carr DJ, Caldwell E *et al* (2014) Bony debris ingress into the lungs due to gunshot. 28th International Symp Ballist, Atlanta
30. Osorio FA, Bilbao E, Bustos R, Alvarez F (2007) Effects of concentration, bloom degree, and pH on gelatin melting and gelling temperatures using small amplitude oscillatory rheology. *Int J Food Prop* 10:841–851

31. Rousselot (2014) Gelatine bloom. <http://www.rousselot.com/en/rousselot-gelatine/gelatine-characteristics/definitions/gelatine-bloom/>
32. Breeze J, Carr DJ, Mabbott A *et al* (2015) Refrigeration and freezing of porcine tissues does not affect the retardation of fragment simulating projectiles. *J Forensic Leg Med* 32:77–83

A comparison of ballistic impacts into armoured 10% gelatine and armoured porcine samples arranged to simulate a thorax.

A. Mabbott¹, D.J. Carr¹, S. Champion², C Malbon³, D. Miller¹ and M. Teagle¹

¹ Impact and Armour Group, Centre for Defence Engineering, Cranfield Defence and Security, Cranfield University at the Defence Academy of the United Kingdom, Shrivenham, SN6 8LA, UK.

² Weapons and Vehicle Systems Group, Centre for Defence Engineering, Cranfield Defence and Security, Cranfield University at the Defence Academy of the United Kingdom, Shrivenham, SN6 8LA, UK.

³ Mechanical Engineering, Material Science and Civil Engineering, Centre for Applied Science and Technology, Home Office Science, Woodcock Hill, Sandridge, St Albans, Hertfordshire, AL4 9HQ.

Abstract: Many tissue simulants have been and continue to be used in the study of ballistics as substitutes for biological tissues such as skin, muscles and organs. Perhaps the most widely used are gelatine and glycerine soap. Early studies found that using 10% gelatine produced similar penetration depths to those observed in soft tissue, whilst demonstrating the mechanics of the temporary and permanent cavities that resulted from a ballistic impact. However, questions still remain regarding how damage recorded in tissue simulants compares to damage in living tissue and to specific areas of a human body. Although 10% gelatine has been shown to be a close match for thigh muscle of both humans and pigs when comparing densities, as well as being shown to produce depths of penetration that are within 3% of living porcine muscle, a typical priority area on a human target is not the thigh muscle. An area of the body that is more commonly targeted during a ballistic attack is the thorax, which is composed of many differing materials (skin, muscle, bone, heart, lungs, blood vessels, fatty deposits, nerves etc.) and is thus very different to the composition of thigh muscle. Along with the head, the thorax is where the majority of body armour is worn, giving protection to the heart and vital organs contained there. The aim of the work discussed in this paper was to consider how damage in 10% gelatine compared to damage observed in a simulated thorax after ballistic attack, when both target types were protected by typical UK police body armour (CAST certified; HOSDB 39/07). Targets were either formed of 10% gelatine, protected either side by armour panels, or from porcine thoracic walls (ribs, intercostal muscles, underlying tissue and skin; vertebra and the sternum were removed) which were placed either side of a 10% gelatine block, forming a thorax arrangement, which was protected on both the front and rear faces by armour panels. Ballistic impacts were carried out using .223 Remington (62 grain; Federal Premium® Tactical® Bonded®; strike velocity of 845m/s \pm 10m/s) / 9mm Luger (124 grain; DM11 A1B2; strike velocity of 420m/s \pm 10m/s). All impacts were filmed using a Phantom V12 high-speed camera. Post-firing analysis and dissection of the swine samples and gelatine blocks was carried out; depth of penetration, level of damage and presence of debris was recorded and compared for the two target types.

Mabbott, A., Carr, D.J., Champion, S., Malbon, C. and Tickler, C., (2013) Comparison of 10% gelatine, 20% gelatine and Perma-Gel™ for ballistic testing, in: *Proceedings of the 27th International Symposium on Ballistics*, 22nd – 26th April, Freiburg, Germany, pp. 648-654:

27TH INTERNATIONAL SYMPOSIUM ON BALLISTICS
FREIBURG, GERMANY, APRIL 22–26, 2013

COMPARISON OF 10% GELATINE, 20% GELATINE AND PERMA-GEL™ FOR BALLISTIC TESTING

A. Mabbott¹, D. J. Carr¹, S. Champion², C. Malbon³ and C. Tichler³

¹*Impact and Armour Group, Department of Engineering and Applied Science, Cranfield Defence and Security, Cranfield University, Defence Academy of the United Kingdom, Shrivenham, Wiltshire, SN6 8LA, U*

²*Weapons and Vehicle Systems Group, Department of Engineering and Applied Science, Cranfield Defence and Security, Cranfield University, Defence Academy of the United Kingdom, Shrivenham, Wiltshire, SN6 8LA, UK*

³*Mechanical Engineering, Material Science and Civil Engineering, Centre for Applied Science and Technology, Home Office Science, Woodcock Hill, Sandridge, St Albans, Hertfordshire, AL4 9HQ, UK*

Soft tissue simulants are used in ballistic testing as a tool for capturing the interaction projectiles have with living tissue. No internationally agreed standard exists for the preparation of such tissue simulants; a factor that has led to questions regarding reliability and reproducibility of results presented in the open literature. A calibration method for 10% gelatine has been suggested utilising low velocity projectiles [1]. However, recent work has suggested that gelatine is strain rate sensitive [2]. Therefore it may be more appropriate to test at velocities representative of the projectile under investigation.

This paper presents a modified method to assess the differences in penetration depth in three simulants. Non-deformable ball bearings (BBs) of similar diameter to ammunition of interest (5.5 mm BBs, 5.56 mm x 45 mm) at a range of velocities representative of different engagement ranges (150m/s, 250m/s, 500m/s, 750m/s and 1050m/s) were used.

INTRODUCTION

Gelatine has long been used as a simulant in terminal ballistics, albeit typically in two different concentrations by mass: 10% and 20% [3; 4]. However, an internationally agreed standard for the preparation and use of either of these types of gelatine does not exist, and although calibration methods have been proposed, many of these remain in-house, and are not available in the open literature. There is currently no known conversion method to

¹ Impact and Armour Group, Department of Engineering and Applied Science, Cranfield Defence and Security, Cranfield University, Defence Academy of the United Kingdom, Shrivenham, Wiltshire, SN6 8LA, UK.

² Weapons and Vehicle Systems Group, Department of Engineering and Applied Science, Cranfield Defence and Security, Cranfield University, Defence Academy of the United Kingdom, Shrivenham, Wiltshire, SN6 8LA, UK.

³ Mechanical Engineering, Material Science and Civil Engineering, Centre for Applied Science and Technology, Home Office Science, Woodcock Hill, Sandridge, St Albans, Hertfordshire, AL4 9HQ, UK.

confidently compare results from different concentrations of gelatine, with work in the open literature which has tested both concentrations limited e.g. [5].

Perma-Gel™ is a commercially available, clear, synthetic material which was developed specifically as a soft tissue simulant that reportedly behaves in a similar manner to 10% gelatine [6]. A further claimed advantage of Perma-Gel™ is that it can be re-melted and reused, although the number of times this can be done maintaining repeatable results is undefined. Developed in 2005, independent validation of Perma-Gel™ in the open literature appears lacking [7].

Thus the aim of work undertaken in this study was to test and record the differences between the three simulants for depth of penetration of 5.5mm diameter BBs at velocities between 150m/s and 1050m/s.

MATERIALS AND METHODS

Type 3 (265 Bloom) ballistic photographic grade gelatine¹ from the same batch was used to manufacture all 10% and 20% gelatine blocks. Two days prior to testing the blocks were made in moulds measuring 250mm (h) x 250mm (w) x 500mm (l), with both longer sides tapered 1 ° to facilitate set gelatine removal. Blocks were left to set overnight, before being transferred to a refrigerator at either 4 ° C or 10 ° C (10% and 20% gelatine respectively) for at least 24 hours before testing.

Perma-Gel™ blocks were purchased in the raw base media form; dimensions were approximately 127mm (h) x 279mm (w) x 432mm (l). These blocks were placed into a roaster oven and following the manufacturer's instructions, melted to form blocks ready for testing.

Depth of penetration (DoP) tests were conducted using 5.5mm diameter steel ball bearings (BBs). The BBs were secured into a polymeric sabot which was then fitted into a 7.62mm x 51mm cartridge before firing from an Enfield Number 3 Proof Housing. The simulant targets were placed 10 m down range from the end of the muzzle. Multiple firings were conducted at both faces of the blocks, ensuring the wound tracts and permanent cavities of each individual shot did not breach the simulant nor come into contact with another shot.

Impact velocities were recorded using a Weibel W-700 Doppler radar. DoP into the simulant by the BBs was measured using a metal rod (1mm diameter) and a 1 m steel ruler (Figure 1).

Summary statistics (mean (\bar{x}), standard deviation (s.d.) and coefficient of variation (CV)) were calculated for the penetration data. In order to do this, recorded impact velocities were grouped into bins (Table I).

TABLE I VELOCITY BINS USED FOR DATA ANALYSIS

Velocity bins (m/s)*	Range of velocity bins (m/s)
150	110 – 190
250	210 – 290
500	460 – 540
750	710 – 790
1050	1010 – 1090

*n = 12-15 per velocity bin.

¹ Gelita UK Ltd., 3 Macclesfield Road, Cheshire, CW4 7NF, UK

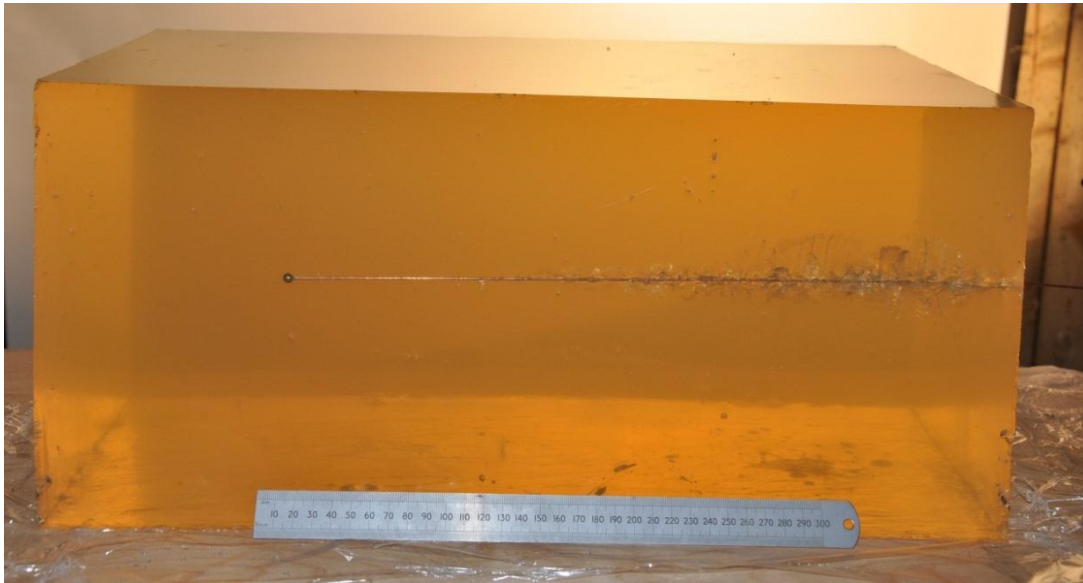


Figure 1. Gelatine block with penetration depth being measured.

RESULTS

Figure 2 helps to answer the question “Does the depth of penetration vary amongst tissue simulants?” Plotted on the graph is mean DoP for 5.5mm diameter BBs into 10% gelatine, 20% gelatine and Perma-Gel™ blocks against velocity bins. The DoP of BBs was longer at faster impact velocities for all simulants. The preliminary Perma-Gel™ data² suggested that for faster velocities, DoP was typically longer compared to both concentrations of gelatine.

Penetration of 5.5mm diameter BBs into the 10% and 20% gelatine followed a very similar pattern, albeit with 10% gelatine resulting in longer DoP at comparable velocities (e.g. velocity bin 500m/s: 10% gelatine mean DoP = 302.42mm; 20% gelatine mean DoP = 184.40mm). In comparison, the DoP results for BBs penetrating Perma-Gel™ did not follow the same pattern as gelatine; BB impact velocities of approximately 250m/s in Perma-Gel™ produced a shorter mean DoP than in 10% gelatine, however, for 500m/s and 750m/s bins, BBs penetrated Perma-Gel™ further compared to 10% gelatine at similar impact velocities.

² Not all Perma-Gel™ data was available at the time of paper submission. Complete results will be presented in the poster.

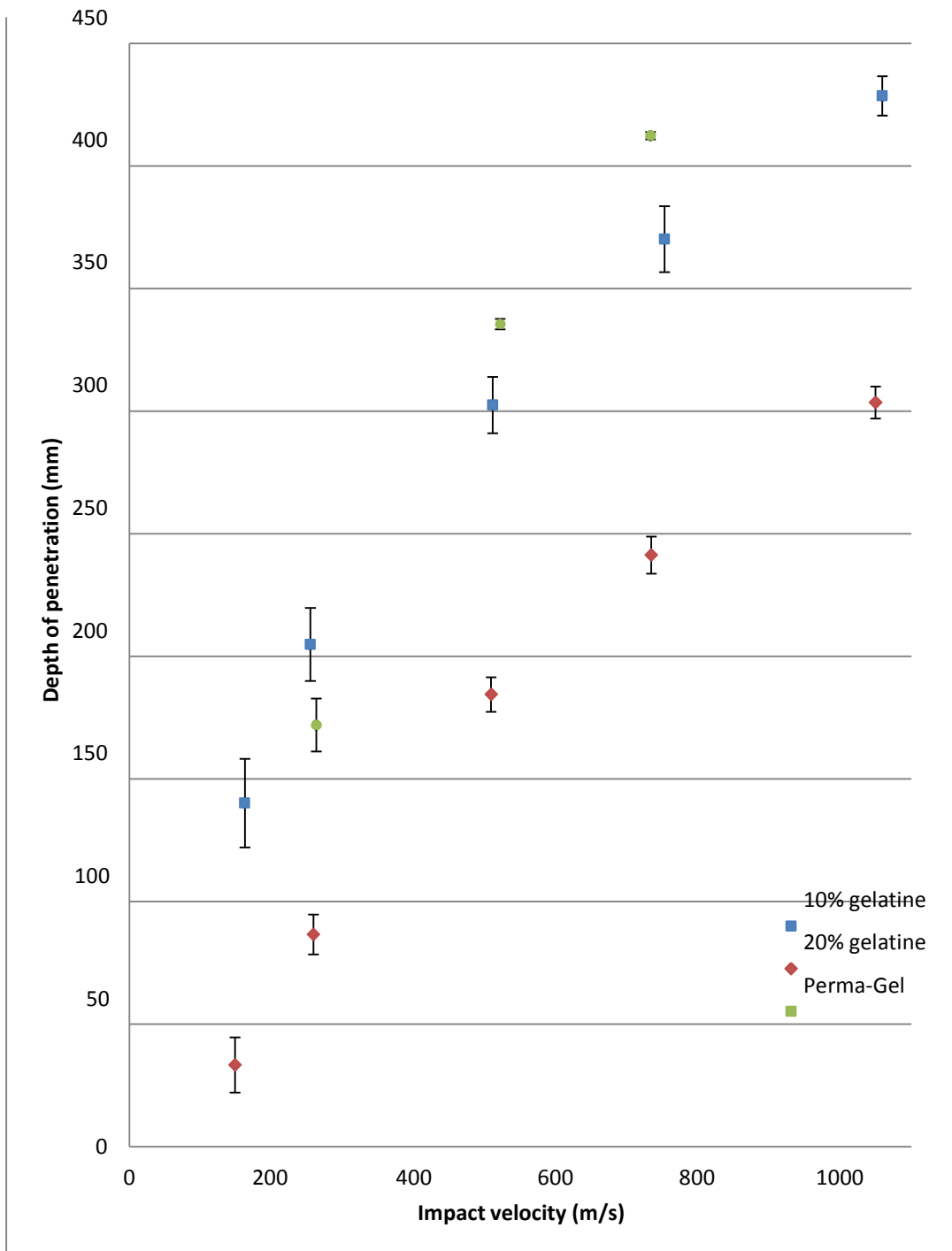


Figure 2. Comparison of mean penetration depths (with s.d.) of 5.5mm diameter BBs through three tissue simulants at a range of velocities.

Data obtained is summarised in Table II. The longest DoP was recorded in 10% gelatine (mean = 428.50mm, s.d. = 8.05mm), over 100mm longer than the longest DoP in 20% gelatine (mean = 303.50mm, s.d. = 6.56mm). In both concentrations of gelatine, the fastest velocity bin (1050m/s) caused the longest DoP (10% mean = 428.50mm, s.d. = 8.05mm; 20% mean = 303.50mm, s.d. = 6.56mm) and the

slowest velocity bin (150m/s) created the shortest DoP (10% mean = 140.14mm, s.d. = 18.09mm; 20% mean = 33.27mm, s.d. = 11.26mm).

Preliminary data for Perma-Gel™ demonstrated that DoP at 250m/s was more than 30mm shorter in comparison to 10% gelatine (mean = 172.00mm, s.d. = 10.78mm), but when compared at both 500m/s and 750m/s, DoP in Perma-Gel™ was over 35mm and 40mm longer respectively compared to 10% gelatine (mean = 335.50mm, s.d. = 2.12mm; mean = 412.33, s.d. = 1.53mm). DoP into Perma-Gel™ at 750m/s was more similar to the DoP at 1050m/s in 10% gelatine than to 750m/s in 10% gelatine.

TABLE II: DEPTH OF PENETRATION IN 10% AND 20% GELATINE

Velocity bin (m/s)	n*	Mean (mm)	s.d. (mm)	CV (%)
10% gelatine				
150	14	140.14	18.09	12.90
250	13	204.77	14.89	7.27
500	12	302.42	11.48	3.80
750	12	370.08	13.47	3.64
1050	12	428.50	8.05	1.88
20% gelatine				
150	15	33.27	11.26	33.84
250	14	86.50	8.13	9.40
500	15	184.40	7.05	3.82
750	14	241.29	7.57	3.14
1050	12	303.50	6.56	2.16
Perma-Gel™				
250	5	172.00	10.78	6.26
500	2	335.50	2.12	0.63
750	3	412.33	1.53	0.37

*Incomplete data set for Perma-Gel™, full data to be presented in the poster presentation.

DISCUSSION

A penetration function for verification of 10% gelatine quality that involved the use of BBs had been suggested [1]. Using 4.5mm diameter BBs at velocities of approximately 110m/s, 150m/s, 170m/s and 190m/s, an equation from which expected penetration could be predicted from impact velocity was proposed. The research presented here also used BBs, however, 5.5mm diameter BBs were used as a closer representation of specific rifle ammunition of interest in a wider research programme (i.e. 5.56mm x 45mm). With 500m/s quoted as the lower limit of low velocity ammunition [8], measuring gelatine DoP at a variety of impact velocities up to 1050m/s gave a much closer representation of an expected rifle ammunition impact velocity. Comparison of results in 10% gelatine against Jussila's [1] proposed linear regression function for DoP revealed large differences, with DoP greater in the current study at comparable velocities. The use of BBs with a 1.0mm larger diameter possibly affected DoP, as did measuring to the back of the BB instead of the front, as Jussila did. Bourget *et al.* presented DoPs for 5.5mm steel spheres in both 10% gelatine and 20% gelatine from a series of independent tests carried out in France, the Netherlands and Belgium [5]. Results from the current study on the whole follow the same pattern;

however, DoPs were shorter at comparable impact velocities when compared to those presented by Bourget *et al.*

However, the gelatine DoP results collected in the current study are comparable to the results previously published when DoPs are plotted against kinetic energy rather than impact velocity. Results for 10% gelatine follow the same configuration except for kinetic energy values equivalent to approximately 500m/s which result in a notable difference in DoPs. When comparing 20% gelatine the results follow the same formation, apart from DoPs at kinetic energy values equivalent to approximately 750m/s showing a noticeable difference. The larger range of velocities displayed in the current study gives a better idea of DoP in gelatine as a whole, rather than just at very low velocity levels.

There is a paucity of studies into the capabilities of Perma-Gel™ with one exception [7]. BBs were used; but they were much larger (1/2 inch, 12.7mm diameter) and tested at a smaller velocity range (61m/s – 274m/s). No data on DoP was presented, however, remarks regarding the behaviour of Perma-Gel™, such as traces of the BB backtracking through the gel, and the permanent cavity collapsing leaving an incomplete wound tract behind were found; similar observations were made during the current study. The complete collapse of the wound tract did not occur in either concentration of the gelatine; the process of the temporary cavity subsiding to form the permanent cavity left a smaller cavity and wound tract, conversely, the whole tract remained clearly visible, unlike in Perma-Gel™. The BBs backtracking through gelatine during the ballistic event was witnessed with the aid of high-speed filming, yet, visible traces in the gelatine were not clearly identifiable.

CONCLUSIONS

Depth of penetration was assessed in three different tissue simulants. The results show that at comparable velocities DoP followed a similar pattern in both 10% and 20% gelatine; however DoP was longer in 10% gelatine over a range of impact velocities (150m/s – 1050m/s). In Perma-Gel™, a synthetic simulant that is marketed as having similar properties as 10% gelatine, provisional results suggested this simulant produced the longest DoP of the three simulants at higher velocities (>500m/s), though this was not the case at lower velocities (>400).

ACKNOWLEDGEMENTS

The authors would like to thank the Engineering and Physical Science Research Council, The Impact and Armour Group (CDS) and the Worshipful Company of Armourers and Brasiers for their funding and support.

REFERENCES

- [1] Jussila, J. (2004), Preparing ballistic gelatine—review and proposal for a standard method, *Forensic science international*, 141(2–3), pp. 91-98.

- [2] Shepherd, C. J., Appleby-Thomas, G. J., Hazell, P. J. and Allsop, D. F. (2009), "The dynamic behaviour of ballistic gelatine", *Proceedings of the American Physical Society Topical Group on Shock Compression of Condensed Matter*, 28th June – 3rd July, Nashville (Tennessee), USA, American Institute of Physics, pp. 1399-1402.
- [3] Fackler, M. L. and Malinowski, J. A. (1985), "The wound profile: A visual method for quantifying gunshot wound components", *Journal of Trauma*, 25(6), pp. 522-529.
- [4] Knudsen, P. J. T. and Vignaes, J. S. (1995), "Terminal ballistics of 7.62mm NATO bullets: experiments in ordnance gelatine", *International Journal of Legal Medicine*, 108(2), pp. 62-67.
- [5] Bourget, D., Dumas, S. and Bouamoul, A. (2012), "Preliminary estimate for injury criterion to immediate incapacitation by projectile penetration", *Proceedings of the Personal Armour Systems Symposium*, 16th–20th September, Nuremberg, Germany, The International Personal Armour Committee, pp. 449-456.
- [6] Amick, D. (2006), *Perma-Gel Product Overview*, available at: <http://www.perma-gel.com/overview.htm> (accessed March, 15th 2012).
- [7] Ryckman, R. A., Powell, D. A. and Lew, A. J. (2011), "Ballistic penetration of Perma-Gel", *Proceedings of the 17th American Physical Society Topical Conference on Shock Compression of Condensed Matter*, 26th June–1st July, Chicago, Illinois, American Institute of Physics, pp. 143-148.
- [8] Tobin, L. and Iremonger, M. (2006), *Modern body armour and helmets: An introduction*, Argos Press, Canberra, Australia.

Comparison of 10% gelatine, 20% gelatine and Perma-Gel™ for ballistic testing



*Mabbott, A.¹, Carr, D.J.¹,
Champion, S.², Malbon, C.³
and Tichler, C.³

Cranfield
UNIVERSITY

Introduction

Gelatine has been used as a simulant in terminal ballistics, albeit typically in two different concentrations by mass: 10% and 20% (1; 2). However, an internationally agreed standard for the preparation and use of either of these types of gelatine does not exist. Although calibration methods have been proposed, many of these are not available in the open literature. There is currently no known adaptive method to compare results from different concentrations of gelatine, with work in the open literature which has tested both concentrations limited e.g. (3).

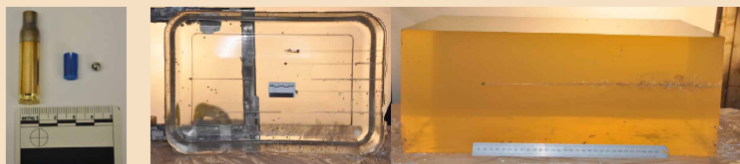
Perma-Gel™ is a commercially available, clear, synthetic material which was developed specifically as a soft tissue simulant that reportedly behaves in a similar manner to 10% gelatine (4). A further claimed advantage of Perma-Gel™ is that it can be re-melted and reused. Developed in 2005, independent validation of Perma-Gel™ in the open literature appears lacking (5).

The aim of work undertaken in this study was to test and record the differences between the three simulants for depth of penetration of 5.5 mm diameter ball bearings (BBs) at velocities between 150 m/s and 1050 m/s.

Materials and Methods

Both 10% and 20% gelatine blocks were made using Type 3 (265 Bloom) ballistic photographic grade gelatine from the same batch (Manufacturer: Gelita UK Ltd, 3 Macclesfield Road, Cheshire, CW4 7NF, UK). Blocks were made two days prior to testing, following guidelines from the Centre for Applied Science and Technology (CAST). The gelatine solution was poured and left to set in moulds measuring 250 mm (h) x 250 mm (w) x 500 mm (l), with both longer sides tapered 1° to facilitate set gelatine removal. Blocks were left to set overnight, before being transferred to a refrigerator at either 4°C or 10°C (10% and 20% gelatine respectively) for at least 24 hours before testing. Perma-Gel™ blocks were purchased in the raw base media form (dimensions approximately 127 mm (h) x 279 mm (w) x 432 mm (l)). These blocks were prepared following the manufacturer's instructions.

Depth of penetration (DoP) tests were conducted using 5.5 mm diameter steel BBs. The BBs were placed into a polymeric sabot which was fitted into a 7.62 x 51 mm cartridge before firing from an Enfield Number 3 Proof Housing. The simulant targets were placed 10 m down range from the end of the muzzle. Multiple firings were conducted at both faces of the blocks, ensuring the wound tracts and permanent cavities of each individual shot did not breach the simulant nor come into contact with another shot. Impact velocities were recorded using a Weibel W-700 Doppler radar. DoP into the simulant by the BBs was measured using a metal rod (1 mm diameter) and a 1 m steel ruler.



References

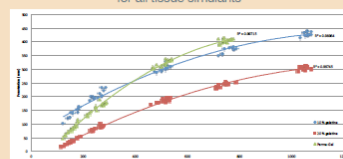
- 1 Fackler, M. L. and Malinowski, J. A. (1985), "The wound profile: A visual method for quantifying gunshot wound components", *Journal of Trauma*, 25(6), pp. 522-529.
- 2 Knudsen, P. J. T. and Vignaes, J. S. (1995), "Terminal ballistics of 7.62 mm NATO bullets: experiments in ordnance gelatine", *International Journal of Legal Medicine*, 108(2), pp. 62-67.
- 3 Bourget, D., Dumas, S. and Bouamoul, A. (2012), "Preliminary estimate for injury criterion to immediate incapacitation by projectile penetration", *Proceedings of the Personal Armour Systems Symposium*, 16th-20th September, Nuremberg, Germany, The International Personal Armour Committee, pp. 449-456.
- 4 Amick, D. (2006), *Perma-Gel Product Overview*, available at: <http://www.perma-gel.com/overview.htm> (accessed March, 15th 2012).
- 5 Ryckman, R. A., Powell, D. A. and Lew, A. J. (2011), "Ballistic penetration of Perma-Gel", *Proceedings of the 17th American Physical Society Topical Conference on Shock Compression of Condensed Matter*, 26th June-1st July, Chicago, Illinois, American Institute of Physics, pp. 143-148.

Results

Impact velocities were grouped into five separate velocity bins: 150, 250, 500, 750 and 1050 m/s. Analysis of 10% gelatine, 20% gelatine and Perma-Gel™ at velocity bins 150 m/s – 750 m/s showed that DoP varied significantly amongst velocity bins ($F_{3,152} = 3190.385$, $p < 0.05$). Tukey's HSD multiple comparison test indicated that each velocity bin resulted in significantly different DoPs. In each tissue simulant the longest DoP occurred with the fastest velocity bin and the shortest DoP occurred with the slowest velocity bin. Results showed that the type of tissue simulant had a significant effect on DoP of 5.5 mm BBs ($F_{2,152} = 1395.52$, $p < 0.05$). Tukey's HSD multiple comparison test indicated that each simulant type resulted in significantly different DoPs. DoP for velocity bins varied between the different tissue simulants, although weakly compared to the main effects ($F_{2,152} = 72.86$, $p < 0.05$). At 750 m/s, the longest DoP was recorded in Perma-Gel™ (mean = 403.47 mm, s.d. = 7.84 mm), over 30 mm longer than the next longest DoP which was in 10% gelatine (mean = 367.64 mm, s.d. = 10.98 mm), with 20% gelatine producing the shortest DoP at 750 m/s (mean = 241.29 mm, s.d. = 7.57 mm). However, at 150 m/s, the longest DoP was recorded in 10% gelatine (mean = 137.42 mm, s.d. = 18.15 mm), over 50 mm longer than the next longest DoP which was in Perma-Gel™ (mean = 81.47 mm, s.d. = 18.95 mm), with 20% gelatine again producing the shortest DoP (mean = 33.27 mm, s.d. = 11.26 mm).

Analysis of 10% gelatine and 20% across all five velocity bins revealed that gelatine concentration had a significant effect on DoP of BBs ($F_{1,123} = 3703.4500$, $p < 0.05$). The longest DoP was recorded in 10% gelatine (mean = 428.50 mm, s.d. = 8.05 mm), over 100 mm longer than the longest DoP in 20% gelatine (mean = 303.50 mm, s.d. = 6.56 mm). The DoP varied significantly amongst velocity bins ($F_{4,123} = 2713.33$, $p < 0.05$). Tukey's HSD multiple comparison test indicated that each velocity bin resulted in significantly different DoPs. DoP for velocity varied between the two gelatine concentrations, although weakly compared to the main effects ($F_{4,123} = 3.76$, $p < 0.05$).

Comparison of velocity bins and depth of penetration for all tissue simulants



Conclusions

- Depth of penetration of 5.5 mm BBs at a range of velocity bins is repeatable in all three simulants, with the level of penetration following a similar pattern for both concentrations of gelatine.
- The type of tissue simulant had a significant effect on depth of penetration of 5.5 mm BBs.
- The depth of penetration varied significantly amongst velocity bins.

Acknowledgements

The authors acknowledge the assistance of Mr. D. Miller and Mr. M. Teagle with ballistic testing. Also a big thank you to CAST for providing materials to support this project. Thank you also to the Worshipful Company of Armourers and Brasiers for their funding and support.

Mabbott, A., Carr, D.J., Malbon, C., Tickler, C. and Champion, S., (2012) Behind soft armour wounding by penetrating ammunition, in: *Proceedings of the Personal Armour Systems Symposium*, 17th – 21st September, Nuremberg, Germany, pp. 574-580:

Behind soft armour wounding by penetrating ammunition

Mabbott, A.¹, Carr, D.J.¹, Malbon, C.², Tickler, C.² and Champion, S.³

¹ *Impact and Armour Group, Department of Engineering and Applied Science, Cranfield Defence and Security, Cranfield University, Defence Academy of the United Kingdom, Shrivenham, Wiltshire, SN6 8LA, UK.*

² *Mechanical Engineering, Material Science and Civil Engineering, Centre for Applied Science and Technology, Home Office Science, Woodcock Hill, Sandridge, St Albans, Hertfordshire, AL4 9HQ.*

³ *Weapons and Vehicle Systems Group, Department of Engineering and Applied Science, Cranfield Defence and Security, Cranfield University, Defence Academy of the United Kingdom, Shrivenham, Wiltshire, SN6 8LA, UK.*

Abstract. There is a paucity of studies in the peer-reviewed literature that investigate behind soft armour wounding caused by over-matching rifle (high-velocity) ammunition; exceptions include [1-4]. There is some suggestion in the literature that in situations where a greater threat than expected is present, the specific body armour worn may not aid protection; rather it could exacerbate the wounding effect [1]. However, the evidence in the literature is contradictory [compare 1-4], and the need for further research has been noted [3, 4]. This poster describes work investigating behind (soft) armour wounding caused by two Federal Tactical rounds which are of interest to the UK Police i) 5.56mm x 45mm and ii) 7.62mm x 51mm. The armour investigated was typical of that worn by UK Police Officers. For each shot, the body armour panel was mounted in front of gelatine blocks, thus producing permanent cavities from which wound analysis was carried out. Additionally, each impact was recorded using a Phantom V12 high-speed video camera. Results demonstrated that the ammunition types behaved differently, and was supported by statistical tests performed on the wound measurements. Analysis of the effect body armour had on the wounding revealed inconsistent wound profiles. Debris (lead and fabric) was observed through the wound track.

Curriculum Vitae for Alex Mabbott

2011ff PhD researcher

Impact and Armour Group, Department of Engineering and Applied Science, Cranfield Defence and Security, Cranfield University, Defence Academy of the United Kingdom

Broad research area: wound ballistics; supported by EPSRC DTA (Engineering and Physical Sciences Research Council Doctoral Training Account), Department of Engineering and Applied Science and Home Office Centre for Applied Science and Technology

2010 – 2011 MSc Forensic Ballistics, 71%

Cranfield Forensic Institute and Impact and Armour Group, Department of Engineering and Applied Science, Cranfield Defence and Security, Cranfield University, Defence Academy of the United Kingdom

Thesis *Penetration of soft body armour by rifle ammunition* [UK RESTRICTED]

(commissioned by the Home Office Centre for Applied Science and Technology)

2007 – 2010 BSc (Hons) Forensic Science, awarded 2:1

University of Lincoln

Dissertation *An evaluation of the reproducibility of pore area in latent fingerprints*

Behind soft armour wounding by penetrating ammunition

Mabbott, A.¹, Carr, D.J.¹, Malbon, C.², Tickler, C.² and Champion, S.³

¹ *Impact and Armour Group, Department of Engineering and Applied Science, Cranfield Defence and Security, Cranfield University, Defence Academy of the United Kingdom, Shrivenham, Wiltshire, SN6 8LA, UK.*

² *Mechanical Engineering, Material Science and Civil Engineering, Centre for Applied Science and Technology, Home Office Science, Woodcock Hill, Sandridge, St Albans, Hertfordshire, AL4 9HQ.*

³ *Weapons and Vehicle Systems Group, Department of Engineering and Applied Science, Cranfield Defence and Security, Cranfield University, Defence Academy of the United Kingdom, Shrivenham, Wiltshire, SN6 8LA, UK.*

1. INTRODUCTION

Table 1 summarises the studies in the peer-reviewed literature that investigate behind soft armour wounding caused by over-matching rifle (high-velocity) ammunition.

Table 1. Summary of previous studies

	Previous studies			
	Lanthier <i>et al.</i> , 2004 [2]	Knudsen and Sørensen, 1997 [3]	Missliwetz <i>et al.</i> , 1995 [1]	Prather, 1994 [4]
Ammunition tested	5.45mm x 39mm (AK-74) and 5.56mm x 45mm (SS109)	7.62mm x 39mm (AK-47 FMJ;LAPUA, Finland)	9mm x 19mm (S-Patr P 08) 7.62mm x 39mm (AK-47) 7.62mm x 51mm (S-Patr StG 58) 5.56mm x 45mm (S-Patr StG 77)	7.62mm x 39mm (AK-47)
Velocity	600m/s and 900m/s	N/A	N/A	430m/s to 855m/s +
Firing range	10 m	30 m	10 m and 100 m	10 m to 500 m
Body armour tested	18 layers of para- aramid woven fabric	14 and 28 layers of Kevlar® fabric (Danish military Kevlar 29 type 964)	Nylon vest (4340 g), Kevlar® vest (4406 g), Kevlar® vest (2928g)	Configurations of 8 and 28 plies of 1000 Kevlar® fabric
Body simulant used	Glycerine soap blocks (250mm x 250mm x 400mm)	None	Soap blocks (300mm in length)	20% gelatine blocks (150mm high x 150mm wide x 400mm long)
Findings	<ul style="list-style-type: none"> Results showed that the armour did not cause an earlier transfer of energy from the projectile into the soap. Volume and maximum diameter of the cavity produced were smaller when body armour was in place. 	<ul style="list-style-type: none"> With the body armour tested at varying angles, the yaw of the projectile after perforation was measured. Results showed that perforation of the soft body armour resulted in an increased yaw angle. The yaw increased with the number of armour layers. 	<ul style="list-style-type: none"> Results demonstrated that the projectiles created a shorter narrow channel for both 5.56mm x 45mm and 7.62mm x 39mm bullets. While the cavity produced by the 7.62mm x 39mm projectile had a reduced maximum diameter, the cavity caused by the 5.56mm x 45mm projectile had increased significantly. It was concluded that another factor which could not be defined affected the wounding observed; possibly how the body armour material was processed 	<ul style="list-style-type: none"> At velocities lower than 430m/s, upon exit of the armour, projectiles were observed tumbling and exhibited a velocity loss of over 10% For velocities simulating target ranges over 500 m the projectiles remained visibly stable and did not tumble after passing through the 28 ply sample. There appeared to be no significant effect produced by soft armour on the wounding characteristics after realistic engagement (500 m) with ak-47 ammunition. Called for a more rigorous study involving different small arms projectiles and other armour
Critical review	<ul style="list-style-type: none"> Soap will only capture the temporary cavity, not the permanent cavity; therefore it would be hard to comment on overall wounding potential. Only one form of soft armour tested, could more or less layers have an effect? 	<ul style="list-style-type: none"> No body simulant was used, therefore wounding potential could not be analysed. With no backing material present, would this affect the behaviour of the body armour? 	<ul style="list-style-type: none"> Permanent cavity not captured as soap was used instead of gelatine. 	<ul style="list-style-type: none"> The findings were for realistic battle engagements (500 m), wounding from rifle ammunition could occur at close range too.

The armours, body simulants and ammunition used in these studies varied, thus results are not easily compared, highlighting and reiterating the need for further research as noted by several researchers [3, 4].

The aim of the research summarised in this paper was to determine whether the effects of high velocity ammunition are exacerbated when fired through soft (fabric) body armour.

2. MATERIALS AND METHODS

2.1 Materials

A soft body armour panel was provided by the Home Office Centre for Applied Science and Technology (CAST) and will be referred to as Soft Body Armour A in the article. Two types of ammunition were also provided by CAST which are of interest to UK Police Forces (Figure 1):

- i) 5.56mm x 45mm (62 grain; Federal Premium® Tactical Bonded®)
- ii) 7.62mm x 51mm (165grain; Federal Premium® Tactical Bonded®)



Figure 1. Comparison of both bullet types; (left to right) 7.62mm x 51mm and 5.56mm x 45mm

Gelatine blocks, 20% by mass, were prepared using 250 Bloom grade A gelatine¹¹ in 45 L plastic containers (540mm x 350mm x 240mm¹²). These blocks were then cut in half (270mm x 350mm x 240mm).

2.2 Methods

Ballistic testing was conducted using HOSDB *Body Armour Standards for UK Police Part 2: Ballistic Resistance, 2007* as a guideline [5]. The target was placed 10 m from the end of the muzzle. Two barrel types (SA80 and SLR) were fitted to an Enfield Number 3 Proof Housing to fire the .223 Remington and 7.62mm x 51mm bullets respectively.

For every test shot, a new gelatine block was used. To achieve a set of baseline results three rounds of each ammunition type were fired into separate gelatine blocks i.e. no body armour was used. Following this, body armour panel A was mounted in front of gelatine blocks. One bullet was fired into each panel A/gelatine block combination, with a total of three bullets of each ammunition fired into the armour panel. Impact sites were located at least 50mm from the edge of the body armour and 50mm from previous impact

¹¹Weishardt International, France.

¹²The Range, Swindon, Wiltshire, SN1 2NN.

sites, conforming to the HOSDB regulations [5]. Testing was blocked by bullet calibre, that is, all the 7.62mm x 51mm tests were conducted first and all the 5.56mm x 45mm tests were conducted second.

Gelatine blocks were dissected after testing. Lead and fabric debris present in the cavities were noted and photographed (Nikon D90, Nikon DX AF-S NIKKOR 18-105mm lens). Measurements of the permanent cavities produced in the gelatine blocks were then taken, giving the following key dimensions: neck length, 'body' length, 'body' width, 'body' height and (when possible) distance to bullet (Figure 2). From the 'body' width and height dimensions, an estimated maximum ellipse area was calculated. A final calculation predicted the wound volume.

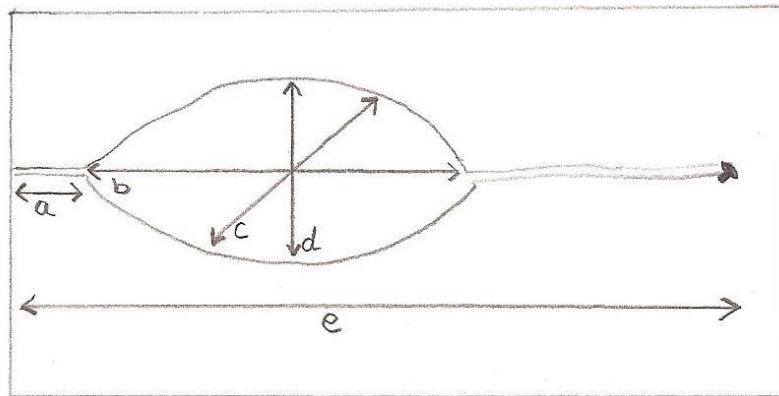


Figure 2. Schematic diagram of permanent cavity measurements; a – neck length, b – 'body' length, c – 'body' width, d 'body' height and e – distance to bullet

Summary statistics (mean (\bar{x}), standard deviation (s.d.) and coefficient of variation (CV)) were calculated for the permanent cavity data. Analysis of variance (ANOVA) and Tukey analysis were used to determine when significant differences among the baseline and body armour data set occurred for each type of ammunition (IBM SPSS Statistics 19.0) Normality of data and equality of variance were checked for each data set.

3. RESULTS

3.1 General observations

All three 5.56mm x 45mm bullets that were fired at gelatine blocks with no body armour present fully perforated the blocks. Of these three bullets, one was found 2.2 m away from the rear of the gelatine block, one was found in the sand butt of the range, and one was not recovered. Of the three shots fired into body armour A, all defeated the armour and although they partially perforated the gelatine blocks, the projectiles remained in the blocks. All six 7.62mm x 51mm bullets fired perforated the gelatine blocks, regardless of the body armour A being present.

3.2 Neck length

Bullet calibre had no significant effect on the resultant mean neck length ($F_{1,8} = 0.97, \rho = \text{NS}$), nor did the presence of body armour ($F_{1,8} = 0.97, \rho = \text{NS}$). That said, for both 5.56mm x 45mm and 7.62mm x 51mm bullet types, the neck length was longest when no body armour was present (mean = 9.00mm, s.d. = 6.56mm; mean = 8.33mm, s.d. = 10.41mm) (Table 2a).

3.3 Body length

The bullet calibre had no significant effect on the mean body length ($F_{1,8} = 0.05, \rho = \text{NS}$), neither did the presence of body armour ($F_{1,8} = 0.97, \rho = \text{NS}$). However, the mean body lengths were shortest when body armour A was present for both bullet types (5.56mm x 45mm mean = 223.33mm, s.d. = 25.17mm; 7.62 x 51mm mean = 220.00mm, s.d. = 36.06mm) (Table 2b).

3.4 Body width

The mean body width was not significantly affected by bullet type ($F_{1,8} = 3.02, \rho = \text{NS}$). Nor was it significantly affected by the presence of body armour ($F_{1,8} = 4.02, \rho = \text{NS}$). The shortest body width for the 5.56mm x 45mm was against body armour A (mean = 65.00mm, s.d. = 8.66mm); the shortest for the 7.62mm x 51mm was against body armour A too (mean = 75.00mm, s.d. = 5.00mm) (table 2c).

3.5 Body height

The bullet calibre had a significant effect on the mean body height ($F_{1,8} = 7.03, \rho \leq 0.05$), with the 7.56mm x 51mm causing the largest mean body height. The presence of body armour had no significant effect on the mean body height ($F_{1,8} = 0.50, \rho = \text{NS}$). The largest mean body height for the 5.56mm x 45mm was against no body armour (mean = 75.00mm, s.d. = 5.00mm); a different result was witnessed for the 7.62mm x 51mm, which produced the largest mean body height against body armour A (mean = 106.67mm, s.d. = 25.16mm) (table 2d).

3.6 Debris

Forensic examination of the gelatine blocks that were fired at with body armour A attached revealed a common pattern; fabric debris was present on the face of the gelatine block that had been in contact with the body armour. The colour of the fabric present correlated with the colour of the body armour cover. When 7.62mm x 51mm ammunition was used, the fabric debris was primarily distributed around the entrance wound; a much wider spread of fabric debris occurred when the 5.56mm x 45mm ammunition was used.

The gelatine blocks were dissected; debris (lead and fabric) was common in the wound tracts for both ammunition types (e.g. Figure 3). Wounds caused by the 5.56mm x 45mm bullets contained a greater number of fibres/pieces of fabric; fabric debris was larger in size as if ‘punched’ out. In comparison fabric debris resulting from 7.62mm x 51mm bullets was smaller as if the material had been torn through. Lead debris was concentrated at the entrance wound for both ammunition types; however the wound tracts contained lead debris throughout.

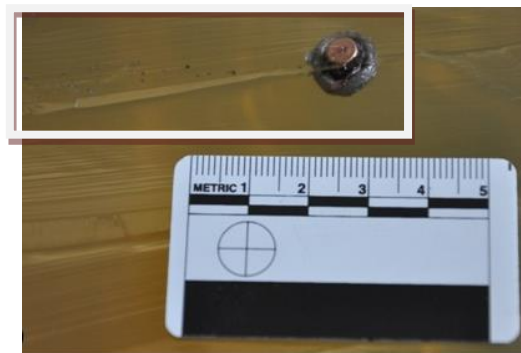


Figure 3. Example of lead debris and bullet in wound tract after perforation by 5.56mm x 45mm

Table 2. Selection of descriptive statistics

	Mean	s.d.	CV (%)
<u>a Neck length (mm)</u>			
5.56mm x 45mm			
None	9.00	6.56	72.86
A	8.33	2.89	34.66
7.62mm x 51mm			
None	8.33	10.41	124.95

A	6.67	2.89	43.28
b Body length (mm)			
5.56mm x 45mm			
None	256.67	30.55	11.90
A	223.33	25.17	11.27
7.62mm x 51mm			
None	246.67	90.74	36.79
A	220.00	36.06	16.39
c Body Width (mm)			
5.56mm x 45mm			
None	76.67	2.88	3.75
A	65.00	8.66	13.32
7.62mm x 51mm			
None	88.33	18.93	21.43
A	75.00	5.00	6.67
d Body height (mm)			
5.56mm x 45mm			
None	75.00	5.00	6.67
A	61.67	10.41	16.88
7.62mm x 51mm			
None	80.00	17.32	21.65
A	106.67	25.16	23.59

4. DISCUSSION

There are two points which require further discussion, effect of i) ammunition and ii) body armour on wounding.

4.1 Ammunition

The 7.62mm x 51mm ammunition expanded early in the gelatine, the energy it transferred appeared to be spread over a longer distance. Fibres were mostly displaced and not broken; similar failure mechanisms have been reported before, but for 5.45mm x 39mm rounds at 900m/s [2]. Observations regarding the perforation mechanism of soft body armour in other previously published studies were not been reported.

In comparison, the 5.56mm x 45mm bullets ‘punched’ through the armour and gelatine blocks, transferring energy from the bullet to the gelatine over a shorter distance compared to the 7.62mm x 51mm ammunition. High-speed video footage supported this observation. This interaction is different to that observed for the 5.45mm x 39mm ammunition used by Lanthier *et al.* [2] suggesting differing ammunition could have different effects. Although the mechanisms of transferring energy from the bullets to both the body armour and gelatine were noticeably different, the resulting wounds were just as likely to be fatal from both ammunition types, regardless of which armour was present.

The yaw observed after perforation of body armour in the current work is in agreement with previous studies [2, 3]. Bullet instability or tumbling after body armour perforation was not observed in the current work; this contradicts previous studies [1, 4].

4.2 Effect of body armour on wounding compared to no body armour

The body armour panel that was tested was designed to protect the thoracic region. Therefore, information regarding anthropometric measurement of the chest is useful. Laing *et al.* [6] reported that the mean anterior-posterior chest depth was 245.8mm, with a transverse chest breadth being 327.3mm for New Zealand firefighters. Such measurements assist with understanding the potential area where wounding

could occur within the human torso. The neck of the permanent cavity identified the route the bullet has taken, and the length reveals the distance the bullet has travelled before it dissipates energy. A short neck length indicates a quicker transfer of energy into the body in comparison to a longer neck length. If the neck length is too long, i.e. if the distance the bullet travels before dissipating its energy is too long, the bullet may have perforated and exited a target before it has transferred its kinetic energy, meaning wounding has not maximised.

The area of energy deposition for the wounds considered in this paper was named the 'body'. Statistical analysis revealed the presence of body armour type A did not affect the wound measurements that were taken for the body, nor the neck of the wound.

5. CONCLUSIONS

The wounding caused by both ammunition types, with or without soft body armour investigated in this research, would be fatal in the majority of cases. Although diversity was seen for both ammunition types, and for when body armour was used, no common trend was observed.

References

- [1] Misliwetz, J., Denk, W. and Wieser, I., Study on the wound ballistics of fragmentation protective vests following penetration by handgun and assault rifle bullets, *Journal of Forensic Sciences*, 40 (1995), 582-584.
- [2] Lanthier, J.M., Iremonger, M.J., Lewis, E.A., Horsfall, I. and Gotts, P.L., Is the wounding potential of high velocity military bullets increased after perforation of textile body armour, *Personal Armour Systems Symposium*, The International Personal Armour Committee, The Hague, Netherlands, 6th -10th September, (2004), 225-232.
- [3] Knudsen, P.J.T. and Sørensen, O.H., The destabilising effect of body armour on military rifle bullets, *International Journal of Legal Medicine*, 110 (1997), 82-87.
- [4] Prather, R.N., Small arms vs. soft armour – A pilot study, *Proceedings of the Personal Armour Systems Symposium*, Colchester, UK, 21st – 25th June, (1994), 137-141.
- [5] Croft, J. and Longhurst, D., *HOSDB Body Armour Standards for UK Police (2007) Part 2: Ballistic Resistance*, Home Office Scientific and Development Branch, St Albans, UK, 2007.
- [6] Laing, R.M., Holland, E.J., Wilson, C.A. and Niven, B.E., Development of sizing for protective clothing for the adult male, *Ergonomics*, 42 (1999), 1249-1257.



College of Management and Technology

Behind soft armour wounding by penetrating ammunition

Introduction

The amount of protection body armour is required to provide is threat-based; with numerous examples available in the open literature testing body armour against a wide range of threats that includes blunt objects, knives and fragments. What happens when the threat is greater than predicted is not well understood. More poignantly, could this scenario result in a greater wounding potential? Focusing specifically on fabric (soft) body armour systems, there is some suggestion in the limited literature available on this topic, that where a greater threat than expected is present the body

armour worn may not aid protection; rather it could exacerbate the wounding. However, the evidence in the literature is contradictory, with some studies calling for further research. The work summarised in this poster investigated the effect of over matching a UK police soft body armour with two types of high velocity rifle ammunition, with the aim of discovering whether the body armour exacerbated wounding compared to when no body armour was present.

Mabbott, A.¹, Carr, D.J.¹, Malbon, C.², Tichler, C.² and Champion, S.³

- 1 Impact and Armour Group, Department of Engineering and Applied Science, Cranfield Defence and Security, Cranfield University, Defence Academy of the United Kingdom, Shrivenham, SN6 8LA, UK.
- 2 Mechanical Engineering, Material Science and Civil Engineering, Centre for Applied Science and Technology, Home Office Science, Woodcock Hill, Sandridge, St Albans, Hertfordshire, AL4 9HQ, UK.
- 3 Weapons and Vehicle Systems Group, Department of Engineering and Applied Science, Cranfield Defence and Security, Cranfield University, Defence Academy of the United Kingdom, Shrivenham, Wiltshire, SN6 8LA, UK.

Materials and Method

Materials

Two types of ammunition of interest to UK police were used: (i) 5.56 mm x 45 mm (62 grain; Federal® Premium® Tactical Bonded®) and (ii) 7.62 mm x 51 mm (165 grain; Federal® Premium® Tactical Bonded®). 20% gelatine blocks were used as a tissue simulant.

Methods

The target set up (Figure 1) was 10 m down range from the Enfield Number 3 Proof Housing that was used to fire the ammunition. Three rounds of each ammunition type were fired into three separate gelatine blocks. The body armour was mounted in front of non-tested

gelatine blocks and one bullet fired into each panel / gelatine block combination, with a total of three bullets of each ammunition fired into the armour. Gelatine blocks were dissected after testing; lead and fabric debris were recorded, and a series of measurements of the permanent cavities in the gelatine blocks taken (Figure 2).

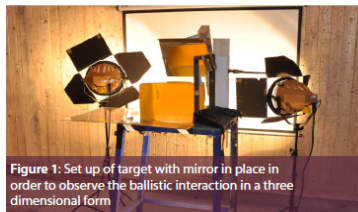


Figure 1: Set up of target with mirror in place in order to observe the ballistic interaction in a three dimensional form

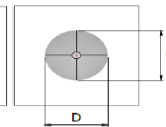
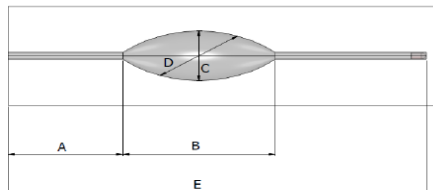


Figure 2: Schematic diagram of permanent measurements; A- neck length, B-'body' length, C-'body' height, D-'body' width and E-distance to bullet.

Results

General

All three 5.56 mm x 45 mm bullets that were fired at gelatine blocks with no body armour present, fully perforated the blocks. Of the three shots fired into the body armour, all defeated the armour and although they penetrated the gelatine blocks, the projectiles remained in the blocks. All six 7.62 mm x 51 mm bullets perforated the gelatine blocks, regardless of body armour being present.

Bullet calibre had no significant effect on the resultant mean neck length ($F_{1,8} = 0.97, p = NS$), nor did the presence of body armour ($F_{1,8} = 0.97, p = NS$).

The bullet calibre had no significant effect on the mean body length ($F_{1,8} = 0.05, p = NS$), neither did the presence of body armour ($F_{1,8} = 0.97, p = NS$). The mean body width was not significantly affected by bullet type ($F_{1,8} = 3.02, p = NS$), nor was it significantly affected by the presence of body armour ($F_{1,8} = 4.02, p = NS$). The bullet calibre had a significant effect on the mean body

height ($F_{1,8} = 7.03, p \leq 0.05$), with the 7.62 mm x 51 mm causing the largest mean body height. The presence of body armour had no significant effect on the mean body height ($F_{1,8} = 0.50, p = NS$). The largest mean body height for the 5.56 mm x 45 mm was against no body armour (mean = 75.00 mm, s.d. = 5.00 mm); a different result was witnessed for the 7.62 mm x 51 mm, which produced the largest mean body height against the body armour.

Conclusion

- Both ammunition types, regardless of the presence of body armour, produced wounds that would be fatal in the majority of cases.
- Diversity in permanent cavity measurements was seen for both ammunition types, and for when body armour was used, but no common trend was observed.
- Further work required.

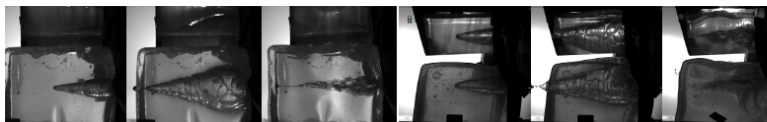


Figure 3: Stills of high speed imagery of (i) 5.56mm x 45mm and (ii) 7.62mm x 51mm after perforation of body armour A into 20% gelatine blocks (mirror located above gelatine block)

Acknowledgments

CAST for providing materials to support this project. David Miller and Mike Teagle for their support on the Cranfield Small Arms Experimental Range.

**APPENDIX L – Other publications the author was involved in during
this research**

Breeze, J., Carr, D.J., Mabbott, A., Beckett, S. and Clasper, J.C. (2015), Refrigeration and freezing of porcine tissue does not affect the retardation of fragment simulating projectiles, *Journal of Forensic and Legal Medicine*, 32, pp. 77-83.

Breeze, J., Mabbott, A. and Carr, D.J., Experimental penetration of 5mm spherical fragment simulating projectiles into 20% gelatine in: *Proceedings of the Personal Armour Systems Symposium*, 8th – 13th September, Cambridge, UK, (2014).

Burrell, G., Mabbott, A., Carr, D.J., Malbon, C., O'Rourke, S., Miller, D., Teagle, M. and Robbins, S., Do underwire bras affect wounding potential during non-perforating ballistic impacts onto police body armour, in: *Proceedings of the Personal Armour Systems Symposium*, 8th – 13th September, Cambridge, UK, (2014).

Carr, D.J., Kieser, J., Mabbott, A., Mott, C., Champion, S., Girvan, E. (2014), Damage to apparel layers and underlying tissue due to hand-gun bullets, *International Journal of Legal Medicine*, 128(1), pp. 83-93.

Kieser, D., Carr, D.J., Jermy, M., Mabbott, A. and Kieser, J., (In Press), Chapter 16 Biomechanics, in Freeman, M.D. (Ed.) *Forensic Epidemiology*, Elsevier, USA.

Mabbott, A., Carr, D.J., Caldwell, E., Miller, D. and Teagle, M., Bony debris ingress into the lungs due to gunshot, in: *28th International Symposium on Ballistics*, 22nd – 26th September, Atlanta, USA, (2014).

Mabbott, A., Robbins, S., Carr, D.J., Breeze, J., Malbon, C., O'Rourke, S. and Miller, D., Do Zips in front of body armour increase the wounding potential of non-perforating ballistic attacks? – A pilot study, in: *Proceedings of the Personal Armour Systems Symposium*, 8th – 13th September, Cambridge, UK, (2014).

Co-supervisor of the following MSc theses:

Burrell, G.M.R. (2013), *Do underwire bras effect wounding potential during non-perforating ballistic impacts onto police body armour?* (unpublished MSc thesis), Cranfield University, UK.

Caldwell, E.J. (2013), *Bone debris ingress into lungs from gunshot wounds* (unpublished MSc thesis), Cranfield University, UK.

De Friend, J.P. (2015), *Over matching of military soft body armour* (unpublished MSc thesis), Cranfield University, UK.

Milliner, M.S. (2014), *An investigation into the effect of ancillary equipment on behind armour blunt trauma (BABT)* (unpublished MSc thesis), Cranfield University, UK.

**APPENDIX M – Spreadsheets of tracking data collected from high
speed videos (CD attachment)**